Removal of various contaminants from water by renewable lignocellulose -derived biosorbents: A comprehensive and critical review

Hai Nguyen Tran[1]*, Hoang Chinh Nguyen[2], Seung Han Woo[3], Tien Vinh Nguyen[4], Saravanamuth Vigneswaran[4], Ahmad Hosseini-Bandegharaei[5,6], Jörg Rinklebe[7,8], Ajit Kumar Sarmah[9], Andrei Ivanets[10], Guilherme Luiz Dotto[11], Tho Truong Bui[12], Ruey-Shin Juang[13,14]*, Huan-Ping Chao[15]*

[1]Institute of Fundamental and Applied Sciences, Duy Tan University, Ho Chi Minh city 700000, Vietnam

[2]Faculty of Applied Sciences, Ton Duc Thang University, Ho Chi Minh city 700000, Vietnam
[3]Department of Chemical and Biological Engineering, Hanbat National University, 125 Dongseodaero, Yuseong-Gu, Daejeon 305-719, Republic of Korea
[4]Faculty of Engineering and IT, University of Technology, Sydney (UTS), Sydney, Australia
[5]Wastewater Division, Faculty of Health, Sabzevar University of Medical Sciences, PO Box 319, Sabzevar, Iran
[6]Department of Engineering, Kashmar Branch, Islamic Azad University, PO Box 161, Kashmar, Iran
[7]University of Wuppertal, School of Architecture and Civil Engineering, Institute of Foundation Engineering, Water- and Waste-Management, Laboratory of Soil- and Groundwater-Management, Pauluskirchstraße 7, 42285 Wuppertal, Germany
[8]Department of Environment and Energy, Sejong University, 98 Gunja-Dong, Guangjin-Gu, Seoul, Republic of Korea
[9]Department of Civil & Environmental Engineering, Faculty of Engineering, The University of Auckland, Private Bag 92019, Auckland 1142, New Zealand
[10]Institute of General and Inorganic Chemistry of National Academy of Sciences of Belarus, 220072 Minsk, Belarus
[11]Chemical Engineering Department, Federal University of Santa Maria–UFSM, 1000, Roraima Avenue, 97105-900 Santa Maria, RS, Brazil
[12]The Centre of Hi-tech Application in Agriculture, Chau Thanh district, Ben Tre province, Vietnam
[13]Department of Chemical and Materials Engineering, Chang Gung University, Guishan, Taoyuan 33302, Taiwan
[14]Division of Nephrology, Department of Internal Medicine, Chang Gung Memorial Hospital, Linkou, Taiwan
[15]Department of Environmental Engineering, Chung Yuan Christian University, Chung Li District, Taoyuan City 32023, Taiwan

----

Corresponding authors:

H.N. Tran (trannguyenhai@duytan.edu.vn); R.-S. Juang (rsjuang@mail.cgu.edu.tw); and H.-P. Chao (hpchao@cycu.edu.tw)

Abstract

Contaminants in water bodies cause potential health risks for humans and great environmental threats. Therefore, the development and exploration of low-cost, promising adsorbents to remove contaminants from water resources as a sustainable option is one focus of the scientific community. Here, we conducted a critical review regarding the application of pristine and modified/treated biosorbents derived from leaves for the removal of various contaminants. These include potentially toxic cationic and oxyanionic metal ions, radioactive metal ions, rare earth elements, organic cationic and anionic dyes, phosphate, ammonium, and fluoride from water media. Similar to lignocellulose-based biosorbents, leaf-based biosorbents exhibit a low specific surface area and total pore volume but have abundant surface functional groups, high concentrations of light metals, and a high net surface charge density. The maximum adsorption capacity of biosorbents strongly depends on the operation conditions, experiment types, and adsorbate nature. The absorption mechanism of contaminants onto biosorbents is complex; therefore, typical experiments used to identify the primary mechanism of the adsorption of contaminants onto biosorbents were thoroughly discussed. It was concluded that byproduct leaves are renewable, biodegradable, and promising biosorbents which have the potential to be used as a low-cost green alternative to commercial activated carbon for effective removal of various contaminants from the water environment in the real-scale plants.

Keywords: Leaf; biosorbent; biosorption; adsorption mechanism; water treatment; critical review.

Contents

1. Introduction

The increasingly uncontrolled discharge of contaminated effluents from various industrial activities has adversely affected the quality of water resources. Numerous alternative water treatment techniques, such as membrane filtration, chemical oxidation, precipitation, coagulation, and biological treatments, have been applied to remove hazardous chemicals from wastewater (Tchobanoglous and Angelakis, 1996). Although these methods could be applied to remove contaminants in the water bodies or wastewater, the operation cost and removal efficiency are the crucial factors to determine the selected method. Precipitation is a low-cost method, but it is only used for high concentrations of contaminants. Ion exchange resins and membrane filtration with high removal of contaminants are the expensive technologies. They are seldom used in wastewater treatment. The biological treatment often focuses on the biodegradable contaminants. Among current advanced technologies, adsorption is considered to be the most favorable alternative method for the removal of a variety of contaminants from polluted water resources (Abdolali et al., 2014; De Gisi et al., 2016). The advantages for the removal of contaminants from water bodies or wastewater by renewable leaf-derived biosorbents include a high removal efficiency for the contaminants at low concentrations, simplicity of design, cost effectiveness, and minimal generation of secondary byproducts such as sludge (Ali and Gupta, 2007; Fomina and Gadd, 2014).

In water purification, activated carbon (AC) has been proven to be an excellent adsorbent that can remove a great variety of toxins from contaminated water due to its highly developed porosity, large surface area, and high total pore volume (Giannakoudakis et al., 2016; Wong et al., 2018; Yagub et al., 2012). However, expensive production and regeneration costs restrict the application of AC in larger-scale industries and developing countries (Vu et al., 2018). The total adsorbent preparation cost of aluminate-treated *Casuarina equisetifolia* leaves is US$48/t (Khan Rao and Khatoon, 2017), which is remarkably lower than that of available commercial AC (US$400–1500/t). Unlike carbonaceous materials (i.e., AC and biochar), biosorbents are low energy-consuming materials (**Section 2.1**) because they do not require a further pyrolysis process at high temperature (often >700 °C for AC or

>300 °C for biochar). Furthermore, AC is highly carbonaceous porous material and has few functional groups on its surface; consequently, it has a very low ability to absorb charged chemicals such as heavy metals (Huang et al., 2014). Notably, several researchers found that biosorbents exhibit a higher adsorption capacity than AC under the same operation conditions (Amarasinghe and Williams, 2007; Aoyama et al., 2000a). In fact, Aoyama et al. (2000a) compared the removal efficiency of harmful metal cations from dilute solution by biosorbents obtained from the leaves of 34 conifer species with that of three different types of commercial ACs. They reported a removal efficiency of Cr(III) by leaves ranging from to 60% to 97%, while the corresponding values for commercial ACs are between 24% and 52%.

The literature survey indicates that many authors reviewed the use of various adsorbents derived from various feedstock resources for the removal of diverse contaminants from water media. Such alternative adsorbents include agricultural byproducts (i.e., banana, coffee, eggshell, and coconut wastes), industrial wastes (i.e., fly ash, sludge and slag, red mud, black liquor lignin, and waste slurry), activated carbon, biochar, bentonite, montmorillonite, zeolites, layered double hydroxides, iron oxide nanomaterials, and geopolymers (Abdolali et al., 2014; De Gisi et al., 2016; Neris et al., 2019; Siyal et al., 2018; Wong et al., 2018). Among the existing lignocellulosic materials-derived biosorbent, the plant-derived biomass has been acknowledged as a promising biosorbent to remove various contaminants from water environment. Notably, some researchers found that in the same experimental operation conditions, the biosorbent prepared from tree's leaves often exhibited a higher adsorption capacity than the biosorbent originated from its barks (Arshad et al., 2008), branches (Al-Masri et al., 2010), stems (Liu et al., 2010a; Prasad and Freitas, 2000), and roofs (Prasad and Freitas, 2000). The leaves are selected as target adsorbents in this study because (1) most abundant research data among them are present in literature, (2) other plant parts have significantly different characteristics from leaves—elemental composition, surface area, and adsorption performance—which may cause diverse results and intensify the confusion, and (3) the leaf biomass can be easily collected, consequently used, and economically advanced.

Here, we collected information from previous scientific papers (approximately 295 relevant original papers and review articles, mainly published from 1994 to 2018) on applying leaves (approximately 240 types of leaves) as green biosorbents for the removal of diverse pollutants from water environments (**Figure S1**). The biosorbent properties play a paramount role in estimating the adsorption capacity of these contaminants and proposing the primary adsorption mechanism. Thus, in **Section 2**, we summarize principal and relevant properties of leaves, such as textural, physicochemical, thermal, and crystal properties, especially the surface chemistry. We also clarify the effects of prevailing operational conditions on adsorption processes in batch and column experiments (see **Figure 1**; **Sections 3** and **4**). The potential application of biosorbents in wastewater is discussed in **Section 5**. Several problems regarding the direct use of biosorbents for water treatment are mentioned in **Section 6**. Importantly, the adsorption mechanism plays an integral role in elucidating the corresponding interactions between contaminant and biosorbent. Therefore, we focus on summarizing common techniques/experiments in **Section 7** to identify adsorption mechanism pathways. Lastly, we provide a critical analysis and discussion, which are integral to this study.

2. Preparation and characterization of leaf-derived biosorbents

2.1. Preparation of leaf-derived biosorbents

Leaf-derived biosorbents are composed mainly of molecules of organic origin, such as, cellulose, lignin, hemicellulose, pectin and extractive compounds (Liu et al., 2010c). From one side, this is an interesting characteristic, since these organic compounds contain a series of functional groups which can act as active sites for biosorption. On the other side, the structure and functionality of these organic molecules can be easily damaged by the temperature, pH, air humidity, oxygen, and others (Escudero et al., 2018). Because of this, a detailed preparation of the leaf-derived biosorbents is fundamental. **Figure 1** indicates the leaf can be synthesized adsorbents through various processes. In recent studies, the leaf-derived biosorbents were widely applied in the batch and column experiments of adsorption. Furthermore, the important parameters, which have a strong effect on the

adsorption process, are also represented in **Figure 1**.
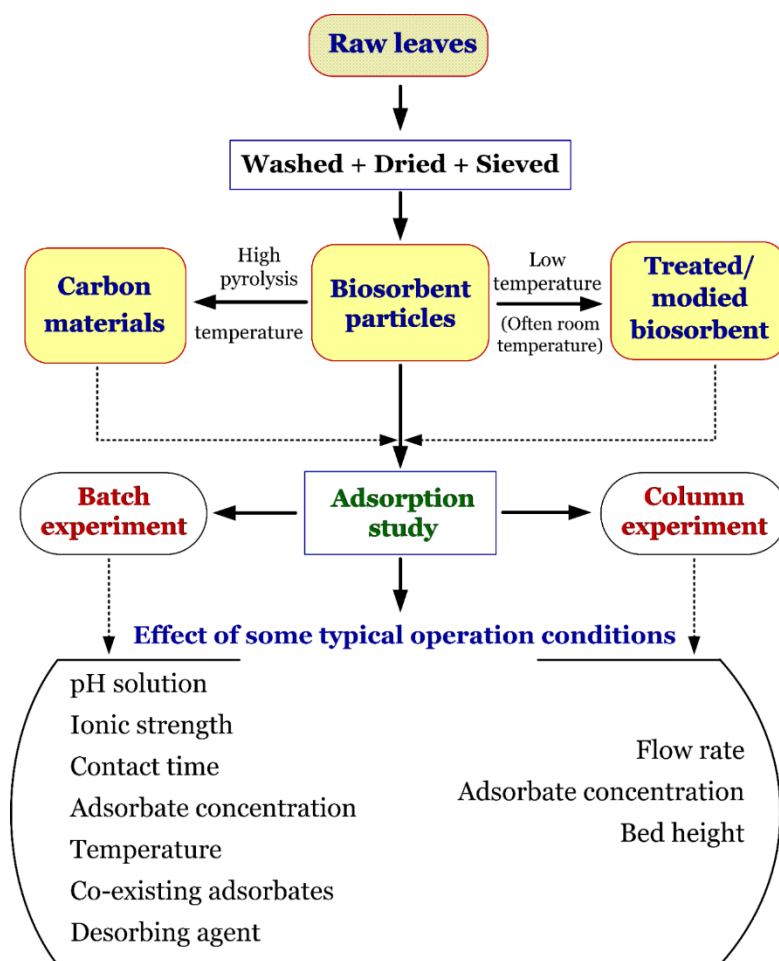
Figure 1. Preparation of the biosorbent for several typical adsorption batch and column experiments

In general, the leaf-derived biosorbents are prepared by consecutive steps as follows (Dotto et al., 2017; Dotto et al., 2015): (1) firstly, the raw material is thoroughly washed with deionized or distilled water to remove any adhering dirt and water-soluble impurities; (2) the material is then dried under controlled temperature and time. Drying operation should guarantee that the moisture content remains below to the monolayer, in order to avoid the physicochemical or microbiological degradation of the material. Normally the air-drying temperature is around 40–60 °C to avoid thermal degradation; and (3) finally the material is ground to attain a specific particle size. In cases where the biosorbent is composed by extractive molecules, the material is extracted with solvents, such as *n*-hexane and ethanol (Chao et al., 2014; Chao and Chen, 2012), chloroform and methanol (Chao et al., 2014; Chao and Chen, 2012), and hexane (Immich et al., 2009). This operation aims the removal of the extractive compound from the solid matrix, to avoid its released during the biosorption operation

(Georgin et al., 2018). After these preparation steps, the biosorbent material can be stored in tightly closed bottles or plastic bags for several months, or even years, and their physicochemical characteristics are unchanged.

2.2. Textural properties

Several methods to determine the specific surface area of solid materials are described in literature. The specific surface area of spent tea leaves was determined in Agarry et al. (2013) using the methylene blue adsorption method. They reported that the surface area of tea leaves is approximately 175 m^2/g. The sample method was applied in Kahina and Nasser (2017) and Baruah et al. (2017) to determine the specific surface areas of globe artichoke and bael leaves; surface areas of 723 and 110 m^2/g, respectively, were reported. Clearly, the specific surface areas of tea, globe artichoke, and bael leaves determined by the methylene blue adsorption method are much higher than that of other leaf-derived biosorbents obtained by using the nitrogen adsorption/desorption isotherm. **Table S1** indicates the specific surface area (S_{BET}) ranged from 0.08 to 67.0 m^2/g for agriculture products or wastes in literatures. The different synthesis processes and the unique properties of leaves might lead to a high diversity in the S_{BET} value.

In a recent study, Tran (2017) suggested that the specific surface area of an adsorbent can be determined by the nitrogen adsorption/desorption isotherm but that it is impractical to analyze it using methylene blue or iodine adsorption methods. A typical nitrogen adsorption/desorption isotherm of arborvitae leave-developed biosorbent is presented in **Figure S2**. Based on Tran et al. (2017a), the S_{BET} of a solid material can be calculated with the Brunauer–Emmett–Teller method (**Section S1**).

Essentially, S_{BET} is one of the characteristics that affect the maximum adsorption capacity of an adsorbent toward certain contaminants. Generally, any adsorbent with a large specific surface area is supposed to exhibit a superb adsorption capacity. Similar to other types of biosorbents, leaf-derived biosorbents can be classified as nonporous materials because of their poor textural properties. In fact, the S_{BET} and V_{total} of leave-originated biosorbents range from 0.08 to 67 m^2/g and 0.001 to 0.11 cm^3/g,

respectively (see **Table S1**). Meanwhile, other types of biosorbents, such as peanut shell (1.8 m^2/g and 0.003 cm^3/g), sawdust (1.6 m^2/g and 0.004 cm^3/g) (Ahmad et al., 2017), golden shower pod (5.7 m^2/g and 0.0099 cm^3/g), coconut shell (3.2 m^2/g and 0.0041 cm^3/g), orange peel (2.1 m^2/g and 0.0042 cm^3/g) (Tran et al., 2017c), cantaloupe peel (5.2 m^2/g and 0.0049 cm^3/g), pine cone (4.6 m^2/g and 0.0042 cm^3/g), litchi fruit peel (5.2 m^2/g and 0.0041 cm^3/g), annona squamosal peel (4.3 m^2/g and 0.0032 cm^3/g), sugarcane bagasse (7.9 m^2/g and 0.0056 cm^3/g), and bamboo shoot (2.6 m^2/g and 0.0019 cm^3/g) (Tran and Chao, 2018b), have lower S_{BET} and V_{total} values. Moreover, Figure S3a shows the morphology of a typical leaves-based biosorbent before adsorption. The SEM image also indicated the non-porous structure of the biosorbent.

Furthermore, Pandey et al. (2015) reported that the porosity of Kush grass and bamboo leaves only accounts for 0.11% and 0.15%, respectively. Therefore, the role of the pore filling mechanism in the biosorption process of contaminants in aqueous media is negligible. In this case, the available presence of active functional groups (hydroxyl, carboxylic, and amino), alkaline earth metals (Ca and Mg), and alkali metals (K and Na) on the biosorbent surface will play a major role in adsorbing adsorbate ions in solution.

2.3. Physical and chemical properties

Table 1 summarizes the major polysaccharide constituents including cellulose hemicellulose and lignin of leaf-based materials. Clearly, polymer carbohydrates (cellulose and hemicellulose) and lignin are the most abundant components of such materials. These constituents possibly contain polar surface functional groups, for instance alcohols, aldehydes, ketones, carboxyl, phenol, and ether (Liu et al., 2010c). Notably, the percentage of such constituents varies depending on the unique properties of each leaf type (**Table 1**).

Table 1. Polysaccharide components (%) of leaf-based materials

Leaves	Cellulose	Hemicellulose	Lignin	Reference

9

Southern cattail	34.1	31.2	4.16	Abdel-Ghani et al., 2009
Roxburgh fig	35.6	18.8	9.96	Rangabhashiyam et al., 2015
Pineapple	66.2	19.5	4.20	Daud et al., 2014
Oriental plane	32.5	19.7	30.1	Li et al., 2017
Pineapple	36.3	22.9	27.5	Santos et al., 2013
Oil palm	44.5	3.17	—	Setiabudi et al., 2016
Bamboo	18.6	16.5	12.3	Peng et al., 2013
Tea	37.0	—	14.7	Bajpai and Jain, 2012
Sakura	16.6	10.4	18.3	Wenfang et al., 2015
Maguey	80	5	15	Hamissa et al., 2010
Esparto grass	45.3	23.7	23.9	Lafi et al., 2015
Average	40.6	17.1	16.0	—
Standard deviation	18.6	8.67	9.01	—
Minimum	16.6	3.17	4.16	—
Maximum	80.0	31.2	30.1	—
Median	36.3	19.2	14.9	—

The element composites of leaf-derived adsorbents can be analyzed by energy-dispersive X-ray spectroscopy (EDS; **Figure S3b**) or other instruments. The contents of carbon (C) and oxygen (O) can affect the functional groups on the surface of adsorbent. Alkaline earth (Ca and Mg) and alkali (K and Na) metals on the biosorption surface play an essential role in adsorbing potentially toxic metals through ion exchange mechanisms (**Figures S3b–c**) (Wan Ngah and Hanafiah, 2008).

Figure 2 and **Table S2** demonstrate that carbon and oxygen are the primary elements of leaf composites. The leaf-generated biosorbent exhibits high oxygen content (31.4–64.1%), suggesting

that the biosorbent has many oxygen-containing functional groups on its surface (i.e., carboxylic and phenolic groups). Furthermore, the leaf-produced biosorbent has higher atomic oxygen/carbon (0.4–1.81) and hydrogen/carbon (1.2–2.8) ratios because of the presence of organic plant residues (i.e., main hemicellulose, cellulose, and lignin).

The proximate analysis (**Figure 2** and **Table S2**) shows that leaf-derived biosorbent (average ± SD) has low moisture (5.9±2.7%), total ash (11.5±6.8%; water-soluble substances), and fixed carbon (20.3±20.3%) contents but a high volatile content (60.4±20.6%). A low moisture contents is because the biosorbent has been dried during the preparation process (see **Section 2.1**). In contrast, high volatility is evident because cellulose, hemicellulose, and lignin are present in large amounts. Moreover, the average pH value and density of the leaf-based absorbent are 6.12±0.87 ($n = 16$) and 0.33±0.17 g/cm^3 ($n = 9$), respectively (**Table S4**). Accordioning to **Figure 2**, it can be concluded that proximate analysis and ultimate analysis possess the high bias. Moreover, surface chemistry becomes the important factors to determine the adsorption capacities of contaminants.
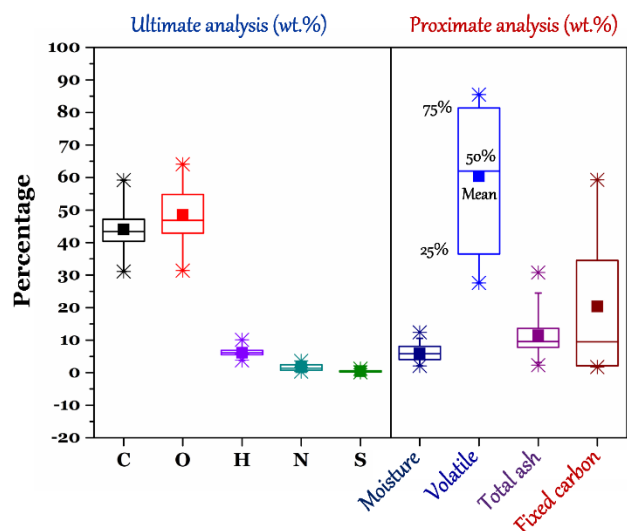

Figure 2. Ultimate and proximate analyses (wt.%) of leaf-based biosorbents (Data taken from Tables S2–S3)

2.4. Surface chemistry

The presence of the main functional groups on the external surface of the biosorbent can be

qualitatively evaluated by Fourier transform infrared spectroscopy (FTIR) or X-ray photoelectron spectroscopy (XPS). As mentioned above, leaves are considered to be lignocellulosic biomass-rich material (**Table 1**). Consequently, they exhibit surface functional properties that resemble that of other waste substances (i.e., coconut shell, pistachio nut shell, and orange peel). A typical FTIR spectrum of a leaf-based biosorbent is shown in **Figure S4a** and the spectroscopic assignment of the functional groups is provided in **Figure S4b**. Similarly, the surface chemistry properties of leaf-based biosorbent can be analyzed by XPS (**Figures S4c–d**). The leaf-derived biosorbent exhibits abundant oxygen functional groups on its surface, similar to other biosorbents (i.e., orange peel, golden shower pod, coconut shell) (Tran et al., 2017c).

Unlike the FTIR and XPS techniques, conductometric (Boehm) or potentiometric titration can be used to obtain quantitative information on the oxygen-containing functionality (acid and basic groups) of the biosorbent surface. The standardization of the Boehm titration has been investigated by Goertzen et al. (2010). Several researchers found that the results obtained by the two methods differ insignificantly (Fourest and Volesky, 1995; Komy et al., 2006). Although acidic groups (i.e., carboxylic and phenolic) attached to the biosorbent surface have been acknowledged as active groups when adsorbing various contaminants in solution onto biosorbent, quantitative information on such functionality is scarce in the literature. **Table S5** shows pristine biosorbent derived from leaves exhibits a concentration of total acid groups (1.5–6.2 mmol/g) similar to that from agricultural waste-derived biosorbents (e.g., 8.7 mmol/g for golden shower pod, 6.9 mmol/g for orange peel, and 4.21 mmol/g for coconut shell) (Tran et al., 2017c). The relatively higher acid groups facilitate the adsorption of cationic contaminants.

The surface electrostatic state of any adsorbent in aqueous phase is typically characterized by the point of zero charge (PZC) or the isoelectric point (IEP). The difference between them has been discussed by many scholars and summarized in the recent review work (Tran et al., 2017b). **Figure S5** shows the point of zero charge of leaf-based biomaterials. The pH_{PZC} is defined as the pH value at which the net surface charge density (external and internal) of the adsorbent equals zero (**Figures**

S5a–b). In contrast, the pH value at which the electrokinetic (ζ) potential at the shear plane equals zero is defined as pH_{IEP} (**Figures S5c–d**). The surface charge of adsorbent is negative when the solution pH approximates 7.0. The result favors cationic ion adsorption in solution. **Table S6** summarizes the pH_{PZC} and pH_{IEP} of leaf-based biosorbents, and **Table S7** lists the ζ potential of several biosorbents at a given $pH_{solution}$. Essentially, any adsorbent often is amphoteric. Almost all pH_{PZC} values of the observed biosorbents are lower than 7.0, suggesting that the total amount of acidic groups on the biosorbent surface will dominate.

2.5. Crystal structure and thermal stability

The crystallinities of leaf biomass can be determined by X-ray diffraction (XRD). As represented in **Figure S6**, two reflections at approximately 15° and 22° are characteristic for crystalline cellulose material (Khan Rao and Khatoon, 2017; Wang et al., 2016). Cellulose in the leaf biomass has a parallel alignment and crystalline structure, which is the consequence of hydrogen bonds and van der Waals interactions between adjacent molecules, while lignin and hemicellulose are amorphous (Percival and Lynd, 2004; Tran et al., 2018).

The thermal stability of the adsorbent was evaluated by thermogravimetric analysis (TGA). **Figure S7b** shows thermal decomposition peaks at approximately 330 °C and 450 °C that can be assigned to the thermal degradation of cellulose and lignin, which is in good agreement with observations of some researchers (Tran et al., 2017c; Tongpoothorn et al., 2011; Lafi et al., 2015). Notably, lignin component is more difficult to decompose because it contains the full of aromatic rings with various branches. Therefore, the degradation of lignin often occurs within a wide temperature range (between 160 °C and 900 °C) (Yang et al., 2007). The endpoint temperature of the leaf-based biosorbent is approximately 500 °C (**Figure S7**), suggesting that complete carbonization of the biosorbent requires a minimum temperature of 500 °C.

3. Batch experiment

3.1. Effect of the solution pH

The pH of a certain solution is the most important parameter in adsorption analysis because it has a strong effect on the charge of the adsorbent surface (**Figure S5**) and speciation of the adsorbate (**Figure S8**). **Figure 3** shows that the biosorption process strongly depends on the solution pH value. Generally, the adsorption capacity of the biosorbent with respect to cationic adsorbates usually increases when the $pH_{solution}$ value increases. The surface charge of the biosorbent becomes more negative when the $pH_{solution}$ value increases (**Figure S5**). Therefore, the electrostatic attraction between the negatively charged surface of the biosorbent and adsorbate cations in solution is also simulated. Another possible reason is a decrease in the adsorption competition between adsorbates (i.e., Cd^{2+}) and H^+ ions for active adsorption sites (i.e., $—COO^-$) on the surface of the biosorbent. This can be confirmed by the experimental conditions of the adsorption isotherm (**Tables S8–S9**).
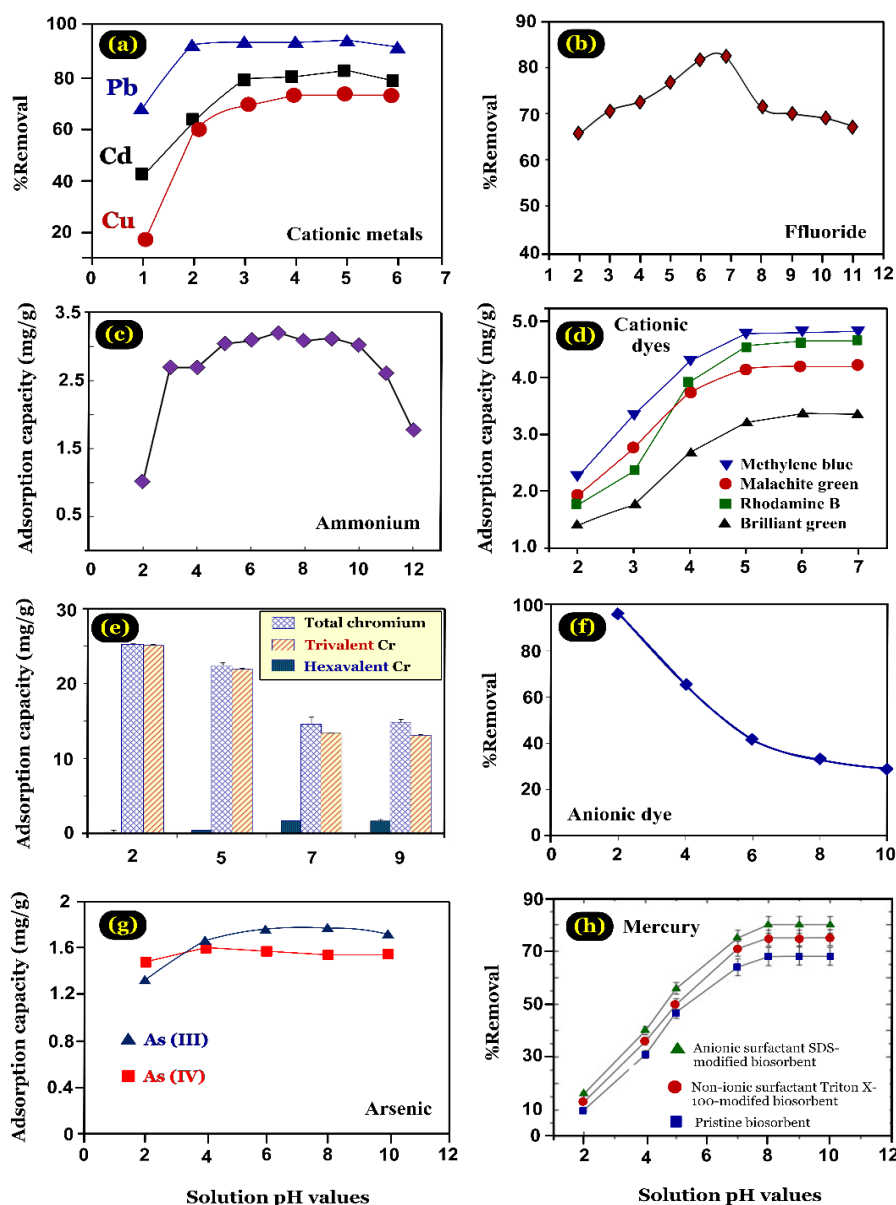
Figure 3. Effect of the pH solution on the adsorption process on (a) potentially toxic metal cations onto *Fraxinus excelsior* tree leaf-biosorbent (Sangi et al., 2008) [License number: 4435910682650], (b) fluoride onto *Azadirachta indica* tree leaf-biosorbent (Bharali and Bhattacharyya, 2015; Sangi et al., 2008) [License number: 4440010650238], (c) ammonium onto *Parthenocissus tricuspidata* tree leaf-biosorbent (Liu et al., 2010b) [License number: 4435910810287], (d) cationic dyes onto *Saraca asoca* tree leaf-biosorbent (Gupta et al., 2012) [License number: 4435910987708], (e) hexavalent chromium onto *Melaleuca diosmifolia* tree leaf-biosorbent (Kuppusamy et al., 2016) [License number: 4435911095229], (f) acid violet 17 dye onto activated *Ficus racemosa* tree leaf-adsorbent (Jain and Gogate, 2017b), [License number: 4435911196015] (g) arsenic onto *Psidium guajava* leaf tree leaf-biosorbent (Kamsonlian et al., 2012) [License number: 4435940299690], and (h) mercury onto pristine and modified bamboo leaf tree leaf-biosorbents (Mondal et al., 2013) [License number: 4435920032442]

In contrast, the biosorbent adequately adsorbs adsorbate anions such as chromate or dichromate at a low $pH_{solution}$ value (**Figure 3**) because the biosorbent exhibits a positively charged surface at a low $pH_{solution}$ value, which results in the protonation of hydroxyl groups (i.e., —$COOH_2^+$ or —OH_2^+). The biosorbent has a high affinity to contaminant anions in the solution during electrostatic attraction. This hypothesis is consistent with the literature. Some authors emphasized that the adsorption of hexavalent chromium onto leaf-based biosorbents reaches the optimal adsorption efficiency at a $pH_{solution}$ of 2.0 (Ahmad et al., 2017; Babu and Gupta, 2008; Nag et al., 2016; Nakkeeran et al., 2016; Rangabhashiyam et al., 2015; Saha and Saha, 2014; Wenfang et al., 2015). A similar optimal $pH_{solution}$ was found for the adsorption of acid violet 17 dye onto activated cluster fig tree leaves (Jain and Gogate, 2017b), acid blue 25 dye onto NaOH-treated cluster fig leaves (Jain and Gogate, 2017c) and neem leaves (Sarma et al., 2011), acid orange 52 onto princess-tree leaves (Deniz and Saygideger, 2010), acid green 25 onto NaOH-treated almond leaves (Jain and Gogate, 2018), two anionic dyes (Sumfixe Supra red and Alpacelle Lumiere brown) onto maguey leaves (Hamissa et al., 2007), Eosin dye (a fluorescent red dye) onto Eucalyptus tree leaves (Rostami and Niazi, 2013), Rhodamine B onto neem leaves (Sarma et al., 2008), methyl orange onto pristine and modified pineapple leaves (Kamaru et al., 2016), and Pd(II) and Pt(IV) onto tropical almond leaves (Ramakul et al., 2012).

However, other investigators emphasized the negligible effect of the $pH_{solution}$ on the adsorption efficiency at a given $pH_{solution}$. Namely, Zaidi et al. (2018) recognized that the adsorption of cationic methyl violet 2B dye onto pristine and NaOH-treated terap leaves is insignificantly depends on the $pH_{solution}$, between pH 3.0 and 10. Similar observations were made for the adsorption of hexavalent chromium onto NaOH-treated false ashoka leaves (Anwar et al., 2011); As(III) and As(V) onto guava leaves (Kamsonlian et al., 2012); cationic methyl violet 2B dye onto pristine and treated terap leaves (Lim et al., 2016); malachite green dye onto *Glossogyne tenuifolia* leaves (Yang and Hong, 2018); and methylene blue onto citric acid-treated lawn grass (Chen et al., 2011), activated carbon prepared from Neptune grass (Dural et al., 2011), and pineapple leaves (Kamaru et al., 2016).

3.2. Effect of the ionic strength

Similar to the solution pH, the adsorption capacity of biosorbents is adversely affected by the addition of a salt (**Table S10**) such as $NaNO_3$, $NaClO_4$, $CaCl_2$, $NaCl$, Na_2SO_4, KNO_3, $(NH_4)_2SO_4$, $NaHCO_3$, and $Ca(NO_3)_2$. Among these, NaCl is the most common salt used for the investigation of the effect of the ionic strength on biosorption. Generally, the presence of salt causes a profound decline in the removal efficiency of both anionic and cationic contaminants from aqueous solutions. **Figure S9** shows a typical example of the impact of the ionic strength on the biosorption of various potentially toxic metals onto *Ulmus carpinifolia* leaves (Sangi et al., 2008). Many scholars also documented a similar decrease in the adsorption capacity of leaf-based biosorbents towards potentially toxic metals, which is caused by the presence of inorganic salts (Al-Haidary et al., 2011; Ngah and Hanafiah, 2008; Rao et al., 2011a;2010b; Srinivasa Rao et al., 2010; Weng and Wu, 2012; Zhang et al., 2015). However, the ion strength is difficultly controlled in the realistic wastewater treatment. The ion strength is only regarded as a reference.

Furthermore, the adsorption process of cationic and anionic dyes is also examined due to the presence of a specific salt. In fact, many researchers concluded that the addition of salt results in a significant decrease of the adsorption efficiency of leaf-based biosorbents toward methylene green (Han et al., 2014; Kushwaha et al., 2014), malachite green (Han et al., 2014), methylene blue (Ansari et al., 2016; Han et al., 2007; Han et al., 2011; Kushwaha et al., 2014; Yagub et al., 2012), basic red 46 (Wahab et al., 2012), acid blue 113 (Jain and Gogate, 2017a), and toluidine blue and crystal violet (Lafi et al., 2015).

The deceased adsorption ability of adsorbent due to an increase in the inorganic salt concentration is possibly attributed to a screening effect (known as electrostatic screening) between the positively charged biosorbent surface and cationic pollutants. When the adsorbent is added to the adsorbate solution, the latter will be surrounded by an electrical double layer (EDL; **Section S2**). Nevertheless, the EDL can be significantly expanded by the presence of a certain electrolyte agent

(Krishnan and Anirudhan, 2003; Ngah and Hanafiah, 2008; Wang et al., 2007; Weng et al., 2009). This expansion prevents adsorbent particles and adsorbate ions from being very close to each other, which causes a remarkable electrostatic attraction. As a consequence, the adsorption capacity of the adsorbent to adsorbate will decrease. For example, Weng et al. (2009) pointed out that an increase in the $NaNO_3$ concentration causes a remarkable decrease in the EDL thickness (**Figure S10**) and an increase in the amount of indifferent ions approaching the surface of the biosorbent. This outcome demonstrates the increasing competition between cationic methylene blue dye molecules and Na^+ ions for available adsorbing sites on the biosorbent surface when the salt concentration increases.

However, some authors suggested that the biosorption phenomenon is insignificantly impacted by the addition of salt (Chen et al., 2010; Lim et al., 2016). For example, Chen et al. (2010) used camphor leaves to remove Cu(II) from aqueous media. They concluded that the adsorption efficiency of leaves only slightly decreases (by 7%) in the presence of external electrolytes, even at high salt concentrations up to 0.5M NaCl.

3.3. Adsorption kinetics

Generally, the effect of contact time plays an important role in determining the (1) true equilibrium, (2) adsorption rate, and (3) activation energy of the adsorption process. The equilibrium time and adsorption rate strongly depend on the biosorbent properties, adsorbate nature, and especially in the operation conditions—the initial adsorbate concentration, solution temperature, solution pH, particle size of biosorbent, coexisting ions, ionic strength, and shaking speed.

Unlike porous adsorbents (i.e., spherical and non-spherical activated carbon and biochar, zeolite, and macroreticular resin), the adsorption of contaminants onto nonporous biosorbents often takes less time to reach true equilibrium because the adsorption phenomenon mainly occurs on the biosorbent surface. For example, King et al. (2007; 2008) reported that the biosorption of Pb^{2+} and Zn^{2+} ions on jambolan leaves reaches an equilibrium within 10 min of contact, which agrees with the conclusions of other scholars (**Tables S9–S10**). Moreover, Amarasinghe and Williams (2007)

18

compared the adsorption rate of potentially toxic metals onto tea leave waste and granular activated carbon. They concluded that the rate constant (k_2; g/mg × min) of the pseudo-second-order equation of tea leaves (0.0091 and 0.0133) to Pb(II) and Cu(II) is significantly higher than that of granular AC (0.0064 and 0.0020, respectively). This means that, under the same operation conditions, the metal ion removal by leaf-based biosorbents occurs faster than that by AC.

When the adsorption process reaches a real equilibrium, specific adsorption kinetic models can possibly be applied to determine relative adsorption parameters. Common models that are extensively used in adsorption studies are the pseudo-first-order, pseudo-second-order, Elovich, and intraparticle diffusion equations. The true derivation and accurate application of such models in the field of adsorption science and technology have been discussed by Tran et al. (2017b). Generally, most studies revealed that the pseudo-second-order model (Equation 9) can adequately describe all experimental kinetics data in an adsorption batch experiment. In this case, the adsorption rate constant (k_2; g/mg × min) is useful to describe the adsorption process. A higher k_2 value corresponds to an adsorption process that reaches saturation faster. The effects of typical operation conditions on the adsorption rate constant are presented in **Figure 4**; the values in parentheses represent the amount of adsorbate adsorbed onto biosorbents in equilibrium (q_e; mg/g), which was calculated using the pseudo-second-order equation (**Section S3).** As showed in **Figure 4**, the adsorption rate constants are proportional to solid/liquid ratio and stirring speed, and inversely proportional to initial adsorbate concentration, ionic strength, and adsorbent's particle size. Especially in temperature, whether or not the adsorption rate constant increases with the increasing temperature. The adsorption mechanism is an important factor to determine it.
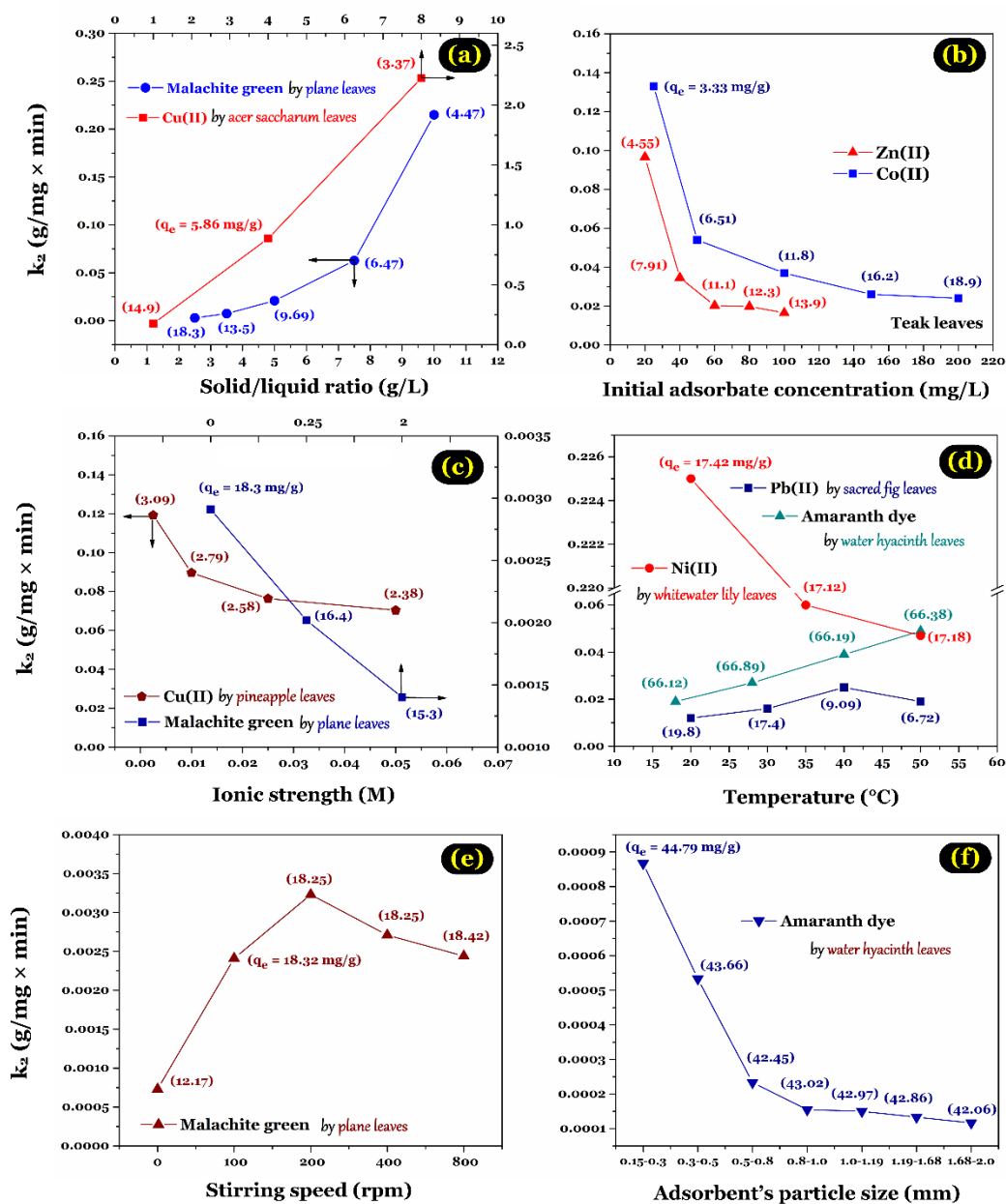
Figure 4. Effect of typical operation conditions on the rate constant (k_2) of the pseudo-second-order equation, such as (a) solid/liquid ratio [(Hamdaoui et al., 2008) for malachite green adsorption and (Amirnia et al., 2016) for Cu(II) adsorption]; (b) initial adsorbate metal concentration [(Kumar et al., 2006) for Zn(II) adsorption and (Vilvanathan and Shanthakumar, 2016) for Co(II) adsorption]; (c) ionic strength [(Weng and Wu, 2012) for Cu(II) adsorption and (Hamdaoui et al., 2008) for malachite green adsorption]; (d) temperature [(Zahedi et al., 2015) for Ni(II) adsorption, (Qaiser et al., 2009) for Pb(II) adsorption, and (Guerrero-Coronilla et al., 2015) for amaranth dye adsorption]; (e) shaking speed (Hamdaoui et al., 2008); and (f) adsorbent particle size (Guerrero-Coronilla et al., 2015)

In most cases, the k_2 constant is applied to determine the activation energy (Ea). The Ea of the adsorption process (in kJ/mol) is defined as the minimum energy that must be overcome by the adsorbate molecules and can be computed through the Arrhenius equation (**Section S3**). For example, Weng and Wu (2012) applied pineapple leaf powder to absorb Cu(II) ions in a water solution. They reported a magnitude of Ea of the biosorption of 7.0 kJ/mol (**Figure S11**), which is similar to the E_a value (5.2 kJ/mol) of Cu(II) biosorption onto peanut hull (Ali et al., 2016). The low E_a magnitude (typically <40 kJ/mol) suggests that the biosorption process was primarily physical adsorption. Conversely, Lin et al. (2011) examined the removal behavior of Cu^{2+} ions by humic acid-immobilized surfactant-modified zeolite, concluding that the adsorption process was chemisorption (E_a = 63.1 kJ/mol). In addition, Boparai et al. (2011) claimed that the E_a value of chemisorption of Cd(II) cations onto nano-zero-valent iron particles is approximately 55 kJ/mol.

Some activation energy highlights are of concern here. Firstly, the value of the activation energy is strongly dependent on the operation conditions, especially the initial adsorbate concentration (C_o; mg/L). For example, Ren et al. (2015) investigated crystal violet dye biosorption from aqueous solution using the leaves of the phoenix tree at three solution temperatures (20, 30, and 40 °C). They discovered that the E_a value of the biosorption process is 25.3 kJ/mol at 100 mg/L, 45.8 kJ/mol at 300 mg/L, and 37.7 kJ/mol at 400 mg/L. Similarly, Guerrero-Coronilla et al. (2015) highlighted that the E_a value of the biosorption process of amaranth dye onto water hyacinth leaves at different solution temperatures (18, 28, 40, and 50 °C) increases if the C_o value increases. They reported that the E_a values increases in the following order: 19.8 kJ/mol at C_o of 50 mg/L < 23.5 kJ/mol at 100 mg/L < 34.8 kJ/mol at 200 mg/L.

Secondly, the activation energy strongly depends on the derivation of the rate constant. For example, Agarry et al. (2013) applied the rate constants of the pseudo-first-order (k_1) and pseudo-second-order (k_2) equations to calculate the activation energy of naphthalene adsorption onto spent tea. An E_a value of 15.9 kJ/mol and 28.9 kJ/mol was obtained when applying the k_1 and k_2 constants, respectively. Furthermore, in some cases, an accurate activation energy was not obtained because of

the low R^2 value of the Arrhenius equation such as $R^2 = 0.1671$ (k_1 value) and $R^2 = 0.5671$ (k_2 value) (Wahab et al., 2012).

Table 2 indicates the estimated E_a values in the literature. A calculation mistake has been found in previous publications (Chakraborty et al., 2012; Chowdhury et al., 2011). According to the reported k_2 values, the correct E_a values of the biosorption process of basic green 4 and crystal violet onto pineapple leaves should be –58.9 kJ/mol and –46.1 kJ/mol, while the E_a values reported in the original papers are 58.9 and 45.8, respectively. Thirdly and lastly, because the rate constant is important for the accurate calculation of E_a, the adsorption rate constant at different solution temperatures should be reported in adsorption kinetic studies. Unfortunately, some authors ignored the presentation of the rate constant and readers therefore cannot verify the accuracy of the E_a values (see **Table 2**).

Table 2. Activation energy (Ea; kJ/mol) of the biosorption process

Leaves	Adsor-bate	Ea	Remark	Ref.
Bael	Pb(II)	22.2*	Corrected	Chakravarty et al., 2010
Treated Australian pine	Pb(II)	6.38	Re-calculated	Khan Rao and Khatoon, 2017
Pineapple	Cu(II)	6.99*	Corrected	Weng and Wu, 2012
NaOH-treated tea	Cu(II)	4.12*	Corrected	Weng et al., 2014
Treated Australian pine	Cu(II)	12.53	Re-calculated	Khan Rao and Khatoon, 2017
Treated Australian pine	Ni(II)	11.98	Re-calculated	Khan Rao and Khatoon, 2017
Black tea	Cr(VI)	16.2	Corrected	Hossain et al., 2005
London plane	MB	14.26*	Re-calculated (11.67)	Kong et al., 2015
Pine	MB	3.081	Re-calculated	Yagub et al., 2012b

Oriental plane	MG	7.13*	Corrected	Hamdaoui et al., 2008
Treated maize husk	MG	21.5*	Unreported k_2	Jalil et al., 2012
Pineapple	BG4	45.79*	Re-calculated (-46.1)	Chowdhury et al., 2011
Princess-tree	AO52	9.64*	Corrected	Deniz and Saygidege,r 2010
Pineapple	CV	58.9*	Re-calculated (-59.06)	Chakraborty et al., 2012
Jackfruit	CV	-45.99	Re-calculated	Saha et al., 2012
Phoenix	CV	25.3–45.8	Re-calculated	Ren et al., 2015
Pine	BR46	38.39*	Unreported k_2	Deniz and Karaman, 2011
Water hyacinth	AR27	19.8–34.8*	Corrected	Guerrero-Coronilla et al., 2015
Treated cluster fig	AV17	7.07	Unreported k_2	Jain and Gogate 2017b
Treated almond	AG25	6.22	Corrected	Jain and Gogate, 2018
Spent tea	$C_{10}H_8$	15.89	Re-calculated (28.9)	Agarry et al., 2013
Treated almond	AB113	6.54*	Unreported k_2	Jain and Gogate, 2017a

Note: The E_a values were calculated from the Arrhenius equation at different k_2 constant rates of the pseudo-second-order equation. *the data were reported in the original data. "Re-calculated" means that the E_a value was re-calculated from the k_2 value of the original paper; "Corrected" means that the E_a values re-calculated and reported are the same; "Unreported k_2 means that the k_2 valuwas not reported in the original paper. Adsorbate: MB (methylene blue), CV (crystal violet), MG (malachite green), AO52 (acid orange 52), BG4 (basic green 4), BR46 (basic red 46), AB113 (acid blue 113), AR27 (acid red 27), AG25 (acid green 25), AV17 (acid violet 17), and $C_{10}H_8$ (naphthalene).

3.4. Adsorption isotherm

In batch adsorption studies, the adsorption isotherm (**Figure 5**) plays a key role in recognizing the regions (e.g., Henry, Freundlich, Langmuir, and BET) containing the actual experimental data corresponding to the adsorption equilibrium. In particular, two methods used to obtain an adsorption isotherm have been reported in the literature. Firstly, the adsorption isotherm (**Figure 5a**) is most commonly determined at different initial adsorbate concentrations under fixed experimental conditions (i.e., temperature, solution pH, solid/liquid ratio, ionic strength, adsorbent particle size, and contact time) (Kılıç et al., 2009). Secondly, the adsorption isotherm (**Figure 5b**) can be examined at different solid/liquid ratios under constant experimental conditions including the temperature, solution pH, initial adsorbate concentration, ionic strength, adsorbent particle size, and reaction time (Chen et al., 2010).
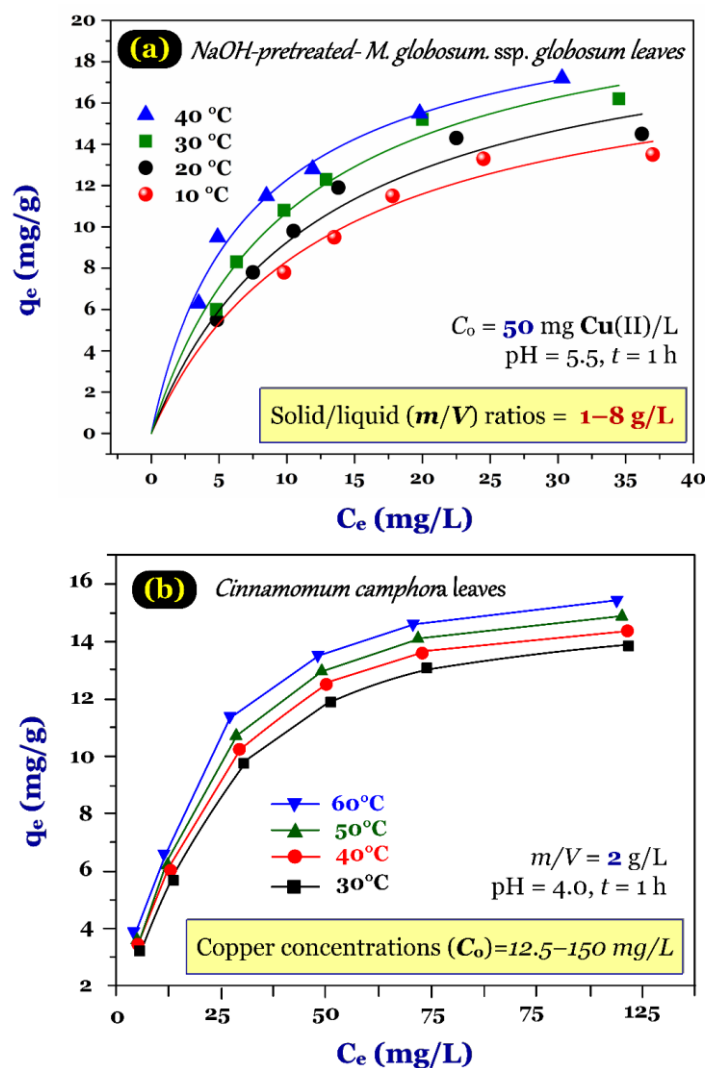
Figure 5. Typical adsorption isotherm determined by two different methods, that is by changing (a) solid/liquid ratio (Kılıç et al., 2009) [License number: 501431317], and (b) initial adsorbate concentrations (Chen et al., 2010) [License number: 4435921407628]

Several adsorption isothermal models have been used in the scientific literature such as the Langmuir, Freundlich, Dubinin–Radushkevich, and Redlich–Peterson models. Among these, the Langmuir model **(Section S4)** is the most commonly used one because the maximum adsorption capacity of a certain adsorbent can be calculated under given experimental conditions. When the adsorption process reaches a true equilibrium under optimal conditions, the Q^o_{max} parameter is helpful to (1) compare the adsorption efficiency among adsorbents and (2) design the adsorption study in a fixed-bed column. **Tables S8–S9** summarize the Langmuir maximum adsorption capacities (Q^o_{max}) of various pristine and treated biosorbents derived from leaves from previous literature. Based on the data in **Tables S8–S9**, basic statistical analyses were performed, and the results are listed in **Figure 6**. **Figure 6** indicates Q^o_{max} of modified/treated leaves are quite higher those of pristine leaves. Furthermore, the of modified/treated leaves also exhibit the relatively higher bias in the estimated Q^o_{max} values.
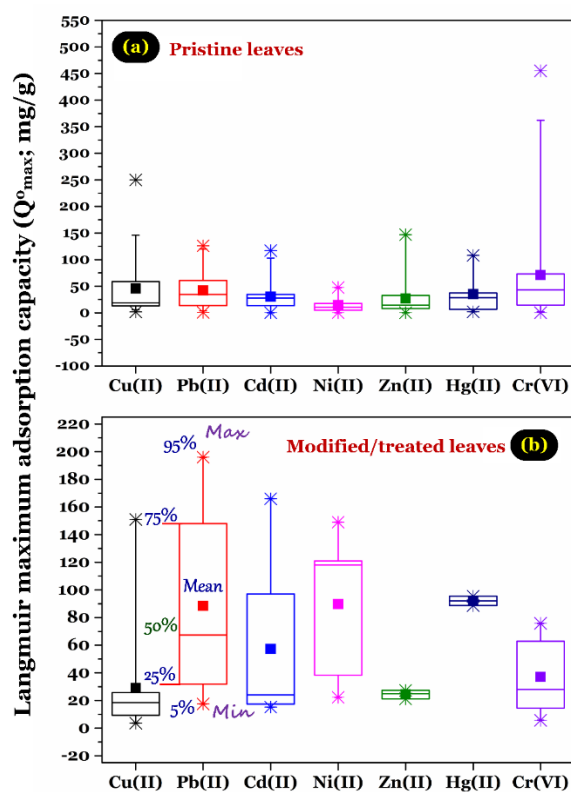
Figure 6. The Langmuir maximum adsorption capacity (Q^o_{max}, mg/g) of leaf-based biosorbent (batch experiment) to some typical toxic metal ions (Data were analyzed based on summarizing data reported in the literature; see Tables S8–S9)

Notably, although the Q^o_{max} value plays an important role in adsorption studies, the maximum adsorption capacity of an adsorbent to a certain adsorbate strongly depends on the properties of the adsorbent (mainly its particle size) and operation conditions. The Q^o_{max} value is often inversely proportional to the particle size of the adsorbent. For example, Hanafiah and Ngah (2009) reported that the Q^o_{max} value of protonated rubber leaf biosorbent deceases in the following order when its particle size increases from less than 180 μm to 180–355 μm and to 355–500 μm: 8.4 mg/g > 6.9 mg/g > 5.8 mg/g. An analogous conclusion was drawn by Ngo et al. (2014).

In addition, the effects of the operation conditions on the Q^o_{max} value often comprise the solid/liquid ratio, solution pH, and temperature. First, Bhattacharyya et al. (2009) applied neem leaves to remove Ni(II) from an aqueous medium. They reported that the Q^o_{max} values (mg/g) decrease when the solid/liquid ratios (g/L) increase, as follows: 9.1 mg/g (at 0.5 g/L) > 6.3 mg/g (1.0 g/L) > 5.0 mg/g

(1.5 g/L) > 4.2 (2.0 g/L) > 3.0 mg/L (3.0 g/L) > 2.4 mg/g (4.0 g/L). Similar reports were found in the literature (Baruah et al., 2017; Bhattacharyya and Sarma, 2003; Bhattacharyya et al., 2010; Bhattacharyya and Sharma, 2004; Gowda et al., 2012; Sharma and Bhattacharyya, 2005). However, there is a potential problem regarding true equilibrium adsorption, which should be carefully considered. For example, Baruah et al. (2017) applied bael leaves to remove methylene blue dye from synthetic water. They determined the adsorption isotherm at very low initial dye concentrations (from 10 mg/L to 50 mg/L). The Q^o_{max} values (mg/L) at different solid/liquid ratios (g/L) were 500 mg/L (at 0.2 g/L), 167 mg/L (0.4 g/L), 100 mg/L (0.6 g/L), 91 mg/L (0.8 g/L), and 52 mg/L (1.0 g/L). Unfortunately, they did not include the adsorption isotherm in the published paper. A similar problem has been found in reference (Bhattacharyya and Sharma, 2004), with the Q^o_{max} value for Pb(II) biosorption onto neem leaves at a C_o range (50–150 mg/L) being 833 mg/g (at a solid/liquid ratio = 0.2 g/L), 270 mg/g (0.4 g/L), 196 mg/g (0.6 g/L), 119 mg/g (0.9 g/L), and 82 mg/L (1.2 g/L). Therefore, the critical question is whether the adsorption process can reach a true equilibrium at low initial adsorbate concentrations (i.e., 10–50 mg/L) and high solid/liquid ratio (i.e., 1.0 g/L). If the adsorption process cannot reach a true equilibrium in the adsorption isotherm, the calculated Q^o_{max} values are invalid. This mistake has been discussed by many scholars (Hai, 2017; Kumar, 2006; Tran et al., 2017b; Vasanth Kumar and Sivanesan, 2006).

Second, Sharma and Forster (1994) reported the Q^o_{max} values of leaf mould with respect to chromium adsorption at different initial $pH_{solution}$ values (1.5, 2.0, 2.5, 3.0, 4.0, 6.0, and 10), that is, 27.6, 43.1, 23.4, 8.9, 7.1, 3.9, and 2.5 mg/g, respectively. In another study, it was also reported that the Q^o_{max} value greatly depends on the initial $pH_{solution}$ (Chen et al., 2009). Third, some studies demonstrated that the Q^o_{max} values increase when the temperatures increase, while others indicated the opposite trend. For example, Yuvaraja et al. (2014) hightlighted that the Q^o_{max} values of *Solanum melongena* leaf biosorbent toward Pb(II) decrease in the following order: 71.4 mg/g (at 50 °C) > 62.5 mg/g (40 °C) > 55.6 mg/g (30 °C). In constrast, Kılıç et al. (2009) reported that the Q^o_{max} values of

NaOH-pretreated *Marrubium globosum ssp. globosum* leaves to copper ions decrease in the following order: 21.1 mg/g (at 20 °C) > 20.3 mg/g (30 °C) > 19.7 mg/g (40 °C) > 18.5 mg/g (45 °C).

3.5. Adsorption thermodynamics

The study of adsorption thermodynamics is an indispensable part for the estimation of the adsorption mechanism (i.e., physical or chemical). Taking the adsorption of heavy metals as a typical example, physical adsorption involves relatively weak interactions (i.e., van der Waals force), while chemical adsorption is generated from stronger chemical interactions (i.e., coordination) with associated transfer of electrons between the adsorbent and adsorbate.

The thermodynamic parameters of a reaction, including the changes in Gibbs energy (ΔG), entropy (ΔS), and enthalpy (ΔH), can be obtained from calorimetric measurements (Ferreira et al., 2017) or based on the van't Hoff approach (Tran et al., 2017b). However, we found that the van't Hoff approach was used in almost all publications relevant for this work (**Section S5**). **Tables S11–S15** compile the thermodynamic parameters for the biosorption process of various contaminants onto pristine and treated biosorbents derived from leaves. The signs and magnitudes of the parameters strongly depend on the properties of both the biosorbent and adsorbate. In addition, the effects of temperature on the amount of adsorbate adsorbed on the biosorbent are reflected by the sign of the enthalpy change. The biosorption capacity of the biosorbent is enhanced when the temperature rises, suggesting that the biosorption is an endothermic process ($\Delta H > 0$). On the other hand, the negative ΔH reflects the exothermic nature of the biosorption process, which is demonstrated by a decreased biosorption capacity at higher temperatures. For example, NaOH-treated dead leaves of *Ficus racemose* were applied to remove anionic dyes from synthetic water. Based on the results, the ΔH value of the adsorption of acid green 25 is +7.0 kJ/mol (Jain and Gogate, 2018), that of acid blue 25 is +29.9 kJ/mol (Jain and Gogate, 2017c), and that of acid blue 113 is −31.3 kJ/mol (Jain and Gogate, 2017a). This means that the adsorption process of acid green 25 and acid blue 25 is endothermic, but that of acid blue 113 is exothermic. These results were very consistent with the equilibrium study (i.e., the

adsorption isotherms at different temperatures and the Langmuir maximum adsorption capacity; Q^o_{max}). The Q^o_{max} value for acid green 25 adsorption increases in the following order: 44.3 mg/g (at 20 °C) < 46.6 mg/g (30 °C) < 48.9 mg/g (40 °C) < 50.8 C (50 °C); thus, ΔH is positive. In contrast, the Q^o_{max} value for acid blue 113 adsorption decreases in the following order: 97.1 mg/g (at 20 °C) > 93.5 mg/g (at 30 °C) > 90.1 mg/g 40 °C) > 87.0 mg/g (50 °C); thus, ΔH is negative. Based on **Tables S11–S15**, it can be concluded that most biosorbent processes are endothermic in nature (accounting for approximately 70% of the processes, $n = 65/93$).

Generally, the removal process of contaminants from aqueous solutions (adsorption onto the biosorbent) occurs spontaneously or naturally (accounting for approximately 90%, $n = 84/93$), which is supported by the negative ΔG values (**Tables S11–S15**). Furthermore, the sign of the entropy change reflects whether the organization of the adsorbate at the solid/solution interface during the biosorption becomes less random ($\Delta S < 0$). As shown in **Tables S11–S15**, raw and modified biosorbents exhibit a positive ΔS value in most cases (~71%, $n = 66/93$), suggesting that the organization of the adsorbate ions at the solid/solution interface becomes more random during the biosorption process.

Figure 7 illustrates the relationship between ΔH and ΔS for the adsorption of heavy metal ions and organic dyes on the biosorbents. However, the results indicated that the enthalpy–entropy compensation (plot of ΔH versus ΔS) shows a relative strong linear relationship (exclusion of some unlogic points). This phenomenon seems strange and is difficult to explain because the results are based on different studies with different experimental conditions. One possible explanation is that both ΔH and ΔS are calculated using the same equation.

Other significant concerns are that the sign and magnitude of ΔS and ΔH demonstrate a confused representation because the thermodynamic parameters given in **Tables S11–S15** were calculated based on the equilibrium constant K_c, which is assumed from different alternatives (i.e., K_L, K_p^o, and K_d) and units (i.e., L/mol, L/mg, L/g, and dimensionless). Moreover, the operating conditions of biosorption

experiments are dissimilar. For example, Shah et al. (2015) applied the distribution coefficient ($K_d = q_e/C_e$; L/g) at an initial Ni(II) concentration of 5 mg/L, but Kushwaha et al. (2014) applied the distribution coefficient [$K_d = (q_e/C_e) \times (m/V)$; dimensionless] at an initial dye concentration of 10 mg/L to compute the thermodynamic parameters. Meanwhile, Jalil et al. (2012) calculated the thermodynamic parameters from the partition coefficient ($K_p = C_s/C_e$; dimensionless) at an initial dye concentration of 200 mg/L and different temperatures (313–363 K). In contrast, Yuvaraja et al. (2014) applied the Langmuir constant (K_L; L/mg) at different initial Pb(II) concentrations (30–90 mg/L), and Jain and Gogate (2018) applied the Langmuir constant (K_L; dimensionless) at different initial dye concentrations (50–300 mg/L) to calculate the thermodynamic parameters.
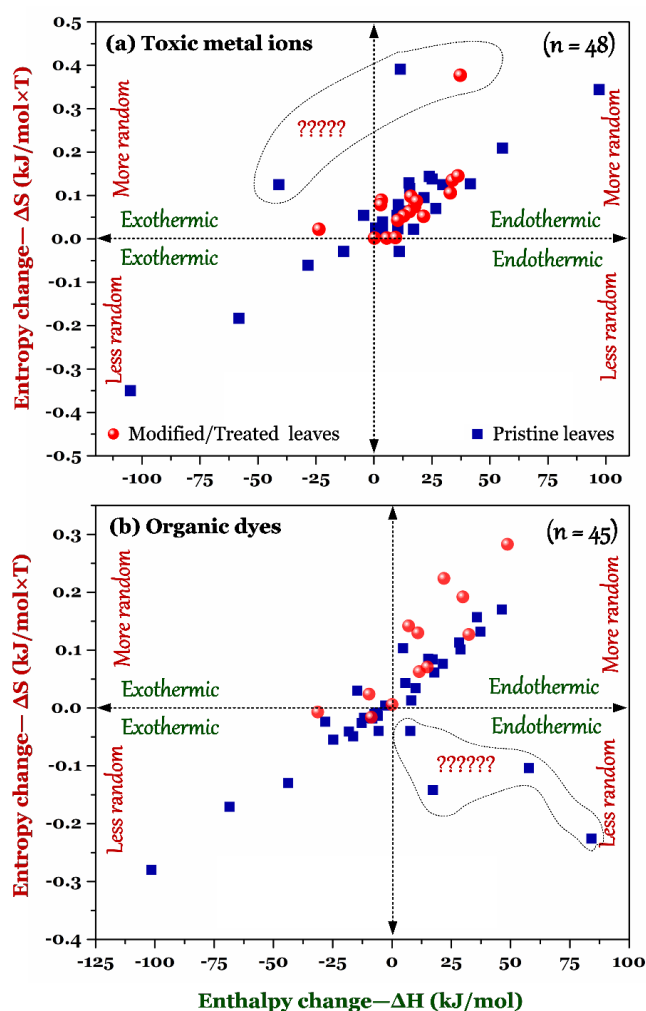
Figure 7. Enthalpy–entropy compensation plot for the biosorption of (a) potential toxic metals and (b) organic dyes onto the raw and modified biosorbents derived from leaves (data collected from Tables S11–S15)

It is accepted that the following two steps consecutively occur during adsorption in aqueous solution: (1) release of pre-adsorbed water molecules from adsorption sites ($\Delta H_1 > 0$, $\Delta S_1 > 0$) and (2) adsorption of the adsorbate on the solid surface in a more ordered manner than that in bulk liquid phase ($\Delta H_2 < 0$, $\Delta S_2 < 0$). In this regard, a highly positive ΔH and/or highly positive/negative ΔS of the adsorption appears abnormal, unless sufficient experimental evidence is provided. Therefore, to obtain an appropriate conclusion or remark at this stage, several requirements need to be met in the existing studies. First, the alternative of the equilibrium constant K_c must be dimensionless. Second, the linear regression coefficient (R^2) of the van't Hoff equation must be high. Third, the initial concentration of the adsorbate utilized in adsorption studies must be low or high. If the initial concentrations of the adsorbate are very high, the distribution and partition coefficients might not be appropriate for the calculation of thermodynamic adsorption parameters (Chang et al., 2016; Tran et al., 2016; Tran et al., 2017b).

3.6. Desorption and regeneration

The adsorption reversibility is often determined by desorption studies. To some extent, the desorption study can help to understand the uppermost reaction between adsorbent and adsorbate in solution. Because leaf-based biosorbents are nonporous carbonaceous materials, surface interaction (i.e., electrostatic attraction) greatly contribute to the adsorption mechanism. In general, if electrostatic attraction is mainly responsible for the adsorption of cationic adsorbates (i.e., Cu^{2+}), the adsorption process is highly reversible when pure water at a low pH value (often pH 2.0) is used as the desorbing agent. For example, Chakravarty et al. (2010) speculated about Pb(II) biosorption by bael leaves, concluding that the desorption efficiency of Pb(II) from bael leaves has the following other: 85% (at pH 2.0) > 35% (pH 3.0) > 10% (pH 4.0–7.0).

In contrast, highly alkaline conditions (often pH 12) simulate the desorption efficiency of anionic adsorbates (i.e., $Cr_2O_7^{2-}$) from the surface of the adsorbent if the adsorption process primarily involves electrostatic attraction. **Figure 8** collects the plots regarding to the research of desorption

from biosorbents in the literature. A typical example was described in Hamissa et al. (2007) for the biosorption of two anionic dyes (Sumfixe Supra Red and Alpacelle Lumiere Brown) onto maguey leaves (**Figures 8a–b**), which agrees with the findings of other authors (Guerrero-Coronilla et al., 2015; Jain and Gogate, 2018; Namasivayam et al., 1996; Singh et al., 2009). Similarly, Guerrero-Coronilla et al. (2015) concluded that the decline in the acid red 27 desorption efficiency has the following order: strongly alkaline (0.01 M NaOH and KOH; pH ≈ 12) > weakly alkaline (0.1 M Na_2CO_3; pH ≈ 11.5) > neutral salt (0.1 M NaCl, $NaNO_3$, and Na_2SO_4; pH ≈ 7.0) > weak acid (0.1 M NH_4Cl; pH ≈ 5.1) > strong acid (0.1 M HCl, H_2SO_4, and HNO_3; pH ≈ 1.0) solutions.
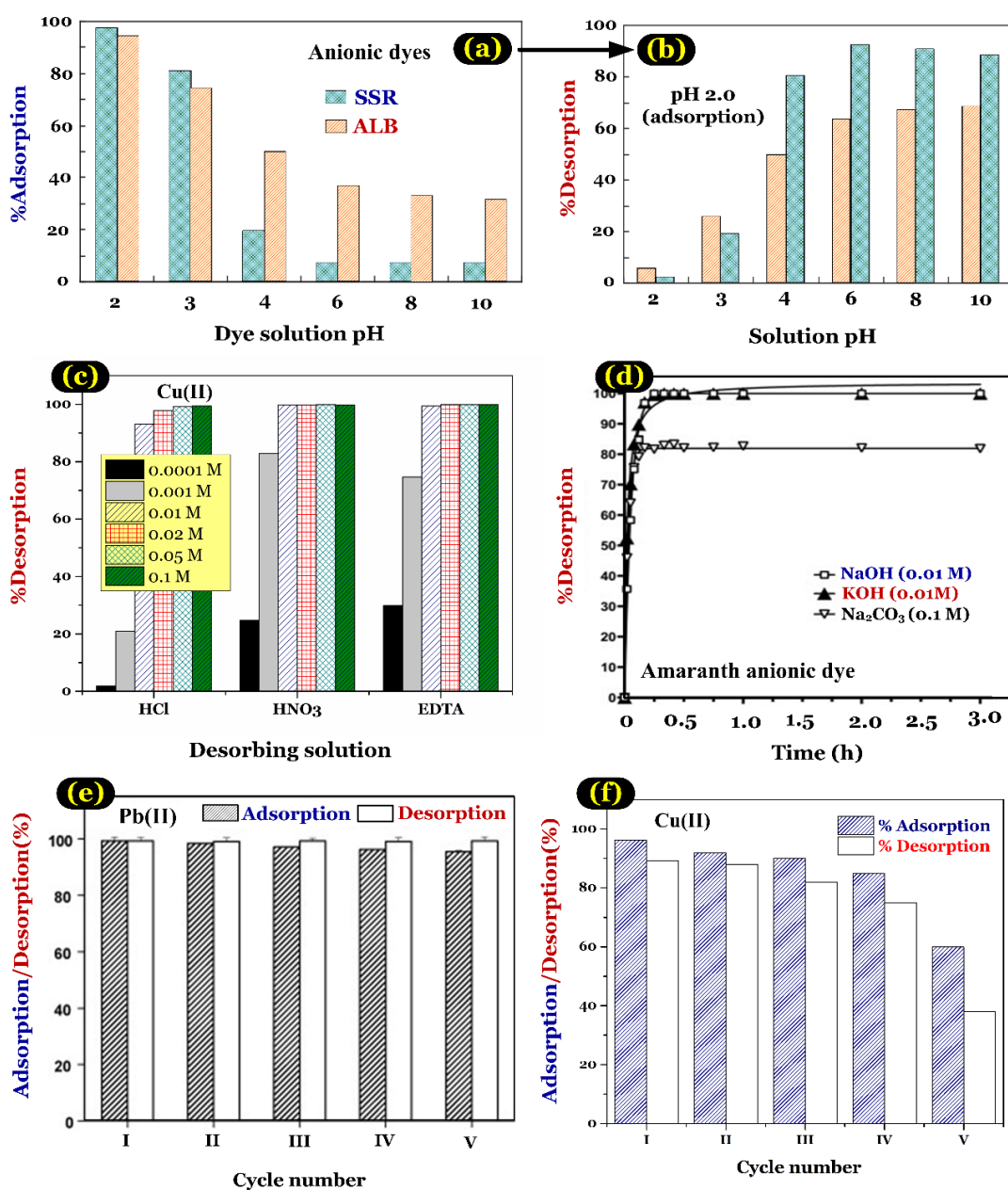
Figure 8. (a) Effect of solution pH on the adsorption of two anionic dyes ([Sumfixe Supra red (SSR) and Alpacelle Lumiere brown (ALB)] onto *Agave americana* leaves, and (b) effect of pH on the dye desorption (Hamissa et al., 2007) [Creative Commons CC-BY by SAGE]; (c) Effect of different eluents on copper desorption from treated rubber leaves (Ngah and Hanafiah, 2008) [License number: 4443540449114]; (d) Desorption kinetics of anionic Amaranth dye from water hyacinth leaves (Guerrero-Coronilla et al., 2015) [License number: 4435930384912]; (e) Five cycles of Pb(II) adsorption–desorption with 0.4 M HCl (Reddy et al., 2010) [License number: 4435930464723]; (f) Biosorption-desorption cycles for regenerating SATCEL with 0.1 N HCl (Khan Rao and Khatoon, 2017) [License number: 4435930646149]

Generally, the desorption efficiency of potential toxic metals is enhanced when the solution concentration of used desorbing agent increases. For example, Chen et al. (2011) found that the desorption efficiency of Cu(II) ions from NaOH-treated rubber leaves increases from 1.9% to 99.4%, 24.7% to 99.9%, and 29.9% to 99.9% when the concentrations of HCl, HNO_3, and EDTA increase from 0.0001 M to 0.1 M, respectively (**Figure 8c**). They suggested that ion exchange is the primary desorption mechanism. The exact performance was reported by other scholars (Al Rmalli et al., 2008; Chen et al., 2011; Chojnacka et al., 2005; Mambo et al., 2016; Ngah and Hanafiah, 2009; Qi and Aldrich, 2008; Reddy et al., 2012; Saha et al., 2017; Serencam et al., 2008; Yuvaraja et al., 2012).

Similar to the adsorption process, the desorption process of adsorbate from the laden biosorbent derived from leaves reaches a fast equilibrium (Cengiz and Cavas, 2010; Guerrero-Coronilla et al., 2015; Hossain et al., 2012; Jain and Gogate, 2017b; Rao et al., 2011b). In fact, Guerrero-Coronilla et al. (2015) reported that the desorption process of amaranth anionic dye from laden water hyacinth leaves reaches a desorption equilibrium at approximately 15 min within all assayed alkaline eluents (i.e., NaOH, KOH, and Na_2CO_3; **Figure 8d**). In addition, Rao et al. (2011b) reported very fast desorption kinetics fast, where approximately 95.6% Cd(II) in the jambolana leaf-based biosorbent were desorbed within a short period of time, that is, 5 min. However, Qi and Aldrich (2008) found that the desorption process of potentially toxic metals (i.e., Ni, Zn, Cd, Cu, and Pb)

from tobacco leaves reaches an equilibrium after 8 h.

When the adsorption is highly reversible, an adsorption–desorption cycle is performed to explore the possibility of spent biosorbent regeneration and adsorbate recovery. Generally, the adsorption–desorption efficiency progressively decreases with increasing regeneration cycle number (Abedi et al., 2016; Amirnia et al., 2016; Cheraghi et al., 2015; Jain and Gogate, 2017a;2018; Kong et al., 2015; Khan Rao and Khatoon, 2017; Nag et al., 2016; Peydayesh and Rahbar-Kelishami, 2015; Qaiser et al., 2009; Serencam et al., 2008; Setiabudi et al., 2016; Xiao et al., 2016). For example, Khan Rao and Khatoon (2017) asserted that the percentage of Cu(II) adsorbed onto Australian pine leaves decreased from 96.3% to 60% after five consecutive cycles using 0.1 N HCl as a desorbing solution and the percentage of Cu(II) desorbed from laden biosorbent decreased from 89.2% to 37.9% (**Figure 8f**).

In contrast, many researchers postulated that the reusability percentages insignificantly decrease after several adsorption–desorption cycles (Çay et al., 2004; Chakravarty et al., 2010; Chen et al., 2010; Gupta et al., 2012; Han et al., 2014; Hossain et al., 2014a; Jain and Gogate, 2017b; Jain and Gogate, 2017c; Khorshidi et al., 2015; Lim et al., 2016; Ngah and Hanafiah, 2009; Reddy et al., 2010; Reddy et al., 2012; Ruiyi et al., 2016; Yu et al., 2016). For example, Reddy et al. (Reddy et al., 2010) assessed that the desorption of Pb(II) from chemically modified drumstick leaves in all four cycles remained at very high efficiency, with more than 98% recovery of Pb(II) in each cycle (**Figure 8e**). In conclusion for **Figure 8**, the desorption/regeneration processes of heavy metals or dyes form the biosorbents are easily carried out. The adsorption efficiency often decreases with the increasing cycles in regeneration.

However, other authors claimed that the adsorption affinity of biosorbents to adsorbate is enhanced after each adsorption–desorption cycle (Muhammad et al., 2009; Saha et al., 2017). For example, Saha et al. (2017) found that the adsorption and desorption efficiency noticeably increased after the first cycle. They concluded that the HNO_3 solution (used as desorbing agent) could dissolve the organic portion of the leaves, activating the binding site and consequently enhancing the

adsorption efficiency. A similar phenomenon was found for the desorption of Cu(II) from laden banana peel using a H_2SO_4 desorbing agent (Hossain et al., 2012), Pb(II) and Cd(II) from laden mango peel using HCl (Iqbal et al., 2009), and Zn(II) and Ni(II) from grapefruit peel using HCl (Muhammad et al., 2009). Similarly, Yazıcı et al. (2008) also discovered that the adsorption capacity of Cu(II) onto lamiaceae leaves was improved when the leaves were pretreated with H_2SO_4 and HNO_3 because the pretreatment with such acids possibly causes the protonation of the biomass surface and consequently an increased ion exchange capacity. In addition, Hanafiah and Ngah (2009) found that the pretreatment of rubber leaves with HCl contributes to increasing protonation of silanol, carboxyl, amino, and hydroxyl groups on the leaf surface. This presumably results in an increased adsorption capacity of copper cations in the bulk solution.

The adsorption of anionic contaminants is a process that often occurs adequately at a low solution pH because of the large contribution of electrostatic attraction. Therefore, desorption will be favored at a higher pH (alkaline condition). For example, Jain and Gogate (2017c) reported that the process of acid blue 25 adsorption onto NaOH-treated cluster fig leaves reaches the highest adsorption efficiency at pH 2.0. The results of a desorption–adsorption study using distilled water at pH 12 as a desorbing agent signify that the adsorption capacity of the biosorbent slightly declines, from 24.6 ± 0.34 mg/g in the first cycle to 24.4 ± 0.42 mg/g in the seventh cycle at $C_o = 100$ mg/L.

With respect to desorption competition, Çay et al. (2004) found that the desorption efficiency of toxic metals from laden tea waste in single and binary systems is similar. An amount of 0.1 M HCl can desorb 97.2% Cu(II) and 98.1% Pb(II) in the single system and approximately 97% Cu(II) and Pb(II) in the binary system.

3.7. Adsorption competition

Adsorption competition occurs in a multi-adsorbate system. In fact, the adsorption capacity of the adsorbent is strongly impacted by the presence of multi-adsorbates because of (1) the competitive adsorption phenomenon of adsorbates in the mixed system for adsorption sites on the

adsorbent surface and (2) their antagonistic effect.

For example, Shi et al. ([2016](#)) reported that the Langmuir maximum adsorption capacity (Q^o_{max}) of arborvitae leaves toward potentially toxic metals in non-competitive adsorption (35.8 mg/g for Pb, 7.9 mg/g for Cu, and 6.8 mg/g for Co) is much higher than in competitive adsorption (9.3 mg/g for Pb, 3.1 mg/g for Cu, and 1.54mg/g for Co). Similarly, Kamar Firas et al. ([2017](#)) stated that the Q^o_{max} values of cabbage leaves with respect to Pb(II), Cu(II), and Cd(II) in a single system (6.3, 5.8, and 5.1 mg/g) are higher than the corresponding values in a ternary system (4.54, 3.35, and 2.48 mg/g). In addition, Khan Rao and Khatoon ([2017](#)) reported Q^o_{max} values of Cu (44.5 and 13.0 mg/g), Pb (28.6 and 21.7 mg/g), and Ni (39.9 and 7.79 mg/g) adsorption onto aluminate-treated Australian pine leaves in single and multi-metal systems, respectively. A similar tendency was discussed elsewhere (Çay et al., 2004; Hossain et al., 2014b; Yu et al., 2015). Furthermore, Salim et al. ([2008](#)) explored the Cd(II) removal efficiency from aquatic environments of 20 species of plant leaves. They concluded that the existence of foreign ions (Zn, Pb, and Cu) or complexing agents (EDTA) causes a significant decrease in the biosorption efficiency of cadmium onto the plant leaves.

With respect to adsorption selectivity, the Q^o_{max} value (mmol/g) of leaf-based biosorbent decreases in the following order: Cu(II) > Pb(II) > Co(II) (Shi et al., 2016); Cu(II) > Cd(II) > Pb(II) (Kamar Firas et al., 2017); Cu(II) > Ni(II) > Pb(II) (Khan Rao and Khatoon, 2017); Cu(II) > Cd(II) (Çay et al., 2004); Cu(II) > Cd(II) > Pb(II), Zn(II) > Cd(II) > Pb(II), Zn(II) > Cu(II) > Cd(II), and Cu(II) > Cd(II) > Zn(II) (Hossain et al., 2014b); Cu(II) > Cd(II) (Nag et al., 2016); Cu(II) > Zn(II) > Cd(II) (Yu et al., 2015); and Cu(II) > Pb(II) > Zn(II) > Cd(II) > Ni(II) (Qi and Aldrich, 2008).

Furthermore, Zolgharnein et al. ([2017](#)) used XPS to identify the biosorption affinity of modified Buxus sempervirens tree leaves to a ternary mixture of metal ions. The surface composition (atomic percentage) was ranked as Cu (0.3%) > Cd (0.3%) ~ Ni (0.3%). Clearly, the leaf-developed biosorbent favors the adsorption of Cu(II) and not the mixture containing the metal ion solution.

Because the limitation of adsorption competition study in multi-adsorbate system using leaves

as biosorbent in the literature, we compared the Q^o_{max} values of biosorbents to potentially toxic metals in the single system. The Q^o_{max} values (mmol/g) exhibit a decreasing order: Cu(II) > Ni(II) > Cd(II) (Reddy et al., 2012), Cu(II) > Cd(II) > Pb(II) (Kamar Firas et al., 2017; Wan et al., 2014), Hg(II) > Cu(II) > Pb(II) (Zhang et al., 2015), Cr(III) > Cr(VI) > Pb(II) (Copello et al., 2011), Cr(III) > Cd(II) > Cr(VI) (Sawalha et al., 2006), Co(II) > Ni(II) (Vilvanathan and Shanthakumar, 2016), Cu(II) > Ni(II) > Pb(II) (Khan Rao and Khatoon, 2017), Cr(III) > Cu(II) > Pb(II) > Zn(II) (Abedi et al., 2016), Cr(III) > Cu(II) > Zn(II) (Rawat et al., 2014), Pb(II) > Cd(II) (Hossain et al., 2014c), Cu(II) > Pb(II) > Cd(II) (Sangi et al., 2008), Cr(III) > Cu(II) > Cd(II) (Chojnacka et al., 2005), Cu(II) > Zn(II) > Cd(II) (Yu et al., 2015), Cu(II) > Ni(II) > Pb(II) (Salehi et al., 2008), Cu(II) > Zn(II) > Pb(II) > Cd(II) (Abdolali et al., 2016), and Cu(II) > Co(II) > Ni(II) > Cr(III) > Zn(II) > Cd(II) > Pb(II) (Batool et al., 2017).

4. Column experiment

Continuous fixed-bed analysis is often performed to comprehend the effects of various process parameters, such as the bed height, flow rate, and initial adsorbate concentrations, on the dynamic adsorption process. To analyze the breakthrough profiles in the fixed-bed adsorption process, various mathematical models have been applied to describe the dynamic adsorption behavior of adsorbates in the fixed-bed column including the Thomas, Adams–Bohart, and Yoon–Nelson models. Similar to the Langmuir model, the Thomas model (**Section S6**) is commonly applied to estimate the maximum adsorption capacity of the adsorbent (q_o; mg/g) under given experimental conditions.

Generally, breakthrough and exhaustion times significantly decrease when the flow rate and initial adsorbate concertation increase, while they increase with increasing bed height (used adsorbent mass). For example, Tamez Uddin et al. (2009) conducted a fixed-bed column study of methylene blue removal from water media using jackfruit leaf powders (**Figure S12**). With respect to the effect of the flow rate (Q; mL/min), the breakthrough and exhaustion times exhibited the following order: 3350 and 530 min (at 30 mL/min) > 250 and 390 min (at 40 mL/min) > 190 and 300 min (at 50

mL/min), respectively. Meanwhile, the breakthrough time (t_b; min) and exhaustion time (t_s; min) decreased from 490 and 780 min to 250 and 390 min and then to 170 and 270 min when the initial dye concentration (C_o; mg/L) increased from 100 mg/L to 200 mg/L and then to 300 mg/L, respectively. In contrast, the t_b and t_s values increased when the bed height (Z; cm) rose as follows: 170 and 270 min (at 5 cm), 275 and 390 min (at 7.5 cm), and 400 and 490 min (at 10 cm), respectively. Notably, although the breakthrough and exhaustion times strongly depend on the operation conditions (i.e., Z, Q, and C_o), the Thomas maximum adsorption capacity (q_o; mg/g) of jackfruit leaves is almost the same under different operation conditions. The q_o values ranged from 245 to 251 mg/g (for the flow rate study), from 256 to 266 mg/g (bed height), and from 245 to 256 mg/g (initial dye concentration). Similar results were reported elsewhere (Amirnia et al., 2016; Das et al., 2016; Han et al., 2009; Rao et al., 2011b; Yu et al., 2015), but contrary findings were also documented (Amin et al., 2017; Jain and Gogate, 2018; Nag et al., 2016; Saha et al., 2012). **Table 3** summarizes the maximum equilibrium adsorption capacity in the column of the Thomas model of various pollutants onto leaf-based biosorbents. In **Table 3**, the adsorption capacities significantly vary with the operation conditions.

Table 3. Thomas maximum adsorption capacity (q_o; mg/g) of leaf-based bisorbents (column experiment) at different operation conditions including flow rate (Q; mL/min), bed height (Z; cm), and initial adsorbate concentration (C_o; mg/L)

Leaves	Adsor-bate	Operation conditions			q_o (mg/g)	Reference
		Q	Z	C_o		
Sacred fig	Pb(II)	5	50	100	16.42	Qaiser et al., 2009
Tea waste	Pb(II)	20	15[a]	100	46.0	Amarasinghe and Williams 2007
MSG-treated rubber	Pb(II)	NA	1.0	20	75.8	Fadzil et al., 2016

HNO$_3$-treated rubber	Pb(II)	NA	1.0	20	48.7	Fadzil et al., 2016
Jambolan	Cd(II)	20	5.0	100	25.2	Rao et al., 2011b
Tea waste	Cu(II)	20	15[a]	100	13.0	Amarasinghe and Williams 2007
Date palm	Cu(II)	3	5	150	5.19	Amin et al., 2017
MA-treated date palm	Cu(II)	2	5	100	9.64	Amin et al., 2017
Rubber	Cr(VI)	15	3	10	19.2	Nag et al., 2016
Castor	Hg(II)	2	1.0[a]	100	35.5	Al Rmalli et al., 2008
Neptune grass	MB	7.3	9.0	100	482	Cavas et al., 2011
Jackfruit	MB	40	7.5	300	266	Tamez Uddin et al., 2009
Phoenix	MB	8	15	100	149	Han et al., 2009
Pineapple	MG	10	5	200	85.2	Das et al., 2016
NaOH-treated almond	AG25	8	4	200	38.1	Jain and Gogate 2018
Jackfruit	CV	5	12	50	66.7	Saha et al., 2012
Treated cluster fig	AV17	8	4	200	70.9	Jain and Gogate, 2017b

Note: [a]The used adsorbent mass (g); data unreported in the original paper (NA); malachite green (MG); methylene blue (MB); crystal violet (CV); acid violet 17 (AV17); acid green 25 (AG25); monosodium glutamate (MSG); and mercaptoacetic acid (MA).

Furthermore, the maximum adsorption capacity of an adsorbent in batch experiments (Q^o_{max}; mg/g) is often higher than that in column experiments (q_o; mg/g). For example, Jain and Gogate (2017b) reported that the Q^o_{max} value of treated cluster fig leaves toward acid violet 17 dye (111 mg/g) is significantly higher than the q_o value (35.8–70.9 mg/g). Similarly, Fadzil et al. (2016) found that

the Q^o_{max} values of citric acid-modified rubber leaves and monosodium glutamate-modified rubber leaves toward Pb(II) are 97.2 and 110 mg/g, respectively, that is, significantly higher than the q_o values (37.7–48.7 mg/g and 51.3–75.8 mg/g, respectively). In addition, Amarasinghe and Williams (2007) reported that the maximum adsorption capacity of tea waste to Cu(II) and Pb(II) exhibits the following order: Q^o_{max} (48 and 65 mg/g) > q_o (13 and 46 mg/g), respectively. A higher Q^o_{max} value (46.6 mg/g) compared with q_o (20.5–38.1 mg/g) was also reported by Jain and Gogate (2018) for acid green 25 adsorption onto NaOH-treated almonds.

Moreover, Amarasinghe and Williams (2007) highlighted that the column adsorption capacity of tea waste [13 mg/g for Cu(II) adsorption and 46 mg/g for Pb adsorption] is remarkably higher than that of coconut shell-based granular activated carbon (8 and 19 mg/g, respectively). A comparable result was observed for Cr(VI) adsorption onto rubber leaves, $Q^o_{max} = 23.0$ mg/g > q_o (8.2–18.8 mg/g) (Nag et al., 2016), and Pb(II) adsorption onto sacred fig leaves, $Q^o_{max} = 37.5$ mg/g > q_o (13.4–16.4 mg/g) (Qaiser et al., 2009).

However, Al Rmalli et al (2008) found that the Q^o_{max} (35.5 mg/g) and q_o (37.2 mg/g) values of Hg(II) adsorption onto castor leaves are similar. In contrast, Saha et al. (2012) proposed that jackfruit leaves have a higher q_o value (57.3–66.7 mg/g) than Q^o_{max} (41.1 mg/g) based on an adsorption study of crystal violet dye. A similar trend was reported by Rao and Khan (2017) for Cu(II) adsorption onto Boston fern leaves: q_o (37.5 mg/g) > Q^o_{max} (27.0 mg/g).

The column adsorption could be assumed as a plug flow reactor. In the realistic operation, the adsorption difficultly reaches equilibrium. On the other hand, the adsorption equilibrium can be regarded as a batch reaction. The maximum adsorption capacity can be estimated through Langmuir equation. Thus, the adsorption capacities in the batch adsorption equilibrium frequently are higher than those in the column adsorption. The adsorption capacity in the column adsorption varies with the operation conditions such as bed height, flowrate and initial concentration. The adsorption capacity in the adsorption equilibrium only varies with the properties of solution such as pH and temperature. In addition, the column adsorption is frequently used in the realistic wastewater

treatment operation. However, the particle sizes of biosorbents might affect the adsorption efficiencies toward heavy metal ions or dyes. When the biosorbents are applied to treat the realistic wastewater using column, the particle size is regarded as a crucial factor. The produced biosorbents possess the relatively lower particle size, which wastewater needs to take a long period to pass the column.

5. Application of biosorption technology to real samples

To explore the feasibility of the application in realistic wastewater, it is necessary to examine the adsorption efficiency of the leaf-based biosorbent in a real-life scenario. For example, Ruiyi et al. (2016) applied NaOH-treated biosorbent derived from fallen persimmon leaves to treat industrial wastewater from the GEM High-Tech Co., Ltd., China. The results indicated that the treated biosorbent can effectively remove approximately 96% Zn(II), 88% Ni(II), and 82% Pb(II) from industrial wastewater. Similarly, Tewari (2013) reported that approximately 99% Cr(VI), 95% Cu(II), and 93% Zn(II) were removed from brass and electroplating industry effluent by pine leaves. Meanwhile, diethylenetriamine functionalized sago palm leaves were applied to remove uranium from nuclear industry wastewater at different U(VI) concentrations. The removal efficiency decreased in the following order: 87.7% (at C_o = 200 µg/L) > 84.3% (at 10 µg/L) > 82.8% (at 5 µg/L) (Xiao et al., 2016). For the removal efficiency of various potentially toxic metals from different wastewater samples, refer to **Table 4.** It can be found in **Table 4** that removal efficiencies of contaminants are highly affected by the initial concentration, solid/liquid ratio and solution pH.

Table 4. Removal efficiency (R%) of toxic metal by leaf-based biosorbents at different real water samples

Site	Leaves	Chemical Adsorbate	C_o (mg/L)	m/V (g/L)	pH	R%	Ref.

No.	Biosorbent	Treatment	Metal					Ref.
1.	Poplar	—	Pb(II)	0.17	—	—	99.8	(1)
2.	Poplar	—	Cd(II)	1.65	—	—	95.0	(1)
3.	potato	NaOH	Cu(II)	15.5	50	5.2	95.8	(2)
4.	Persimmon	NaOH	Pb(II)	4.73	10	5.0	81.6	(3)
4.	Persimmon	NaOH	Zn(II)	16.6	10	5.0	95.9	(3)
4.	Persimmon	NaOH	Ni(II)	8.23	10	5.0	87.9	(3)
5.	Chinaberry	NaOH+HCl	Pb(II)	5.86	—	—	75.1	(4)
6.	Taro	—	Pb(II)	10	1	6.0	99.8	(5)
7.	Waste tea	Formaldehyde	Ni(II)	0.5	25	7.0	99.8	(6)
8.	Waste tea	Formaldehyde	Ni(II)	0.5	25	7.0	99.7	(6)
9.	Waste tea	Formaldehyde	Ni(II)	0.5	25	7.0	99.8	(6)
10.	Gum arabic	—	Cr(VI)	—	—	2.0–8.0	65.0	(7)
11.	Bael	—	Pb(II)	55.4	1	6.2	88.1	(8)
12.	Pine	—	Cr(VI)	2.74	40	4	99.8	(9)
12.	Pine	—	Cu(II)	4.55	40	4	94.5	(9)
12.	Pine	—	Zn(II)	5.53	40	4	93.1	(9)
13.	Sotetsu	DETA	U(VI)	0.2	0.2	—	87.7	(10)

Sites: [1]Pb-battery factory disposal site; [2]Disposal sites of Phosphogypsum piles; [3]Copper plating effluent; [4]Industrial wastewater from GEM high-tech Co. Ltd., China; [5]Industrial sample; [6]River water; [7]Tap water; [8]River Badabaira, Peshawar; [9]River Swat, Charsadda; [10]Real industrial wastewater collected from a metal finishing industry in Tirupur near to Coimbatore; [11]Battery waste effluent;

[12]Industrial effluent obtained from brass and electroplating industry; and [13]Nuclear industry wastewater. DETA means diethylenetriamine.

Reference: (1) (Al-Masri et al., 2010), (2) (Mambo et al., 2016), (3) (Ruiyi et al., 2016), (4) (Khokhar et al., 2015), (5) (Saha et al., 2017), (6) (Shah et al., 2015), (7) (Prasad and Thirumalisamy, 2013), (8) (Chakravarty et al., 2010), (9) (Tewari, 2013), (10) (Xiao et al., 2016).

Interestingly, Prasad and Thirumalisamy (2013) applied gum arabic leaves to remove hazardous Cr(VI) from industrial and synthetic wastewater. They found that the removal process is independent of the $pH_{solution}$ ranging from 2.0 to 8.0. However, their finding is dissimilar to that of Chakravarty et al. (2010) for the removal of Pb(II) ions from battery waste effluent using bael leaves.

6. Concerns

Similar to other lignocellulose materials-derived biomass, the leaf-based biosorbent can release solute organic compounds (i.e., lignin, pectin, and tannin) during the adsorption process, which results in a high chemical oxygen demand (COD) of the water. This organics release may lead to a second form of pollution, which can turn the color of treated water into light yellow or brown. For example, Çekim et al. (2015) reported that, although pristine tobacco leaf-derived biosorbent exhibits an excellent adsorption capacity to Cu(II) with its high removal efficiency (90.7%), it results in organic-originated pollution of the biosorption system. They reported that the COD levels in water after adsorption varied between 208–235 mg/L at varying temperatures.

However, many researchers found that the leaching problem of organic solutes can be overcome if the biosorbent is pretreated. For example, Ngah and Hanafiah (2009) reported that formaldehyde rubber leaves can minimize the COD concentration in treated water. The results showed that the COD level rose from 7 to 37 mg/L when the solid/liquid ratio rose from 2 to 10 g/L, respectively. Similarly, Šćiban et al. (2006) reported that the leaching of organic matter during Zn(II) biosorption from modified wood sawdust-derived biosorbent is significantly lower than that of pristine wood sawdust. The COD level exhibited the following order: pristine fir sawdust (82 mg/L)

> NaOH-treated fir sawdust (63 mg/L) and pristine poplar sawdust (31.5 mg/L) > NaOH-treated poplar sawdust (29 mg/L).

Another problem is the disposal of metal ion-adsorbed adsorbent that can create another serious environmental issue because acid rain can wash out adsorbed metal ions of the adsorbent surface into the environment (Çay et al., 2004). A number of investigators have studied the desorption of heavy metal ions from the biosorbents (see **Section 3.6**). When the metal ions release from the ion-adsorbed adsorbent through the extraction process, the adsorbents can be used repeatedly. The extractive solution needs to be treated or recycled according to the characteristics of the solution. The metal-load adsorbents might be regarded as hazardous waste if the adsorbent cannot be used continuously. The safe disposal of hazardous waste needs to be evaluated carefully. For example, Nag et al. (2016) were interested in the safe disposal of Cr(VI)-loaded rubber leaf powder. The laden leaves were first incinerated at 700 °C and then mixed in deionized water. Surprisingly, they reported that Cr(VI) was not found in the ash sample; therefore, the ash can be disposed in a landfill. This mistake might result from their analysis method of chromium (VI) ions that is the colorimetric method. This method cannot distinguish Cr(VI) from total Cr (Tran et al., 2017b). In fact, if Cr(VI) would go into the air during incineration, it would be serious problem. The question is whether the reduction mechanism plays a primary role in removing Cr(VI) from the aqueous phase (see **Section 7.5**). This means that most Cr(VI) anions are reduced to Cr(III) cations into solution without adsorbing onto the surface of the biosorbent. Furthermore, Ruiyi et al. (2016) observed the thermogravimetry (TG) and differential thermogravimetry (DTG) curves of NaOH-treated persimmon leaves before and after adsorption of Pb(II). They concluded that the ash contains abundant Pb(II) metals after incineration, which can be recycled as secondary lead resource or disposed of properly. A similar outcome was reported by Saha et al. (2017).

It is essential to separate the contaminants before disposing the exhausted adsorbents. At their end of life, the exhausted leaf biosorbents can be regenerated, dried, and burned. Although the final products can be disposed in landfills, some researchers have suggested exploiting them in preferable

ways, like in the preparation of hybrid inorganic–organic composites. The prepared composites are often used for padding in the stone blocks (Visa, 2012) and incorporating in brick, cement, and road construction (De Gisi et al., 2016). As mentioned in **Section 3.6**, various reagents and chemicals can be used for desorption of contaminants and their separation from the exhausted biosorbents.

Overall, from real-life application point of view, the usage of untreated leaves has an obvious drawback related to considerable amounts of potentially hazardous contaminants leached into the environment and increase of COD levels of the treated water bodies. In this regard, the pretreatment of leaves with some certain chemical regents can serve as a superior option to lessen the leaching problems. On the other hand, although by-product leaves are promising alternatives that can be potentially utilized in full-scale plants, almost all of the reported studies are referred to using the biosorbents for the removal of various contaminants from synthetic solutions in lab-scale systems. Also, the studies related to regeneration of adsorbents and, specially, safe disposal or using the exhausted biosorbents for other purposes are not very high. To overcome the practical limitations in using by-product leaves as an alternative to commercial activated carbon, in the future studies, more focus should be placed on finding suitable low-cost strategies for eliminating of leaching contaminants from the leave bodies. Further studies should also focus on the biosorbent performances with real water and wastewater samples. Regeneration and reuse of the adsorbents for several adsorption-desorption cycles, and environmentally safe disposal of the biosorbents should be looked at.

7. Adsorption mechanism

As previously discussed, the adsorption capacity and mechanism of an adsorbent essentially depend on the adsorbent properties and its adsorbate nature. For example, in adsorption studies of cadmium, Salim et al. (2008) utilized 20 species of plant leaves and concluded that the most efficient types of leaves for cadmium biosorption are that of styrax, walnut, pomegranate, and plum plants. A similar study was conducted by Sayrafi et al. (1999) with respect to Cd(II) adsorption onto cypress,

pine, and oak leaves. Whilst these followed important adsorption mechanisms, others have been discussed and reported in the literature.

7.1. Negligible role of the pore filling

Generally, the adsorption capacity of the adsorbent is directly proportional to its specific surface area. However, as aforementioned in **Section 2.1**, leaf-based biosorbent is nonporous material due to its lack of porosity properties (i.e., low surface area and pore volume). Consequently, the contribution of the pore filling mechanism to the adsorption process of contaminants (i.e., potentially toxic cationic and anionic metal ions, cationic and anionic dyes, and others) is less important. In addition, Setiabudi et al. (2016) reported that the S_{BET} and V_{total} of oil palm leaves before adsorption (2.6 m^2/g and 0.0020 cm^3/g, respectively) are similar to those of methylene after blue dye adsorption (2.3 m^2/g and 0.0008 cm^3/g, respectively). This result further proved the insignificant role of the pore filling. Similarly, Nag et al. (2016) found that the S_{BET} of rubber leaves slightly decreases after Cr(VI) adsorption, from 29.2 to 13.1 m^2/g. While studying Ni(II), Zn(II), and Co(II) adsorption onto industrial waste-derived biosorbent, Ramrakhiani et al. (2017) noted the S_{BET} values of pristine and laden biosorbents of 23.6 and 18.7 m^2/g, respectively.

Although the leaves are nonporous biosorbents, they exhibit abundant surface functional groups (i.e., carboxylic and amine groups) and high concentrations of light metal ions (i.e., Ca, Mg, K, and Na) on their surface. Such functionalities and inorganic salts will play a decisive role in the adsorption mechanism. This means that the adsorption process will occur on the external surface of the biosorbent, which is visible when subjected to scanning electron microscope (SEM; **Figure S13**) and atomic force microscopy (AFM; **Figure S14**) analyses. For example, Khan Rao and Khatoon (2017) compared the AFM data before and after adsorption of Cu(II) and concluded that the average roughness of Australian pine leaves increases from 8.41 to 18.46 nm (**Figure S14**). This outcome confirmed that the biosorption process mainly took place on the leaf surface. An identical result was reported by Deng et al. (2003) for adsorption of Pb(II) and Cu(II) onto aminated polyacrylonitrile

fibers (APANF). The surface roughness of APANF increased from 1.174 nm to 1.616 nm and 1.555 nm after the adsorption of Pb(II) and Cu(II) ions, respectively.

7.2. Identifying electrostatic attraction

Similar to other adsorbents, leaf-based biosorbents typically coexist with both acidic and basic solutions (amphoteric nature). Hence, the biosorbents can adsorb both cationic and anionic contaminants through electrostatic attraction. Several common experiments have been used to identify the presence of electrostatic attraction such as the effect of the solution pH (see **Section 3.1**) and ionic strength (**Section 3.2**) and desorption studies (**Section 3.6**).

With respect to the adsorption of potentially toxic metals, electrostatic attraction is known as outer-sphere complexation, while non-electrostatic attraction is known as inner-sphere complexation (Goldberg, 2013). The hydroxyl and carboxylic groups play a predominant role in the adsorption process. The outer-sphere (electrostatic: weakly bonded ions) interaction results from a dipole–ion attraction between the metallic cation and the dipole of the oxygen from the –OH or –COOH groups. In contrast, the inner-sphere (surface coordination or surface complexation: strongly bonded ions) interaction is caused by covalent bonding between one pair of electrons of the oxygen (donor) from the –OH or –COOH groups and the metallic cation (acceptor) (Davis and Kent, 1990). To identify the existence of electrostatic attraction between tobacco leaves and a toxic metal, Qi and Aldrich (2008) compared the leaves' zeta potential before and after adsorption. They found that the magnitude of the zeta potential value significantly decreased after adsorption, by approximately 40%.

Notably, a new classification of the metal biosorption mechanism has been proposed by Robalds et al. (2016). A special case of complexation in which the ligand bonds at two or more places to a metal ion is usually regarded as chelation (chemisorption) (Manahan, 2000). **Figure S15** presents several active binding functional groups for adsorption (Volesky, 2007) and the binding mechanism of a metal ion (M^{2+}) by oxygen-containing functional groups (Manahan, 2000). For biosorption, the elements of oxygen, nitrogen and sulfur might generate complexation reaction with the metal ions.

47

7.3. Identifying complexation and chelation

Among the current advanced techniques, FTIR is widely used to identify the main functional groups present on the adsorbent surface. However, with respect to the adsorption of potentially toxic metals, FTIR cannot distinguish between outer- and inner-sphere complexes. In contrast, XPS can help to identify the inner-sphere complexes (complexation) between toxic metal ions and the functional groups on the adsorbent surface.

For example, Ruiyi et al. (2016) applied the XPS technique to investigate the Pb(II) adsorption mechanism onto NaOH-treated persimmon fallen leaves and suggested that there is an interaction between Pb(II) in the solution and O elements in the functional groups of the leaves. This outcome after Pb(II) adsorption, the peak of Pb 4f at 138.85 eV demonstrated that: firstly, bonding occurred between Pb(II) ions and the carboxyl group of the biosorbent; and secondly, the peak at 143.65 eV further confirmed the fixation of Pb onto the biosorbent. The O 1s peak at 530.70 eV confirmed the presence of PbO after Pb(II) adsorption. Therefore, the authors concluded that there is chelation between the carboxylate ligand and hydroxyl group on the biosorbent and Pb(II) in the solution, forming the Pb(II) complex.

In their study, Chen and Yang (2006) applied pristine and formaldehyde-modified *Sargassum sp.* biosorbent to remove heavy metals from water media. Based on the XPS data before and after adsorption, they concluded that the —COO^- group is the uppermost functional group in the formation of the metal complexes. During the formation of carboxyl–metal complexes, the oxygen atom donated electrons to the metal ions. Therefore, the electron density at the adjacent carbon atom in C=O and C–O significantly decreased.

In addition, Ramrakhiani et al. (2017) studied the adsorption process of Ni(II), Co(II), Zn(II), and Cd(II) onto industrial waste-derived biosorbent. They reported that the deconvolution of N 1s and C 1s XPS spectra produced two and one additional peaks, respectively, suggesting the formation of amino-metal complexes. The N atom derived from the R—NH_2 and R—NH_3^+ groups is mainly in

nitrogen form and interacts with toxic metal ions. A lone pair of electrons in the N atom is donated to the covalent bond between nitrogen and metal ions. The formation of amino-metal complexes comprises $R—NH_2Ni^{2+}$, $R—NH_2Co^{2+}$, $R—NH_2Zn^{2+}$, and $R—NH_2Cd^{2+}$. Correspondingly, the electron cloud density of the N atom decreases, and a higher binding energy peak is observed. An increase in the atomic concentration of total oxygen and a decrease in the atomic concentration of total carbon on the surface of metal-loaded biosorbent further explain the formation of different metal complexes on the biosorbent surface.

The change of pH_{PZC} before and after adsorption of potentially toxic metals might confirm that the adsorption process is chemisorption. For example, Rao et al. (2010a) found that the pH_{PZC} of guava leaves (pH_{PZC} = 6.54) increased by 0.74 units after Cd(II) adsorption (pH_{PZC} = 7.01). They concluded that the positive shift is indicative of Cd(II) ion adsorption involved in chemisorption. In another study, they reported that the pH_{PZC} value of teak leaves shifted 0.83 units after Cd(II) adsorption; the pH_{PZC} of pristine and laden biosorbents was 7.85 and 7.02, respectively (Srinivasa Rao et al., 2010). Similarly, Mohapatra and Anand (2007) concluded that the pH_{PZC} value exhibits the following order: 6.48 (pristine adsorbent) < 7.8 (Cd-loaded adsorbent). In contrast, Babić et al. (1999) reported that the pH_{PZC} of activated carbon cloth decreased after toxic metals adsorption from 7.0 to 6.0 (for Zn adsorption) and to 6.5 (for Cd adsorption). They explained that the decrease in the pH_{PZC} of AC occurs due to the specific adsorption of Zn^{2+} and Cd^{2+} ions. However, it should be noted that the term "specific adsorption" is too general.

7.4. Identifying the ion exchange mechanism

As previously discussed in **Section 2.2**, the leaf-based biosorbent contains a high concentration of light metal ions (i.e., Ca, Mg, K, and Na). Thus, ion exchange is expected to be the primary adsorption mechanism between potentially toxic metals and the biosorbent. Based on the literature, many methods have been applied to identify the presence of ion exchange during the adsorption process. Here, we summarize and analyze several common and useful methods.

The first method is a comparison between the amount of adsorbed toxic metal ions and the amount of exchanged metal ions. The ion exchange mechanism during adsorption of potentially toxic metals onto adsorbent can be quantitatively investigated by following the release of alkali metal ions (Na^+ and K^+), alkaline earth metal ions (Ca^{2+} and Mg^{2+}), and proton binding H^+ ions from the adsorbent after the adsorption process reached an equilibrium. However, the release of light metal ions from the adsorbent is often divided into two types: "*dissolved*" and "*released*" ions (Shin et al., 2007). The light metal ions can be transferred to the solution (control or blank sample only consisting of adsorbent and double-distilled water) by simple dissolution without ion exchange with toxic metals (i.e., Cd^{2+}), which is referred to as "dissolved." Meanwhile, the metal ions released in the presence of Cd^{2+} are called "*released*." The net release amount of metal ions from the adsorption process ("*exchanged*") is defined as the difference between the amount of "*released*" and "*dissolved*" metals (**Figure S3**). In addition, the displacement of H^+ ions (effect of protons in the exchange mechanism) can be determined by the corresponding values of the solution pH before and after adsorption (Fiol et al., 2006; Ruiyi et al., 2016; Šćiban et al., 2006). Meanwhile, researchers proposed an alternative method to calculate the amount of released protons during the adsorption process based on the amount of NaOH added to maintain the pH at 5.0 until reaching the adsorption equilibrium (Iqbal et al., 2009; Zolgharnein et al., 2013).

According to the stoichiometric ratio of cations, the release of one divalent ion would be equivalent to releasing two monovalent ions. Therefore, the sum of exchanged cations [E] can be calculated as $Ca^{2+} + Mg^{2+} + Na^+/2 + K^+/2 + H^+/2$. The ion exchange mechanism is given by the $R_{[A]/[E]}$ ratio, which has been acknowledged by researchers working in adsorption science and with the relevant technology (Fiol et al., 2006; Hanafiah et al., 2009; Iqbal et al., 2009; Ngah and Hanafiah, 2009; Šćiban et al., 2006; Villaescusa et al., 2004; Zolgharnein et al., 2013; Zolgharnein et al., 2015):

$$R_{[A]/[E]} = \frac{[A]}{[E]} = \frac{[i.e., Cd^{2+}]}{[Ca^{2+}] + [Mg^{2+}] + 1/2[K^+] + 1/2[Na^+] + 1/2[H^+]} \tag{1}$$

where the concentration of all cations is commonly expressed as mmol/L or meq/g and [A] is the amount of toxic metal ions (i.e., Cd^{2+}) adsorbed onto the adsorbent in equilibrium. If the coefficient $R_{[A]/[E]}$ is equal to 1, the adsorption process involves a pure ion exchange mechanism.

For example, Ngah and Hanafiah (2009) investigated the Cu(II) adsorption onto surface-modified rubber leaves. They noted that the calculated $R_{[A]/[E]}$ ratio is 1.42. A $R_{[A]/[E]}$ value greater than unity corresponds to the amount of Cu(II) ions adsorbed on the biosorbent; it is greater than the sum of cations released into the solution during the adsorption. This result suggests that ion exchange and complexation primarily involve the removal of copper ions, which is in line with Ngah and Hanafiah's EDS analysis, that is, the peaks corresponding to Mg and Ca ions disappeared after copper adsorption. Similarly, Fiol et al. (2006) reported that the $R_{[A]/[E]}$ value of the adsorption of Pb(II), Ni(II), Cu(II), and Cd(II) cations onto olive stone waste is 1.7, 0.9, 1.4, and 2.3, respectively. They asserted that another mechanism (surface complexation), in addition to ion exchange, must be involved in the adsorption process of such metals. A comparable result was reported by other scholars (**Table 5**). Furthermore, for the multi-adsorbate system (Pb^{2+}, Cd^{2+}, Ni^{2+}, and Cu^{2+}), Abdolali et al. (2016) reported that the total amounts of adsorbed heavy metal ions (1.43 mmol/L) and exchanged alkali ions (1.51 mmol/L) were approximately equal. The ion exchange can be regarded as one of primary adsorption mechanisms but being the unique adsorption mechanism.

Table 5. The R[A]/[E] ratio between the net amount of adsorbed toxic metals [A] and exchanged cations [E]

Adsorbent	Toxic Metal	[A]	[E]	Concentration of cations (exchanged)*					$R_{[A]/[E]}$	Ref.
				Ca^{2+}	Mg^{2+}	$Na^+/2$	$K^+/2$	$H^+/2$		
Leaves-biosorbent										
Treated weed	Cu	0.132	0.159	0.043	0.031	0.069	0.011	0.0045	0.83	(1)
Treated rubber	Cu	0.136	0.146	0.045	0.079	0.069	—	-0.048	0.93	(2)

Adsorbent	Metal									Ref.
Modified rubber	Cu	0.103	0.073	0.011	0.004	0.017	—	0.041	1.42	(3)
Judas[b]	Ag	0.093	0.029	—	—	—	—	—	3.21	(4)
Hardy catalpa[b]	Pb	0.163	0.128	—	—	—	—	—	1.27	(5)
Other kinds of biosorbent										
Juniper bark[a]	Cd	91.6	95.4	—	—	—	—	—	1.04	(6)
Juniper wood[a]	Cd	24.8	19.5	—	—	—	—	—	0.78	(7)
Grape stalk	Cu	0.234	0.247	0.131	0.031	—	0.063	0.022	0.95	(8)
Grape stalk	Ni	0.186	0.206	0.119	0.030	—	0.049	0.008	0.90	(9)
Oil palm bunche	Pb	0.038	0.042	0.017	0.005	0.055	0.007	-0.041	0.91	(10)
Mango peel[b]	Cd	0.914	1.197	0.513	0.118	0.007	0.142	0.135	1.32	(11)
Mango peel[b]	Pb	0.783	0.937	0.506	0.123	0.006	0.119	0.030	1.20	(12)
Grapefruit peel[b]	Ni	1.331	1.166	0.718	0.293	0.020	0.049	0.085	1.14	(13)
Grapefruit peel[b]	Zn	1.512	1.285	0.749	0.323	0.018	0.051	0.145	1.18	(14)

Note: The unit of [a](μmol/g) and [b](meq/g); [A] is total metal adsorbed (mmol/L); [E] is total metal exchanged (mmol/L) = $[Ca^{2+}] + [Mg^{2+}] + [Na^+/2] + [K^+/2] + [H^+/2]$; *concentration of cations (exchanged) = concentration of cations (released) – concentration of cations (dissolved).

References: (1) (Hanafiah et al., 2009), (2) (Ngah and Hanafiah, 2008), (3) (Ngah and Hanafiah, 2009), (4) (Zolgharnein et al., 2013b), (5) (Zolgharnein et al., 2015), (6) (Shin et al., 2007), (7) (Shin et al., 2007), (8) (Villaescusa et al., 2004), (9) (Villaescusa et al., 2004), (10) (Ibrahim et al., 2010), (11) (Iqbal et al., 2009), (12) (Iqbal et al., 2009), (13) (Muhammad et al., 2009), (14) (Muhammad et al., 2009).

Another method is the comparison of the Langmuir adsorption capacity of the adsorbent (Q^o_{max}; mmol/g) and target toxic cationic metal with the cation exchange capacity (CEC; mmol/g) of the adsorbent. Because the CEC of the adsorbent plays a key role in estimating the maximum adsorption capacity of potentially toxic metal onto the adsorbent and primary adsorption mechanism,

Chao and Chen ([2012](#)) defined a parameter α as the ratio of Q^o_{max} to CEC. If the adsorption process only involves ion exchange, the α value is unity (Chao and Chang, 2012; Tran and Chao, 2018b). In contrast, the external cation exchange capacity (ECEC) plays a vital role in estimating the maximum adsorption capacity of adsorbent to toxic anionic metal and parameter β is defined as the ratio of Q^o_{max} to ECEC (Chao and Chen, 2012). Although the CEC and ECEC values of leaf-based biosorbents play a deciding role in estimating the maximum adsorption capacity of potentially toxic metals onto adsorbents and primary adsorption mechanism, these important properties were not reported in the literature. Therefore, we summarized the α and β values of other adsorbents with similar ion exchange characteristics such as zeolite and agricultural waste-based biosorbents (**Table S16**).

Thirdly, many researchers applied the EDS technique (**Figure S3b–c**) to quantitatively analyze the presence of ion exchange by comparing the EDS spectra of the adsorbent before and after adsorption of divalent toxic metals (Hanafiah et al., 2009; Iqbal et al., 2009; Muhammad et al., 2009; Yuvaraja et al., 2012; Zhang et al., 2015). For example, Chen et al. ([2010](#)) found that the intensity of the Ca, Na, K, and S peaks in the EDS spectrum decreased after copper adsorption and copper peaks are visible in the spectrum. They suggested that ion exchange is an integral part of the adsorption process. Similarly, Yuvaraja et al. ([2012](#)) concluded that several light metal cations (Ca^{2+}, Mg^{2+}, and Na^+) disappeared from the EDX spectrum of Cu(II)-laden biosorbent, suggesting the involvement of an ion exchange mechanism in the adsorption process.

Similar to the EDS technique, the advanced instrumental analyses of XRF are also used to quantitatively identify ion exchange (Dabbagh et al., 2016; Zahedi et al., 2015). For example, Dabbagh et al. ([2016](#)) concluded that the changed Mg^{2+} and Ca^{2+} ions possibly resulted from ion exchange or replacing cobalt ions with such ions. They found that the composition of CaO and MgO (42.3% and 4.9%, respectively) significantly decreased after adsorption (16.1% and 0.97%, respectively).

Lastly, some authors used the magnitude of the mean adsorption energy (E; calculated from the Dubinin–Radushkevich equation) to propose whether the adsorption process primarily involved

ion exchange. More relevant information on such equations has been discussed in our recent work (Tran et al., 2016; Tran et al., 2017b). As acknowledged by many researchers, the adsorption energy of physical adsorption often ranges from 1–8 kJ/mol, while an ion exchange process usually involves a higher adsorption energy (8–16 kJ/mol). For example, Hanafiah and Ngah (2009) investigated the Cu(II) removal process by HCl-treated rubber leaves. Based on the EDS data (no Ca peak detected in the EDS spectrum after adsorption) and E value (12.7–14.4 kJ/mol at different leaf particle sizes), they concluded that the main adsorption mechanism is ion exchange. In addition, Ngah and Hanafiah (2008) proposed that ion exchange is primarily responsible for Cu(II) biosorption onto NaOH-treated rubber leaves because (1) the E value was 8.8 kJ/mol and (2) the ratio of adsorbed cations (Cu^{2+}) to cations (H^+, Na^+, Ca^{2+}, and Mg^{2+}) released from the leaves was almost unity. Similarly, Chen et al. (2010) pointed out that the E values at different temperatures (302–332 K) range from 10.0 to 11.6 kJ/mol. Based on a combination of the analysis of EDS and FTIR data, they also concluded that ion exchange is the primary Cu(II) biosorption mechanism of camphor leaves. Similar results were reported by Hanafiah et al. (2009) for Cu(II) biosorption onto NaOH-treated weed leaves (14.1–14.4 kJ/mol at 300–310 K); by Brahman et al. (2016) for biosorption of inorganic arsenic species onto rohida leaves [15.8 kJ/mol for As(III) and 12.9 kJ/mol for As(V)]; by Hymavathi and Prabhakar (2017) for Co(II) biosorption onto banyan leaves (12.9 kJ/mol); and by Sawalha et al. (2006) for Cr(III), Cr(VI), and Cd(II) adsorption onto saltbush leaves (10.8, 9.5, and 9.1 kJ/mol, respectively).

7.5. Identifying the reduction mechanism

The reduction mechanism during adsorption mainly involves certain redox active elements such as chromium. This type of mechanism is also known as "adsorption-coupled reduction". **Figure 9** shows the potential adsorption mechanisms of Cr(VI) on the biosorbents presented in the literature. The adsorption–reduction mechanism can be summarized as follows: (1) Cr(VI) anions are electrostatically attracted by the positively charged adsorbent surface (i.e., —NH_3^+ or —OH_2^+) when $pH_{solution} < pH_{PZC}$ or pH_{IEP}; and (2) Cr(VI) anions are directly reduced to Cr(III) cations when they are in contact with electron donor groups of the adsorbent (i.e., amino and carboxylic groups) under

strongly acidic conditions. Notably, the converted Cr(III) cations were neither retained in the functional groups on the adsorbent surface through the complexation of converted Cr(III) with the adjacent functional groups capable of Cr-binding nor released (desorbed) to the solution due to electrostatic repulsion between the positively charged groups and Cr(III) cations (Gagrai et al., 2013; Gardea-Torresdey et al., 2000; Mohan and Pittman, 2006; Park et al., 2006;2005; Qi et al., 2016; Zhou et al., 2016).
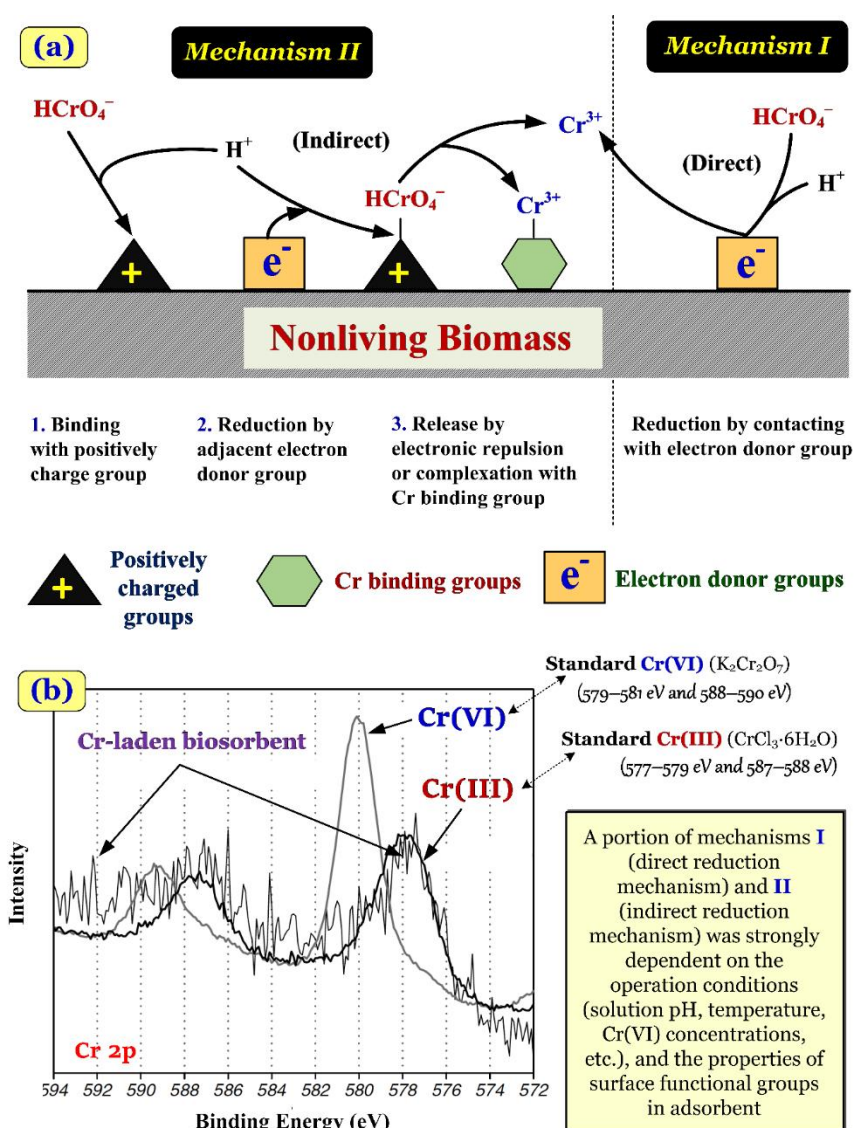
Figure 9. (a) Mechanisms proposed for Cr(VI) biosorption by nonliving biomass (Park et al. 2005) [License number: 4440510789887]; and (b) high-resolution spectra collected from the Cr 2p core regions of the Cr-laden biosorbent derived from Korean red pine tree leaves as well as standard Cr(III) and Cr(VI) chemicals (Park et al., 2011) [License number: 4435931207985]

In the aqueous phase, Cr(III) and Cr(VI) are the prevalent species. Meanwhile, hexavalent ($HCrO_4^-$ and $Cr_2O_7^{2-}$) and trivalent (Cr^{3+} and $CrOH^{2+}$) chromium species are dominant in industrial wastewater (Park et al., 2005). In addition, Aoyama and Tsuda (2001) reported that the hydrogen chromate ion ($HCrO_4^-$) is the dominant anionic chromium species in the solution when the initial pH of $K_2Cr_2O_7$ solution ranges from 1.0 to 5.0 [see Cr(VI) speciation diagram as a function of the pH in **Figure S16**]. This is similar to the assumption of other scholars (Abdolali et al., 2014; Aoyama, 2003b; Park et al., 2004;2005; Weng et al., 2006). Previous studies demonstrated that biomass-derived biosorbent can reduce toxic Cr(VI) to less toxic Cr(III). Aqueous Cr(VI) commonly exists as five species: H_2CrO_4, $HCrO_4^-$, CrO_4^{2-}, $Cr_2O_7^{2-}$, and $HCr_2O_7^-$ (Abdolali et al., 2014; Mukherjee et al., 2016; Park et al., 2004). It has been noted that protons and electrons are consumed during the reduction of Cr(VI), as presented in Equations 2–5. Therefore, the reduction of Cr(VI) to Cr(III) occurs in a strongly acidic environment.

$$Cr_2O_7^{2-} + 14H^+ + 6e^- \leftrightarrow 2Cr^{3+} + 7H_2O \qquad E° = +1.33 \text{ V} \qquad (2)$$

$$CrO_4^{2-} + 8H^+ + 3e^- \leftrightarrow Cr^{3+} + 4H_2O \qquad E° = +1.48 \text{ V} \qquad (3)$$

$$HCrO_4^- + 7H^+ + 3e^- \leftrightarrow Cr^{3+} + 4H_2O \qquad E° = +1.35 \text{ V} \qquad (4)$$

$$H_2CrO_4 + 6H^+ + 3e^- \leftrightarrow Cr^{3+} + 4H_2O \qquad E° = +1.33 \text{ V} \qquad (5)$$

Generally, when Cr(VI) oxyanions in solution are in contact with organic substances or reducing agents (especially in an acidic medium), the Cr(VI) species are easily reduced to Cr(III) species because of the redox reaction (Aoyama et al., 2000b) because Cr(VI) has a high redox (oxidation/reduction) potential (often higher than +1.3 V) under standard conditions (Park et al., 2005). As reported in the literature, when Cr(VI) oxyanions are in contact with electron donor groups of the biosorbent (i.e., amino and carboxylic groups), Cr(VI) spontaneously reduces to Cr(III). The electron-donor groups must have a reduction potential lower than 1.3 V. This mechanism is called direct reduction (**Figure 9a**).

Interestingly, the Cr(IV) concentration is often determined with the colorimetric method. The

pink-colored complex, which was formed from 1,5-diphenylcarbazide and chromium ions in an acidified solution, can be spectrophotometrically analyzed at 540 nm. Meanwhile, the total Cr concentration can be determined as follows: Cr(III) is converted to Cr(VI) at high temperature (130 –140 °C) and an oxidation treatment with $KMnO_4$ is performed before the 1,5-diphenylcarbazide reaction. The Cr(III) concentration can be calculated from the difference between the total Cr and Cr(VI) concentrations (Park et al., 2008; Singh et al., 2009).

Generally, some organic carbons of the adsorbent are completely oxidized into inorganic carbon (i.e., HCO_3^- and CO_2) during Cr(IV) reduction. The reduction rate of Cr(VI) to Cr(III) strongly depends on the $pH_{solution}$. The reduction rate of Cr(VI) decreases with increasing $pH_{solution}$ because the proton consumption decreases during Cr(VI) reduction **(Table S17).** For example, Aoyama et al. (1999) found that approximately 33% Cr(VI) are reduced to Cr(III) at pH 2.0 during the adsorption process by coniferous leaves because of increased proton consumption in the acidic solution. However, the reduction rate of Cr(VI) seems negligible when the $pH_{solution}$ is higher than 3.0, which agrees with the findings of other studies (Abdolali et al., 2014; Aoyama, 2003a; Aoyama and Tsuda, 2001). Notably, Abdolali et al. (2014) concluded that a reduction of Cr(VI) to Cr(III) did not occur in the absence of the biosorbent.

Furthermore, XPS, X-ray absorption spectroscopy (XAS), and extended X-ray absorption fine structure (EXAFS) analysis are three useful advanced techniques to ascertain the oxidation state of the chromium bound on the biomass-derived adsorbent. For example, Gardea-Torresdey et al. (2000) studied the Cr(VI) binding and reduction to Cr(III) by oat biomass (containing different ligands). Their XAS analysis indicated that the biomass catalyzes the reduction of the much more toxic (VI) state of chromium to the less toxic (III) state. The EXAFS study indicated that the reduced Cr(III) is bound to the oxygen-containing functional group (possibly carboxyl groups) on the biomass surface. Meanwhile, based on the XPS data, Zhou et al. (2016) concluded that the binding energies at 577.2 and 579.2 eV (in the Cr $2p_{3/2}$ orbitals) correspond to Cr(III) and Cr(VI) after Cr(VI) adsorption. The results indicated that the Cr(III) and Cr(VI) ions coexist on the surface of the adsorbent, with the

former and the latter accounting for 93.33% and 6.67%, respectively. This result agrees with that of other investigators (Dambies et al., 2001; Park et al., 2011; Qi et al., 2016). Notably, the Cr 2p3/2 and Cr 2p1/2 binding energies of Cr(VI) and Cr(III) chemicals were thoroughly reviewed by (Tran (2019) to avoid the undesirable mistakes and the propagation of incorrect information in the scientific literature.

Notably, Park et al. (2007) applied sixteen natural biomaterials (i.e., pine needle, pine cone, rice husk, pine bark, sawdust, fungal biomass of Rhizopus, walnut shell, green tea waste, peanut shell, banana skin, orange peel, oak leaf, rice straw, seaweed biomasses of *Sargassum*, *Ecklonia*, and *Enteromorpha*) to thoroughly investigate the adsorption-coupled reduction mechanism of Cr(VI) removal from aqueous solution. Based on the XPS data before and after adsorption, they concluded that the spectra of the Cr-adsorbed biomaterials are consistent with that of the standard Cr(III) compound (CrCl$_3$•6H$_2$O). This suggests that the chromium bound to the surface of the selected sixteen biosorbents was mainly or totally in Cr(III) form. Therefore, the evidence indicates that the removal mechanism of Cr(VI) by natural biosorbents is an adsorption-coupled reduction.

Similarly, Park et al. (2011) applied the emerging XPS technique to propose the adsorption-coupled reduction mechanism for the removal of Cr(VI) or total Cr by the leaves of *Pinus densiflora*. They compared the XPS spectrum of Cr-loaded biosorbents and standard Cr(III) compounds (CrCl$_3$•6H$_2$O) and standard Cr(VI) compounds (K$_2$Cr$_2$O$_7$) in the Cr 2p core regions. The direct comparison demonstrated that the spectrum of the Cr-loaded biosorbent matches that of the standard Cr(III) compound (**Figure 9b**). An analogous conclusion was proposed by Qi et al. (2016).

7.6. Identification of functional groups relevant for the adsorption mechanism

Similar to lignocellulose-derived biosorbent, leaf-based biosorbents exhibit abundant functional groups on their surface, which have been regarded as active groups important for the adsorption of various adsorbates (i.e., potentially toxic metals and dyes). However, the functional

properties of each biosorbent are unique and the functionality, which is part of the adsorption process, is generally dissimilar. Compared with the XPS technique, the FTIR technique is widely used for the identification of the main functional groups of certain adsorbents. The main functionality corresponding to the adsorption process can be identified by comparing the FTIR spectra of pristine and laden adsorbents.

7.6.1. Adsorption of potentially toxic metals, fluoride, uranium, and ammonium

The potential adsorption mechanisms between toxic metals and biosorbents are illustrated in **Figure 10**. The electrostatic attraction, complexation and ion exchange were regarded as the main adsorption mechanisms. These mechanisms highly correlated with the functional groups and element composites on the surface of biosorbents.

M^{2+} represents Cu^{2+}, Pb^{2+}, Zn^{2+}, Ni^{2+}, and Cd^{2+}
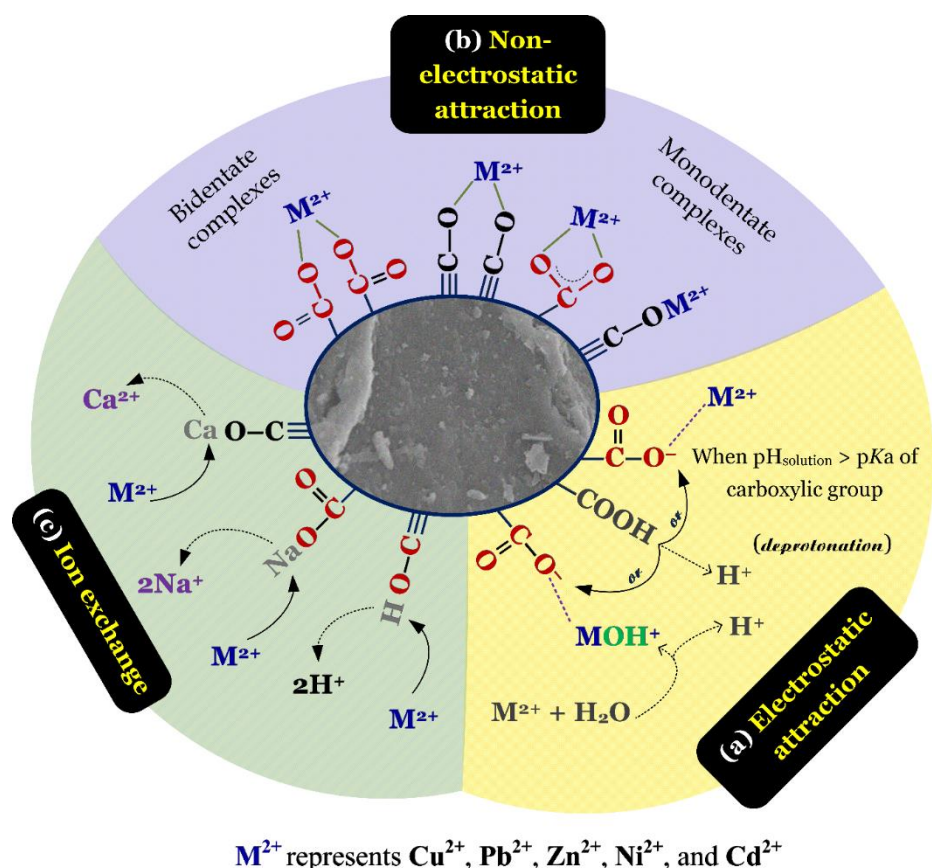
Figure 10. The potential adsorption mechanisms between toxic metals and biosorbents (Tran and Chao, 2018a) [License number: 4525340872276]

Because of the length limitation required by the journal, more information on adsorption of

potentially toxic metals, fluoride, uranium, and ammonium is summarized in **Section S7**. For example, Rao and Khan (2017) compared the FTIR spectrum of Boston fern leaves before and after Cu(II) adsorption, concluding that the peak shifts from 3391 to 3397 cm^{-1} (—OH), 1244 to 1246 cm^{-1} (C=O), and 534 to 537 cm^{-1} (C–H) are due to the binding of Cu(II) ions with carboxyl and hydroxyl groups. Similarly, some authors proposed that the hydroxyl, carbonyl, and carboxyl groups greatly contribute to binding Cu(II) ions onto grey nicker leaves (Yuvaraja et al., 2012), Cr(VI) onto mango leaves (Saha and Saha, 2014), Cd(II) and Pb(II) onto mango peel (Iqbal et al., 2009), Ni(II) and Zn(II) onto grapefruit peel (Muhammad et al., 2009), and Cd(II) onto guava leaves (Rao et al., 2010a) and teak leaves (Srinivasa Rao et al., 2010).

A comprehensive study on the application of FTIR and electron paramagnetic resonance (EPR) to identify the main functional groups participating in Cu(II) biosorption onto dried leaves was conducted by Carvalho et al. (2003). Based on their FTIR analysis, the molecular bonds affected by the existence of the copper ions are C=C, C–H, and O–H bonds; these are all present in the carbon rings of the biosorbent. The EPR analysis indicated that Cu(II) ions are incorporated into the biosorbent, at sites with strong axial symmetry (**Figure S17**).

7.6.2. Dye adsorption

Figure 11 indicates the typical interactions contributing to the adsorption of cationic methylene green 5 dye onto biosorbent. Similarly, the functional groups can determine the adsorption capacities of dyes on the biosorbent. Dissimilar to the adsorption of potentially toxic metals, the adsorption mechanism of organic compounds onto the adsorbent can be determined by comparing the FTIR spectra of the adsorbent before and after adsorption. For example, Tran et al. (2017c) studied the adsorption mechanism of cationic methylene green 5 onto various biosorbents. Based on adsorption (effect of pH, NaCl salt, temperature, and initial dye concentration) and desorption studies and FTIR analysis, they proposed that the primary involved adsorption mechanisms are electrostatic attraction, dipole–dipole and Yoshida hydrogen bonding formations, and n–π interaction. Their FTIR spectra verified that the –OH, C=O, and C–O peaks shift and decrease in intensity after dye adsorption.
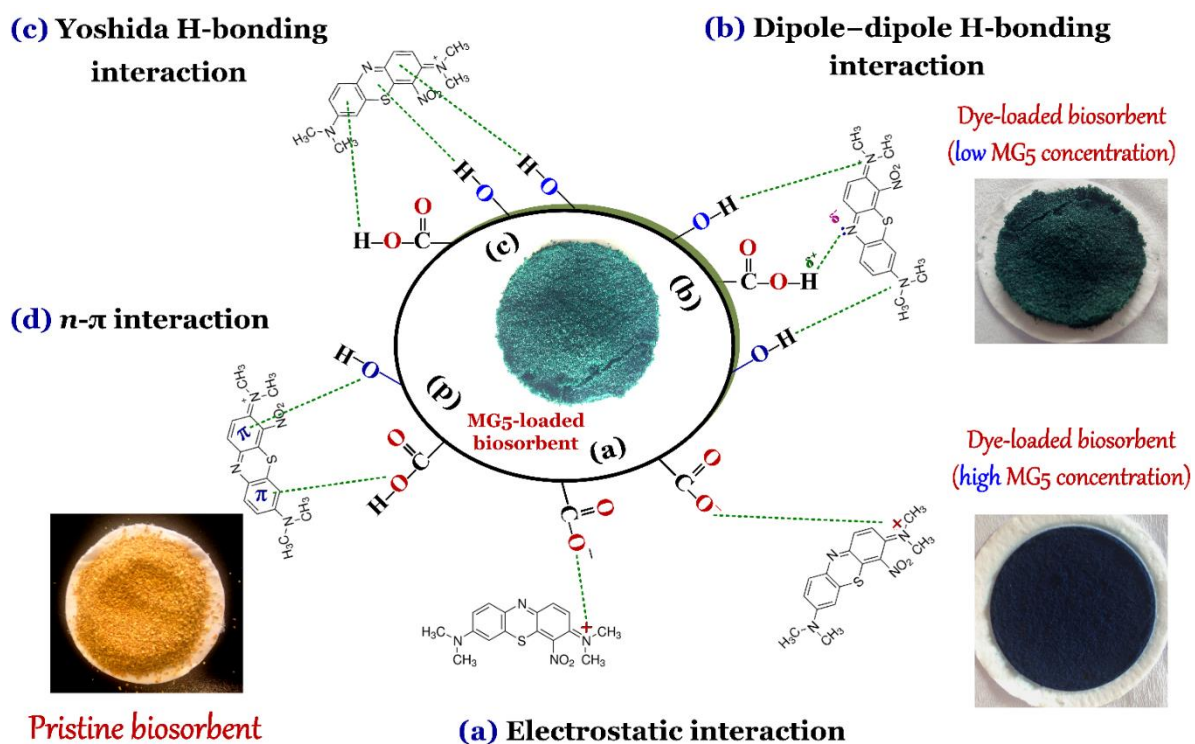
Figure 11. Typical interactions contributing to the adsorption of cationic methylene green 5 dye onto biosorbent (Tran et al., 2017c) License number: 4435940108341]

Based on FTIR spectral analysis, Saha et al. (2012) suggested the major role of the C=O, O–H, and C–O groups in the biosorption of crystal violet dye onto jackfruit leaves. Similarly, Setiabudi et al. (2016) concluded that the C=O, C–O, O–H, and C–H groups play a vital role in removing cationic methylene blue using oil palm leaves. Its performance has been documented by other scholars (Han et al., 2011; Han et al., 2014; Jain and Gogate, 2017c; Lafi et al., 2015; Lim et al., 2016; Tamez Uddin et al., 2009; Zhu et al., 2016).

8. Conclusions

Based on the viewpoints discussed in the literature and this study, it can be concluded that:

• The leaves by-products can be made ready for sorption usages by several consecutive simple steps, i.e., thoroughly washing of raw material with water, drying under controlled temperature and time, grounding the material to attain a specific particle size and, if needed, pre-treating of

61

the material for lessening the leaching problems.

• Leaf-based biosorbents are nonporous materials with average S_{BET} and V_{total} values of 9.9±13.4 m^2/g ($n = 60$) and 0.019±0.027 cm^3/g ($n = 25$), respectively. Therefore, the pore filling mechanism was ruled out in the adsorption study of contaminants.

• Depending on the unique surface chemistry properties of the biosorbent, the adsorption affinity and mechanism of each biosorbent are dissimilar. Among the existing functional groups on the biosorbent surface, the carboxylic group (—COOH) plays a more important role in interacting with various contaminants than the amino (—NH$_2$), sulfhydryl (—SH), and phenolic (—OH) groups.

• Leaf-based biosorbents (pristine and modified/treated) have been used as promising adsorbents to remove potentially toxic cationic metal and oxyanionic metal ions, organic cationic and anionic dyes, radioactive metal ions, rare earth elements, phosphate, ammonium, and fluoride.

• The adsorption process rapidly reaches an equilibrium (approximately 60–180 min for almost all contaminants). The optimal pH value strongly depends on the target adsorbate; acidic conditions are favorable for anionic adsorbate biosorption, while neutral or alkaline conditions are favorable for cationic adsorbate biosorption. The presence of specific salts (i.e., NaCl and NaNO$_3$) causes a significant decrease in the adsorption capacity of the biosorbent to most adsorbates.

• The characteristic thermodynamic parameters for the biosorption process using pristine and modified leaves are ΔG <0 (96%, $n = 46/48$), ΔH >0 (83%, $n = 40/48$), and ΔS >0 (88%, $n = 42/48$) for toxic metal ions and ΔG <0 (84%, $n = 38/45$), ΔH >0 (55%, $n = 25/45$), and ΔS >0 (53%, $n = 24/45$) for organic dyes.

• Among toxic metals, copper is adsorbed most by the biosorbent in both single and multi-component adsorption studies.

• Desorption studies indicate that the adsorption process of contaminants onto the biosorbent is normally reversible when the primary adsorption mechanism is electrostatic attraction and/or ion exchange.

• The removal efficiency of potentially toxic metals from the water samples collected from different industrial effluents by leaves ranges from 65% to 99.8%, depending on the operation conditions.

• Electrostatic attraction plays an important role in the adsorption of most adsorbates. Ion exchange mainly involves the adsorption process of potentially toxic cationic metals and ammonium. The adsorption mechanism of Cr(VI) is regarded to be adsorption-coupled reduction. Meanwhile, the hydrogen bond formation and n–π interaction are primarily responsible for the adsorption of most organic dyes.

Nontoxic leaf-derived biosorbents are promising dual-electronic adsorbents for the removal of various anionic and cationic adsorbates from water media. However, in order to take advantages of these sorbents in real treatment plants, future studies should address the limitations which confront their full-scale usages. For example, such studies should consider the strategies by which the leaching of organic chemicals can be satisfactorily lessened, the reusability of biosorbents after regeneration via suitable cheap manners, and their performances towards real waters and wastewaters, as well as exploring adequate safe methods for their end-of-life disposal or exploiting the possibility of using the exhausted sorbents for other purposes.

References

Abdel-Ghani, N.T., Hegazy, A.K. and El-Chaghaby, G.A., 2009. Typha domingensis leaf powder for decontamination of aluminium, iron, zinc and lead: Biosorption kinetics and equilibrium modeling. *International Journal of Environmental Science & Technology, 6*, 243-248.

Abdolali, A., Guo, W.S., Ngo, H.H., Chen, S.S., Nguyen, N.C. and Tung, K.L., 2014. Typical lignocellulosic wastes and by-products for biosorption process in water and wastewater

treatment: A critical review. *Bioresource Technology, 160*, 57-66.

Abdolali, A., Ngo, H.H., Guo, W., Lu, S., Chen, S.-S., Nguyen, N.C., Zhang, X., Wang, J. and Wu, Y., 2016. A breakthrough biosorbent in removing heavy metals: Equilibrium, kinetic, thermodynamic and mechanism analyses in a lab-scale study. *Science of The Total Environment, 542*, 603-611.

Abedi, S., Zavvar Mousavi, H. and Asghari, A., 2016. Investigation of heavy metal ions adsorption by magnetically modified aloe vera leaves ash based on equilibrium, kinetic and thermodynamic studies. *Desalination and Water Treatment, 57*, 13747-13759.

Agarry, S.E., Ogunleye, O.O. and Aworanti, O.A., 2013. Biosorption equilibrium, kinetic and thermodynamic modelling of naphthalene removal from aqueous solution onto modified spent tea leaves. *Environmental Technology, 34*, 825-839.

Ahmad, A., Ghazi, Z.A., Saeed, M., Ilyas, M., Ahmad, R., Muqsit Khattak, A. and Iqbal, A., 2017. A comparative study of the removal of Cr(VI) from synthetic solution using natural biosorbents. *New Journal of Chemistry, 41*, 10799-10807.

Al-Haidary, A.M.A., Zanganah, F.H.H., Al-Azawi, S.R.F., Khalili, F.I. and Al-Dujaili, A.H., 2011. A study on using date palmfibers and leaf base of palm as adsorbents for Pb(II) ions from its aqueous solution. *Water, Air, & Soil Pollution, 214*, 73-82.

Al-Masri, M.S., Amin, Y., Al-Akel, B. and Al-Naama, T., 2010. . Biosorption of cadmium, lead, and uranium by powder of poplar leaves and branches. *Applied Biochemistry and Biotechnology, 160*, 976-987.

Al Rmalli, S.W., Dahmani, A.A., Abuein, M.M. and Gleza, A.A., 2008. Biosorption of mercury from aqueous solutions by powdered leaves of castor tree (*Ricinus communis* L.). *Journal of Hazardous Materials, 152*, 955-959.

Ali, I. and Gupta, V.K., 2007. Advances in water treatment by adsorption technology. *Nature protocols, 1*, 2661.

Ali, R.M., Hamad, H.A., Hussein, M.M. and Malash, G.F., 2016. Potential of using green adsorbent of heavy metal removal from aqueous solutions: Adsorption kinetics, isotherm, thermodynamic, mechanism and economic analysis. *Ecological Engineering, 91*, 317-332.

Amarasinghe, B.M.W.P.K. and Williams, R.A., 2007. Tea waste as a low cost adsorbent for the

removal of Cu and Pb from wastewater. *Chemical Engineering Journal, 132*, 299-309.

Amin, M., Alazba, A. and Shafiq, M., 2017. Batch and fixed-bed column studies for the biosorption of Cu (II) and Pb (II) by raw and treated date palm leaves and orange peel. *Global Nest Journal, 19*, 464-478.

Amirnia, S., Ray, M.B. and Margaritis, A., 2016. Copper ion removal by *Acer saccharum* leaves in a regenerable continuous-flow column. *Chemical Engineering Journal, 287*, 755-764.

Ansari, S.A., Khan, F. and Ahmad, A., 2016. Cauliflower leave, an agricultural waste biomass adsorbent, and its application for the removal of MB dye from aqueous solution: Equilibrium, kinetics, and thermodynamic studies. *International Journal of Analytical Chemistry, 2016*, 10.

Anwar, J., Shafique, U., Waheed uz, Z., un Nisa, Z., Munawar, M.A., Jamil, N., Salman, M., Dar, A., Rehman, R., Saif, J., Gul, H. and Iqbal, T., 2011. Removal of chromium on *Polyalthia longifolia* leaves biomass. *International Journal of Phytoremediation, 13*, 410-420.

Aoyama, M., 2003a. Comment on "Biosorption of chromium(VI) from aqueous solution by cone biomass of *Pinus sylvestris*". *Bioresource Technology, 89*, 317-318.

Aoyama, M., 2003b. Removal of Cr(VI) from aqueous solution by London plane leaves. *Journal of Chemical Technology & Biotechnology, 78*, 601-604.

Aoyama, M., Sugiyama, T., Doi, S., Cho, N.S. and Kim, H.E., 1999. Removal of hexavalent chromium from dilute aqueous solution by coniferous leaves. *Holzforschung*, 365.

Aoyama, M. and Tsuda, M., 2001. Removal of Cr(VI) from aqueous solutions by larch bark. *Wood Science and Technology, 35*, 425-434.

Aoyama, M., Tsuda, M., Cho, N.-S. and Doi, S., 2000a. Adsorption of trivalent chromium from dilute solution by conifer leaves. *Wood Science and Technology, 34*, 55-63.

Aoyama, M., Tsuda, M., Seki, K., Doi, S., Kurimoto, Y. and Tamura, Y., 2000b. Adsorption of Cr(VI) from Dichromate Solutions onto Black Locust Leaves. *Holzforschung*, 340.

Arshad, M., Zafar, M.N., Younis, S. and Nadeem, R., 2008. The use of Neem biomass for the biosorption of zinc from aqueous solutions. *Journal of Hazardous Materials, 157*, 534-540.

Babić, B.M., Milonjić, S.K., Polovina, M.J. and Kaludierović, B.V., 1999. Point of zero charge and intrinsic equilibrium constants of activated carbon cloth. *Carbon, 37*, 477-481.

Babu, B.V. and Gupta, S., 2008. Adsorption of Cr(VI) using activated neem leaves: kinetic studies. *Adsorption, 14*, 85-92.

Bajpai, S.K. and Jain, A., 2012. Equilibrium and thermodynamic studies for adsorption of crystal violet onto spent tea leaves (STL). *Water, 4*, 52-71.

Baruah, S., Devi, A., Bhattacharyya, K.G. and Sarma, A., 2017. Developing a biosorbent from *Aegle Marmelos* leaves for removal of methylene blue from water. *International Journal of Environmental Science and Technology, 14*, 341-352.

Batool, F., Iqbal, S. and Akbar, J., 2017. Impact of metal ionic characteristics on adsorption potential of *Ficus carica* leaves using QSPR modeling. *Journal of Environmental Science and Health, Part B*, 1-6.

Bharali, R.K. and Bhattacharyya, K.G., 2015. Biosorption of fluoride on Neem (*Azadirachta indica*) leaf powder. *Journal of Environmental Chemical Engineering, 3*, 662-669.

Bhattacharyya, K.G. and Sarma, A., 2003. Adsorption characteristics of the dye, Brilliant Green, on Neem leaf powder. *Dyes and Pigments, 57*, 211-222.

Bhattacharyya, K.G., Sarma, A. and Sarma, J., 2010. Adsorption of Cu(II) ions onto a cellulosic biosorbent, *Azadirachta Indica* leaf powder: Application in water treatment. *Adsorption Science & Technology, 28*, 869-883.

Bhattacharyya, K.G., Sarma, J. and Sarma, A., 2009. *Azadirachta indica* leaf powder as a biosorbent for Ni(II) in aqueous medium. *Journal of Hazardous Materials, 165*, 271-278.

Bhattacharyya, K.G. and Sharma, A., 2004. Adsorption of Pb(II) from aqueous solution by *Azadirachta indica* (Neem) leaf powder. *Journal of Hazardous Materials, 113*, 97-109.

Boparai, H.K., Joseph, M. and O'Carroll, D.M., 2011. Kinetics and thermodynamics of cadmium ion removal by adsorption onto nano zerovalent iron particles. *Journal of Hazardous Materials, 186*, 458-465.

Brahman, K.D., Kazi, T.G., Afridi, H.I., Baig, J.A., Abro, M.I., Arain, S.S., Ali, J. and Khan, S., 2016. Simultaneously removal of inorganic arsenic species from stored rainwater in arsenic endemic area by leaves of *Tecomella undulata*: A multivariate study. *Environmental Science and Pollution Research, 23*, 15149-15163.

Carvalho, d.R.P., Freitas, J.R., de Sousa, A.M.G., Moreira, R.L., Pinheiro, M.V.B. and Krambrock, K., 2003. Biosorption of copper ions by dried leaves: chemical bonds and site symmetry. *Hydrometallurgy, 71*, 277-283.

Cavas, L., Karabay, Z., Alyuruk, H., Doğan, H. and Demir, G.K., 2011. Thomas and artificial neural network models for the fixed-bed adsorption of methylene blue by a beach waste *Posidonia oceanica* (L.) dead leaves. *Chemical Engineering Journal, 171*, 557-562.

Çay, S., Uyanık, A. and Özaşık, A., 2004. Single and binary component adsorption of copper(II) and cadmium(II) from aqueous solutions using tea-industry waste. *Separation and Purification Technology, 38*, 273-280.

Çekim, M., Yildiz, S. and Dere, T., 2015. Biosorption of copper from synthetic waters by using tobacco leaf: Equilibrium, inetic and thermodynamic tests. *Journal of Environmental Engineering and Landscape Management, 23*, 172-182.

Cengiz, S. and Cavas, L., 2010. A promising evaluation method for dead leaves of *Posidonia oceanica* (L.) in the adsorption of methyl violet. *Marine Biotechnology, 12*, 728-736.

Copello, G.J., Garibotti, R.E., Varela, F., Tuttolomondo, M.V. and Diaz, L.E., 2011. Exhausted yerba mate leaves (*Ilex Paraguariensis*) as biosorbent for the removal of metals from aqueous solutions. *Journal of the Brazilian Chemical Society, 22*, 790-795.

Chakraborty, S., Chowdhury, S. and Saha, P.D., 2012. Insight into biosorption equilibrium, kinetics and thermodynamics of crystal violet onto *Ananas comosus* (pineapple) leaf powder. *Applied Water Science, 2*, 135-141.

Chakravarty, S., Mohanty, A., Sudha, T.N., Upadhyay, A.K., Konar, J., Sircar, J.K., Madhukar, A. and Gupta, K.K., 2010. Removal of Pb(II) ions from aqueous solution by adsorption using bael leaves (*Aegle marmelos*). *Journal of Hazardous Materials, 173*, 502-509.

Chang, Y., Lai, J.-Y. and Lee, D.-J., 2016. Thermodynamic parameters for adsorption equilibrium of heavy metals and dyes from wastewaters: Research updated. *Bioresource Technology, 222*, 513-516.

Chao, H.-P. and Chang, C.-C., 2012. Adsorption of copper(II), cadmium(II), nickel(II) and lead(II) from aqueous solution using biosorbents. *Adsorption, 18*, 395-401.

Chao, H.-P., Chang, C.-C. and Nieva, A., 2014. Biosorption of heavy metals on Citrus maxima peel,

passion fruit shell, and sugarcane bagasse in a fixed-bed column. *Journal of Industrial and Engineering Chemistry, 20*, 3408-3414.

Chao, H.-P. and Chen, S.-H., 2012. Adsorption characteristics of both cationic and oxyanionic metal ions on hexadecyltrimethylammonium bromide-modified NaY zeolite. *Chemical Engineering Journal, 193-194*, 283-289.

Chen, H., Dai, G., Zhao, J., Zhong, A., Wu, J. and Yan, H., 2010. Removal of copper(II) ions by a biosorbent—*Cinnamomum camphora* leaves powder. *Journal of Hazardous Materials, 177*, 228-236.

Chen, J.P. and Yang, L., 2006. Study of a heavy metal biosorption onto raw and chemically modified *Sargassum* sp. via spectroscopic and modeling analysis. *Langmuir, 22*, 8906-8914.

Chen, L., Ramadan, A., Lü, L., Shao, W., Luo, F. and Chen, J., 2011. Biosorption of methylene blue from aqueous solution using lawny grass modified with citric acid. *Journal of Chemical & Engineering Data, 56*, 3392-3399.

Chen, Y., Tang, G., Yu, Q.J., Zhang, T., Chen, Y. and Gu, T., 2009. Biosorption properties of hexavalent chromium on to biomass of tobacco-leaf residues. *Environmental Technology, 30*, 1003-1010.

Cheraghi, E., Ameri, E. and Moheb, A., 2015. Adsorption of cadmium ions from aqueous solutions using sesame as a low-cost biosorbent: kinetics and equilibrium studies. *International Journal of Environmental Science and Technology, 12*, 2579-2592.

Chojnacka, K., Chojnacki, A. and Górecka, H., 2005. Biosorption of Cr^{3+}, Cd^{2+} and Cu^{2+} ions by blue–green algae *Spirulina sp.*: Kinetics, equilibrium and the mechanism of the process. *Chemosphere, 59*, 75-84.

Chowdhury, S., Chakraborty, S. and Saha, P., 2011. Biosorption of Basic Green 4 from aqueous solution by *Ananas comosus* (pineapple) leaf powder. *Colloids and Surfaces B: Biointerfaces, 84*, 520-527.

Dabbagh, R., Ashtiani Moghaddam, Z. and Ghafourian, H., 2016. Removal of cobalt(II) ion from water by adsorption using intact and modified *Ficus carica* leaves as low-cost natural sorbent. *Desalination and Water Treatment, 57*, 19890-19902.

Dambies, L., Guimon, C., Yiacoumi, S. and Guibal, E., 2001. Characterization of metal ion

interactions with chitosan by X-ray photoelectron spectroscopy. *Colloids and Surfaces A: Physicochemical and Engineering Aspects, 177*, 203-214.

Das, P., Das, P. and Datta, S., 2016. Continuous biosorption of Malachite Green by *Ananus comosus* (pineapple) leaf powder in a fixed bed reactor: Experimental, breakthrough time and mathematical modeling. *Desalination and Water Treatment, 57*, 25842-25847.

Daud, Z., Awang, H., Kassim, M., Sari, A., Hatta, M., Zainuri, M. and Aripin, A.M., 2014. Comparison of pineapple leaf and *Cassava* peel by chemical properties and morphology characterization. *Advanced Materials Research, 974*.

Davis, J.A. and Kent, D., 1990. Surface complexation modeling in aqueous geochemistry. *Reviews in Mineralogy and Geochemistry, 23*, 177-260.

De Gisi, S., Lofrano, G., Grassi, M. and Notarnicola, M., 2016. Characteristics and adsorption capacities of low-cost sorbents for wastewater treatment: A review. *Sustainable Materials and Technologies, 9*, 10-40.

Deniz, F. and Karaman, S., 2011. Removal of Basic Red 46 dye from aqueous solution by pine tree leaves. *Chemical Engineering Journal, 170*, 67-74.

Deniz, F. and Saygideger, S.D., 2010. Equilibrium, kinetic and thermodynamic studies of Acid Orange 52 dye biosorption by *Paulownia tomentosa Steud*. leaf powder as a low-cost natural biosorbent. *Bioresource Technology, 101*, 5137-5143.

Deng, S., Bai and Chen, J.P., 2003. Aminated polyacrylonitrile fibers for lead and copper removal. *Langmuir, 19*, 5058-5064.

dos Santos, R.M., Neto, W.P.F., Silvério, H.A., Martins, D.F., Dantas, N.O. and Pasquini, D., 2013. Cellulose nanocrystals from pineapple leaf, a new approach for the reuse of this agro-waste. *Industrial Crops and Products, 50*, 707-714.

Dotto, G.L., Salau, N.P.G., Piccin, J.S., Cadaval, T.R.S.A. and de Pinto, L.A.A., 2017. . Adsorption kinetics in liquid phase: Modeling for discontinuous and continuous system. In A. Bonilla-Petriciolet et al. (eds.) *Adsorption Processes for Water Treatment and Purification*, 53-76). Cham: Springer International Publishing.

Dotto, G.L., Sharma, S.K. and Pinto, L.A., 2015. Biosorption of organic dyes: Research opportunities and challenges. *Green Chemistry for Dyes Removal from Wastewater: Research Trends and*

Applications, 295-329.

Dural, M.U., Cavas, L., Papageorgiou, S.K. and Katsaros, F.K., 2011. Methylene blue adsorption on activated carbon prepared from *Posidonia oceanica* (L.) dead leaves: Kinetics and equilibrium studies. *Chemical Engineering Journal, 168*, 77-85.

Escudero, L.B., Quintas, P.Y., Wuilloud, R.G. and Dotto, G.L., 2018. Recent advances on elemental biosorption. *Environmental Chemistry Letters*.

Fadzil, F., Ibrahim, S. and Hanafiah, M.A.K.M., 2016. Adsorption of lead(II) onto organic acid modified rubber leaf powder: Batch and column studies. *Process Safety and Environmental Protection, 100*, 1-8.

Ferreira, G.M.D., Ferreira, G.M.D., Hespanhol, M.C., de Paula Rezende, J., dos Santos Pires, A.C., Gurgel, L.V.A. and da Silva, L.H.M., 2017. Adsorption of red azo dyes on multi-walled carbon nanotubes and activated carbon: A thermodynamic study. *Colloids and Surfaces A: Physicochemical and Engineering Aspects, 529*, 531-540.

Fiol, N., Villaescusa, I., Martínez, M., Miralles, N., Poch, J. and Serarols, J., 2006. Sorption of Pb(II), Ni(II), Cu(II) and Cd(II) from aqueous solution by olive stone waste. *Separation and Purification Technology, 50*, 132-140.

Fomina, M. and Gadd, G.M., 2014. Biosorption: current perspectives on concept, definition and application. *Bioresource Technology, 160*, 3-14.

Fourest, E. and Volesky, B., 1995. Contribution of sulfonate groups and alginate to heavy metal biosorption by the dry biomass of *Sargassum fluitans*. *Environmental Science & Technology, 30*, 277-282.

Gagrai, M.K., Das, C. and Golder, A.K., 2013. Reduction of Cr(VI) into Cr(III) by *Spirulina* dead biomass in aqueous solution: Kinetic studies. *Chemosphere, 93*, 1366-1371.

Gardea-Torresdey, J.L., Tiemann, K.J., Armendariz, V., Bess-Oberto, L., Chianelli, R.R., Rios, J., Parsons, J.G. and Gamez, G., 2000. Characterization of Cr(VI) binding and reduction to Cr(III) by the agricultural byproducts of *Avena monida* (Oat) biomass. *Journal of Hazardous Materials, 80*, 175-188.

Georgin, J., da Silva Marques, B., da Silveira Salla, J., Foletto, E.L., Allasia, D. and Dotto, G.L., 2018. Removal of Procion Red dye from colored effluents using H2SO4-/HNO3-treated avocado

shells (*Persea americana*) as adsorbent. *Environmental Science and Pollution Research, 25*, 6429-6442.

Goertzen, S.L., Thériault, K.D., Oickle, A.M., Tarasuk, A.C. and Andreas, H.A., 2010. Standardization of the Boehm titration. Part I. CO_2 expulsion and endpoint determination. *Carbon, 48*, 1252-1261.

Goldberg, S., 2013. Surface Complexation Modeling. *Reference Module in Earth Systems and Environmental Sciences*: Elsevier.

Gowda, R., Nataraj, A. and Rao, N.M., 2012. Coconut leaves as a low cost adsorbent for the removal of nickel from electroplating effluents. *Int J Sci Eng Res, 2*, 1-5.

Guerrero-Coronilla, I., Morales-Barrera, L. and Cristiani-Urbina, E., 2015. Kinetic, isotherm and thermodynamic studies of amaranth dye biosorption from aqueous solution onto water hyacinth leaves. *Journal of Environmental Management, 152*, 99-108.

Gupta, N., Kushwaha, A.K. and Chattopadhyaya, M.C., 2012. Adsorption studies of cationic dyes onto Ashoka (*Saraca asoca*) leaf powder. *Journal of the Taiwan Institute of Chemical Engineers, 43*, 604-613.

Giannakoudakis, D.A., Kyzas, G.Z., Avranas, A. and Lazaridis, N.K., 2016. Multi-parametric adsorption effects of the reactive dye removal with commercial activated carbons. *Journal of Molecular Liquids, 213*, 381-389.

Hai, T.N., 2017. Comments on "Effect of temperature on the adsorption of methylene blue dye onto sulfuric acid–treated orange peel". *Chemical Engineering Communications, 204*, 134-139.

Hamdaoui, O., Saoudi, F., Chiha, M. and Naffrechoux, E., 2008. Sorption of malachite green by a novel sorbent, dead leaves of plane tree: Equilibrium and kinetic modeling. *Chemical Engineering Journal, 143*, 73-84.

Hamissa, A.M.B., Brouers, F., Mahjoub, B. and Seffen, M., 2007. Adsorption of textile dyes using *Agave americana* (L.) fibres: Equilibrium and kinetics modelling. *Adsorption Science & Technology, 25*, 311-325.

Hamissa, A.M.B., Lodi, A., Seffen, M., Finocchio, E., Botter, R. and Converti, A., 2010. Sorption of Cd(II) and Pb(II) from aqueous solutions onto *Agave americana* fibers. *Chemical Engineering Journal, 159*, 67-74.

Han, R., Wang, Y., Zhao, X., Wang, Y., Xie, F., Cheng, J. and Tang, M., 2009. Adsorption of methylene blue by phoenix tree leaf powder in a fixed-bed column: Experiments and prediction of breakthrough curves. *Desalination, 245*, 284-297.

Han, R., Zou, W., Yu, W., Cheng, S., Wang, Y. and Shi, J., 2007. Biosorption of methylene blue from aqueous solution by fallen phoenix tree's leaves. *Journal of Hazardous Materials, 141*, 156-162.

Han, X., Wang, W. and Ma, X., 2011. Adsorption characteristics of methylene blue onto low cost biomass material lotus leaf. *Chemical Engineering Journal, 171*, 1-8.

Han, X., Yuan, J. and Ma, X., 2014. Adsorption of malachite green from aqueous solutions onto lotus leaf: Equilibrium, kinetic, and thermodynamic studies. *Desalination and Water Treatment, 52*, 5563-5574.

Hanafiah, M.A.K.M. and Ngah, W.S.W., 2009. Preparation, characterization and adsorption mechanism of Cu(II) onto protonated rubber leaf powder. *CLEAN – Soil, Air, Water, 37*, 696-703.

Hanafiah, M.A.K.M., Zakaria, H. and Wan Ngah, W.S., 2009. Preparation, characterization, and adsorption behavior of Cu(II) Ions onto alkali-treated weed (*Imperata cylindrica*) leaf powde. *Water, Air, and Soil Pollution, 201*, 43-53.

Hossain, M.A., Kumita, M., Michigami, Y. and Mori, S., 2005. Optimization of parameters for Cr (VI) adsorption on used black tea leaves. *Adsorption, 11*, 561-568.

Hossain, M.A., Ngo, H.H., Guo, W., Zhang, J. and Liang, S., 2014a. A laboratory study using maple leaves as a biosorbent for lead removal from aqueous solutions. *Water Quality Research Journal of Canada, 49*, 195-209.

Hossain, M.A., Ngo, H.H., Guo, W.S., Nghiem, L.D., Hai, F.I., Vigneswaran, S. and Nguyen, T.V., 2014b. Competitive adsorption of metals on cabbage waste from multi-metal solutions. *Bioresource Technology, 160*, 79-88.

Hossain, M.A., Ngo, H.H., Guo, W.S. and Nguyen, T.V., 2012. Biosorption of Cu(II) from water by banana peel based biosorbent: Experiments and models of adsorption and desorption. *Journal of Water Sustainability, 2*, 87-104.

Hossain, M.A., Ngo, H.H., Guo, W.S., Nguyen, T.V. and Vigneswaran, S., 2014c. Performance of

cabbage and cauliflower wastes for heavy metals removal. *Desalination and Water Treatment, 52*, 844-860.

Huang, F.-C., Lee, C.-K., Han, Y.-L., Chao, W.-C. and Chao, H.-P., 2014. Preparation of activated carbon using micro-nano carbon spheres through chemical activation. *Journal of the Taiwan Institute of Chemical Engineers, 45*, 2805-2812.

Hymavathi, D. and Prabhakar, G., 2017. Studies on the removal of Cobalt(II) from aqueous solutions by adsorption with *Ficus benghalensis* leaf powder through response surface methodology. *Chemical Engineering Communications, 204*, 1401-1411.

Ibrahim, M.N.M., Ngah, W.S.W., Norliyana, M.S., Daud, W.R.W., Rafatullah, M., Sulaiman, O. and Hashim, R., 2010. A novel agricultural waste adsorbent for the removal of lead (II) ions from aqueous solutions. *Journal of Hazardous Materials, 182*, 377-385.

Immich, A.P.S., Ulson de Souza, A.A. and Ulson de Souza, S.M.d.A.G., 2009. Removal of Remazol Blue RR dye from aqueous solutions with Neem leaves and evaluation of their acute toxicity with *Daphnia magna*. *Journal of Hazardous Materials, 164*, 1580-1585.

Iqbal, M., Saeed, A. and Zafar, S.I., 2009. FTIR spectrophotometry, kinetics and adsorption isotherms modeling, ion exchange, and EDX analysis for understanding the mechanism of Cd^{2+} and Pb^{2+} removal by mango peel waste. *Journal of Hazardous Materials, 164*, 161-171.

Jain, S.N. and Gogate, P.R., 2017a. Acid Blue 113 removal from aqueous solution using novel biosorbent based on NaOH treated and surfactant modified fallen leaves of *Prunus Dulcis*. *Journal of Environmental Chemical Engineering, 5*, 3384-3394.

Jain, S.N. and Gogate, P.R., 2017b. Adsorptive removal of acid violet 17 dye from wastewater using biosorbent obtained from NaOH and H_2SO_4 activation of fallen leaves of *Ficus racemosa*. *Journal of Molecular Liquids, 243*, 132-143.

Jain, S.N. and Gogate, P.R., 2018. Efficient removal of Acid Green 25 dye from wastewater using activated *Prunus Dulcis* as biosorbent: Batch and column studies. *Journal of Environmental Management, 210*, 226-238.

Jain, S.N. and Gogate, P.R., 2017c. NaOH-treated dead leaves of *Ficus racemosa* as an efficient biosorbent for Acid Blue 25 removal. *International Journal of Environmental Science and Technology, 14*, 531-542.

Jalil, A.A., Triwahyono, S., Yaakob, M.R., Azmi, Z.Z.A., Sapawe, N., Kamarudin, N.H.N., Setiabudi, H.D., Jaafar, N.F., Sidik, S.M., Adam, S.H. and Hameed, B.H., 2012. Utilization of bivalve shell-treated Zea *mays L.* (maize) husk leaf as a low-cost biosorbent for enhanced adsorption of malachite green. *Bioresource Technology, 120*, 218-224.

Kahina, L. and Nasser, S.M., 2017. Adsorption of Auramine-O using activated Globe artichoke leaves: Kinetic and isotherm studies. *Asian Journal of Chemistry, 29*.

Kamar Firas, H., Nechifor Aurelia, C., Nechifor, G., Al-Musawi Tariq, J. and Mohammed Asem, H., 2017. Aqueous phase biosorption of Pb(II), Cu(II), and Cd(II) onto cabbage leaves powder *International Journal of Chemical Reactor Engineering*.

Kamaru, A.A., Sani, N.S. and Malek, N.A.N.N., 2016. Raw and surfactant-modified pineapple leaf as adsorbent for removal of methylene blue and methyl orange from aqueous solution. *Desalination and Water Treatment, 57*, 18836-18850.

Kamsonlian, S., Suresh, S., Majumder, C.B. and Chand, S., 2012. Biosorption of arsenic from contaminated water onto solid *Psidium guajava* leaf surface: Equilibrium, kinLetics, thermodynamics, and desorption study. *Bioremediation Journal, 16*, 97-112.

Kılıç, M., Yazıcı, H. and Solak, M., 2009. A comprehensive study on removal and recovery of copper(II) from aqueous solutions by NaOH-pretreated *Marrubium globosum* ssp. globosum leaves powder: Potential for utilizing the copper(II) condensed desorption solutions in agricultural applications. *Bioresource Technology, 100*, 2130-2137.

King, P., Rakesh, N., Beenalahari, S., Prasanna Kumar, Y. and Prasad, V.S.R.K., 2007. Removal of lead from aqueous solution using *Syzygium cumini* L.: Equilibrium and kinetic studies. *Journal of Hazardous Materials, 142*, 340-347.

King, P., Rakesh, N., Lahari, S.B., Kumar, Y.P. and Prasad, V.S.R.K., 2008. Biosorption of zinc onto *Syzygium cumini* L.: Equilibrium and kinetic studies. *Chemical Engineering Journal, 144*, 181-187.

Komy, Z.R., Gabar, R.M., Shoriet, A.A. and Mohammed, R.M., 2006. Characterisation of acidic sites of *Pseudomonas* biomass capable of binding protons and cadmium and removal of cadmium via biosorption. *World Journal of Microbiology and Biotechnology, 22*, 975-982.

Kong, L., Gong, L. and Wang, J., 2015. Removal of methylene blue from wastewater using fallen leaves as an adsorbent. *Desalination and Water Treatment, 53*, 2489-2500.

Krishnan, K.A. and Anirudhan, T., 2003. Removal of cadmium (II) from aqueous solutions by steam-activated sulphurised carbon prepared from sugar-cane bagasse pith: Kinetics and equilibrium studies. *Water Sa, 29*, 147-156.

Kumar, K.V., 2006. Comments on "Adsorption of acid dye onto organobentonite". *Journal of Hazardous Materials, 137*, 638-639.

Kumar, Y.P., King, P. and Prasad, V.S.R.K., 2006. Zinc biosorption on *Tectona grandis* L.f. leaves biomass: Equilibrium and kinetic studies. *Chemical Engineering Journal, 124*, 63-70.

Kuppusamy, S., Thavamani, P., Megharaj, M., Venkateswarlu, K., Lee, Y.B. and Naidu, R., 2016. Potential of *Melaleuca diosmifolia* leaf as a low-cost adsorbent for hexavalent chromium removal from contaminated water bodies. *Process Safety and Environmental Protection, 100*, 173-182.

Kushwaha, A.K., Gupta, N. and Chattopadhyaya, M.C., 2014. Removal of cationic methylene blue and malachite green dyes from aqueous solution by waste materials of *Daucus carota*. *Journal of Saudi Chemical Society, 18*, 200-207.

Khan Rao, R.A. and Khatoon, A., 2017. Aluminate treated *Casuarina equisetifolia* leaves as potential adsorbent for sequestering Cu(II), Pb(II) and Ni(II) from aqueous solution. *Journal of Cleaner Production, 165*, 1280-1295.

Khokhar, A., Siddique, Z. and Misbah, 2015. Removal of heavy metal ions by chemically treated *Melia azedarach* L. leaves. *Journal of Environmental Chemical Engineering, 3*, 944-952.

Khorshidi, N., Niazi, A. and Mohammad Nazari, B., 2015. Optimization of pyrocatechol violet biosorption by *Robinia pseudoacacia* leaf powder using response surface methodology: kinetic, isotherm and thermodynamic studies. *Journal of Water Reuse and Desalination*.

Lafi, R., Hamdi, N. and Hafiane, A., 2015. Study of the performance of Esparto grass fibers as adsorbent of dyes from aqueous solutions. *Desalination and Water Treatment, 56*, 722-735.

Li, Y., Zhang, Z., Jing, Y., Ge, X., Wang, Y., Lu, C., Zhou, X. and Zhang, Q., 2017. Statistical optimization of simultaneous saccharification fermentative hydrogen production from *Platanus* orientalis leaves by photosynthetic bacteria HAU-M1. *International Journal of Hydrogen Energy, 42*, 5804-5811.

Lim, L.B.L., Priyantha, N. and Mohamad Zaidi, N.A.H., 2016. A superb modified new adsorbent,

Artocarpus odoratissimus leaves, for removal of cationic methyl violet 2B dye. *Environmental Earth Sciences, 75*, 1179.

Lin, J., Zhan, Y. and Zhu, Z., 2011. Adsorption characteristics of copper (II) ions from aqueous solution onto humic acid-immobilized surfactant-modified zeolite. *Colloids and Surfaces A: Physicochemical and Engineering Aspects, 384*, 9-16.

Liu, H., Dong, Y., Liu, Y. and Wang, H., 2010a. Screening of novel low-cost adsorbents from agricultural residues to remove ammonia nitrogen from aqueous solution. *Journal of Hazardous Materials, 178*, 1132-1136.

Liu, H., Dong, Y., Wang, H. and Liu, Y., 2010b. Adsorption behavior of ammonium by a bioadsorbent – Boston ivy leaf powder. *Journal of Environmental Sciences, 22*, 1513-1518.

Liu, H., Dong, Y., Wang, H. and Liu, Y., 2010c. Ammonium adsorption from aqueous solutions by strawberry leaf powder: Equilibrium, kinetics and effects of coexisting ions. *Desalination, 263*, 70-75.

Mambo, M., Admire, C. and Tichaona, N., 2016. Removal of Copper from Aqueous Solution Using Chemically Treated Potato (*Solanum tuberosum*) Leaf Powder. *CLEAN – Soil, Air, Water, 44*, 488-495.

Manahan, S., 2000. *Chapter 3. Fundamentals of Aquatic Chemistry. Environmental chemistry*: CRC press.

Mohan, D. and Pittman, C.U., 2006. Activated carbons and low cost adsorbents for remediation of tri- and hexavalent chromium from water. *Journal of Hazardous Materials, 137*, 762-811.

Mohapatra, M. and Anand, S., 2007. Studies on sorption of Cd(II) on Tata chromite mine overburden. *Journal of Hazardous Materials, 148*, 553-559.

Mondal, D.K., Nandi, B.K. and Purkait, M.K., 2013. Removal of mercury (II) from aqueous solution using bamboo leaf powder: Equilibrium, thermodynamic and kinetic studies. *Journal of Environmental Chemical Engineering, 1*, 891-898.

Muhammad, I., Silke, S. and Randall, C., 2009. Mechanistic elucidation and evaluation of biosorption of metal ions by grapefruit peel using FTIR spectroscopy, kinetics and isotherms modeling, cations displacement and EDX analysis. *Journal of Chemical Technology & Biotechnology, 84*, 1516-1526.

Mukherjee, K., Ghosh, D. and Saha, B., 2016. Reliable bioremediation of hexavalent chromium from wastewater using mango leaves as reductant in association with the neutral and anionic micellar aggregation as redox accelarators. *Desalination and Water Treatment, 57*, 16919-16926.

Nag, S., Mondal, A., Mishra, U., Bar, N. and Das, S.K., 2016. Removal of chromium(VI) from aqueous solutions using rubber leaf powder: Batch and column studies. *Desalination and Water Treatment, 57*, 16927-16942.

Nakkeeran, E., Saranya, N., Giri Nandagopal, M.S., Santhiagu, A. and Selvaraju, N., 2016. Hexavalent chromium removal from aqueous solutions by a novel powder prepared from Colocasia esculenta leaves. *International Journal of Phytoremediation, 18*, 812-821.

Namasivayam, C., Muniasamy, N., Gayatri, K., Rani, M. and Ranganathan, K., 1996. Removal of dyes from aqueous solutions by cellulosic waste orange peel. *Bioresource Technology, 57*, 37-43.

Neris, J.B., Luzardo, F.H.M., da Silva, E.G.P. and Velasco, F.G., 2019. Evaluation of adsorption processes of metal ions in multi-element aqueous systems by lignocellulosic adsorbents applying different isotherms: A critical review. *Chemical Engineering Journal, 357*, 404-420.

Ngah, W.S.W. and Hanafiah, M.A.K.M., 2008. Biosorption of copper ions from dilute aqueous solutions on base treatedrubber (*Hevea brasiliensis*) leaves powder: Kinetics, isotherm, and biosorption mechanisms. *Journal of Environmental Sciences, 20*, 1168-1176.

Ngah, W.S.W. and Hanafiah, M.A.K.M., 2009. Surface modification of rubber (*Hevea brasiliensis*) leaves for the adsorption of copper ions: kinetic, thermodynamic and binding mechanisms. *Journal of Chemical Technology & Biotechnology, 84*, 192-201.

Ngo, H.H., Guo, W. and Liu, C., 2014. Biosorbent for heavy metal removal: Google Patents.

Pandey, R., Prasad, R.L., Ansari, N.G. and Murthy, R.C., 2015. Utilization of NaOH modified *Desmostachya bipinnata* (Kush grass) leaves and Bambusa arundinacea (bamboo) leaves for Cd(II) removal from aqueous solution. *Journal of Environmental Chemical Engineering, 3*, 593-602.

Park, D., Lim, S.-R., Yun, Y.-S. and Park, J.M., 2007. Reliable evidences that the removal mechanism of hexavalent chromium by natural biomaterials is adsorption-coupled reduction. *Chemosphere, 70*, 298-305.

Park, D., Yun, Y.-S., Kim, J.Y. and Park, J.M., 2008. How to study Cr(VI) biosorption: Use of fermentation waste for detoxifying Cr(VI) in aqueous solution. *Chemical Engineering Journal, 136*, 173-179.

Park, D., Yun, Y.-S., Lee, D.S. and Park, J.M., 2011. Optimum condition for the removal of Cr(VI) or total Cr using dried leaves of Pinus densiflora. *Desalination, 271*, 309-314.

Park, D., Yun, Y.-S. and Park, J.M., 2006. Mechanisms of the removal of hexavalent chromium by biomaterials or biomaterial-based activated carbons. *Journal of Hazardous Materials, 137*, 1254-1257.

Park, D., Yun, Y.-S. and Park, J.M., 2004. Reduction of Hexavalent Chromium with the Brown Seaweed Ecklonia Biomass. *Environmental Science & Technology, 38*, 4860-4864.

Park, D., Yun, Y.-S. and Park, J.M., 2005. Studies on hexavalent chromium biosorption by chemically-treated biomass of Ecklonia sp. *Chemosphere, 60*, 1356-1364.

Peng, H., Zhou, M., Yu, Z., Zhang, J., Ruan, R., Wan, Y. and Liu, Y., 2013. Fractionation and characterization of hemicelluloses from young bamboo (*Phyllostachys pubescens Mazel*) leaves. *Carbohydrate polymers, 95*, 262-271.

Percival, Z.Y.H. and Lynd, L.R., 2004. Toward an aggregated understanding of enzymatic hydrolysis of cellulose: Noncomplexed cellulase systems. *Biotechnology and Bioengineering, 88*, 797-824.

Peydayesh, M. and Rahbar-Kelishami, A., 2015. Adsorption of methylene blue onto Platanus orientalis leaf powder: Kinetic, equilibrium and thermodynamic studies. *Journal of Industrial and Engineering Chemistry, 21*, 1014-1019.

Prasad, A.L. and Thirumalisamy, S., 2013. Evaluation of the use of acacia nilotica leaf as an ecofriendly adsorbent for Cr(VI) and its suitability in real waste water: Study of residual errors. *Journal of Chemistry, 2013*, 7.

Prasad, M.N.V. and Freitas, H., 2000. Removal of toxic metals from solution by leaf, stem and root phytomass of *Quercus ilex L.* (holly oak). *Environmental Pollution, 110*, 277-283.

Qaiser, S., Saleemi, A.R. and Umar, M., 2009. Biosorption of lead from aqueous solution by *Ficus religiosa* leaves: Batch and column study. *Journal of Hazardous Materials, 166*, 998-1005.

Qi, B.C. and Aldrich, C., 2008. Biosorption of heavy metals from aqueous solutions with tobacco dust. *Bioresource Technology, 99*, 5595-5601.

Qi, W., Zhao, Y., Zheng, X., Ji, M. and Zhang, Z., 2016. Adsorption behavior and mechanism of Cr(VI) using Sakura waste from aqueous solution. *Applied Surface Science, 360*, 470-476.

Ramakul, P., Yanachawakul, Y., Leepipatpiboon, N. and Sunsandee, N., 2012. Biosorption of palladium(II) and platinum(IV) from aqueous solution using tannin from Indian almond (*Terminalia catappa* L.) leaf biomass: Kinetic and equilibrium studies. *Chemical Engineering Journal, 193-194*, 102-111.

Ramrakhiani, L., Halder, A., Majumder, A., Mandal, A.K., Majumdar, S. and Ghosh, S., 2017. Industrial waste derived biosorbent for toxic metal remediation: Mechanism studies and spent biosorbent management. *Chemical Engineering Journal, 308*, 1048-1064.

Rangabhashiyam, S., Nakkeeran, E., Anu, N. and Selvaraju, N., 2015. Biosorption potential of a novel powder, prepared from *Ficus auriculata* leaves, for sequestration of hexavalent chromium from aqueous solutions. *Research on Chemical Intermediates, 41*, 8405-8424.

Rao, K., Anand, S. and Venkateswarlu, P., 2010a. *Psidium guvajava* L. leaf powder—a potential low-cost biosorbent for the removal of cadmium(II) Ions from wastewater. *Adsorption Science & Technology, 28*, 163-178.

Rao, K.S., Anand, S. and Venkateswarlu, P., 2011a. Adsorption of cadmium from aqueous solution by *Ficus religiosa* leaf powder and characterization of loaded biosorbent. *CLEAN – Soil, Air, Water, 39*, 384-391.

Rao, K.S., Anand, S. and Venkateswarlu, P., 2010b. Cadmium removal from aqueous solutions using biosorbent *Syzygium cumini* leaf powder: Kinetic and equilibrium studies. *Korean Journal of Chemical Engineering, 27*, 1547-1554.

Rao, K.S., Anand, S. and Venkateswarlu, P., 2011b. Modeling the kinetics of Cd(II) adsorption on *Syzygium cumini* L. leaf powder in a fixed bed mini column. *Journal of Industrial and Engineering Chemistry, 17*, 174-181.

Rao, R.A.K. and Khan, U., 2017. Adsorption studies of Cu(II) on Boston fern (*Nephrolepis exaltata* Schott cv. Bostoniensis*) leaves. *Applied Water Science, 7*, 2051-2061.

Rawat, A.P., Giri, K. and Rai, J.P.N., 2014. Biosorption kinetics of heavy metals by leaf biomass of

Jatropha curcas in single and multi-metal system. *Environmental Monitoring and Assessment, 186*, 1679-1687.

Reddy, D.H.K., Harinath, Y., Seshaiah, K. and Reddy, A.V.R., 2010. Biosorption of Pb(II) from aqueous solutions using chemically modified *Moringa oleifera* tree leaves. *Chemical Engineering Journal, 162*, 626-634.

Reddy, D.H.K., Seshaiah, K., Reddy, A.V.R. and Lee, S.M., 2012. Optimization of Cd(II), Cu(II) and Ni(II) biosorption by chemically modified *Moringa oleifera* leaves powder. *Carbohydrate Polymers, 88*, 1077-1086.

Ren, X., Xiao, W., Zhang, R., Shang, Y. and Han, R., 2015. Adsorption of crystal violet from aqueous solution by chemically modified phoenix tree leaves in batch mode. *Desalination and Water Treatment, 53*, 1324-1334.

Robalds, A., Naja, G.M. and Klavins, M., 2016. Highlighting inconsistencies regarding metal biosorption. *Journal of Hazardous Materials, 304*, 553-556.

Rostami, B. and Niazi, A., 2013. Biosorption of a textile dye (Eosin) by eucalyptus tree leaves biomass: estimation of equilibrium, thermodynamic and kinetic parameters. *Advanced Science Focus, 1*, 50-56.

Ruiyi, F., Qingping, Y., Yucong, X., Feng, X., Qinglin, Z. and Zhengrong, L., 2016. Enhanced adsorption and recovery of Pb(II) from aqueous solution by alkali-treated persimmon fallen leaves. *Journal of Applied Polymer Science, 133*.

Saha, G.C., Hoque, M.I.U., Miah, M.A.M., Holze, R., Chowdhury, D.A., Khandaker, S. and Chowdhury, S., 2017. Biosorptive removal of lead from aqueous solutions onto Taro (*Colocasiaesculenta(L.) Schott*) as a low cost bioadsorbent: Characterization, equilibria, kinetics and biosorption-mechanism studies. *Journal of Environmental Chemical Engineering, 5*, 2151-2162.

Saha, P.D., Chakraborty, S. and Chowdhury, S., 2012. Batch and continuous (fixed-bed column) biosorption of crystal violet by *Artocarpus heterophyllus* (jackfruit) leaf powder. *Colloids and Surfaces B: Biointerfaces, 92*, 262-270.

Saha, R. and Saha, B., 2014. Removal of hexavalent chromium from contaminated water by adsorption using mango leaves (*Mangifera indica*). *Desalination and Water Treatment, 52*, 1928-1936.

Salehi, P., Asghari, B. and Mohammadi, F., 2008. Removal of heavy metals from aqueous solutions by *Cercis siliquastrum* L. *Journal of the Iranian Chemical Society, 5*, S80-S86.

Salim, R., Al-Subu, M. and Dawod, E., 2008. Efficiency of removal of cadmium from aqueous solutions by plant leaves and the effects of interaction of combinations of leaves on their removal efficiency. *Journal of Environmental Management, 87*, 521-532.

Sangi, M.R., Shahmoradi, A., Zolgharnein, J., Azimi, G.H. and Ghorbandoost, M., 2008. Removal and recovery of heavy metals from aqueous solution using *Ulmus carpinifolia* and *Fraxinus excelsior* tree leaves. *Journal of Hazardous Materials, 155*, 513-522.

Sarma, J., Sarma, A. and Bhattacharyya, K.G., 2011. Biosorption of Acid Blue 25 on Azadirachta indica (NEEM) leaf powder *World Environmental and Water Resources Congress 2011: Bearing Knowledge for Sustainability*, 3927-3940).

Sarma, J., Sarma, A. and Bhattacharyya, K.G., 2008. Biosorption of commercial dyes on Azadirachta indica leaf powder: A case study with a basic dye Rhodamine B. *Industrial & Engineering Chemistry Research, 47*, 5433-5440.

Sawalha, M.F., Peralta-Videa, J.R., Romero-González, J. and Gardea-Torresdey, J.L., 2006. Biosorption of Cd(II), Cr(III), and Cr(VI) by saltbush (Atriplex canescens) biomass: Thermodynamic and isotherm studies. *Journal of Colloid and Interface Science, 300*, 100-104.

Sayrafi, O., Sayrafi, S.A. and Salim, R., 1999. Removal of cadmium from polluted water using decaying leaves - effect of acidity. *Journal of Environmental Science and Health, Part A, 34*, 835-851.

Šćiban, M., Klašnja, M. and Škrbić, B., 2006. Modified softwood sawdust as adsorbent of heavy metal ions from water. *Journal of Hazardous Materials, 136*, 266-271.

Serencam, H., Gundogdu, A., Uygur, Y., Kemer, B., Bulut, V.N., Duran, C., Soylak, M. and Tufekci, M., 2008. Removal of cadmium from aqueous solution by Nordmann fir *(Abies nordmanniana (Stev.) Spach. Subsp. nordmanniana*) leaves. *Bioresource Technology, 99*, 1992-2000.

Setiabudi, H.D., Jusoh, R., Suhaimi, S.F.R.M. and Masrur, S.F., 2016. Adsorption of methylene blue onto oil palm (*Elaeis guineensis*) leaves: Process optimization, isotherm, kinetics and thermodynamic studies. *Journal of the Taiwan Institute of Chemical Engineers, 63*, 363-370.

Shah, J., Jan, M.R., Haq, A.u. and Zeeshan, M., 2015. Equilibrium, kinetic and thermodynamic studies for sorption of Ni (II) from aqueous solution using formaldehyde treated waste tea leaves. *Journal of Saudi Chemical Society, 19*, 301-310.

Sharma, A. and Bhattacharyya, K.G., 2005. Adsorption of Chromium (VI) on *Azadirachta Indica* (Neem) Leaf Powder. *Adsorption, 10*, 327-338.

Sharma, D.C. and Forster, C.F., 1994. The treatment of chromium wastewaters using the sorptive potential of leaf mould. *Bioresource Technology, 49*, 31-40.

Shi, J., Fang, Z., Zhao, Z., Sun, T. and Liang, Z., 2016. Comparative study on Pb(II), Cu(II), and Co(II) ions adsorption from aqueous solutions by arborvitae leaves. *Desalination and Water Treatment, 57*, 4732-4739.

Shin, E.W., Karthikeyan, K.G. and Tshabalala, M.A., 2007. Adsorption mechanism of cadmium on juniper bark and wood. *Bioresource Technology, 98*, 588-594.

Singh, K.K., Hasan, S.H., Talat, M., Singh, V.K. and Gangwar, S.K., 2009. Removal of Cr (VI) from aqueous solutions using wheat bran. *Chemical Engineering Journal, 151*, 113-121.

Siyal, A.A., Shamsuddin, M.R., Khan, M.I., Rabat, N.E., Zulfiqar, M., Man, Z., Siame, J. and Azizli, K.A., 2018. A review on geopolymers as emerging materials for the adsorption of heavy metals and dyes. *Journal of Environmental Management, 224*, 327-339.

Rao, K.S., Anand, S. and Venkateswarlu, P., 2010. Adsorption of cadmium (II) ions from aqueous solution by *Tectona grandis LF* (teak leaves powder). BioResources, 5, 438-454.

Tamez Uddin, M., Rukanuzzaman, M., Maksudur Rahman Khan, M. and Akhtarul Islam, M., 2009. Adsorption of methylene blue from aqueous solution by jackfruit (*Artocarpus heteropyllus*) leaf powder: A fixed-bed column study. *Journal of Environmental Management, 90*, 3443-3450.

Tchobanoglous, G. and Angelakis, A.N., 1996. Technologies for wastewater treatment appropriate for reuse: Potential for applications in Greece. *Water Science and Technology, 33*, 15-24.

Tewari, H., 2013. Removal of heavy metals from industrial effluent using *Pinus roxburghii* leaves as biosorbent: equilibrium modelling. *Water Science and Technology, 67*, 1894-1900.

Tongpoothorn, W., Sriuttha, M., Homchan, P., Chanthai, S. and Ruangviriyachai, C., 2011.

Preparation of activated carbon derived from Jatropha curcas fruit shell by simple thermo-chemical activation and characterization of their physico-chemical properties. *Chemical Engineering Research and Design, 89*, 335-340.

Tran, H.N., 2019. Comment on "simultaneous and efficient removal of Cr(VI) and methyl orange on LDHs decorated porous carbons". *Chemical Engineering Journal, 359*, 810-812.

Tran, H.N., 2017. Comments on "Characterization and adsorption capacity of raw pomegranate peel biosorbent for copper removal". *Journal of Cleaner Production, 144*, 553-558.

Tran, H.N. and Chao, H.-P., 2018a. Adsorption and desorption of potentially toxic metals on modified biosorbents through new green grafting process. *Environmental Science and Pollution Research, 25*, 12808-12820.

Tran, H.N. and Chao, H.-P., 2018b. Adsorption and desorption of potentially toxic metals on modified biosorbents through new green grafting process. *Environmental Science and Pollution Research*.

Tran, H.N., Chao, H.-P. and You, S.-J., 2018. Activated carbons from golden shower upon different chemical activation methods: Synthesis and characterizations. *Adsorption Science & Technology, 36*, 95-113.

Tran, H.N., Lee, C.-K., Nguyen, T.V. and Chao, H.-P., 2017a. Saccharide-derived microporous spherical biochar prepared from hydrothermal carbonization and different pyrolysis temperatures: synthesis, characterization, and application in water treatment. *Environmental Technology*, 1-14.

Tran, H.N., You, S.-J. and Chao, H.-P., 2016. Thermodynamic parameters of cadmium adsorption onto orange peel calculated from various methods: A comparison study. *Journal of Environmental Chemical Engineering, 4*, 2671-2682.

Tran, H.N., You, S.-J., Hosseini-Bandegharaei, A. and Chao, H.-P., 2017b. Mistakes and inconsistencies regarding adsorption of contaminants from aqueous solutions: A critical review. *Water Research, 120*, 88-116.

Tran, H.N., You, S.-J., Nguyen, T.V. and Chao, H.-P., 2017c. Insight into the adsorption mechanism of cationic dye onto biosorbents derived from agricultural wastes. *Chemical Engineering Communications, 204*, 1020-1036.

Vasanth Kumar, K. and Sivanesan, S., 2006. Equilibrium data, isotherm parameters and process design for partial and complete isotherm of methylene blue onto activated carbon. *Journal of Hazardous Materials, 134*, 237-244.

Villaescusa, I., Fiol, N., Martínez, M.a., Miralles, N., Poch, J. and Serarols, J., 2004. Removal of copper and nickel ions from aqueous solutions by grape stalks wastes. *Water Research, 38*, 992-1002.

Vilvanathan, S. and Shanthakumar, S., 2016. Removal of Ni(II) and Co(II) ions from aqueous solution using teak (*Tectona grandis*) leaves powder: adsorption kinetics, equilibrium and thermodynamics study. *Desalination and Water Treatment, 57*, 3995-4007.

Visa, M., 2012. Tailoring fly ash activated with bentonite as adsorbent for complex wastewater treatment. *Applied Surface Science, 263*, 753-762.

Volesky, B., 2007. Biosorption and me. *Water Research, 41*, 4017-4029.

Vu, M.T., Chao, H.-P., Van Trinh, T., Le, T.T., Lin, C.-C. and Tran, H.N., 2018. Removal of ammonium from groundwater using NaOH-treated activated carbon derived from corncob wastes: Batch and column experiments. *Journal of Cleaner Production, 180*, 560-570.

Wahab, M.A., Boubakri, H., Jellali, S. and Jedidi, N., 2012. Characterization of ammonium retention processes onto *Cactus* leaves fibers using FTIR, EDX and SEM analysis. *Journal of Hazardous Materials, 241-242*, 101-109.

Wan Ngah, W.S. and Hanafiah, M.A.K.M., 2008. Adsorption of copper on rubber (*Hevea brasiliensis*) leaf powder: Kinetic, equilibrium and thermodynamic studies. *Biochemical Engineering Journal, 39*, 521-530.

Wan, S., Ma, Z., Xue, Y., Ma, M., Xu, S., Qian, L. and Zhang, Q., 2014. Sorption of lead(II), cadmium(II), and copper(II) ions from aqueous solutions using tea waste. *Industrial & Engineering Chemistry Research, 53*, 3629-3635.

Wang, C., Wang, H. and Liu, Y., 2016. Purification of Pb (II) ions from aqueous solution by camphor leaf modified with succinic anhydride. *Colloids and Surfaces A: Physicochemical and Engineering Aspects, 509*, 80-85.

Wang, X.-S., Huang, J., Hu, H.-Q., Wang, J. and Qin, Y., 2007. Determination of kinetic and equilibrium parameters of the batch adsorption of Ni(II) from aqueous solutions by Na-

mordenite. *Journal of Hazardous Materials, 142*, 468-476.

Wenfang, Q., Yue, W., Min, J., Yingxin, Z. and Zhenya, Z., 2015. Highly efficient adsorption of Cr (VI) by Sakura leaves from aqueous solution. *Chemistry Letters, 44*, 697-699.

Weng, C.-H., Lin, T.Y., Chu, S.-H. and Yuan, C., 2006. Laboratory-scale evaluation of Cr (VI) removal from clay by electrokinetics incorporated with Fe (O) barrier. *Practice Periodical of Hazardous, Toxic, and Radioactive Waste Management, 10*, 171-178.

Weng, C.-H., Lin, Y.-T., Hong, D.-Y., Sharma, Y.C., Chen, S.-C. and Tripathi, K., 2014. Effective removal of copper ions from aqueous solution using base treated black tea waste. *Ecological Engineering, 67*, 127-133.

Weng, C.-H., Lin, Y.-T. and Tzeng, T.-W., 2009. Removal of methylene blue from aqueous solution by adsorption onto pineapple leaf powder. *Journal of Hazardous Materials, 170*, 417-424.

Weng, C.-H. and Wu, Y.-C., 2012. Potential low-cost biosorbent for copper removal: Pineapple leaf powder. *Journal of Environmental Engineering, 138*, 286-292.

Wong, S., Ngadi, N., Inuwa, I.M. and Hassan, O., 2018. Recent advances in applications of activated carbon from biowaste for wastewater treatment: A short review. *Journal of Cleaner Production, 175*, 361-375.

Xiao, X., Xue, J., Ding, D., He, B., He, D., Tan, L. and Liao, L., 2016. Adsorption of low concentration of Uranium(VI) from aqueous solution by diethylenetriamine functionalized *Cycas revoluta* leaves. *Journal of Radioanalytical and Nuclear Chemistry, 308*, 1027-1037.

Yagub, M.T., Sen, T.K. and Ang, H.M., 2012. Equilibrium, kinetics, and thermodynamics of methylene blue adsorption by pine tree leaves. *Water, Air, & Soil Pollution, 223*, 5267-5282.

Yang, H., Yan, R., Chen, H., Lee, D.H. and Zheng, C., 2007. Characteristics of hemicellulose, cellulose and lignin pyrolysis. *Fuel, 86*, 1781-1788.

Yang, J.-X. and Hong, G.-B., 2018. Adsorption behavior of modified *Glossogyne tenuifolia* leaves as a potential biosorbent for the removal of dyes. *Journal of Molecular Liquids, 252*, 289-295.

Yazıcı, H., Kılıç, M. and Solak, M., 2008. Biosorption of copper(II) by *Marrubium globosum subsp. globosum* leaves powder: Effect of chemical pretreatment. *Journal of Hazardous Materials, 151*, 669-675.

Yu, H., Wang, T., Yu, L., Dai, W., Ma, N., Hu, X. and Wang, Y., 2016. Remarkable adsorption capacity of Ni-doped magnolia-leaf-derived bioadsorbent for congo red. *Journal of the Taiwan Institute of Chemical Engineers, 64*, 279-284.

Yu, J.-x., Feng, L.-y., Cai, X.-l., Wang, L.-y. and Chi, R.-a., 2015. Adsorption of Cu^{2+}, Cd^{2+} and Zn^{2+} in a modified leaf fixed-bed column: competition and kinetics. *Environmental Earth Sciences, 73*, 1789-1798.

Yuvaraja, G., Krishnaiah, N., Subbaiah, M.V. and Krishnaiah, A., 2014. Biosorption of Pb(II) from aqueous solution by *Solanum melongena* leaf powder as a low-cost biosorbent prepared from agricultural waste. *Colloids and Surfaces B: Biointerfaces, 114*, 75-81.

Yuvaraja, G., Subbaiah, M.V. and Krishnaiah, A., 2012. *Caesalpinia bonducella* leaf powder as biosorbent for Cu(II) removal from aqueous environment: Kinetics and isotherms. *Industrial & Engineering Chemistry Research, 51*, 11218-11225.

Zahedi, R., Dabbagh, R., Ghafourian, H. and Behbahanini, A., 2015. Nickel removal by *Nymphaea alba* leaves and effect of leaves treatment on the sorption capacity: A kinetic and thermodynamic study. *Water Resources, 42*, 690-698.

Zaidi, N.A.H.M., Lim, L.B.L. and Usman, A., 2018. Artocarpus odoratissimus leaf-based cellulose as adsorbent for removal of methyl violet and crystal violet dyes from aqueous solution. *Cellulose*.

Zhang, Y., Li, X. and Li, Y., 2015. Influence of solution chemistry on heavy metals removal by bioadsorbent tea waste modified by poly (vinyl alcohol). *Desalination and Water Treatment, 53*, 2134-2143.

Zhou, L., Liu, Y., Liu, S., Yin, Y., Zeng, G., Tan, X., Hu, X., Hu, X., Jiang, L., Ding, Y., Liu, S. and Huang, X., 2016. Investigation of the adsorption-reduction mechanisms of hexavalent chromium by ramie biochars of different pyrolytic temperatures. *Bioresource Technology, 218*, 351-359.

Zhu, L., Wang, Y., He, T., You, L. and Shen, X., 2016. Assessment of potential capability of water bamboo leaves on the adsorption removal efficiency of cationic dye from aqueous solutions. *Journal of Polymers and the Environment, 24*, 148-158.

Zolgharnein, J., Bagtash, M., Feshki, S., Zolgharnein, P. and Hammond, D., 2017. Crossed mixture process design optimization and adsorption characterization of multi-metal (Cu(II), Zn(II) and

Ni(II)) removal by modified *Buxus sempervirens* tree leaves. *Journal of the Taiwan Institute of Chemical Engineers, 78*, 104-117.

Zolgharnein, J., Shariatmanesh, T. and Asanjarani, N., 2013. *Cercis siliquastrum* tree leaves as an efficient adsorbent for removal of Ag(I): Response surface optimization and characterization of biosorption. *CLEAN – Soil, Air, Water, 41*, 1183-1195.

Zolgharnein, J., Shariatmanesh, T., Asanjarani, N. and Zolanvari, A., 2015. Doehlert design as optimization approach for the removal of Pb(II) from aqueous solution by *Catalpa Speciosa* tree leaves: adsorption characterization. *Desalination and Water Treatment, 53*, 430-445.

Removal of various contaminants from water by renewable leaf-derived biosorbents: A comprehensive and critical review

Table of Contents

Supporting Figure

Section S1. Additional discussion on calculating textural properties

Based on Tran et al., 2017a, the specific surface area (S_{BET}) of a solid material can be calculated with the Brunauer–Emmett–Teller method (Equation S1). The calculations of the total pore volume (V_{total}; cm^3/g) and mean pore diameter (L_o; nm) are shown in Equations S4 and S5, respectively.

$$S_{BET} = \frac{(0.1620\,nm^2) \times (6.023 \times 10^{23})}{(22414\,cm^3\,STP) \times (10^{18}\,nm^2/m^2) \times (S_1 + I_1)} \tag{S1}$$

where the constant of 0.162 nm^2 is the molecular cross-sectional area of the analysis gas (N_2); 6.023×10^{23} is the Avogadro number; 22414 cm^3 is the volume of 1 mole gas at standard temperature and pressure (STP); S_1 (g/cm^3 STP) and I_1 (g/cm^3 STP) are the slope (C-1/$Q_{BET} \times C$) and intercept (1/$Q_{BET} \times C$) of a plot of $1/Q(p^\circ/p$-1) versus p/p° (Equation S2), respectively; and the parameter C of the BET equation is obtained using Equation S3.

$$\frac{1}{Q(p^o/p-1)} = \frac{C-1}{Q_{BET} \times C} p/p^o + \frac{1}{Q_{BET} \times C} \tag{S2}$$

$$C = \frac{S_1 + I_1}{I_1} = \frac{1}{Q_{BET} \times I_1} \tag{S3}$$

$$V_{total} = \frac{Q_{0.99}}{647} \tag{S4}$$

$$L_o = \frac{4 \times V_{total}}{S_{BET}} \times 1000 \tag{S5}$$

where Q is the adsorbed quality in volume (cm^3/g STP); $Q_{0.99}$ is the adsorbed quality in volume at a relative pressure (p/p°) of 0.99 (cm^3/g STP); C is indicative of the energy of the adsorption process (positive and dimensionless); Q_{BET} is the monolayer capacity in volume (cm^3/g STP); and p/p° is the relative pressure.

Section S2. Additional discussion electrical double layer (EDL)

Based on several researchers (Doğan et al., 2009; Weng et al., 2009; Weng and Wu, 2012), the thickness of the EDL (1/κ; nm) can be calculated using Equation 6.

$$\frac{1}{\kappa} = \sqrt{\frac{2F^2 I \times 1000}{\varepsilon \varepsilon_o RT}} \qquad (S6)$$

where I is the ionic strength (M); F is the Faraday constant (96500 C/mol); R is the gas constant (8.314 J/mol $\times$ K); ε is the dielectric constant of water (78.5); ε_o is the vacuum permittivity (8.854 $\times$ 10^{12} C/V $\times$ m); and T is the absolute temperature in Kelvin (K).

Section S3. Additional discussion on adsorption kinetics

In the batch adsorption study, the amounts of adsorbate adsorbed onto biosorbent in equilibrium (q_e; mg/g) and at time t (q_t; mg/g) are always calculated using the mass balance equations, as follows:

$$q_e = \frac{(C_o - C_e)}{m} V \qquad (S7)$$

$$q_t = \frac{(C_o - C_t)}{m} V \qquad (S8)$$

where C_o (mg/L), C_e (mg/L), and C_t (mg/L) are the adsorbate concentrations in the beginning, in equilibrium, and at time t, respectively; m (g) is the mass of the used biosorbent; and V (L) is the volume of the adsorbate solution. Therefore, the m/V ratio is defined as solid/liquid ratio.

The pseudo-second-order equation (Blanchard et al., 1984) can be expressed in nonlinear (Equation S9) and linear form (Equation S10):

$$q_t = \frac{q_e^2 k_2 t}{1 + k_2 q_e t} \qquad (S9)$$

$$\frac{t}{q_t} = (\frac{1}{q_e})t + \frac{1}{k_2 q_e^2} \qquad (S10)$$

where q_e and q_t are the amounts of adsorbed adsorbate per adsorbent mass (mg/g) in equilibrium and at time t (min), respectively; and k_2 (g/mg $\times$ min) is the rate constant of the pseudo-second-order equation.

The activation energy (Ea) of the adsorption process (in kJ/mol) is defined as the minimum energy that must be overcome by the adsorbate molecules and can be computed through the Arrhenius equation:

$$\ln k_2 = -(\frac{E_a}{R})\frac{1}{T} + \ln A\,, \tag{S11}$$

where k_2 (g/mg × min) is the rate constant of the second-order reactions; A is the pre-exponential factor (frequent factor); R (8.314 J/mol × K) is the gas constant; and T (K) is the solution temperature in Kelvin.

Section S4. Additional discussion on adsorption isotherm

The Langmuir model (Langmuir, 1918) can be expressed in nonlinear (Equation S12) and linear (common) forms (Equation S13):

$$q_e = \frac{Q^o_{max} K_L C_e}{1 + K_L C_e} \tag{S12}$$

$$\frac{C_e}{q_e} = (\frac{1}{Q^o_{max}})C_e + \frac{1}{Q^o_{max} K_L}\,, \tag{S13}$$

where C_e and q_e are obtained from Equation S7, K_L (L/mg) is the constant related to the affinity between an adsorbent and adsorbate; and Q^o_{max} (mg/g) is the maximum Langmuir adsorption capacity of a certain adsorbent under fixed experimental conditions (i.e., temperature, pH, time, etc.).

Section S5. Additional discussion on adsorption thermodynamics

The thermodynamic parameters for a liquid-phase reaction under non-standard state conditions (concentrations are not all one molar) are calculated using the van't Hoff approach that was described as the following equations:

$$\Delta G = -RT \ln K_C \tag{S14}$$

$$\Delta H = -R\left[\frac{\partial \ln K_C}{\partial (1/T)}\right] \tag{S15}$$

$$\Delta S = -\frac{(\Delta G - \Delta H)}{T} \tag{S16}$$

where K_C is the equilibrium constant (dimensionless) of a reaction based on the molar concentrations; T is the absolute temperature (in Kelvin; K); and R (8.314 J/mol × K) is the universal gas constant.

Equation S15 is the known van't Hoff equation. As shown in Equation S14, the equilibrium constant K_c must be dimensionless for dimension consistency.

The literature survey indicates that there are three ways to obtain the thermodynamic parameters of an adsorption process, depending on the expression of the K_C value in Equations S14 and S15:

(1) The K_C value is directly replaced by the adsorption isotherm constant including the Langmuir, Frumkin, Temkin, Flory–Huggins, Redlich–Peterson, and Henry equations (Chang et al., 2016; Tran et al., 2017b).

(2) The K_c value is substituted by the thermodynamic partition coefficient (K_p^o). The changes in the K_p^o values with temperature were initially studied by Biggar and Cheung (1973) for picloram adsorption on different soils. The thermodynamic partition coefficient is defined as follows:

$$K_p^o = \frac{a_s}{a_e} = \frac{\gamma_s C_s}{\gamma_e C_e} \tag{S17}$$

where a_s and a_e are the activities of the adsorbate adsorbed on the adsorbent and in solution at equilibrium, respectively; γ_s and γ_e are the corresponding activity coefficients; and C_s and C_e, both in mg/L, are the equilibrium concentrations of the adsorbate adsorbed on the adsorbent and in solution, respectively.

When the initial concentration of the adsorbate in solution approaches zero, which results in $C_s \to 0$ and $C_e \to 0$, the value of γ_s and γ_e approaches unity. Equation S17 can thus be written as:

$$\lim_{C_s \to 0} K_P^o = \frac{C_s}{C_e} \tag{S18}$$

In this case, the K_p^o value can be obtained by plotting $\ln(C_s/C_e)$ versus C_s and extrapolating C_s to zero. If a straight line fits the data with a high regression coefficient (R^2) and its intersection with the vertical axis provides the value of K_p^o, the partition coefficient is in unison with the equilibrium constant K_C.

(3) The K_C value is expressed by the distribution coefficient (K_d), which is defined by the following equation (Khan and Singh, 1987):

$$K_d = \frac{q_e}{C_e} \tag{S19}$$

In this case, the K_d values are obtained by plotting $\ln(q_e/C_e)$ against C_e and extrapolating to zero C_e. If a straight line fits the experimental data with a high regression coefficient (R^2), then its intersection with the vertical axis provides the value of K_d. However, the distribution coefficient K_d is dimensional; therefore, it is necessary to convert K_d (dimensional) into K_C (dimensionless) using several appropriate methods (Milonjić, 2009; Tran et al., 2017b). Notably, the distribution and partition coefficients are only appropriate to determine the thermodynamic parameters if the initially used adsorbate concentration is low (infinite dilution). In this situation, the distribution coefficient K_d and partition coefficient K_p will be in unison with the equilibrium constant K_c (Chang et al., 2016).

Section S6. Additional discussion on adsorption dynamics

The Thomas model is commonly applied to estimate the maximum adsorption capacity of the adsorbent under given experimental conditions.

$$\frac{C_t}{C_o} = \frac{1}{1 + \exp(k_{TH} q_o \frac{m_3}{Q} - k_{TH} C_o t)} \tag{S20}$$

$$\ln(\frac{C_o}{C_t} - 1) = k_{TH} q_o \frac{m_3}{Q} - k_{TH} C_o t \tag{S21}$$

where k_{TH} (mL/min × mg) is the Thomas adsorption rate constant; q_o (mg/g) is the maximum equilibrium adsorbate uptake per gram of adsorbent in the column; m_3 (g) is the mass of the adsorbent used in the column; C_o (mg/g) is the adsorbate concentration; and Q (mL/min) is the volumetric flow rate. Notably, the breakthrough time (t_b; min) and exhaustion (or saturation) time (t_s; min) can be obtained when the effluent concentration of the adsorbate reaches approximately 10% and 95% of the influent adsorbate concentration, respectively (Ali and Gupta, 2007).

Section S7. Additional discussion on identifying functional groups relevant for the adsorption mechanism

Adsorption of potentially toxic metals, fluoride, uranium, and ammonium

Meanwhile, Chen et al. (2010a) compared the FTIR spectrum of camphor leaves before and after Cu(II) adsorption. They concluded that the amino and hydroxyl groups play a pivotal role in

retaining Cu(II) ions in the solution, which agrees with the findings of Mambo et al. (2016) for Cu(II) adsorption onto chemically treated potato leaves. In addition, Vilvanathan and Shanthakumar (2016) found that major hydroxyl, carboxyl, and amine functional groups are mainly responsible for capturing Co(II) and Ni(II) ions on the biosorbent based onto teak leaves. This agrees with the observations of Kamar Firas et al., 2017 for Pb(II), Cd(II), and Cu(II), regarding the uptake by cabbage leaves, and of Hossain et al., 2014c, regarding Cu(II), Zn(II), Cd(II), and Pb(II) adsorption onto cabbage leaves.

Moreover, some contributory functional groups (hydroxyl, carboxyl, amino, ether, phe9nolic and phosphate) are 0known as active groups of rubber leaves retaining Cu(II) ions in solution Ngah and Hanafiah, 2009. For example, Amirnia et al. (2016) stated that active functional groups (hydroxide, phosphorous, and carboxyl) present in maple leaves greatly contribute to Cu(II)–biosorbent interactions. Based on FTIR data, Zahedi et al. (2015) proved that the carboxyl and sulfhydryl groups on the surface of $MgCl_2$-treated white water lily leaves mainly interact with Ni(II) of $MgCl_2$-treated white water lily leaves. In contrast, Dabbagh et al. (2016) highlighted that sulfonic acid is a dominant functional group accumulating Co(II) ions onto modified fig leaves. Furthermore, Bose et al. (2016) found that carboxylic, thiol, and sulfahydral groups are primarily responsible for adsorbing Cd(II) ions onto Urticaceae leaves. The great participation of hydroxyl, carboxylate, phosphate, ether, and amino functional groups in the removal of Cu(II) ions by NaOH-treated weed leaves has been identified by Hanafiah et al. (2009b).

In addition, Gebrehawaria et al. (2015) proposed that polar functional groups, such as –OH, –NH and –C=O (amide), are mainly related to Cr(VI) adsorption. However, Mozumder et al. (2008) emphasized that only the amine groups take part in the Cr(VI) adsorption onto tea-leaf waste. In their study, Zhang et al. (2015) reported the great contribution of the –COOH, –NH_2, and O–CH_3 groups of poly(vinyl alcohol)-modified tea waste in removing Pb(II), Hg(II), and Cu(II). In contrast, the comparison of the FTIR spectra of black tea waste before and after adsorption indicated that the functional groups contributing to Cu(II) adsorption are the –OH, –CH, and –C=C groups (Weng et al., 2014a). Based on XPS and FTIR data, Shi et al. (2016b) concluded that the C–C or C–H, C–O, and O–C=O groups provide the vital sites for the adsorption of Pb(II) by arborvitae leaves.

Moreover, Xia et al. (2013) proposed that the uranium adsorption onto Banyan leaves mainly involves the −OH, C=O, P–O, and Si=O groups. With respect to fluoride adsorption, the comparison of the FTIR results of neem leaf powder before and after biosorption revealed that the peak intensities at approximately 3468 cm^{-1} (—OH), 2372 cm^{-1} (−C≡N), and 1640 cm^{-1} (C=O) decreased and the peaks slightly shifted to 3456 cm^{-1}, 2369 cm^{-1}, and 1608 cm^{-1}, respectively. This demonstrates the vital role such functional groups play in the adsorption (Bharali and Bhattacharyya, 2015). Based on

FTIR analysis, researchers proposed that the hydroxyl, phenol, and carboxyl groups predominantly contribute to the adsorption of ammonium onto leaf-produced biosorbents including cactus leaves (Wahab et al., 2012), Boston ivy leaves (Liu et al., 2010c), and strawberry leaves (Liu et al., 2010d).

As noted earlier, FTIR can be used to qualitatively identify the integral role of the biosorbent surface functionality in adsorbing potentially toxic metals. Therefore, some authors used the chemical blocking method involving active functional groups to quantitatively analyze the contribution of principal functional groups (i.e., carboxylic and hydroxyl groups). Based on the literature, carboxylic groups on the adsorbent can be individually blocked by acidified methanol (HCl and CH_3OH), while the hydroxyl group is blocked by formaldehyde (HCHO). For example, Muhammad et al. (2009) compared the adsorption capacity of pristine and functional group-blocked biosorbents. They found that the adsorption capacity of the biosorbents remarkably decreased after blocking of carboxyl groups [by 78.6% for Ni(II) adsorption and 73.3% for Zn(II) adsorption]. Meanwhile, the adsorption capacity of hydroxyl group-blocked biosorbents decreased by 22.6% for Ni(II) adsorption and 28.5% for Zn(II) adsorption.

Likewise, Iqbal et al. (2009) elaborated that the chemical modification of mango peel waste to block carboxyl and hydroxyl groups demonstrates the larger contribution of the carboxylic group (73% and 76%) to the adsorption of Cd(II) and Pb(II) than that of the hydroxyl group (27% and 24%), respectively. The result is consistent with the FTIR analysis; the carboxyl and hydroxyl functional groups are mainly responsible for the adsorption process. Meanwhile, Chojnacka et al. (2005) stated that the Cr(III) adsorption process is hindered when the carboxyl and phosphate groups on the biosorbent surface are esterified, suggesting their significant role in the biosorption process.

To investigate the contribution of functional groups (i.e., carboxyl, carbonyl, amino, phosphate, hydroxyl, and sulfhydryl) to the biosorption of toxic metals, Ramrakhiani et al. (2017) compared the adsorption ability of pristine and chemically modified biosorbents. They reported that the adsorption capacity of pristine biosorbents decreases after chemical modification of these functional groups by esterification of the carboxylic acids, hydroxyl group, and phosphate group. In addition, methylation of amines and modification of the sulfhydryl and carbonyl groups were observed.

Table S1. Textural properties of leaf-derived biosorbents

Leaves	S_{BET} (m²/g)	V_{total} (cm³/g)	Ref.	Leaves	S_{BET} (m²/g)	V_{total} (cm³/g)	Ref.
Almond	67.0	0.062	(1)	Pineapple	5.24	0.021	(31)
Jambolan	53.3	—	(2)	Bamboo	3.41	—	(32)
Neptune grass	38.9	0.041	(3)	Taro	3.33	0.015	(33)
Boston ivy	31.9	—	(4)	Oil palm	2.59	0.002	(34)
Arborvitae	29.5	—	(5)	Mango	2.38	—	(35)
Rubber	29.2	—	(6)	Strawberry	2.05	—	(36)
Eggplant	26.4	0.017	(7)	Mucilaginous	1.85	0.008	(37)
Tiger's claw	25.3	—	(8)	Guava	1.70	—	(38)
Treated cluster fig	21.2	0.066	(9)	Jackfruit	1.66	—	(39)
Neem	21.5	—	(10)	Southern magnolia	1.54	—	(40)
Esparto grass	20.7	0.11	(11)	Used tea	1.34	—	(41)
Treated Potato	17.6	0.007	(12)	Cabbage wastes	1.03	—	(42)
Oriental plane	15.4	0.006	(13)	Brazilian orchid	1.27	—	(43)
Roxburgh fig	15.3	—	(14)	Modified boxwood	1.26	0.005	(44)
Tea	13.0	0.011	(15)	Golden shower	1.09	0.002	(45)
Sugar maple	11.6	0.011	(16)	Cabbage	1.03	—	(46)
Bamboo	11.5	—	(17)	Green honey myrtle	0.99	—	(47)
Jackfruit	11.2	0.004	(18)	Teak	0.96	—	(48)
Tea	11.0	0.009	(19)	Persimmon	0.95	—	(49)
Maple	10.9	0.001	(20)	Cauliflower wastes	0.89	—	(50)
Tomato	8.80	0.003	(21)	Tea waste	0.86	—	(51)
Guava	8.33	—	(22)	Tea waste	0.79	—	(52)
Tea	8.00	0.008	(23)	Hornbeam	0.70	—	(53)
Lotus	7.12	0.009	(24)	Neem	0.57	—	(54)
Tea	7.01	0.005	(25)	Rubber	0.48	—	(55)
Pineapple	6.86	—	(26)	Labill	0.38	—	(56)
Treated persimmon	6.63	—	(27)	Strawberry	0.35	—	(57)
Sacred fig	6.14	0.061	(28)	Coconut	0.24	—	(58)
Tea	6.00	0.003	(29)	Rambai	0.16	—	(59)
Australian pine	5.91	0.006	(30)	Phoenix	0.08	—	(60)

Note: Average: S_{BET} = 9.91 ± 13.37 (n = 60) and V_{total} = 0.019 ± 0.027 (n = 25); Median: S_{BET} = 5.58 and V_{total} = 0.008.

References: (1) Jain and Gogate, 2017b, (2) Rao et al., 2010c, (3) Dural et al., 2011, (4) Liu et al., 2010a, (5) Shi et al., 2016b, (6) Nag et al., 2016, (7) Yuvaraja et al., 2014, (8) Aditya et al., 2012, (9) Jain and Gogate, 2017c, (10) Sharma and Bhattacharyya, 2008, (11) Lafi et al., 2015, (12) Mambo et al., 2016, (13) Peydayesh and Rahbar-Kelishami, 2015, (14) Rangabhashiyam et al., 2015, (15) Peng et al., 2013, (16) Amirnia et al., 2016, (17) Nag et al., 2017, (18) Saha et al., 2012a, (19) Peng et al., 2013, (20) Hossain et al., 2014b, (21) Gutha et al., 2015, (22) Abdelwahab et al., 2015, (23) Peng et al., 2013, (24) Han et al., 2011, (25) Peng et al., 2013, (26) 27 Ruiyi et al., 2016, (28) Qaiser et al., 2009, (29) Peng et al., 2013 (30), Khan Rao and Khatoon, 2017, (31) Weng et al., 2009, (32) Chen et al., 2011a, (33) Nakkeeran et al., 2016, (34) Setiabudi et al., 2016b, (35) Nag et al., 2017, (36) Liu et al., 2010d, (37) Edokpayi et al., 2015, (385) Gaikwad and Kinldy, 2009, (39) Nag et al., 2017, (40) Liu et al., 2010a, (41) Hossain et al., 2005, (42) Hossain et al., 2014d, (43) Jorgetto et al., 2015, (44) Zolgharnein et al., 2017b, (45) Ahmad et al., 2017b, (46) Hossain et al., 2014c, (47) Kuppusamy et al., 2016, (48) Vilvanathan and Shanthakumar, 2016, (49) Ruiyi et al., 2016, (50) Hossain et al., 2014d, (51) Wan et al., 2014, (52) Amarasinghe and Williams, 2007, (53) Zolgharnein et al., 2013a, (54) Singha and Das, 2012, (55) Hanafiah and Ngah, 2009, (56) Yang and Hong, 2018a, (57) Liu et al., 2010a, (58) Gowda et al., 2012, (59) Sen et al., 2011, (60) Li et al., 2009.

Table S2. Ultimate analysis (wt.%) of leaf-based biosorbents

Leaves	C	H	N	S	O*	H/C	O/C	Reference
Roxburgh fig	31.1	4.08	0.77	—	64.1	1.57	1.55	Rangabhashiyam et al., 2015
Esparto grass	44.3	6.5	0.6	—	46.5	1.76	0.79	Lafi et al., 2015
Grey nicker	59.2	7.20	2.20	—	31.4	1.46	0.40	Yuvaraja et al., 2012
Sacred fig	48.4	7.30	1.12	0.12	43.1	1.81	0.67	Qaiser et al., 2009
Neptune grass	38.5	5.60	0.62	—	55.3	1.75	1.08	Meseguer et al., 2016
Taro	37.1	3.81	2.35	0.36	56.4	1.23	1.14	Nakkeeran et al., 2016
Judas	43.3	6.94	3.61	—	46.2	1.92	0.80	Zolgharnein et al., 2013b
Hardy catalpa	43.1	5.50	2.79	—	48.6	1.53	0.85	Zolgharnein et al., 2015
Southern cattail	43.5	10.1	2.49	1.21	42.9	2.79	0.74	Abdel-Ghani et al., 2009
Bamboo	44.0	6.20	2.57	—	47.2	1.69	0.80	Chen et al., 2011a
Globe artichoke	42.4	6.09	1.01	0.21	50.3	1.72	0.89	Benadjemia et al., 2011
Brazilian orchid	46.7	5.57	1.68	0.31	46.1	1.43	0.74	Jorgetto et al., 2015
Hornbeam	41.6	5.95	2.22	—	50.2	1.81	1.81	Zolgharnein et al., 2013a
Almond	40.4	4.44	0.34	—	63.4	1.75	1.75	Jain and Gogate, 2017b
Drumstick	47.2	6.79	2.47	0.59	42.9	1.73	0.68	Reddy et al., 2010
Rubber	51.1	6.89	1.09	—	40.9	1.62	0.60	Ngah and Hanafiah, 2009
NaOH-treated rubber	50.2	6.63	1.09	—	42.1	1.58	0.63	Ngah and Hanafiah, 2008
NaOH-treated almond	40.4	4.44	0.34	—	54.8	1.32	1.02	Jain and Gogate, 2017b
Average	44.0	6.11	1.63	0.47	48.5	1.69	0.94	—
SD	6.12	1.47	0.98	0.40	8.12	0.33	0.39	—
Minimum	31.1	3.81	0.34	0.12	31.4	1.23	0.41	—
Maximum	59.2	10.1	3.61	1.21	64.1	2.79	1.81	—
Median	43.4	6.15	1.40	0.34	46.9	1.71	0.8	—

Note: Calculated by difference; the H/C and O/C atomic ratio; SD means standard deviation

Table S3. Proximate analysis (wt.%) of leaf-based biosorbent

Leaves	Moisture	Volatile	Total ash	Fixed carbon	Reference
Eucalyptus	4.40	57.1	4.10	34.5	Mishra et al., 2010
Gulmohar	4.9.0	85.5	7.80	1.80	Ponnusami et al., 2009b
Teak	8.09	30.8	30.8	30.3	Vilvanathan and Shanthakumar, 2016
Ashoka	12.4	68.5	14.8	4.41	Gupta et al., 2012b
Roxburgh fig	4.03	62.0	24.5	9.50	Rangabhashiyam et al., 2015
Jamun	7.05	27.6	6.11	59.3	Rehman et al., 2014
Guava	5.81	61.5	9.58	34.1	Kamsonlian et al., 2012b
Drumstick	8.08	36.5	12.7	42.8	Bello et al., 2017
Carrot	7.65	81.4	9.21	1.75	Kushwaha et al., 2014b
Potato	8.19	72.1	17.6	2.15	Gupta et al., 2016b
Tomato	2.25	—	2.32	—	Gutha et al., 2015
Eggplant	3.46		3.12	—	Yuvaraja et al., 2014
Gum arabic	8.71	—	9.95	—	Prasad and Thirumalisamy, 2013
Grey nicker	2.10	—	9.12	—	Yuvaraja et al., 2012
Pineapple	5.01	—	6.01	—	Ponou et al., 2011
Neem	8.33	—	13.6	—	Singha and Das, 2012
Jackfruit	4.88	—	16.6	—	Nag et al., 2017
Mango	5.86	—	12.9	—	Nag et al., 2017
Mango	5.80	81.5	9.58	3.13	Kamsonlian et al., 2012c
Grey nicker	2.10	—	9.12	—	Yuvaraja et al., 2012
Bamboo	4.10	—	12.0	—	Nag et al., 2017
Average	5.92	60.4	11.5	20.3	—
SD	2.66	20.6	6.83	20.5	—
Minimum	2.10	27.6	2.32	1.75	—
Maximum	4.40	57.1	4.10	34.5	—
Median	5.81	62.0	9.58	9.50	—

NOTE: SD means standard deviation

Table S4. pH value and density of leaves-based biosorbent

Leaves	pH	Ref.	Leaves	Density (g/cm³)	References
Roxburgh fig	8.10	Rangabhashiyam et al., 2015	Neem	0.710	Singha and Das, 2012
Drumstick	7.08	Bello et al., 2017	Mango	0.367	Nag et al., 2017
Gum arabic	7.02	Prasad and Thirumalisamy, 2013	Used black tea	0.340	Hossain et al., 2005
Phoenix	6.60	Li et al., 2009	Guava	0.333	Gaikwad and Kinldy, 2009
Cauliflower	6.50	Ansari et al., 2016a	Jackfruit	0.299	Nag et al., 2017
Leaf tea	6.48	Jenish and Methodis, 2011	H_2SO_4-treated rubber	0.279	Nag et al., 2017
Castor	6.28	Makeswari and Santhi, 2014	Bamboo	0.214	Nag et al., 2017
Guava	6.20	Gaikwad and Kinldy, 2009	Coconut	0.117	Gowda et al., 2012
Coconut	6.02	Gowda et al., 2012	Gum arabic	0.272	Prasad and Thirumalisamy, 2013
Southern magnolia	6.01	Liu et al., 2010a	Kush grass	0.127	Pandey et al., 2015b
Poplar	5.60	Liu et al., 2010a	Bamboo	0.166	Pandey et al., 2015b
Strawberry	5.80	Liu et al., 2010a			
Boston ivy	5.50	Liu et al., 2010a			
NaOH-treated tea	5.07	Weng et al., 2014a			
Coconut	4.92	Ngah and Hanafiah, 2009			
Tea	4.75	Weng et al., 2014a			

Table S5. Quantitative information on oxygen-containing functional groups (mmol/g)

Leaves	Carboxylic	Phenolic	Lactonic	Total acid	Total basic	Reference
Jamun	1.99	0.003	0.001	1.99	—	Rehman et al., 2014
Castor	—	—	—	4.75	—	Makeswari and Santhi, 2014
Tea industry waste	1.03	0.98	0.46	2.47	—	Gundogdu et al., 2013
Raw lawny	—	—	—	6.20	1.70	Chen et al., 2011b
Esparto grass	0.58	0.96	0.030	1.57	0.40	Lafi et al., 2015
Tea	1.03	0.98	0.46	2.47	—	Gundogdu et al., 2013
Treated-globe artichoke	3.71	3.85	2.30	9.85	2.82	Kahina and Nasser, 2017
Treated-lawny grass	—	—	—	0.75	2.25	Chen et al., 2011b
Palm	0.85[a]	0.65[a]	2.80[a]	4.30[a]	—	Abu Al-Rub, 2006

Note: [a](meq H^+/100g)

Table S6. pH at the point of zero charge (pH$_{PZC}$) of leaf-based biosorbents

Leaves	pH$_{PZC}$	Ref.	Leaves	pH$_{PZC}$	Ref.
Roxburgh fig	8.00	(1)	Arborvitae	5.30	(27)
Sacred fig	7.59	(2)	Brazilian orchid	5.24	(28)
Jambolan	7.53	(3)	Castor	5.06	(29)
Gulmohar	7.50	(4)	Hardy catalpa	4.75	(30)
Modified boxwood	7.10	(5)	Grey nicker	4.51	(31)
Hybrid plane	7.00	(6)	Grey nicker	4.50	(32)
Weeping willow	6.98	(7)	Gum arabic	4.42	(33)
Neem	6.94	(8)	Judas	4.41	(34)
Mango	6.82	(9)	Tea waste	4.20	(35)
Ash	6.41	(10)	Boston fern	4.01	(36)
Chinese ash	6.40	(11)	Jackfruit	3.91	(37)
Esparto grass	6.30	(12)	Australian pine	3.60	(38)
Jackfruit	6.24	(13)	Eggplant	3.52	(39)
Cauliflower	6.23	(14)	Tomato	3.50	(40)
Drago	6.21	(15)	Pineapple	2.81	(41)
Reed	6.20	(16)	Maguey	2.60	(42)
Terap	6.20	(17)	Drumstick	3.72	(43)
Carrot	6.10	(18)	NaOH-treated terap	8.10	(44)
Ashoka	6.10	(19)	NaOH-treated weed	7.34	(45)
Bamboo	6.00	(20)	H$_2$SO$_4$-treated rubber	7.22	(46)
Camphor	5.91	(21)	Ca(OH)$_2$-treated maize	5.51	(47)
Potato	5.90	(22)	NaOH-treated Kush grass	5.50	(48)
Rubber	5.71	(23)	NaOH-treated bamboo	5.00	(49)
Hornbeam	5.70	(24)	NaOH-treated persimmon	3.30*	(50)
Treated Potato	5.50	(25)	Pineapple	2.30*	(51)
Treated Labill	5.30	(26)	Black tea	2.40*	(52)

Note: *pH$_{IEP}$ (pH at the isoelectric point).

References: (1) Rangabhashiyam et al., 2015, (2) Rao et al., 2011b, (3) Rao et al., 2010c, (4) Ponnusami et al., 2009b, (5) Zolgharnein et al., 2017b, (6) Kong et al., 2015, (7) Khodabandehloo et al., 2017, (8) Singha and Das, 2012, (9) Nag et al., 2017, (10) Zolgharnein et al., 2016, (11) Javad et al., 2017, (12) Lafi et al., 2015, (13) Nag et al., 2017, (14) Ansari et al., 2016a, (15) Mahmoud et al., 2016, (16) Markou et al., 2016b, (17) Lim et al., 2016b, (18) Kushwaha et al., 2014b, (19) Gupta et al., 2012b, (20) Mondal et al., 2013, (21) Chen et al., 2010a, (22) Gupta et al., 2016b, (23) Hanafiah and Ngah, 2009, (24) Zolgharnein et al., 2013a, (25) Mambo et al., 2016, (26) Yang and Hong, 2018a, (27) Shi et al., 2016b, (28) Jorgetto et al., 2015, (29) Makeswari and Santhi, 2014, (30) Zolgharnein et al., 2015, (31) Yuvaraja et al., 2012, (32) Yuvaraja et al., 2012, (33) Prasad and Thirumalisamy, 2013, (34) Zolgharnein et al., 2013b, (35) Mozumder et al., 2008, (36) Rao and Khan, 2017, (37) Saha et al., 2012a, (38) Khan Rao and Khatoon, 2017, (39) Yuvaraja et al., 2014, (40) Gutha et al., 2015, (41) Ponou et al., 2011, (42) Hamissa et al., 2010, (43) Reddy et al., 2012, (44) Lim et al., 2016b, (45) Hanafiah et al., 2009b, (46) Nag et al., 2017, (47) Jalil et al., 2012b, (48) Pandey et al., 2015b, (49) Pandey et al., 2015b, (50) Ruiyi et al., 2016, (51) Weng et al., 2009, (52) Weng et al., 2014a.

Table S7. Zeta potential of leaf-based biosorbent at a given solution pH

Leaves	ζ-Potential (mV)	pH	References
Strawberry	−30.0	5.8	Liu et al., 2010a
Boston ivy	−27.4	5.8	Liu et al., 2010a
Southern magnolia	−32.3	5.8	Liu et al., 2010a
Poplar	−24.4	5.8	Liu et al., 2010a
Green honey myrtle	−6.77	7.0	Kuppusamy et al., 2016
Treated persimmon	−6.12	5.0	Ruiyi et al., 2016
Tobacco leaves	−20.5	5.0	Qi and Aldrich, 2008

Table S8. Comparison of maximum adsorption capacity (Q^o_{max}, mg/g) of **pristine** biosorbent calculated from the Langmuir model (single component)

Leaves	Experimental conditions					Q^o_{max} (mg/g)	References
	m/V (g/L)	t (h)	T (°C)	pH	C_o range (mg/L)		
Copper—Cu(II)							
Castor	4.0	2.0	—	5.0	50–200	250	Makeswari and Santhi, 2014
Neem	1.0	2.0	60	5-6	100-1000	146	Ang et al., 2013
Paper mulberry	10	2.0	30	5.0	10-500	127	Nagpal et al., 2011
Sugar maple	1.0	5.0	RT	5.0	15-150	126	Amirnia et al., 2016
Teak	3.33	3.0	RT	5.0	20-100	95.4	King et al., 2006
Sunflower	2.0	7.0	25	5.0	20-500	89.4	Benaïssa and Elouchdi, 2007
Saltbush	5.0	1.0	25	5.0	5-50	67.9	Sawalha et al., 2007
Grey nicker	1.4	2.0	30	5.0	5-125	58.8	Yuvaraja et al., 2012
Tea waste	5.0	6.0	22	5.5	25-200	48.0	Amarasinghe and Williams, 2007
Neem	0.5	2.0	30	5.5	10-50	33.3	Bhattacharyya et al., 2010
Sugar maple	4.0	1.0	RT	5.0	15-150	27.8	Amirnia et al., 2016
Neem	1.5	2.0	30	5.5	10-50	25.1	Bhattacharyya et al., 2010
Papaya	2.0	1.0	RT	6.0	10-50	24.6	V. and Misra, 2018
Phoenix	0.5	0.84	RT	6.0	10-50	20.2	Yu et al., 2015
Tea waste	1.0	3.0	25	5.0	5-50	18.5	Çekim et al., 2015
Tomato	1.0	0.5	25	4.0	10-60	17.2	Çekim et al., 2015
Camphor	2.0	1.0	30	4.0	5-150	16.8	Boparai et al., 2011
Mango	5.0	4.0	RT	5.0	10-80	15.6	Sheen et al., 2013
Teak	3.3	3.0	RT	5.0	20-100	15.4	Prasanna Kumar et al., 2006
Tehran pine	10	1.0	RT	4.0	10-1000	15.3	Asgarzadeh et al., 2016
Brazilian orchid	11	0.5	25	5.0	1-480	15.1	Jorgetto et al., 2015
Cabbage waste	5.0	2.0	RT	6.0	1-500	12.9	Hossain et al., 2014a
Common fig	—	—	—	—	—	12.9	Batool et al., 2017
Judas	5.0	2.0	RT	4.0	5-1000	9.35	Salehi et al., 2008
Judas	10	6.0	RT	4.0	5-1000	9.35	Salehi et al., 2008
Pineapple	0.2	1.0	27	5.0	5-160	9.28	Weng et al., 2009

Arborvitae	2.0	5.0	30	5.5	5-30	7.94	Shi et al., 2016a
Cabbage	10	2.5	25	6.0	10-100	5.75	Kamar Firas et al., 2017
Devdaru	5.0	0.66	25	6.0	30-80	1.71	Rehman et al., 2013

Lead—Pb(II)

Maple	0.05	3.0	20	6.0	1-500	126	Hossain et al., 2014b
Bael	4.0	0.5	30	5.1	8.7-180	125	Chakravarty et al., 2010
Hardy catalpa	18.9	1.0	25	5.0	10-1000	120	Zolgharnein et al., 2015
Neem	0.8	3.0	25	5.0	50-150	119	Bhattacharyya and Sharma, 2004
Paper mulberry	10.0	2.0	30	5.5	10-500	84.7	Nagpal et al., 2011
Camphor	1.0	2.0	30	5.0	50-400	73.2	Chen et al., 2010b
Phoenix	5.0	24.0	30	5.0	100	71.0	Liang et al., 2016
Maple	0.5	3.0	20	6.0	1-500	66.7	Hossain et al., 2014b
Tea waste	5.0	6.0	22	5.5	25-200	65.1	Amarasinghe and Williams, 2007
Cabbage waste	5.0	2.0	RT	6.0	1-500	61.3	Hossain et al., 2014a
Cabbage waste	5.0	3.0	RT	—	1-500	60.6	Hossain et al., 2014d
Mistletoe	2.0	2.5	30	5.5	10-210	59.7	Van Suc and Son, 2016
Eggplant	0.4	1.75	30	5.0	30-90	55.6	Yuvaraja et al., 2014
Maple	1.0	3.0	20	6.0	1-500	50.3	Hossain et al., 2014b
Cauliflower waste	5.0	3.0	RT	—	1-500	47.6	Hossain et al., 2014d
Arborvitae	2.0	5.0	30	5.5	5-30	43.7	Shi et al., 2016b
Diceriocaryum eriocarpum	1.0	0.5	25	4.0	1-50	41.9	Edokpayi et al., 2015
Tropical-almond	2.5	30.0	30	2.0	20-300	41.8	Ramakul et al., 2012
Maguey	5.0	0.5	20	5.0	20-300	40.0	Hamissa et al., 2010
Secred fig	5.0	1.0	25	4.0	10-1000	37.5	Qaiser et al., 2009
Arborvitae	2.0	5.0	30	5.5	5-30	35.8	Shi et al., 2016a
Fig	5.0	1.33	30	6.0	5-200	34.4	Farhan et al., 2013b
Fig	5.0	1.33	30	6.0	10-200	34.3	Farhan et al., 2013a
Jambolan	3.3	1.0	30	6.0	20-100	32.5	King et al., 2007
Hairy fig	3.3	1.0	30	6.0	20-100	32.4	Namdeti and Pulipati, 2014
Tea waste	1.0	3.0	25	5.0	5-50	26.9	Wan et al., 2014

Chickpea	3.0	2.0	30	6.0	50-200	25.6	Nadeem et al., 2006
Neem	10.0	2.0	30	5.0	5-300	22.3	Singha and Das, 2012
Palm	5.0	1.5	25	4.5	180	20.1	Al-Haidary et al., 2011b
Black tea	10.0	3.0	RT	5.0	1-50	19.7	Mohammed et al., 2016
Tehran pine	10.0	1.0	RT	4.0	10-1000	19.7	Asgarzadeh et al., 2016
Common fig	—	—	—	—	—	17.9	Batool et al., 2017
Neem	8.3	2.0	27	4.0	10-300	13.5	Babarinde, 2016
Judas	10.0	6.0	RT	4.0	5-1000	12.5	Salehi et al., 2008
Judas	5.0	2.0	RT	4.0	5-1000	12.4	Salehi et al., 2008
Yerba mate	5.0	16.0	25	3.0	0.5-100	12.3	Copello et al., 2011
Cashew	1.5	2.0	30	4.0	10-140	11.6	Raju et al., 2013
Papaya	1.5	1.0	30	4.0	10-140	11.1	Raju et al., 2013
Star pine	20.0	2.0	30	5.0	30.17	7.66	Sarada et al., 2013b
Star pine	20	2.0	30	5.0	11-105	7.65	Sarada et al., 2013a
Cabbage	10	2.5	25	6.0	10-100	3.61	Kamar Firas et al., 2017
Ashok	4.0	0.5	25	6.5	1-100	3.23	Goyal et al., 2008
Southern cattail	10	2.0	25	2.5	1-30	0.65	Abdel-Ghani et al., 2009

Cadmium—Cd(II)

Neptune grass	1.0	1.0	20	7.0	75-200	117	Kaouah et al., 2014
Fig	2.0	4.0	25	6.0	5-1000	103	Benaïssa, 2006
Sesame	3.33	0.5	25	5.5	2-1000	84.7	Cheraghi et al., 2015
Neptune grass	2.0	3.0	25	6.0	25-1000	77.6	Meseguer et al., 2016
Loquat	0.4	1.0	30	6.0	10-40	48.8	Awwad and Salem, 2014
Mistletoe	2.0	2.5	30	5.5	10-210	44.8	Van Suc and Son, 2016
Tropical-almond	5.0	0.5	30	5.5	50-500	35.8	Rao, 2010
Jambolan	5.0	0.5	30	5.5	50-500	34.5	Rao et al., 2010c
Jambolan	5.0	0.5	30	5.5	50-500	34.5	Rao et al., 2010c
Jambolan	5.0	0.5	30	5.5	50-500	34.5	Rao et al., 2010c
Guava	5.0	0.5	30	5.5	50-500	31.2	Rao et al., 2010a
Fig	5.0	1.33	30	5.0	10-200	30.3	Farhan et al., 2013a
Fig	5.0	1.33	30	6.0	5-60	30.3	Farhan et al., 2013b

Teak	20.0	0.5	30	5.5	50-1000	29.9	Rao et al., 2010b
Loquat	4.0	1.0	30	6.0	5-60	29.2	Al-Dujaili et al., 2012
Loquat	4.0	1.0	30	6.0	5-60	29.2	Al-Dujaili et al., 2012
Jambolan	50.0	1.0	RT	5.5	50-150	29.1	Rao et al., 2011a
Giant reed	2.5	2.0	25	5.5	5-50	27.9	Ammari, 2014
Sacred fig	5.0	0.5	30	5.5	50-500	27.1	Rao et al., 2011b
Paper mulberry	10.0	2.0	30	6.5	10-500	26.1	Nagpal et al., 2011
Cabbage waste	5.0	2.0	RT	6.0	1-500	22.1	Hossain et al., 2014a
Loquat	4.0	1.0	30	6.0	5-60	21.3	Al-Dujaili et al., 2012
Cauliflower waste	5.0	3.0	RT	—	1-500	21.3	Hossain et al., 2014d
Cabbage waste	5.0	3.0	RT	—	1-500	20.6	Hossain et al., 2014d
Guava	5.0	1.0	30	6.7	20-100	17.2	Abdelwahab et al., 2015
Phoenix	0.5	0.84	RT	6.0	10-50	16.3	Yu et al., 2015
Urticaceae	5.0	1.17	27	6.5	10-50	13.8	Bose et al., 2016
Common fig	—	—	—	—	—	12.8	Batool et al., 2017
Brazilian orchid	11.0	0.5	25	5.0	1-480	12.7	Jorgetto et al., 2015
Maguey	5.0	0.5	20	5.0	20-160	12.5	Hamissa et al., 2010
Cabbage	10.0	2.5	25	6.0	10-100	5.07	Kamar Firas et al., 2017
Yerba mate	3.0	—	28	5.8	4.5-100	4.48	Cukierman, 2007
Neem	8.3	2.0	27	4.0	10-300	1.89	Babarinde, 2016
Cypress	13.3	48	22	6.5	0.5-20	1.43	Al-Subu, 2002
Pine	13.3	48	22	6.5	0.5-20	0.11	Al-Subu, 2002
Cinchona	13.3	48	22	6.5	0.5-20	0.10	Al-Subu, 2002

Nickel—Ni(II)

Tomato	0.4	3.0	30	5.5	30-90	47.6	Gutha et al., 2015
Golden shower	1.0	4.0	30	6.0	25-800	34.6	Hanif et al., 2007
Teak	6.0	1.0	30	5.0	25-200	17.8	Vilvanathan and Shanthakumar, 2016
Jackfruit	2.0	3.0	30	5.6	20-100	12.7	Boruah et al., 2015
Tehran pine	10.0	1.0	RT	4.0	10-1000	10.5	Asgarzadeh et al., 2016
Common fig	—	—	—	—	—	10.4	Batool et al., 2017

Neem	0.5	2.5	30	5.6	10-50	9.10	Bhattacharyya et al., 2009
Jamun	16.0	2.0	30	5.0	30-80	6.01	Rehman et al., 2014
Judas	5.0	2.0	RT	4.0	5-1000	4.68	Salehi et al., 2008
Deydaru	5.0	0.66	25	5.0	30-80	4.08	Rehman et al., 2013
Coconut	4.0	4.0	27	8.0	5-27	0.073	Gowda et al., 2012

Zinc—Zn(II)

Neem	1.5	6.0	25	4.0	25-800	147	Arshad et al., 2008
Jambolan	3.3	0.5	RT	6.0	20-100	35.8	King et al., 2008
Saltbush	5.0	1.0	25	5.0	5-50	32.7	Sawalha et al., 2007
Teak	3.3	3.0	30	5.0	20-100	16.4	Kumar et al., 2006
Phoenix	0.5	0.84	RT	6.0	10-50	15.3	Yu et al., 2015
Palm	2.0	0.5	25	5.5	20-300	14.6	Abu Al-Rub, 2006
Indian coral	20	1.0	30	4.5	25-250	12.7	Venkateswarlu et al., 2008
Cabbage waste	5.0	2.0	RT	6.0	1-500	10.9	Hossain et al., 2014a
Common fig	—	—	—	—	—	7.99	Batool et al., 2017
Bael	40	0.5	25	5.0	10-50	2.08	Kumar et al., 2009
Southern cattail	10	2.0	25	2.5	5-32	0.2	Abdel-Ghani et al., 2009

Mercury—Hg(II)

Adulsa	10.0	0.66	30	6.0	25-100	108	Aslam et al., 2013
Castor	2.5	1.0	RT	5.5	5-100	37.2	Al Rmalli et al., 2008
Chinese ash	—	0.5	RT	4.4	50-300	29.5	Zolgharnein and Shahmoradi, 2010
Bamboo	4.0	1.0	27	8.0	100-250	27.1	Mondal et al., 2013
Rambai	2.0	6.0	30	6.0	5-120	6.48	Sen et al., 2011
Phragmites karka	10.0	1.0	25	6.0	10-60	1.79	Raza et al., 2015

Hexavalent chromium—Cr(VI)

Used black tea	0.1	48	25	1.54	50-250	455	Hossain et al., 2005
Sakura	0.2	48	35	1.0	5-500	362	Qi et al., 2016
Mango	0.25	2.0	30	2.0	10-300	178	Saha and Saha, 2014
Sakura	2.0	—	RT	1.0	5-500	148	Wenfang et al., 2015

Neem	14.0	3.0	30	5.5	7-25	146	Sharma and Bhattacharyya, 2005
Tobacco	10.0	1.0	25	1.0	50-1000	125	Chen et al., 2009
Tobacco	10.0	1.0	25	1.0	50-100	113	Chen et al., 2009
Neem	10.0	3.0	30	5.5	7-25	83.6	Sharma and Bhattacharyya, 2005
Tea waste	2.5	8.0	30	2.0	90-160	73.1	Mozumder et al., 2008
Gum arabic	8.0	1.5	RT	6.0	106-176	69.4	Prasad and Thirumalisamy, 2013
Green honey myrtle	5.0	3.0	24	7.0	100-500	62.5	Kuppusamy et al., 2016
Mangrove	4.0	—	25	2.0	50-400	60.2	Sathish et al., 2015
Purple secretia	10.0	—	30	2.0	50-200	54.0	Sinha et al., 2015a
Purple secretia	10.0	5.0	30	2.0	50-200	53.9	Sinha et al., 2015b
Tamarind	4.0	2.0	30	6.0	200-1000	50.7	Muthulaksmi et al., 2016
Tobacco	10.0	1.0	25	2.0	50-1000	50.5	Chen et al., 2009
Taro	1.6	2.0	30	2.0	20-100	47.6	Nakkeeran et al., 2016
Mould	4.0	24.0	25	2.0	10-1000	43.1	Sharma and Forster, 1994
Neem	6.0	3.0	30	5.5	7-25	38.0	Sharma and Bhattacharyya, 2005
Mango	2.0	4.0	30	2.0	10-100	35.7	Nag et al., 2017
Green tea	16.0	3.0	30	2.0	5-500	34.6	Jeyaseelan and Gupta, 2016b
Lechuguilla	—	12.0	22	2.0	5-40	33.2	Romero-González et al., 2005
Jackfruit	2.0	4.0	30	2.0	10-100	32.2	Nag et al., 2017
Rubber	10.0	1.0	25	3.0	50-1000	22.9	Nag et al., 2016
Tobacco	10.0	1.0	25	3.0	50-1000	22.8	Chen et al., 2009
Neem	2.0	3.0	30	5.5	7-25	19.5	Sharma and Bhattacharyya, 2005
Tobacco	10.0	1.0	25	6.0	50-1000	14.6	Chen et al., 2009
Neem	14.0	3.0	30	5.5	7-25	14.4	Sharma and Bhattacharyya, 2005
Bamboo	5.0	4.0	30	2.0	10-100	10.8	Nag et al., 2017
Yerba mate	5.0	16.0	25	2.0	0.5-100	8.80	Copello et al., 2011
Roxburgh fig	5.0	2.0	25	2.0	20-100	6.80	Shi et al., 2016a
Dune guarrie	20.0	1.0	RT	5.6	5-20	3.94	Gebrehawaria et al., 2015
Golden shower	5.0	6.0	30	2.0	30-40	3.84	Ahmad et al., 2017a
Tiger's claw	50.0	3.0	30	2.85	20-180	1.92	Aditya et al., 2012

| Henna | 3.0 | 1.5 | 35 | 6.0 | 5-100 | 0.078 | Shanthi and Selvarajan, 2013 |

Trivalent chromium—Cr(III)

Yerba mate	5.0	16.0	25	3.0	0.5-100	11.8	Copello et al., 2011
Common fig	—	—	—	—	—	8.35	Batool et al., 2017
Neem	8.3	2.0	27	4.0	10-300	4.27	Babarinde, 2016
Jamun	12.0	0.5	30	4.0	30-80	3.82	Rehman et al., 2014
Ashoka	40.0	0.25	30	3.0	50-300	1.83	Anwar et al., 2011

Arsenite—As(III)

| Guava | 4.0 | 8.0 | 30 | 8.0 | 50-250 | 2.59 | Kamsonlian et al., 2012b |
| Rohida | 3.74 | 0.71 | — | 7.56 | 200-600 | 0.05 | Brahman et al., 2016 |

Arsenate—As(V)

Chir pine	20.0	0.5	25	4.0	5-30	3.27	Shafique et al., 2012
Guava	4.0	8.0	30	4.0	50-250	3.25	Kamsonlian et al., 2012b
Rohida	3.60	0.72	—	5.48	200-600	0.12	Brahman et al., 2016

Ammonium—(NH_4^+)

Strawberry	8.0	18	30	—	25-1000	6.71	Liu et al., 2010a
Magnolia	8.0	18	30	—	25-1000	6.22	Liu et al., 2010a
Boston ivy	8.0	18	30	—	25-1000	6.07	Liu et al., 2010a
Strawberry	8.0	24	25	—	25-1000	6.05	Liu et al., 2010d
Boston ivy	8.0	14	25	—	25-1000	5.28	Liu et al., 2010b
Cactus	5.0	2.0	20	6.0	10-50	2.58	Wahab et al., 2012

Cobalt—Co(II)

Teak	6.0	1.0	30	5.0	25-200	29.5	Vilvanathan and Shanthakumar, 2016
Common fig	—	—	—	—	—	11.4	Batool et al., 2017
Arborvitae	2.0	5.0	30	5.5	5-30	6.78	Shi et al., 2016a
Banyan	25.0	2.0	RT	5.0	5-150	5.65	Hymavathi and Prabhakar, 2017
Deydaru	5.0	0.66	25	6.0	30-80	3.99	Rehman et al., 2013
Tiger's claw	40.0	2.0	30	7.2	25-200	2.71	Vijaya Lakshmi et al., 2008

Lanthanum—La(III)

Oriental plane	2.0	1.0	25	4.0	25-300	28.7	Sert et al., 2008
Calabrian pine	4.0	0.5	30	5.0	25-300	22.9	Kütahyali et al., 2010

Cerium

Oriental plane	2.0	1.0	25	4.0	25-300	32.1	Sert et al., 2008
Calabrian pine	4.0	0.25	30	5.0	25-300	17.2	Kütahyali et al., 2010

Zirconium—Zr(IV)

Platanaceae	5.0	0.66	25	3.0	2-500	29.5	Boveiri Monji et al., 2008

Hafnium—Hf(IV)

Platanaceae	5.0	0.66	25	3.0	2-500	14.7	Boveiri Monji et al., 2008

Uranium—U(VI)

Banyan	5.0	1.0	30	3.0	10-400	34.6	Xia et al., 2013
Neptune grass	2.5	0.5	25	3.0	1-25	9.81	Aydin et al., 2012
Poplar	10.0	4.0	25	4.0	1-10	2.3	Al-Masri et al., 2010

Platinum

Tropical-almond	2.5	30.0	30	2.0	20-300	22.5	Ramakul et al., 2012

Methylene blue dye

Lotus	1.0	4.0	20	7.0	30-200	222	Han et al., 2011
Gulmohar	0.5	—	—	7.5	50-200	186	Ponnusami et al., 2009a
Cabbage	1.0	—	RT	9.0	10-200	149	Ansari et al., 2016b
Pine tree	0.3	4.0	30	9.2	10-80	127	Yagub et al., 2012
Phoenix	1.6	1.17	60	12.0	20-180	115	Peydayesh and Rahbar-Kelishami, 2015
Lawny grass	1.0	4.0	—	5.7	40-320	103	Chen et al., 2011c
Bael	0.6	0.33	30	6.7	10-50	100	Baruah et al., 2017
Plane	2.5	7.0	30	7.0	50-500	99.0	Kong et al., 2015
Ashoka	2.0	0.5	30	6.0	10	90.9	Gupta et al., 2012a
Phoenix tree	2.0	3.0	22	7.0	30-180	80.9	Han et al., 2007
Acer tree	5.0	0.67	—	2.7	928	69.2	Zolgharnein and Bagtash, 2015
Carrot	2.0	0.5	30	7.0	10-50	66.6	Kushwaha et al., 2014a

Weeping willow	2.0	2.0	23	7.0	20-200	61.0	Khodabandehloo et al., 2017
Plane	18.0	1.0	25	6.4	1000	55.5	Zolgharnein et al., 2010
Water bamboo	2.0	1.0	10	6.75	50-250	54.2	Zhu et al., 2016
Potato	2.0	0.42	30	7.0	10	52.6	Gupta et al., 2016a
Date palm	10.0	2.67	30	6.5	200	43.1	Gouamid et al., 2013

Malachite green dye

Lotus	1.0	7.0	20	4.5	30-200	114	Han et al., 2014
Ashoka	2.0	0.5	30	6.0	10	83.3	Gupta et al., 2012a
Plane	2.5	7.5	25	—	50-500	77.5	Hamdaoui et al., 2008
Cattail	2.5	4.0	25	4.0	50-500	72.3	Guechi and Hamdaoui, 2013
Carrot	2.0	0.5	30	7.0	10	52.6	Kushwaha et al., 2014a
Potato	2.0	0.42	30	7.0	10	33.3	Gupta et al., 2016a

Crystal violet dye

Pineapple	1.0	3.0	30	8.0	10	159	Neupane et al., 2015
Pineapple	20.0	3.0	30	8.0	20-100	78.2	Chakraborty et al., 2012
Esparto grass	2.0	2.5	25	7.0	20-100	43.5	Lafi et al., 2015
Jackfruit	10.0	2.0	20	7.0	20-100	43.4	Saha et al., 2012b
Sodom apple	10.0	1.0	20	—	10-50	4.14	Ali and Muhammad, 2008

Amaranth dye

Water hyacinth	1.0	7.0	18	2.0	10-500	70.6	Guerrero-Coronilla et al., 2015

Basic Red 46 dye

Pine	1.0	1.25	45	6.0	20-100	71.9	Deniz and Karaman, 2011
Princess	1.0	1.17	25	8.0	20-100	43.1	Deniz and Saygideger, 2011

Methyl violet dye

Platanus carpinifolia	0.11	1.0	25	3.0	500-2500	555	Zolgharnein et al., 2014
Neptune grass	3.33	1.0	25	6.0	10-300	82.7	Cengiz and Cavas, 2010

Remazol Brilliant Blue R dye

Pineapple	100.0	24.0	RT	—	500	42.2	Rahmat et al., 2016

Methyl violet 2B dye

Terap	2.0	4.0	RT	—	500-1000	140	Lim et al., 2016a

Direct Blue-15 dye

Papaya	0.5	0.75	30	7.0	25	3.98	Rehman et al., 2017

Grey BL dye

Mango	1.0	5.0	27	7.0	50-1000	33.7	Murugan et al., 2010

Naphthalene

Spent tea leave	20.0	2.0	45	6.0	100-400	23.81	Agarry et al., 2013

Brilliant Green Dye

Ashoka	2.0	0.5	30	6.0	10	125	Gupta et al., 2012a
Jambolan	60.0	0.33	50	3.0	30-80	4.739	Rehman et al., 2012
Neem	0.4	4.0	27	6.5	10-50	—	Bhattacharyya and Sarma, 2003

Ibuprofen

Fallopia x bohemica	5.0	24.0	20	—	10-800	38.2	Mucha and Mucha, 2017

Acetylsalicyic acid

Fallopia x bohemica	5.0	24.0	20	—	10-1000	17.3	Mucha and Mucha, 2017

Basic Green 4 dye

Pineapple	5.0	2.5	35	9.0	10-100	56.6	Chowdhury et al., 2011

Acid orange 52 dye

Princess	0.1	3.0	25	2.0	10-100	10.5	Deniz and Saygideger, 2010

Auramine dye

Psium guava	40.0	2.0	30	9.0	50-150	7.76	Gaikwad and Kinldy, 2009

Direct solophenyl brown AGL dye

Neptune grass	20.0	24.0	30	2.0	10-100	5.24	Ncibi et al., 2006

Reactive cibacron red FNR dye

Neptune grass	20.0	24.0	30	5.0	10-100	9.62	Ncibi et al., 2006

Remazol blue RR dye

Neem	50.0	—	60	10.0	50-2000	33.9	Immich et al., 2009

Acid blue 193 dye

Parthenium	—	24.0	—	8.66	10-100	10.65	Purai and Rattan, 2012

Fluoride

Neem	1.0	1.0	30	6.8	3-15	9.5	Bharali and Bhattacharyya, 2015

Rhodamine B dye

Ashoka	2.0	0.5	30	6.0	10	66.6	Gupta et al., 2012a

Eosin

Esparto grass	2.0	2.5	25	7.0	20-100	40.0	Lafi et al., 2015
Eucalyptus	1.0	0.5	25	4.0	5-1000	14.5	Rostami and Niazi, 2013

Acid green 25 dye

Almond	14.0	5.5	30	2.0	50-200	22.7	Jain and Gogate, 2018

Table S9. Comparison of maximum adsorption capacity (Q^o_{max}, mg/g) of **modified/treated biosorbent** calculated from the Langmuir model (single component)

Leaves	Chemicals	Experimental conditions					Q^o_{max} (mg/g)	References
		m/V (g/L)	t (h)	T (°C)	pH	Co range (mg/L)		
Copper—Cu(II)								
Drumstick	NaOH, citric acid	0.4	2.0	30	5.0	10-1000	151	Reddy et al., 2012
Tea waste	NaOH	0.4	1.0	26	4.2	—	43.6	Weng et al., 2014a
Phoenix	PMDA	0.5	0.84	RT	6.0	10-50	31.3	Yu et al., 2015
Lamiaceae	NaOH	1-8	1.0	RT	5.5	50	20.3	Kılıç et al., 2009
Lamiaceae	NaOH	2.0	1.0	30	5.5	20-200	20.3	Kılıç and Solak, 2009
Boxwood	NaOH	18	—	—	5.0	50	18.8	Zolgharnein et al., 2017a
Sacred fig	HNO$_3$	10.0	1.0	33	4.4	5-500	18.1	Kazmi et al., 2015
Rubber	NaOH	2.0	1.0	27	4.0	5-50	14.9	Ngah and Hanafiah, 2008
Weed	NaOH	2.0	—	27	—	5-20	10.3	Hanafiah et al., 2009a
Rubber	H$_2$SO$_4$, HCHO	2.0	1.5	27	4.0	5-50	8.36	Ngah and Hanafiah, 2009
Spent tea	CaOH$_2$	—	—	—	—	—	7.81	Ghosh et al., 2015
Henna	H$_2$SO$_4$	3.0	1.5	35	6.0	5-100	3.65	Shanthi and Selvarajan, 2013
Lead—Pb(II)								
Drumstick	NaOH, citric	0.4	1.0	30	5.0	10-1000	196	Reddy et al., 2012
Camphor	NaOH, alcohol, succinic anhydride	—	0.5	RT	5.0	50-1200	186	Wang et al., 2016
Rubber	Monosodium glutamate	0.4-2	2.0	24	5.0	20-60	110	Fadzil et al., 2016
Rubber	Citric acid	0.4-2	2.0	24	5.0	20-60	97.2	Fadzil et al., 2016
Sacred fig	Polysulphone, *n,n*-dimethyl-formamide	5.0	1.0	25	5.3	10-1000	37.5	Qaiser et al., 2009
Chinaberry	NaOH	3.0	1.0	RT	7.0	25	35.1	Khokhar et al., 2015
Chinaberry	HCl	3.0	1.0	RT	7.0	25	28.5	Khokhar et al., 2015
Sacred fig	HNO$_3$	0.4	1.0	30	5.8	10-1000	17.5	Qaiser et al., 2007
Cadmium—Cd(II)								
Drumstick	NaOH, citric acid	0.4	2.0	30	5.0	10-1000	166	Reddy et al., 2012

Phoenix	PMDA	0.5	0.84	RT	6.0	10-50	28.3	Yu et al., 2015
Bamboo	NaOH	1.0	1.0	25	6.5	10-150	19.7	Pandey et al., 2015a
Kush grass	NaOH	1.0	1.0	25	6.5	10-150	15.2	Pandey et al., 2015a

Nickel—Ni(II)

Drumstick	NaOH, citric acid	0.4	2.0	30	5.0	10-1000	149	Reddy et al., 2012
Tea waste	Formaldehyde	2.6	1.5	RT	7.0	0.01-15	121	Shah et al., 2015b
White nenuphar	$MgCl_2$	2.0	2.0	20	6.5	5-100	118	Zahedi et al., 2015
Tea waste	Fe_3O_4 nanoparticle	5.0	3.0	30	4.0	50-100	38.3	Panneerselvam et al., 2011
Boxwood	NaOH	18	—	—	5.0	50	22.3	Zolgharnein et al., 2017a

Zinc—Zn(II)

Phoenix	PMDA	0.5	0.84	RT	6.0	10-50	27.3	Yu et al., 2015
Sacred fig	HNO_3	10.0	1.0	33	5.2	5-500	24.9	Kazmi et al., 2015
Boxwood	NaOH	18	—	—	5.0	50	21.2	Zolgharnein et al., 2017a

Mercury—Hg(II)

Bastard teak	NaOH, $CaCl_2$	4.0	3.0	RT	6.0	150	95.4	Devani et al., 2015
Bastard teak	NaOH, $CaCl_2$	4.0	3.0	RT	6.0	100	88.7	Devani et al., 2015

Hexavalent chromium—Cr(VI)

London plane	HNO_3	2.0	72	30	3.0	53-316	75.8	Aoyama, 2003c
London plane	HNO_3	2.0	72	30	3.0	52.82-315.58	75.7	Aoyama, 2003b
Black locust	HNO_3	2.0	48	30	3.0	5-300	51.6	Aoyama et al., 2000a
Neem	HCl	10.0	72	30	2.0	20-700	62.9	Babu and Gupta, 2008
Rubber	H_2SO_4	5.0	4.0	30	2.0	10-100	29.8	Nag et al., 2017
Sacred fig	HNO_3	10.0	1.0	30	5.2	10-1000	26.3	Qaiser et al., 2007
Ficus nitida	H_2SO_4	8.0	0.42	25	4.0	50-200	21.0	Ali and Alrafai, 2016
Japanese red pine	HNO_3	2.0	24	30	3.0	1-100	14.5	Aoyama et al., 1999a
Lettuce	NaOH	10.0	5.0	40	7.0	10-90	7.15	Li et al., 2014
Mangrove	H_2SO_4, NaOH	10.0	6.0	30	7.0	10-150	5.72	Elangovan et al., 2008

Trivalent chromium—Cr(III)

Mangrove	H_2SO_4, NaOH	10.0	6.0	30	5.0	10-150	6.54	Elangovan et al., 2008

Arsenic—As(III)

Devdaru	HCl	1.0	2.0	30	7.5	1-5	1.51	Choudhary, 2015

Cerium

Calabrian pine	Citric acid	0.5	0.75	40	4.0	10-90	62.1	Kütahyalı et al., 2012

Uranium—U(VI)

Sotetsu	DETA	0.4	2.0	25	8.2	5-30	0.91	Xiao et al., 2016

Vanadium

Neptune grass	HCl	10.0	0.5	RT	3.0	20-40	16.0	Pennesi et al., 2013

Molybdenum

Neptune grass	HCl	10.0	0.5	RT	3.0	20-40	18.0	Pennesi et al., 2013

Methylene blue dye

Lawny grass	Citric acid	1.0	4.0	—	5.7	40-320	301	Chen et al., 2011c
Fig	Fe_3O_4 nanoparticle	3.5	0.5	—	—	4	61.7	Alizadeh et al., 2017
Pineapple	Hexadecyltrimethylammonium bromide	—	2.0	RT	—	5-1000	52.6	Kamaru et al., 2016
Azolla	Fe_3O_4	3.5	0.5	RT	—	4	25.1	Alizadeh et al., 2017

Malachite green dye

Labil	Ammonia, lauric acid	—	—	30	10.0	100-500	370	Yang and Hong, 2018b
Maize	$CaOH_2$	2.5	0.5	50	6.0	10-200	81.5	Jalil et al., 2012a

Crystal violet dye

Phoenix trees	NaOH	1.0	11.0	30	8.0	100-1000	662	Ren et al., 2015
Fig	Fe_3O_4 nanoparticle	2.5	1.0	—	—	4	53.5	Alizadeh et al., 2017
Azolla	Fe_3O_4 nanoparticle	1.5	1.0	—	—	4	30.2	Alizadeh et al., 2017

Acid violet 17 dye

Cluster fig	NaOH, H_2SO_4	3.0	4.0	30	2.0	50-200	111	Jain and Gogate, 2017d

Methyl orange dye

Pineapple	Hexadecyltrimethylammonium bromide	—	2.0	RT	—	5-1000	47.6	Kamaru et al., 2016

Methyl violet 2B dye

Terap	NaOH	2.0	4.0	RT	—	500-1000	1004	Lim et al., 2016a

Direct Blue-15 dye

Tea	Acetone	1.0	0.67	40	3.0	25	90.9	Rehman et al., 2017

Acid Blue 25 dye

Cluster fig	NaOH	4.0	3.0	50	2.0	50-400	83.3	Jain and Gogate, 2017a

Pyrocatechol violet dye

Black locust	NaCl	—	0.83	22	1.82	38.28	82.6	Khorshidi and Niazi, 2016

Brilliant green dye

Jambolan	NaOH	60.0	0.33	50	3.0	30-80	5.13	Rehman et al., 2012
Jambolan	HCl	60.0	0.33	50	3.0	30-80	0.17	Rehman et al., 2012

Acid blue 113 dye

Almond	Surfactant CTAB $C_{19}H_{42}BrN$	10.0	2.5	20	6.5	50-200	97.1	Jain and Gogate, 2017b
Almond	NaOH	10.0	2.5	20	6.5	50-200	25.5	Jain and Gogate, 2017b

Congo red dye

Labil	Ammonia, lauric acid	—	—	30	2.0	100-500	37.2	Yang and Hong, 2018b

Orthophosphate

Kush grass	$CaOH_2$	4.0	24	25	7.0	12.5-200	12.3	Markou et al., 2016b
Kush grass	$CaOH_2$	4.0	24	25	7.0	50-200	12.2	Markou et al., 2016a

Acid green 25 dye

Almond	NaOH	6.0	5.5	30	2.0	50-200	46.6	Jain and Gogate, 2018

Table S10. Some common inorganic salt used for the effect study of ionic strength

Inorganic salt	Adsorbate	Reference
NaCl	Acid blue 113	Jain and Gogate, 2017b
NaCl	Methylene blue, malachite green	Sangi et al., 2008
NaCl	Methylene blue	Ansari et al., 2016a; Han et al., 2007; Han et al., 2011
NaCl	Acid blue 45 and acid black 1	Maleki et al., 2017
NaCl	Heavy metal	Rao et al., 2011b; Ruiyi et al., 2016; Srinivasa Rao et al., 2010
NaCl	Heavy metal	Ngah and Hanafiah, 2008
NaCl	Heavy metal	Zhang et al., 2015
NaCl	Malachite green	Hamdaoui et al., 2008
NaCl	Basic red 46	Deniz and Karaman, 2011
NaCl	Toluidine blue and crystal violet	Lafi et al., 2015
$NaNO_3$	Heavy metal	Sangi et al., 2008
$NaNO_3$	Methylene blue	Weng et al., 2009
Ca_2NO_3	Heavy metal	Sangi et al., 2008
$NaClO_4$	Heavy metal	Weng and Wu, 2012
$CaCl_2$	Methylene blue	Han et al., 2007; Han et al., 2011
Na_2SO_4	Heavy metal	Rao et al., 2011b; Srinivasa Rao et al., 2010
KNO_3	Cationic methyl violet 2B dye	Lim et al., 2016b
$NH_{42}SO_4$	Acid blue 45 and acid black 1	Maleki et al., 2017
$NaHCO_3$	Acid blue 45 and acid black 1	Maleki et al., 2017

Table S11. Thermodynamic parameters for the biosorption of toxic **metal ions** onto **pristine** leaves

Leaves	T (K)	Derivation of K_C (unit)	ΔG° (kJ/mol)	ΔH° (kJ/mol)	ΔS° (kJ/mol × K)	References
Lead (Pb²⁺)						
Camphor	303	K_L	- 23.9	15.1	0.129	Chen et al., 2010b
	313	L/mol	- 25.3			
	323		-26.7			
	333		- 27.8			
Potato	303	K_L	-8.75	3.69	0.039	Yuvaraja et al., 2014
	313	L/mg	-8.51			
	323		-7.98			
Sacred fig	303	K_d	-2.95	-105	-0.350	Qaiser et al., 2009
	313	L/g	-0.12			
	323		4.94			
Tea waste	288	K_d	-14.8	25.1	0.138	Wan et al., 2014
	298	mL/g	-14.6			
	308		-12.8			
	318		-12.6			
	328		-11.3			
Neem	308	K_d	-4.69	10.9	-0.029	Bhattacharyya and Sharma, 2004
	313	mL/g	-4.26			
	318		-3.96			
Palm	283	K_L	-8.23	-16.7	-0.029	Al-Haidary et al., 2011a
	298	L/mg	-8.19			
	308		-7.43			
	323		-7.16			
Cadmium (Cd²⁺)						
Jambolan	303	K_p	-1.40	3.70	0.017	Rao et al., 2010c
	313	No	-1.58			
	323		-1.74			
Loquat	293	K_p	-7.02	29.7	0.125	Awwad and Salem, 2014
	303	No	-8.21			
	313		-9.55			
Hornbeam	298	K_p	-4.29	-13.1	-0.029	Zolgharnein et al., 2013a
	308	No	-4.04			
	318		-3.65			
	328		-3.44			
Date Tree	298	K_p	-7.37	21.6	0.095	Boudrahem et al., 2011
	308	No	-7.52			
	313		-7.92			
	333		-10.8			
Tea waste	288	K_d	-12.5	10.5	0.079	Wan et al., 2014
	298	mL/g	-12.4			
	308		-12.2			
	318		-12.1			
	328		-11.8			
Loquat	293	K_p	-6.33	12.3	0.064	Al-Dujaili et al., 2012
	303	No	-6.98			

	313		-7.60			
Loquat ash	293	K_p	-5.87	10.0	0.054	Al-Dujaili et al., 2012
	303	No	-6.43			
	313		-6.96			
Loquat	293	K_L	-6.33	12.3	0.064	Al-Dujaili et al., 2012
	303	L/mg	-6.98			
	313		-7.62			
Neptune grass	293	K_L	-5.94	55.4	0.209	Kaouah et al., 2014
	303	L/mg	-8.04			
	313		-10.1			
	323		-12.2			

Copper (Cu²⁺)

Boston fern	303	K_p	-10.4	-28.4	-0.061	Rao and Khan, 2017
	313	No	-8.35			
	323		-8.37			
Tea waste	288	K_d	-8.50	11.4	0.064	Wan et al., 2014
	298	mL/g	-7.78			
	308		-7.51			
	318		-7.59			
	328		-7.56			
Neem	303	K_L	-19.8	15.4	0.116	Febriana et al., 2010
	323	L/mol	-22.0			
	343		-24.4			
Neem	298	K_L	-4.66	26.70	0.07	Ang et al., 2013
	313	L/mg	-3.55			
	323		-2.81			
	333		-2.07			
	353		-0.60			

Zinc (Zn²⁺)

Teak	303	K_L	-11.9	-4.45	0.054	Kumar et al., 2006
	313	L/mg	-12.5			
	323		-13.0			
	333		-13.6			

Nickel (Ni²⁺)

Neem	303	K_d	-2.61	-58.2	-0.183	Bhattacharyya et al., 2009
	308	L/g	-1.69			
	313		-3.88			
	323		1.06			
	328		1.41			
	333		2.69			
Tea factory waste	298	K_p	-3.82	17.07	0.022	Malkoc and Nuhoglu, 2005
	318	No	-5.34			
	333		-6.27			

Hexavalent chromium-Cr(VI)

Taro	303	K_d	-8.32	0.75	0.025	Nakkeeran et al., 2016
	313	L/g	-4.41			
	323		-1.43			
	333		-0.79			
Mango	303	K_p	-7.15	97.1	0.344	Saha and Saha, 2014
	308	No	-9.27			

	313		-10.7			
Green tea	298	K_L	-3.96	-41.0	0.125	Jeyaseelan and Gupta, 2016a
	313	L/mg	-1.37			
	323		-0.62			
Purple secretia	303	K_L	-1.85	11.35	0.391	Sinha et al., 2015a
	308	L/mg	-3.09			
	313		-4.22			
	323		-5.28			
Golden shower	293	K_L	4.44			
	303	L/mg	3.20	41.55	0.1267	Ahmad et al., 2017a
	313		1.91			
Mercury (Hg²⁺)						
Bamboo	293	K_d	-0.87	10.3	0.023	Mondal et al., 2013
	300	L/g	-1.25			
	307		-2.03			
Arsenic (III)						
Mango	283	K_d	-17.9	23.9	0.144	Kamsonlian et al., 2012c
	293	L/g	-18.1			
	303		-20.0			
	318		-20.2			
Cadmium (Cd²⁺)						
Java plum	303	K_L	-1.40	3.7	0.017	Rao et al., 2010c
	313	L/mg	-1.58			
	323		-1.74			

NOTE: K_L (the Langmuir constant related to the affinity between an adsorbent and adsorbate that has been defined in Equation 12); K_p (thermodynamic partition coefficient that has been defined in Equation 18); K_d (distribution coefficient that has been defined in Equation 19)

Table S12. Thermodynamic parameters for the biosorption of toxic **metal ions** onto **modified/treated** leaves

Leaves	Chemical	T K	Derivation of K_C (unit)	$\Delta G°$ kJ/mol	$\Delta H°$ (kJ/mol)	$\Delta S°$ (kJ/mol × K)	Ref.
Lead (Pb²⁺)							
Drumstick	HNO₃, NaOH	293 303 313	K_L L/g	-3.94 -4.92 -5.39	17.5	0.074	Reddy et al., 2010
Rubber	NaOH, CD	303 313	K_d mL/g	-5.48 -4.95	21.4	0.052	Khalir et al., 2012
Australian pine	NaAlO₂	303 313 323	K_p no unit	-7.24 -8.87 -9.88	33.8	0.135	Khan Rao and Khatoon, 2017
Cadmium (Cd²⁺)							
Kush grass	NaOH	298 308 318	K_L L/g	-0.39 -1.51 -1.11	5.50	0.002	Pandey et al., 2015b
Bamboo	NaOH	298 308 318	K_L L/g	-0.66 -1.73 -2.05	9.28	0.003	Pandey et al., 2015b
Drumstick	HNO₃, NaOH	293 303 313 323	K_L L/g	-3.68 -4.50 -4.95 -5.42	15.3	0.063	Reddy et al., 2012
Copper (Cu²⁺)							
Rubber	H₂SO₄, HCHO	300 310 320	K_L L/mol	-23.5 -24.4 -25.3	3.20	0.089	Ngah and Hanafiah, 2009
Drumstick	HNO₃, NaOH	293 303 313	K_L L/g	-3.17 -3.75 -4.25	12.8	0.053	Reddy et al., 2012
Australian pine	NaAlO₂	303 313 323	K_p no unit	-7.85 -9.19 -10.7	36.2	0.145	Khan Rao and Khatoon, 2017
Black tea waste	NaOH	277 289 299 311	K_L L/mol	-19.0 -19.9 -20.7 -21.7	2.89	0.079	Weng et al., 2014b
Lamiaceae	NaOH	283 293 303 313 318	K_L L/mg	6.51 6.31 5.32 4.06 2.57	37.2	0.377	Kılıç and Solak, 2009
Mercury (Hg²⁺)							
Bamboo	TX-100	293	K_d	-1.07	15.9	0.098	Mondal et al., 2013

38

		300	L/g	-2.76			
		307		-3.96			
Bamboo	SDS	293	K_d	-1.15	32.9	0.106	Mondal et al., 2013
		300	L/g	-3.00			
		307		-4.19			

Nickel (Ni²⁺)

Adsorbent	Modifier	T	Parameter	Value			Reference
Drumstick	HNO$_3$, NaOH	293	K_L	-2.68	10.3	0.043	Reddy et al., 2012
		303	L/g	-3.08			
		313		-3.56			
Waste tea	FAD	313	K_d	-30.4	-23.7	0.022	Shah et al., 2015a
		323	L/g	-31.1			
		333		-31.8			
		343		-31.5			
		353		-31.9			
		363		-31.6			
Whitewater lily	MgCl$_2$	303	K_d	-1.73	0.21	0.002	Zahedi et al., 2015
		308	L/g	-1.59			
		323		-1.68			
Australian pine	NaAlO$_2$	303	K_p	-8.21	18.3	0.087	Khan Rao and Khatoon, 2017
		313	no unit	-8.60			
		323		-9.28			
Whitewater lily	MgCl$_2$	293	K_L	-1.73	0.21	0.002	Zahedi et al., 2015
		308	L/g	-1.59			
		323		-1.68			

Note: SDS (sodium dodecyl sulfate), FAD (formaldehyde), CD (carbon disulfide);

K_L (the Langmuir constant related to the affinity between an adsorbent and adsorbate that has been defined in Equation 12); K_p (thermodynamic partition coefficient that has been defined in Equation 18); K_d (distribution coefficient that has been defined in Equation 19)

Table S13. Thermodynamic parameters for the biosorption of **organic dyes** onto **pristine** leaves

Leaves	T (K)	Derivation of K_C (Unit)	Thermodynamic parameters			References
			$\Delta G°$ (kJ/mol)	$\Delta H°$ (kJ/mol)	$\Delta S°$ (kJ/mol × K)	
Methylene blue dye						
Carrot	303	K_L	-4.79	-12.7	-0.026	Kushwaha et al., 2014a
	313	L/mg	-4.53			
	323		-4.27			
Weeping willow	293	K_L	-21.1	-28.1	-0.024	Khodabandehloo et al., 2017
	333	L/mg	-20.0			
Phoenix tree	295	K_L	-3.89			Han et al., 2007
	309	L/mg	-4.62	7.77	-0.040	
	323		-5.01			
Potato	303	K_L	-4.38	-7.49	-0.010	Gupta et al., 2016a
	313	L/mg	-4.27			
	323		-4.17			
Brassica oleracea	303	K_d	-5.53	-18.1	-0.041	Ansari et al., 2016b
	313	no unit	-5.12			
	323		-4.71			
Hybrid plane	293	K_L	-4.93	28.3	0.113	Kong et al., 2015
	303	L/mg	-5.38			
	313		-7.45			
	323		-7.76			
Oriental plane	298	K_L	-0.17	9.94	0.034	Peydayesh and Rahbar-Kelishami, 2015
	313	L/mg	-0.70			
	323		-0.99			
	333		-1.37			
Oil palm	303	K_L	-1.41	21.5	0.076	Setiabudi et al., 2016a
	308	L/mg	-1.78			
	313		-2.16			
	318		-2.54			
	323		-2.92			
	328		-3.29			
Pineapple	308	K_L	-4.32	-2.79	0.004	Kamaru et al., 2016
	313	L/mg	-4.33			
	333		-4.44			
Pine	303	K_d	-10.4	15.3	0.085	Yagub et al., 2012
	313	L/g	-11.3			
	323		-12.1			
	333		-12.9			
Water bamboo	283	K_d	-2.39	-16.3	-0.049	Zhu et al., 2016
	293		-2.18			
	303		-1.63			
	313		-0.92			
	323		-0.57			
Date palm	303	K_p	4.13	8.09	0.013	Gouamid et al., 2013
	318	no unit	4.04			
	333		3.73			

Ashoka	303	K_L	-6.56	-11.8	-0.017	Gupta et al., 2012a
	313	L/mg	-6.38			
	323		-6.21			
Lotus	293	K_L	-25.7	4.70	0.103	Han et al., 2011
	303	L/mg	-26.6			
	313		-27.7			

Malachite green dye

Carrot	303	K_L	-2.78	-8.21	-0.018	Kushwaha et al., 2014a
	313	L/mg	-2.60			
	323		-2.42			
Potato	303	K_L	-3.06	-6.30	-0.0107	Gupta et al., 2016a
	313	L/mg	-2.96			
	323		-2.85			
Lotus	296	K_L	-10.7	35.9	0.157	Han et al., 2014
	306	L/mg	-12.4			
	316		-13.9			
Ashoka	303	K_L	-4.19	-6.67	-0.008	Gupta et al., 2012a
	313	L/mg	-4.11			
	323		-4.03			

Crystal violet dye

Pineapple	293	K_L	-18.3	-68.5	-0.171	Chakraborty et al., 2012
	303	L/mg	-16.6			
	313		-14.8			
Esparto grass	298	K_L	2.68	28.9	0.101	Lafi et al., 2015
	308	L/mg	3.74			
	318		4.79			
	328		5.85			

Amaranth dye

Water hyacinth	291	K_L L/mg	58.6	17.3	-0.142	Guerrero-Coronilla et al., 2015
	301		59.9			
	313		61.7			
	323		63.1			

Basic Red 46 dye

Turkish pine	298	K_L L/mg	-4.71	46.4	0.170	Deniz and Karaman, 2011
	308		-7.11			
	318		-8.13			
Princess	298	K_L L/mg	-4.29	-43.8	-0.130	Deniz and Saygideger, 2011
	308		-3.17			
	318		-1.64			

Methyl violet dye

Neptune grass	293	K_L L/mg	-7.37	17.2	0.084	Cengiz and Cavas, 2010
	308		-8.73			
	318		-9.65			
Platanus carpinifolia	298	K_L L/mg	-1.96	37.3	0.132	Zolgharnein et al., 2014
	308		-3.63			
	318		-4.95			
	328		-6.27			

Basic Green 4 dye

Pineapple	298	K_L L/mg	-17.9	-101.40	-0.280	Chowdhury et al., 2011
	308		-14.8			
	318		-12.3			

Acid orange 52 dye

Princess	298	K_L L/mg	6.42	-5.63	-0.040	Deniz and Saygideger, 2010
	308		6.81			
	318		7.23			

Direct solophenyl brown AGL dye

Neptune grass	288	K_L L/mg	-6.73	57.8	-0.104	Ncibi et al., 2006
	303		-6.37			
	318		-5.82			
	333		-5.68			

Reactive cibacron red FNR

Neptune grass	288	K_L L/mg	-5.00	84.1	-0.226	Ncibi et al., 2006
	303		-3.22			
	318		-2.83			
	333		-2.51			

Remazol blue R dye

Neem	298	K_L	5.52	-14.6	0.030	Immich et al., 2009
	313	L/mg	6.62			
	333		7.98			

Brilliant Green dye

Neem	300	K_d	7.15	5.66	0.043	Bhattacharyya and Sarma, 2003
	303		7.28			
	313		7.70			
	323		8.13			
Ashoka	303	K_L L/mg	-7.98	-24.7	-0.055	Gupta et al., 2012a
	313		-7.43			
	323		-6.88			

Rhodamine B

Ashoka	303	K_L L/mg	-1.78	-5.94	-0.014	Gupta et al., 2012a
	313		-1.65			
	323		-1.51			

Toluidine blue dye

Esparto grass	298	K_L L/mg	2.31	17.9	0.061	Lafi et al., 2015
	308		2.99			
	318		3.66			
	328		4.34			

Table S14. Thermodynamic parameters for the biosorption of **organic dyes** onto **modified/treated** leaves

Leaves	Chemical	T K	Derivation of K_C (unit)	ΔG° (kJ/mol)	ΔH° (kJ/mol)	ΔS° (kJ/mol × K)	Ref.
Malachite green dye							
Maize	CaOH₂	303	K_p	-5.93	32.4	0.127	Jalil et al., 2012a
		313	No unit	-7.19			
		323		-8.46			
Labill	Ammoni, lauric acid	293	K_d	-6.88	11.5	0.063	Yang and Hong, 2018b
		303	L/g	-7.85			
		313		-8.12			
		323		-9.72			
Crystal violet dye							
Phoenix tree	NaOH	293	K_p	-5.79	14.9	0.071	Ren et al., 2015
		303	No unit	-6.61			
		313		-7.21			
Acid violet 17 dye							
Cluster fig	NaOH H₂SO₄	293	K_L	-26.6	10.9	0.130	Jain and Gogate, 2017d
		303	L/mg	-27.8			
		313		-29.1			
		323		-30.5			
Pyrocatechol violet							
Black locust	NaCl	296	K_p	-2.43	-9.67	0.024	Khorshidi and Niazi, 2016
		298	No unit	-2.42			
		303		-2.27			
		308		-2.18			
		313		-2.01			
Acid blue 113 dye							
Almond	NaOH, CTAB	293	NA	-29.4	-31.3	-0.007	Jain and Gogate, 2017b
		303		-29.2			
		313		-29.1			
		323		-29.2			
Acid blue 25 dye							
Cluster fig	NaOH	293	K_L	-26.6	29.9	0.192	Jain and Gogate, 2017a
		303	L/mg	-28.3			
		313		-30.3			
		323		-32.4			
Cluster fig	NaOH	293	Temkin	-34.3	48.7	0.283	Jain and Gogate, 2017a
		303	L/mg	-36.8			
		313		-39.7			
		323		-42.8			
Methyl orange dye							
Pineapple	HDTMA	308	K_p	-3.75	-8.75	-0.016	Kamaru et al., 2016
		313	No unit	-3.69			
		333		-3.35			

Acid green 25 dye

Almond	NaOH	293	K_L	-34.7	6.99	0.142	Jain and Gogate, 2018
		303	L/mg	-36.0			
		313		-37.4			
		323		-38.9			
Almond	NaOH	293	Temkin	-43.7	21.9	0.224	Jain and Gogate, 2018
		303	L/mg	-45.7			
		313		-47.9			
		323		-50.4			

Congo red dye

Labill	Ammoni, lauric acid	293	K_d	-1.47	0.004	0.006	Yang and Hong, 2018b
		303	L/g	-2.05			
		313		-2.14			
		323		-2.19			

NOTE: CTAB (cetyltrimethylammonium bromide; hexadecyltrimethylammonium bromide), HDTMA (Hexadecyltrimethylammonium bromide); NA (not clearly mentioned in the original paper)

Table S15. Thermodynamic parameters for the biosorption of **other contaminants** onto **pristine** and **treated/modified** leaves

Leaves	Chemical	T (K)	Derivation of K_C (unit)	Thermodynamic parameters			Ref.
				$\Delta G°$ (kJ/mol)	$\Delta H°$ (kJ/mol)	$\Delta S°$ (kJ/mol $\times$ K)	
Naphthalene							
Spent tea leaves		303	K_d	-0.54	217	0.718	Agarry et al., 2013
		308	(L/g)	-2.29			
		313		-6.32			
		318		-11.2			
Fluoride							
Neem		298	K_L (L/g)	-0.83	-29.9	-0.001	Bharali and Bhattacharyya, 2015
		303		-0.34			
		308		0.15			
		313		0.54			
		318		1.12			
Orthophosphate							
Reed	Ca(OH)$_2$	298	K_p	-15.6	85.0	0.339	Markou et al., 2016a
		308	(No unit)	-20.1			
		318		-22.2			

Table S16. The Q^o_{max} (mmol/kg), CEC (mmol/kg), ECEC (mmol/kg), α or β ratio of bisorbent and zeolite to some cationic and oxyanionic metal ions

Adsorbent	Adsorbate	Q^o_{max}	CEC/ ECEC	α/β	Ref.	Adsorbent	Adsorbate	Q^o_{max}	CEC/ ECEC	α/β	Ref.
Pristine biosorbent						**Modified biosorbent**					
CAN	**Cd(II)**	30.4	66.5	0.81	Tran and Chao, 2018	CAN	**Cd(II)**	45.4	113	0.71	Tran and Chao, 2018
PC	Cd(II)	17.3	43.5	0.71	Tran and Chao, 2018	PC	Cd(II)	30.9	81.3	0.68	Tran and Chao, 2018
LP	Cd(II)	11.5	38.3	0.54	Tran and Chao, 2018	LP	Cd(II)	27.2	76.5	0.63	Tran and Chao, 2018
AS	Cd(II)	7.40	22.6	0.58	Tran and Chao, 2018	AS	Cd(II)	18.9	46.1	0.73	Tran and Chao, 2018
SB	Cd(II)	6.13	11.8	0.92	Tran and Chao, 2018	SB	Cd(II)	14.3	21.1	0.50	Tran and Chao, 2018
BS	Cd(II)	7.03	19.6	0.64	Tran and Chao, 2018	BS	Cd(II)	9.16	32.6	1.03	Tran and Chao, 2018
CAN	**Cu(II)**	23.5	66.5	1.11	Tran and Chao, 2018	CAN	**Cu(II)**	33.1	113	2.67	Tran and Chao, 2018
PC	Cu(II)	14.0	43.5	1.01	Tran and Chao, 2018	PC	Cu(II)	25.4	81.3	5.88	Tran and Chao, 2018
LP	Cu(II)	8.61	38.3	0.70	Tran and Chao, 2018	LP	Cu(II)	22.4	76.5	3.58	Tran and Chao, 2018
AS	Cu(II)	6.14	22.6	0.85	Tran and Chao, 2018	AS	Cu(II)	14.9	46.1	2.82	Tran and Chao, 2018
SB	Cu(II)	6.54	11.8	1.75	Tran and Chao, 2018	SB	Cu(II)	13.9	21.1	2.55	Tran and Chao, 2018
BS	Cu(II)	5.51	19.6	0.88	Tran and Chao, 2018	BS	Cu(II)	8.99	32.6	3.05	Tran and Chao, 2018
CAN	**Pb(II)**	81.1	66.5	1.18	Tran and Chao, 2018	CAN	**Pb(II)**	143	113	1.22	Tran and Chao, 2018
PC	Pb(II)	49.1	43.5	1.09	Tran and Chao, 2018	PC	Pb(II)	78.2	81.3	0.93	Tran and Chao, 2018

LP	Pb(II)	34.5	38.3	0.87	Tran and Chao, 2018	LP	Pb(II)	68.0	76.5	0.86	Tran and Chao, 2018
AS	Pb(II)	23.9	22.6	1.02	Tran and Chao, 2018	AS	Pb(II)	52.9	46.1	1.11	Tran and Chao, 2018
SB	Pb(II)	8.82	11.8	0.72	Tran and Chao, 2018	SB	Pb(II)	33.7	21.1	1.32	Tran and Chao, 2018
BS	Pb(II)	25.4	19.6	1.25	Tran and Chao, 2018	BS	Pb(II)	29.7	32.6	0.88	Tran and Chao, 2018

NaY zeolite						**HDTMA-modified NaY zeolite**					
	Cu(II)	371	3120	0.24	Chao and Chen, 2012		Cu(II)	388	2880	0.27	Chao and Chen, 2012
	Zn(II)	354	3120	0.23	Chao and Chen, 2012		Zn(II)	318	2880	0.22	Chao and Chen, 2012
	Ni(II)	331	3120	0.21	Chao and Chen, 2012		Ni(II)	315	2880	0.22	Chao and Chen, 2012
	Pb(II)	671	3120	0.25	Chao and Chen, 2012		Pb(II)	653	2880	0.45	Chao and Chen, 2012
	Cd(II)	390	3120	0.43	Chao and Chen, 2012		Cd(II)	351	2880	0.24	Chao and Chen, 2012
—	—	—	—	—	—		[a]$Cr_2O_7^{2-}$	184	260	1.42	Chao and Chen, 2012
—	—	—	—	—	—		[b]MnO_4^-	412	260	2.58	Chao and Chen, 2012

Note: CAN (cantaloupe peel), PC (pine cone), LP (litchi fruit peel), AS (annona squamosal), SB (sugarcane bagasse), BS (bamboo shoot); $\alpha = 2Q^o_{max}/\text{CEC}$, [a]$\beta = 2Q^o_{max}/\text{ECEC}$, [b]$\beta = Q^o_{max}/\text{ECEC}$.

Table S17. Removal percentage of Cr(VI) from dichromate solutions by various biosorbents Aoyama, 2003a

pH	Black locust leaves[a]		Coniferous leaves[b]		Larch bark[c]	
	Cr(VI)	Total Cr	Cr(VI)	Total Cr	Cr(VI)	Total Cr
2	100	63.1	100	67.5	99.9	83.1
3	100	99.5	92.5	90.9	95.3	95.3
4	82.7	82.4	76.8	76.5	57.9	57.9
5	77.9	77.3	41.7	41.6	51.4	51.4

Note: [a]Aoyama et al., 2000b, [b]Aoyama et al., 1999b, and [c]Aoyama and Tsuda, 2001
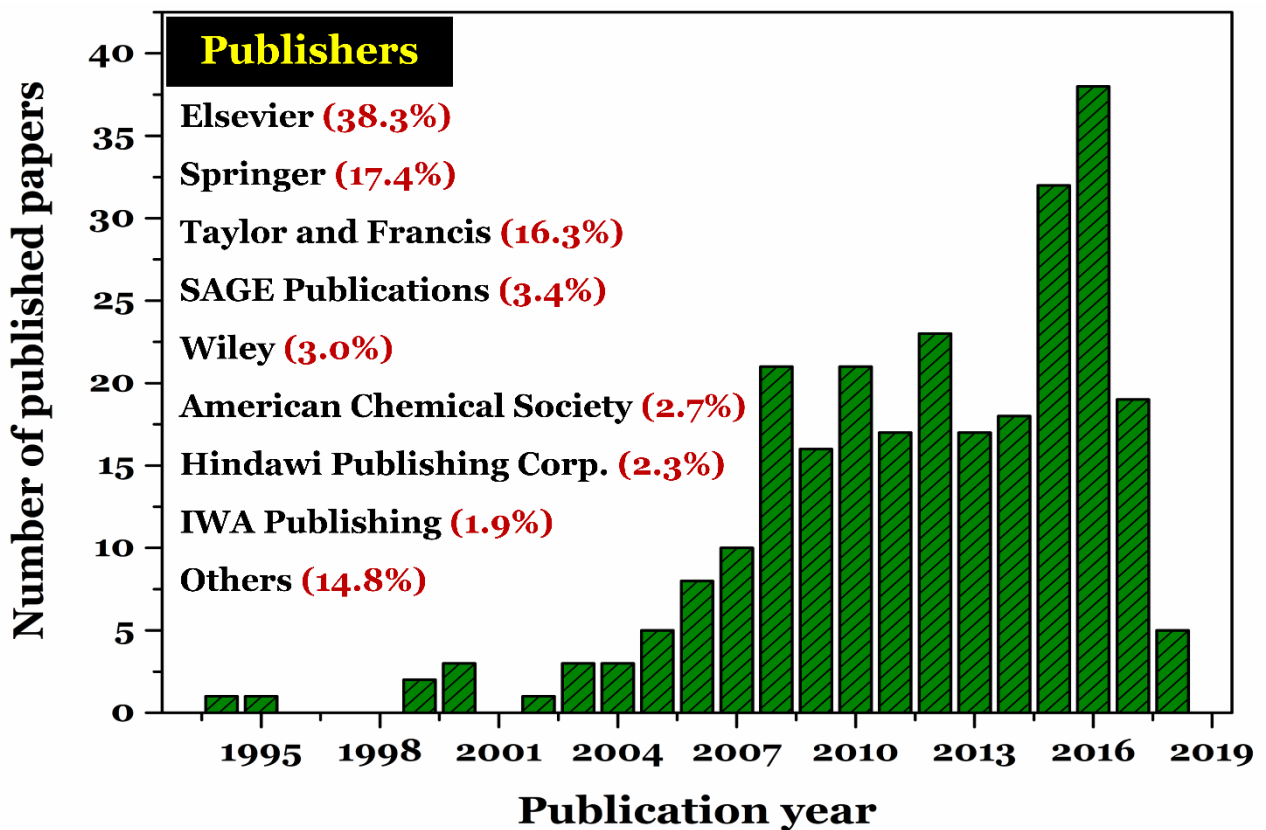
Figure S1. Number of articles published applying leaf-based biosorbent for removal of toxic pollutants from water bodies per year (only for the published original papers) and distribution of publisher relevant to the topic
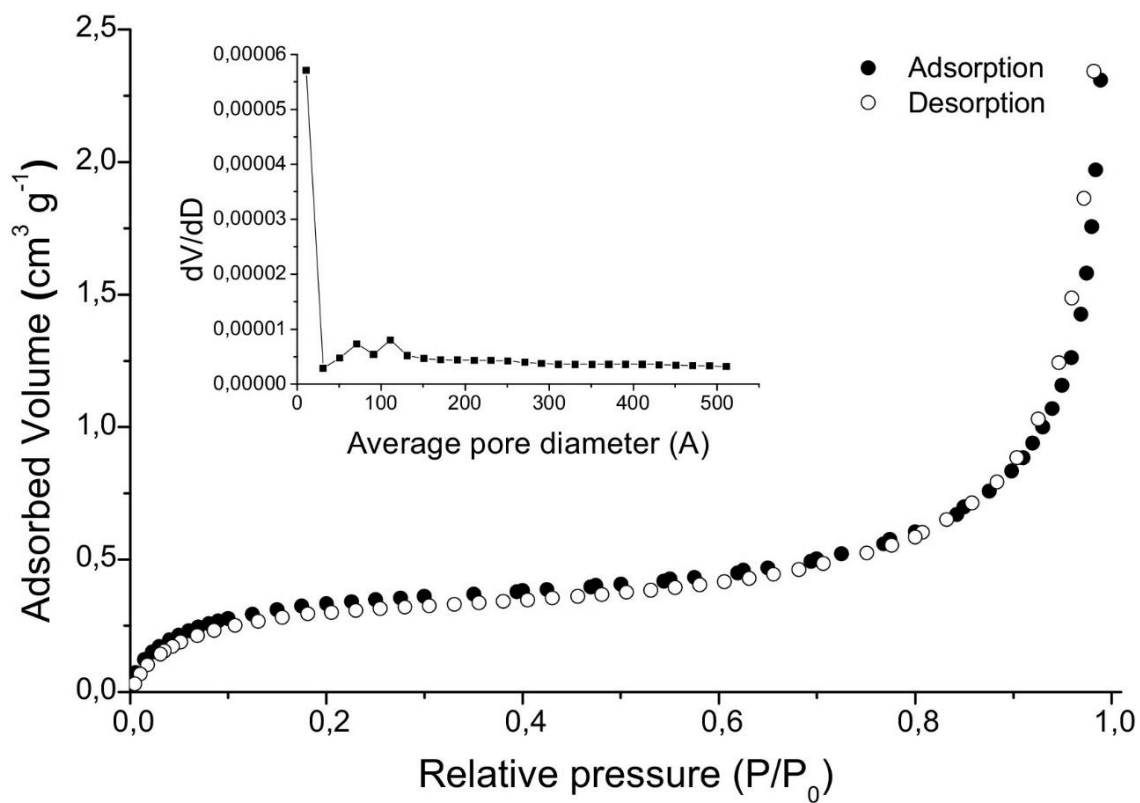
Figure S2. Typical adsorption/desorption isotherm of biosorbent derived from Brazilian orchid tree (pata-de-vaca) leaves and its pore size distribution (Jorgetto et al., 2015)

(a) Before adsorption

× 500

× 1000

(b) Before adsorption

C
Ca

O

Ca   Ca

Si
Au   Au   Ca Ca
Full Scale 5275 cts Cursor: 10.018 keV (1 cts)   keV

(c) After Cu(II) adsorption

C

Ca (No detected)

Cu

O

Cu Si Au Au Au
Full Scale 7912 cts Cursor: 10.018 keV (3 cts)   keV

(d) Cation exchange mechanism

(1) Biosorbent + copper solution ("**Released**")
(2) Biosorbent + deionized water ("**Dissolved**")

Analysis pH and the amount of alkaline earth and alkali metals

(3) The amount of **ion exchange**: (1) "**Released**" − (2) "**Dissolved**"

The ratio of cations bound (Cu^{2+} and 1/2H$^+$) to biosorbent surface and released (Mg^{2+} + Ca^{2+} + 1/2Na$^+$) is **0.85**, suggesting that ion-exchange is the primary adsorption mechanism

Figure S3. (a) SEM image of rubber (*Hevea brasiliensis*) leaf powders, **(b)−(c)** EDS spectra, and **(d)** confirmation of the ion exchange mechanism (Wan Ngah and Hanafiah, 2008)

51

(a) ... **(b)** ... **(c)** ... **(d)**

IR Peaks (cm^{-1})	Functional groups
3420	The (OH) stretching vibration of hydroxyl group
2920 and 2850	The C–H stretching vibration of methyl (–CH$_3$–) methylene (–CH$_2$–) groups
1735	The carbonyl (C=O) groups
1610 and 1515	The skeletal C=C vibrations in aromatic rings
1440	The ionic carboxylic (–COO$^-$) group
1330	The (C=O) vibration in carboxylate group
1250	The C–O–C stretching of aryl-alkyl ether linkages in lignin
1030	The C–O stretching vibrations of cellulose backbone
865	The aromatic C–H out-of-plane bending mode

Figure S4. (a) FTIR spectra of pristine biosorbent derived from fallen *Cinnamomum camphora* leaves (Chen et al., 2010b) and **(b)** the spectroscopic assignment; and **(c)** XPS spectra of arborvitae leaves and **(b)** C 1s XPS spectra of arborvitae leaves (Shi et al., 2016b)

52
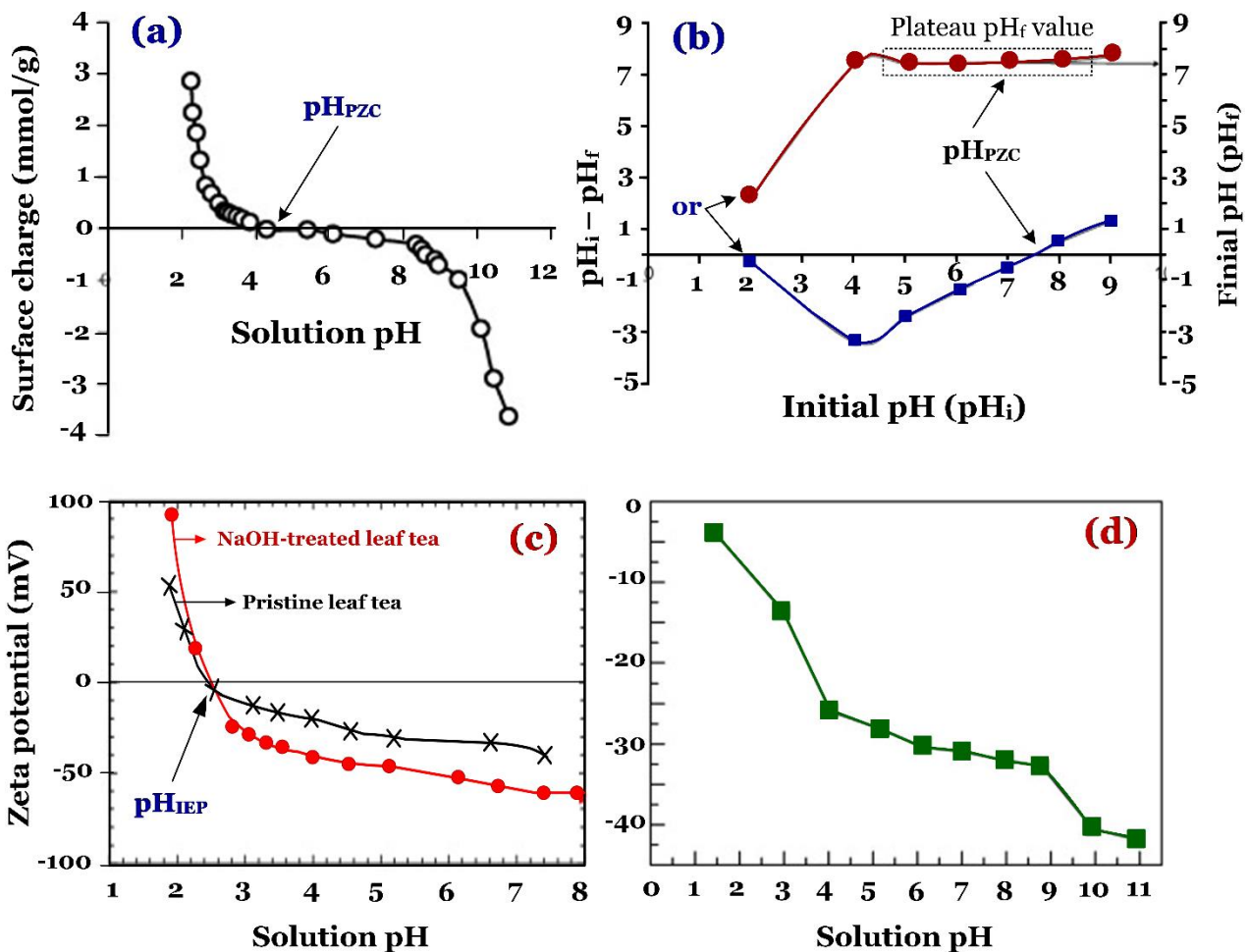
Figure S5. Point of zero charge (PZC) of **(a)** tea waste leaves determined by the acid-base titration method Uddin et al., 2009 [License number: 4435871145286] and **(b)** gulmohar leaves determined by the "drift method" Ponnusami et al., 2009b [License number: 4435871247208]; and isoelectric point (IEP) of **(c)** treated black tea waste leaves determined by a zeta meter Weng et al., 2014a [License number: 4435871464044] and **(d)** strawberry leaves determined by an electrokinetic analyzer Liu et al., 2010d [License Number: 4435880051225]
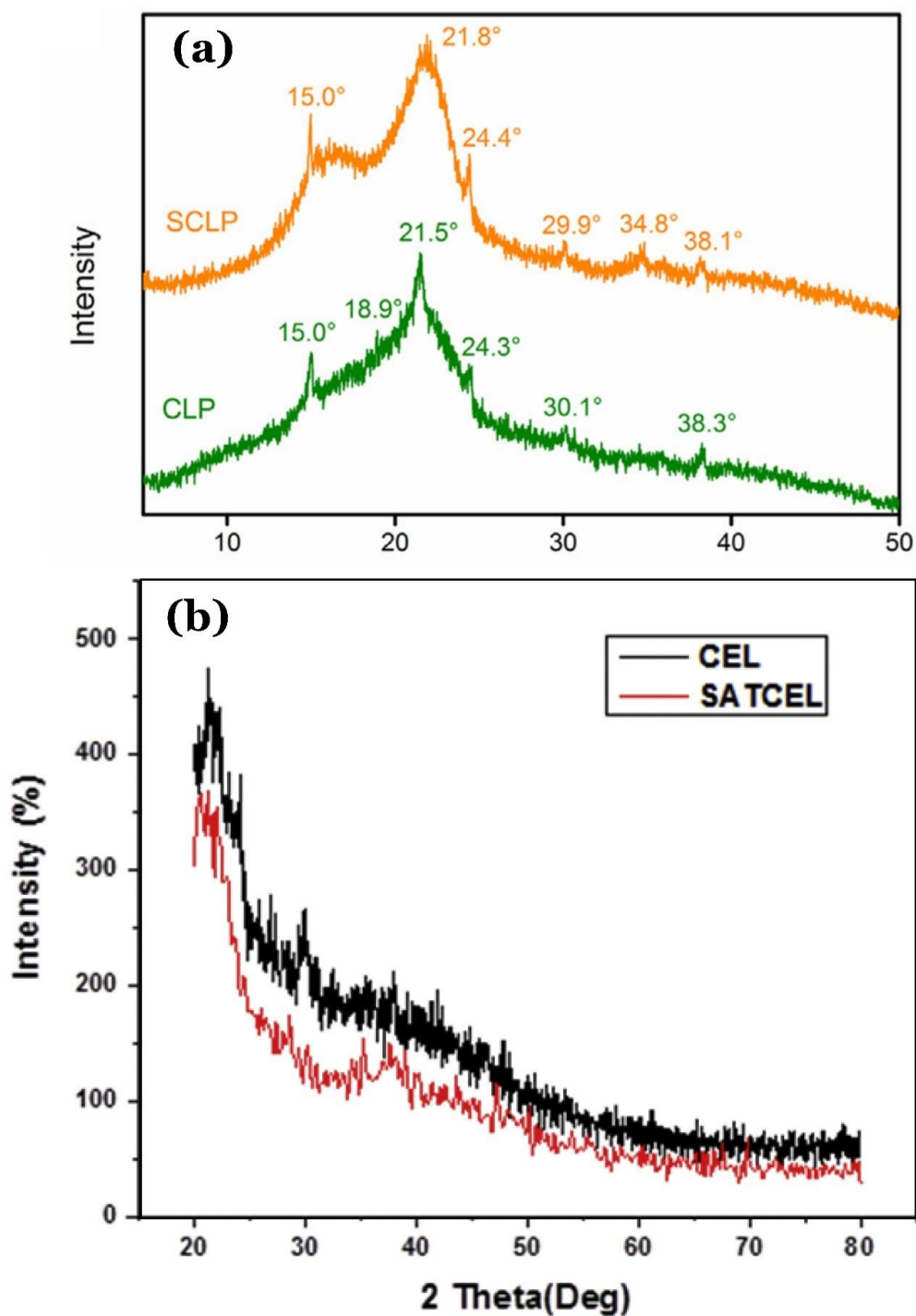
Figure S6. XRD spectra of **(a)** pristine (CLP) and succinic anhydride-modified camphor (SCLP) leaves (Wang et al., 2016), and **(b)** pristine (CEL) and aluminate-treated *Casuarina equisetifolia* (SATCEL) leaves (Khan Rao and Khatoon, 2017)
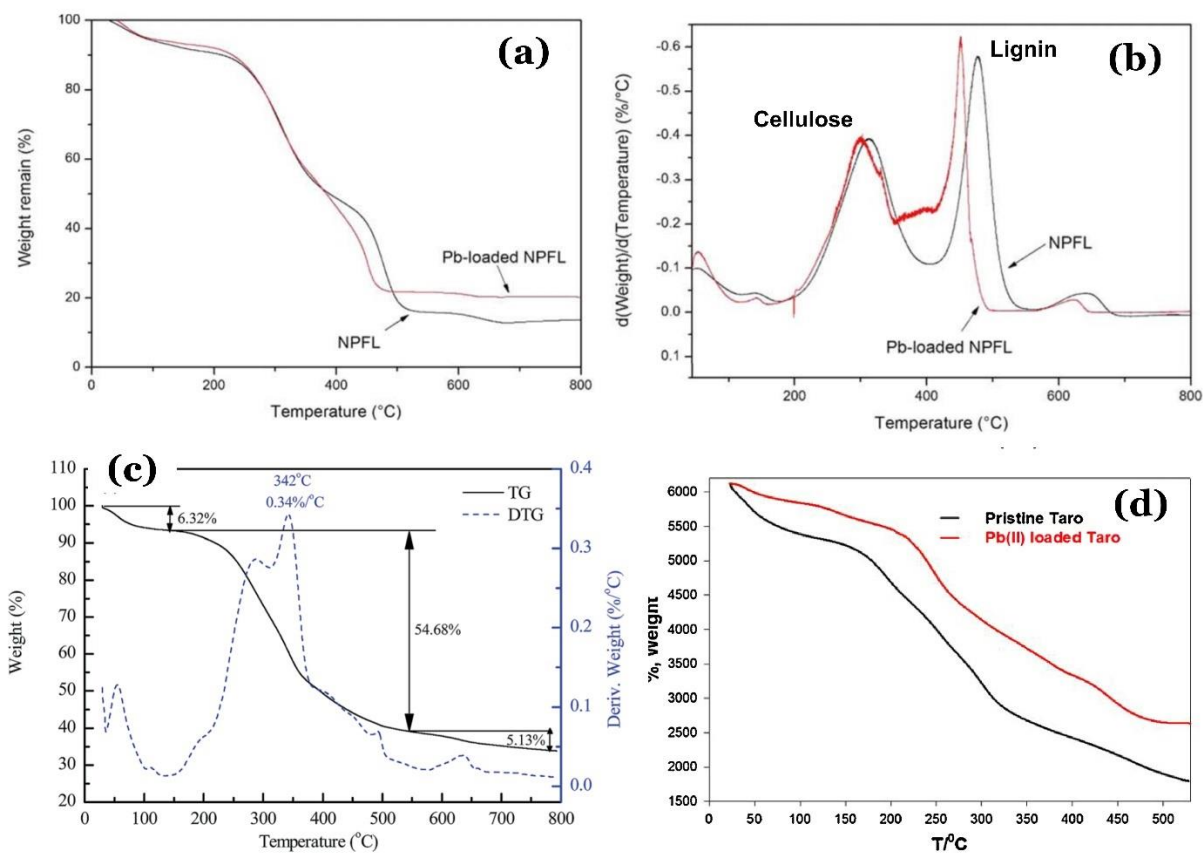
Figure S7. (a) TG and **(b)** DTG curves of alkali-treated persimmon fallen leaves (NPFL) (Ruiyi et al., 2016), **(c)** TG–DTG curves of raw phoenix tree leaves (Liang et al., 2016), and (d) TGA of pristine and Pb-loaded Taro leaves (Saha et al., 2017)
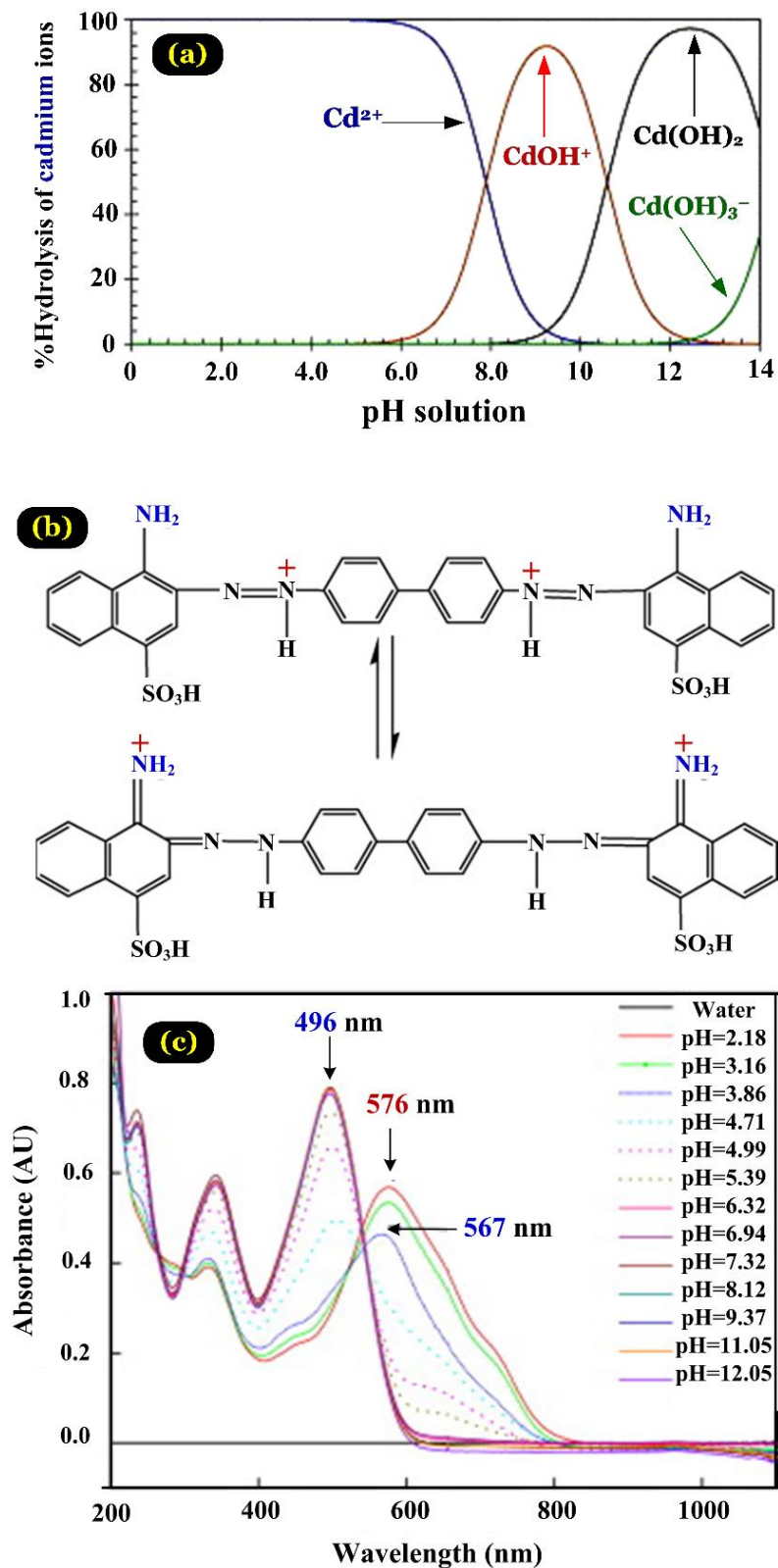
Figure S8. (a) Distribution of various cadmium species as a function of the pH ([Srivastava et al., 2006]); **(b)** chemical structure of Congo Red dye and **(c)** UV–Vis spectra of Congo Red solutions at different solution pH values ([Zhou et al., 2011])
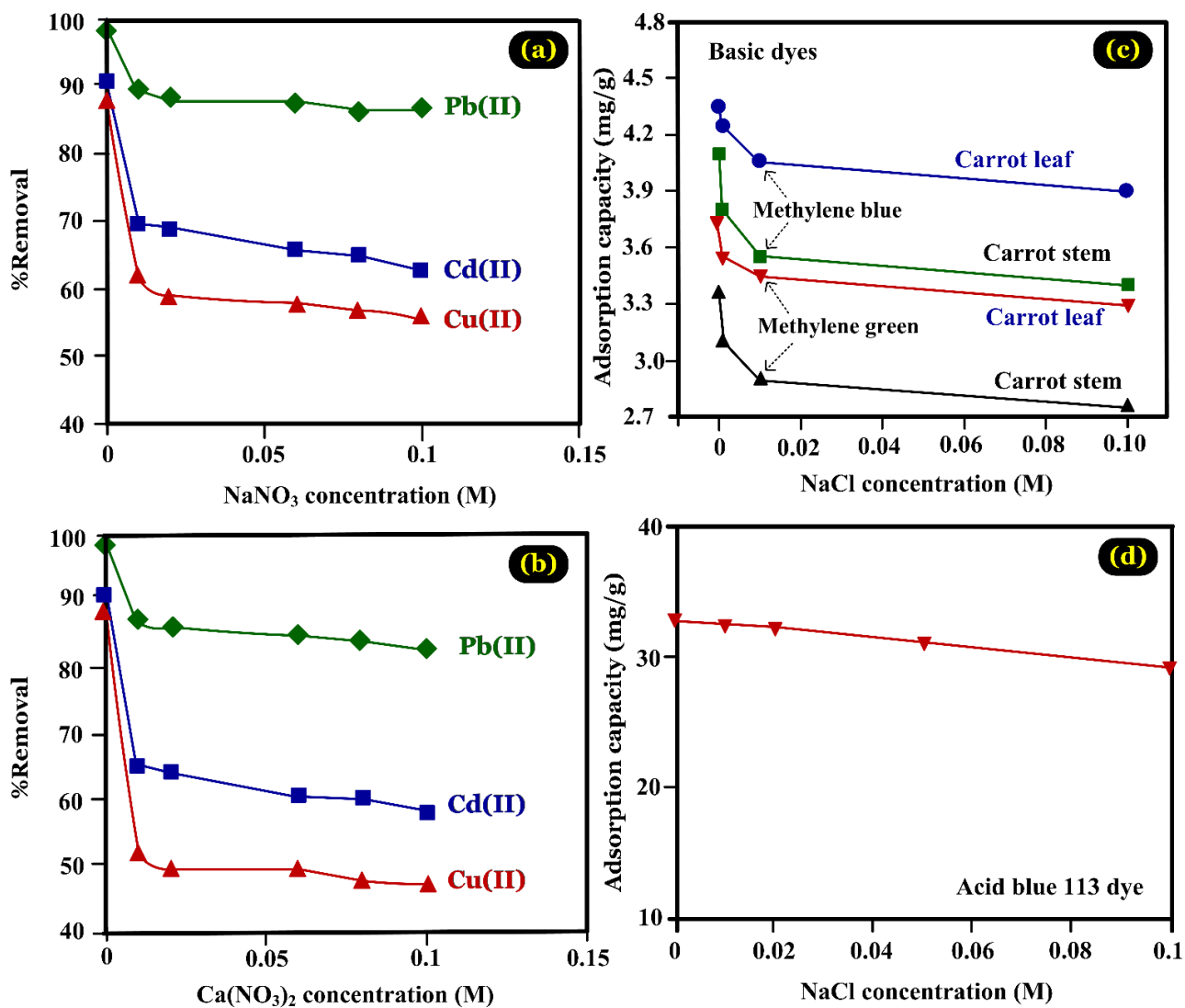
Figure S9. Effect of the ionic strength on the adsorption process of **(a–b)** potentially toxic metals onto *Ulmus carpinifolia* tree leaves (Sangi et al., 2008), **(c)** cationic dyes onto *Daucus carota* stems and leaves (Kushwaha et al., 2014b), and **(d)** anionic dye onto surfactant-modified *Prunus Dulcis* leaves (Jain and Gogate, 2017b)

The plot shows data points labeled "0.005 M", "0.01 M", "0.07 M", and "$I = 0.07$ M" with a red regression line.

Plot annotations:
$y = 1.648 + 0.209\,x$
$R^2 = 0.958$

$$\frac{1}{\kappa} = \left(\frac{2F^2 I \times 1000}{\varepsilon \varepsilon_0 RT} \right)^{-0.5}$$

Y-axis: k_2 (g/mg × min)

X-axis: Electrical double layer thickness ($1/\kappa$; nm)
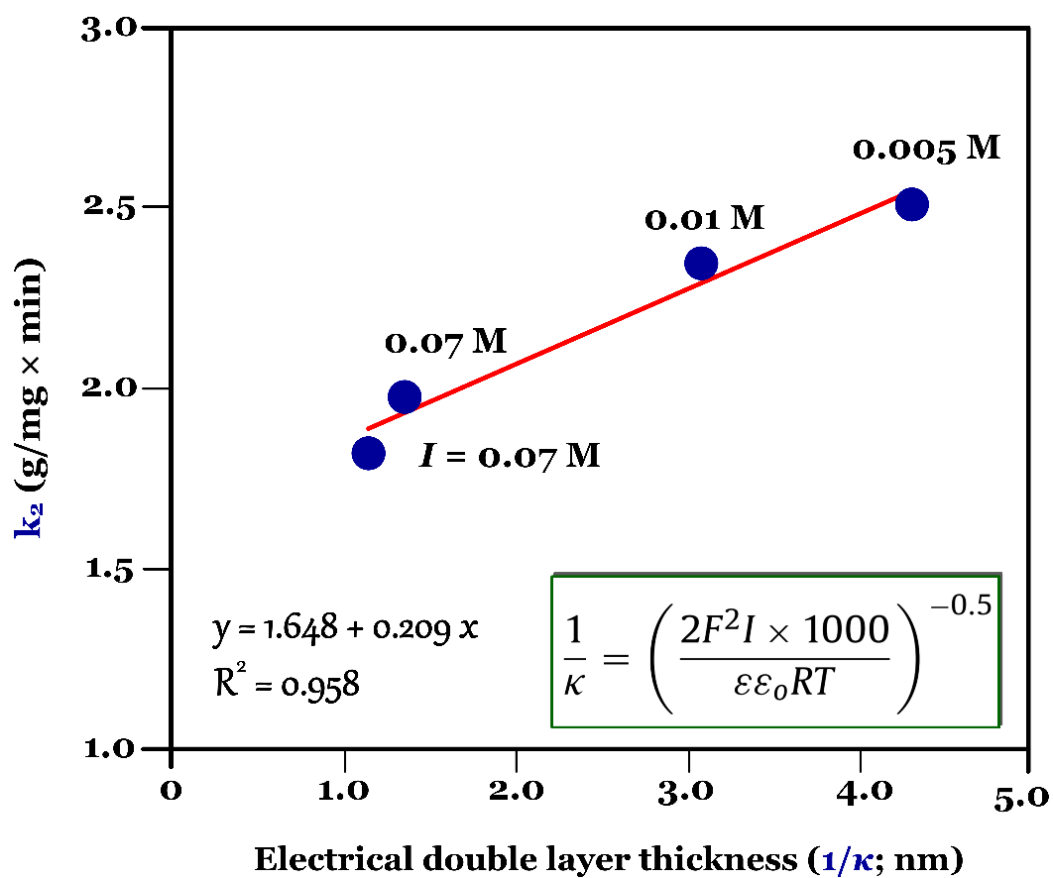
Figure S10. Linear relationship between the rate constant k_2 of pseudo-second-order model and the thickness of the electrical double layer Weng et al., 2009
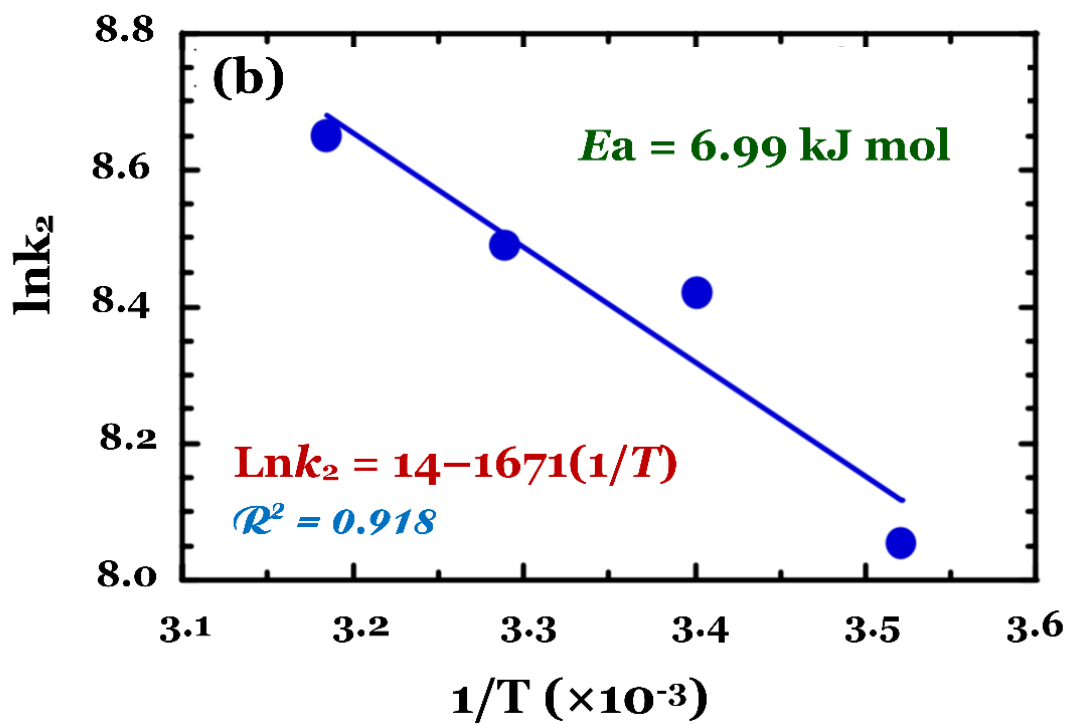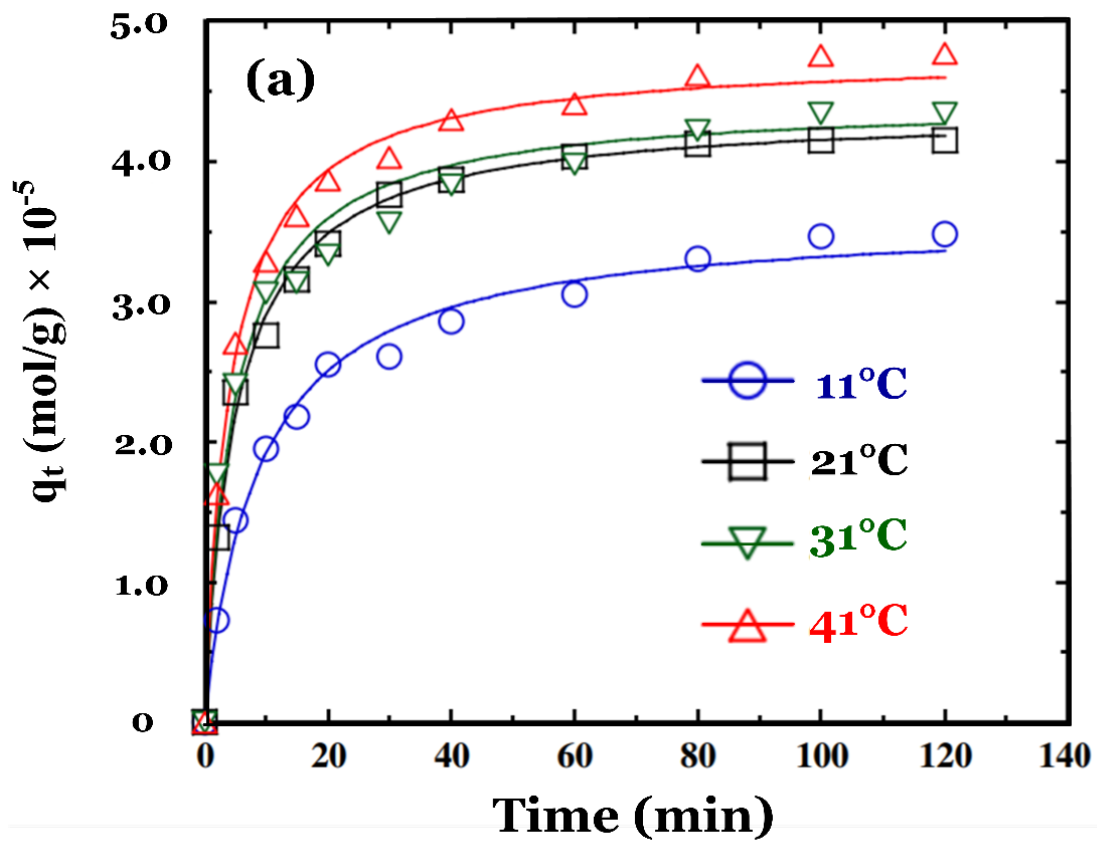
Figure S11. (a) Effect of the contact time on the Cu(II) adsorption process onto pineapple leaf powders at different operation temperatures, and **(b)** plot of the Arrhenius equation (Weng and Wu, 2012)
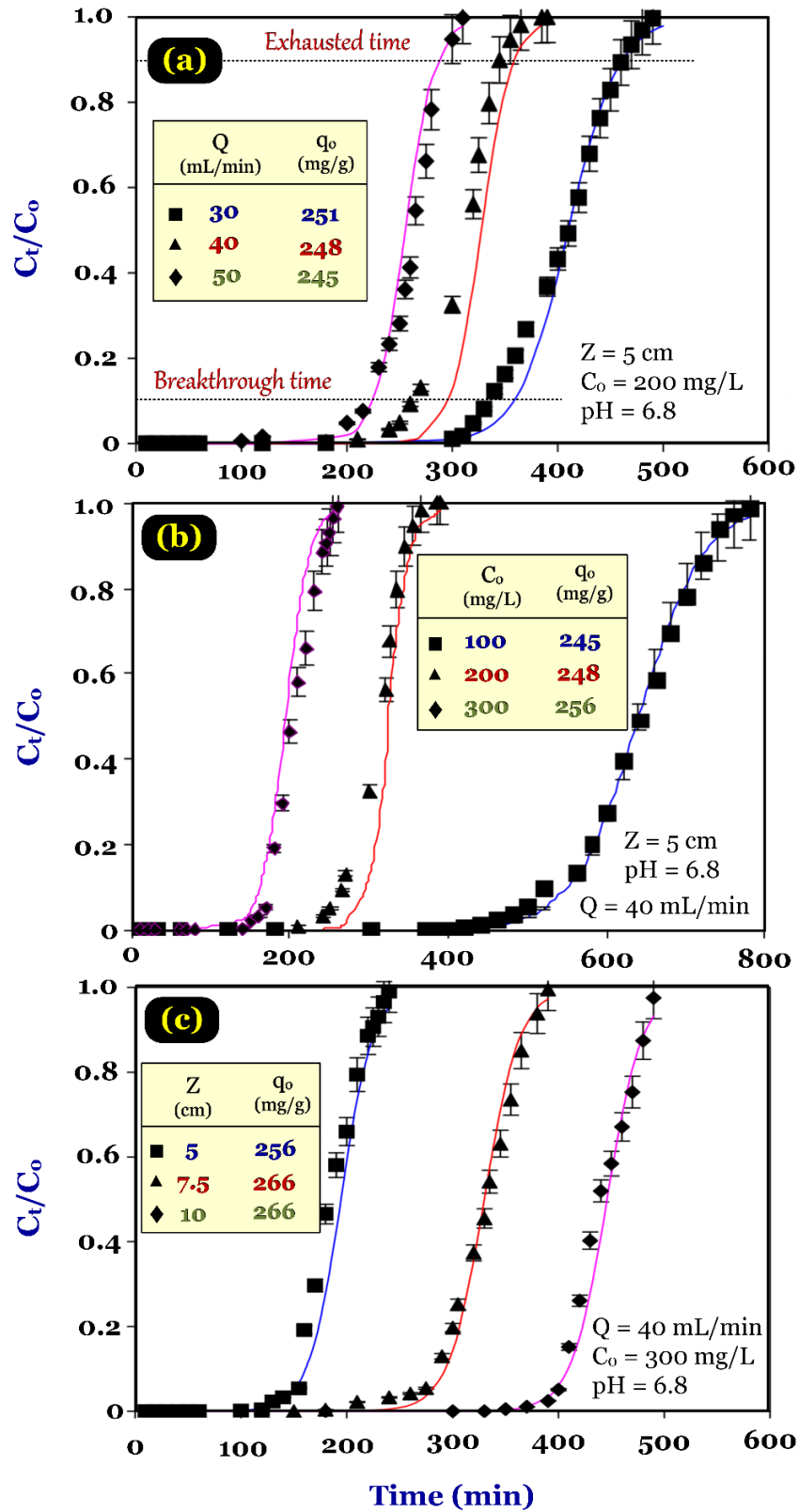
Figure S12. Typical breakthrough curve for methylene blue adsorption onto jackfruit leaves at different **(a)** flow rates, **(b)** feed concentrations, and **(c)** bed heights (Tamez Uddin et al., 2009)

60
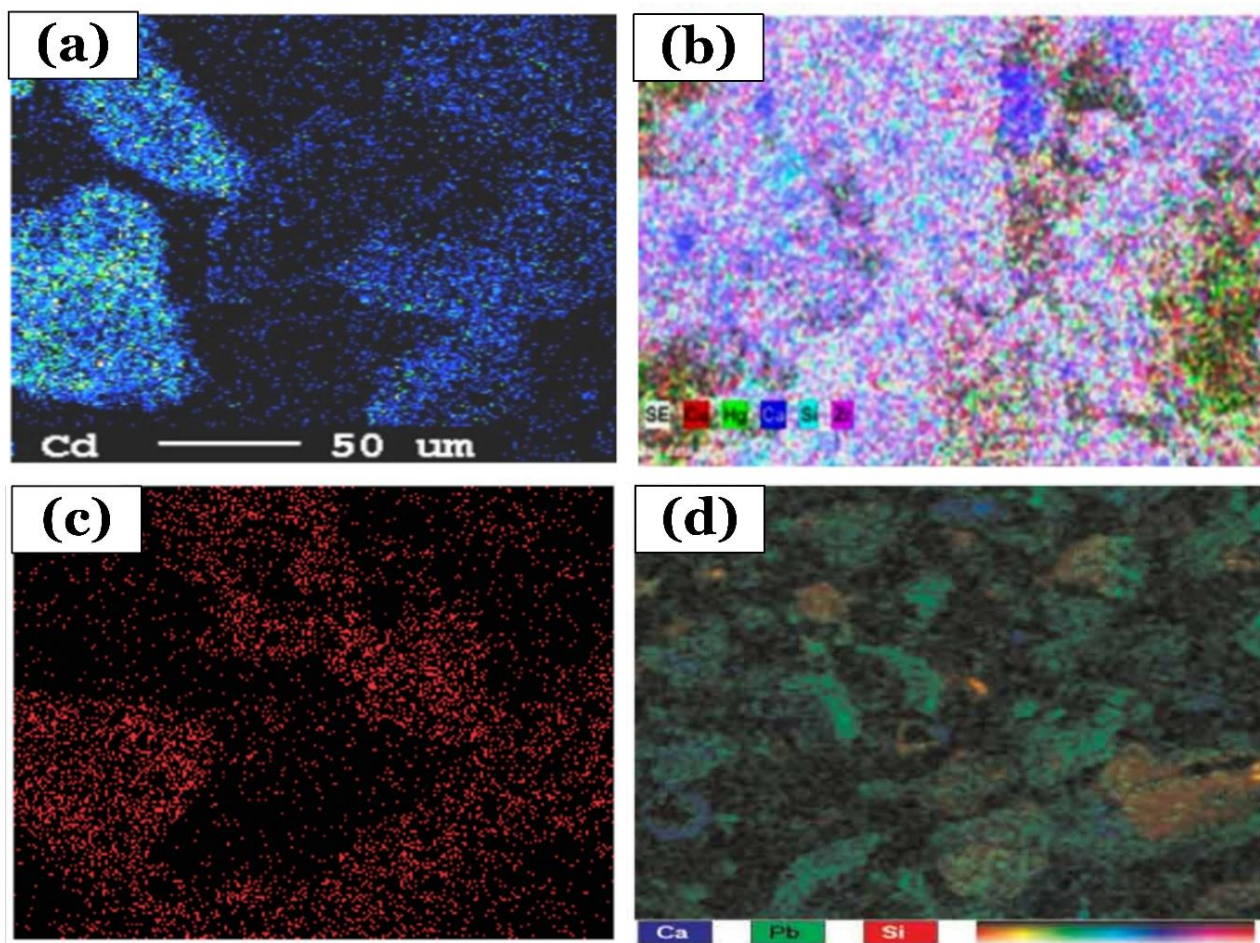
Figure S13. **(a)** Scanning Electron Micrographs of *Syzygium cumini L.* leaves after Cd(II) adsorption (Rao et al., 2010c), **(b)** Element distributions of EDX analysis region of tobacco leaves after Cu(II) biosorption (Çekim et al., 2015), **(c)** Cr mapping of Sakura leaves after Cr (VI) adsorption (Wenfang et al., 2015), and **(d)** X-ray mapping of maple leaves after Pb(II) adsorption (Hossain et al., 2014b)
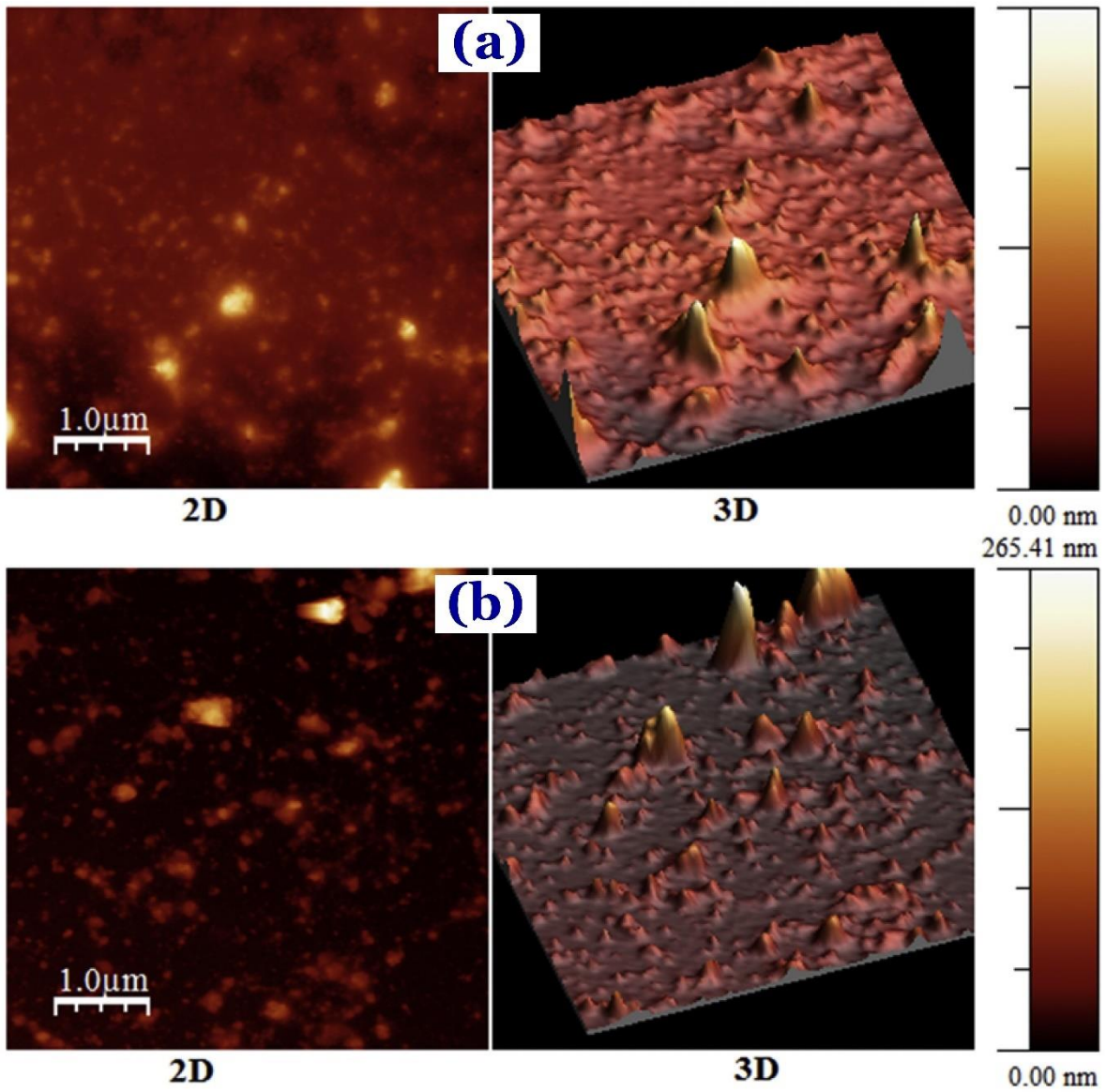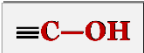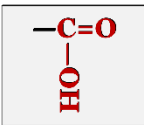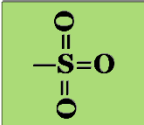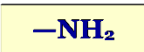
Figure S14. Atomic force microscopy (AFM) image of sodium aluminate-treated *Casuarina equisetifolia* leaves **(a)** before and **(b)** after Cu(II) biosorption (Khan Rao and Khatoon, 2017)

(a)

Binding group	Structural formula	pKa	Ligand atom
Hydroxyl	$\equiv C-OH$	9.5–13	O
Carboxyl	$-C=O$ / OH	1.7–4.7	O
Sulfhydryl (thiol)	$-SH$	8.3–10.8	S
Sulfonate	$-S=O$ (with O, O)	1.3	S
Amine	$-NH_2$	8–11	N

(b)
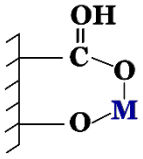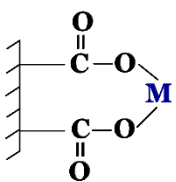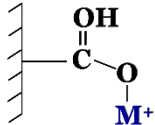
Chelation between carboxyl and phenolic hydroxyl — Chelation between two carboxyl groups — Complexation with a carboxyl group

Figure S15. (a) Some major binding functional groups for adsorption (Volesky, 2007), and **(b)** binding of a metal ion (M^{2+}) by oxygen-containing functional groups (Manahan, 2000).
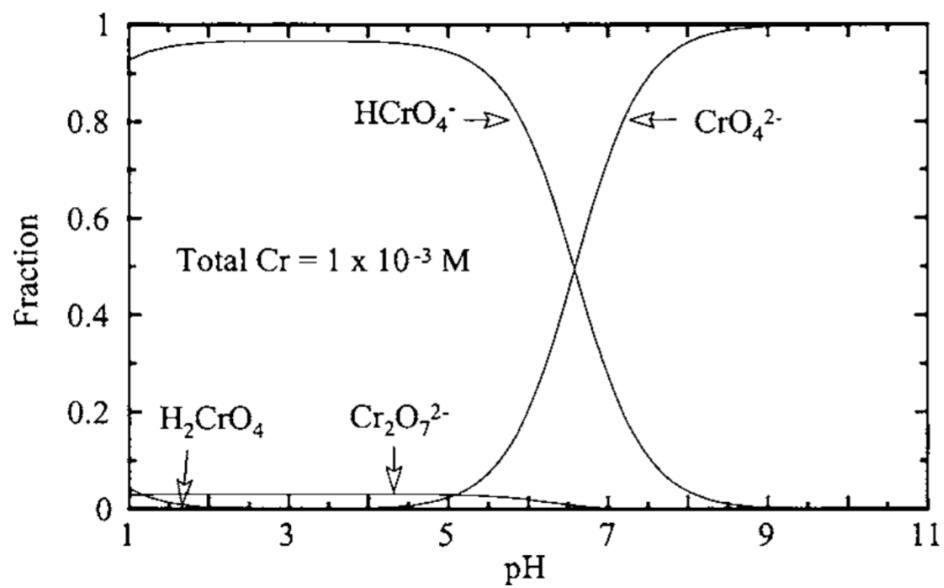
Figure S16. Cr(VI) speciation diagram as function of pH ([Weng et al., 2006](#))
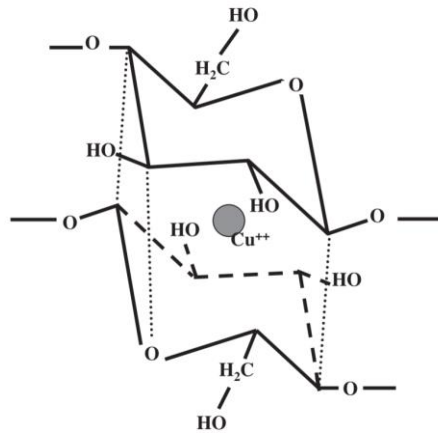
Figure S17. Model for the possible sorption site of a copper ion between two adjacent fibers of the biomass derived from *Maitenus truncata* leaves Carvalho et al., 2003

Licenses

Figure 3. Effect of the pH solution on the adsorption process on **(a)** potentially toxic metal cations onto *Fraxinus excelsior* tree leaf-biosorbent *[Adapted from Sangi et al. Sangi et al., 2008. Copyright (2008), with permission from Elsevier. License Number: 4435910682650]*, **(b)** fluoride onto *Azadirachta indica* tree leaf-biosorbent *[Adapted from Bharali and Bhattacharyya Bharali and Bhattacharyya, 2015. Copyright (2015), with permission from Elsevier. License Number: 4440010650238]*, **(c)** ammonium onto *Parthenocissus tricuspidata* tree leaf-biosorbent *[Adapted from Liu et al. Liu et al., 2010c. Copyright (2010), with permission from Elsevier. License Number: 4435910810287]*, **(d)** cationic dyes onto *Saraca asoca* tree leaf-biosorbent *[Adapted from Gupta et al. Gupta et al., 2012b. Copyright (2012), with permission from Elsevier. License Number: 4435910987708]*, **(e)** hexavalent chromium onto *Melaleuca diosmifolia* tree leaf-biosorbent *[Adapted from Kuppusamy et al. Kuppusamy et al., 2016. Copyright (2016), with permission from Elsevier. License Number: 4435911095229]*, **(f)** acid violet 17 dye onto activated *Ficus racemosa* tree leaf-adsorbent *[Adapted from Jain and Gogate Jain and Gogate, 2017c. Copyright (2017), with permission from Elsevier. License Number: 4435911196015]*, **(g)** arsenic onto *Psidium guajava* leaf tree leaf-biosorbent *[Adapted from Kamsonlian et al. Kamsonlian et al., 2012a. Copyright (2012), with permission from Taylor & Francis. License Number: 4435940299690]*, and **(h)** mercury onto pristine and modified bamboo leaf tree leaf-biosorbents *[Adapted from Mondal et al. Mondal et al., 2013. Copyright (2013), with permission from Taylor & Francis. License Number: 4435920032442]*.

Figure 5. Typical adsorption isotherm determined by two different methods, that is by changing **(a)** solid/liquid ratio *[Adapted from Kılıç et al. Kılıç et al., 2009. Copyright (2009), with permission from Elsevier. License Number: 501431317],* and **(b)** initial adsorbate concentrations *[Adapted from Chen et al. Chen et al., 2010a. Copyright (2010) with permission from Elsevier. License Number: 4435921407628]*.

Figure 8. (a) Effect of solution pH on the adsorption of two anionic dyes [Sumfixe Supra red (SSR) and Alpacelle Lumiere brown (ALB)] onto *Agave americana* leaves, and **(b)** effect of pH on the dye desorption Hamissa et al., 2007 *[Creative Commons CC-BY by SAGE]*; **(c)** Effect of different eluents on copper desorption from treated rubber leaves *[Adapted from Ngah, et al. Ngah and Hanafiah, 2008; Copyright (2008) with permission from Elsevier. License Number:4443540449114]*; **(d)** Desorption kinetics of anionic Amaranth dye from water hyacinth leaves *[Adapted from Guerrero-Coronilla et al. Guerrero-Coronilla et al., 2015. Copyright (2015) with permission from Elsevier. License Number: 4435930384912]*; **(e)** Five cycles of Pb(II) adsorption–desorption with 0.4 M HCl *[Adapted from Reddy et al. Reddy et al., 2010. Copyright (2010) with permission from Elsevier. License Number: 4435930464723]*; **(f)** Biosorption-desorption cycles for regenerating SATCEL with 0.1 N HCl *[Adapted from Khan Rao and Khatoon Khan Rao and Khatoon, 2017. Copyright (2017) with permission from Elsevier. License Number: 4435930646149]*.

Figure 9. (a) Mechanisms proposed for Cr(VI) biosorption by nonliving biomass *[Adapted from Park et al.* *Park et al., 2005. Copyright (2005) with permission from Elsevier. License Number: 4440510789887]*; and **(b)** high-resolution spectra collected from the Cr 2p core regions of the Cr-laden biosorbent derived from Korean red pine tree leaves as well as standard Cr(III) and Cr(VI) chemicals *[Adapted from Park et al.* *Park et al., 2011. Copyright (2011) with permission from Elsevier. License Number: 4435931207985]*.

Figure 10. The potential adsorption mechanisms between toxic metals and biosorbents *[Adapted from* *Tran and Chao, 2018a. Copyright (2018) with permission from Springer. License Number:* 4525340872276]

Figure 11. Typical interactions contributing to the adsorption of cationic methylene green 5 dye onto biosorbent *[Adapted from Tran et al.* *Tran et al., 2017c. Copyright (2017) with permission from Taylor & Francis. License Number: 4435940108341]*.

References

Abdel-Ghani, N.T., Hegazy, A.K. and El-Chaghaby, G.A., 2009. Typha domingensis leaf powder for decontamination of aluminium, iron, zinc and lead: Biosorption kinetics and equilibrium modeling. *International Journal of Environmental Science & Technology, 6*, 243-248.

Abdelwahab, O., Fouad, Y.O., Amin, N.K. and Mandor, H., 2015. Kinetic and thermodynamic aspects of cadmium adsorption onto raw and activated guava (Psidium guajava) leaves. *Environmental Progress & Sustainable Energy, 34*, 351-358.

Abu Al-Rub, F.A., 2006. Biosorption of Zinc on Palm Tree Leaves: Equilibrium, Kinetics, and Thermodynamics Studies. *Separation Science and Technology, 41*, 3499-3515.

Aditya, G.V.V., Pujitha, B.P., Babu, N.C. and Venkateswarlu, P., 2012. Biosorption of chromium onto Erythrina Variegata Orientalis leaf powder. *Korean Journal of Chemical Engineering, 29*, 64-71.

Agarry, S., Ogunleye, O. and Aworanti, O., 2013. Biosorption equilibrium, kinetic and thermodynamic modelling of naphthalene removal from aqueous solution onto modified spent tea leaves. *Environmental technology, 34*, 825-839.

Ahmad, A., Ghazi, Z.A., Saeed, M., Ilyas, M., Ahmad, R., Khattak, A.M. and Iqbal, A., 2017a. A comparative study of the removal of Cr (vi) from synthetic solution using natural biosorbents. *New Journal of Chemistry, 41*, 10799-10807.

Ahmad, A., Ghazi, Z.A., Saeed, M., Ilyas, M., Ahmad, R., Muqsit Khattak, A. and Iqbal, A., 2017b. A comparative study of the removal of Cr(VI) from synthetic solution using natural biosorbents. *New Journal of Chemistry, 41*, 10799-10807.

Al-Dujaili, A.H., Awwad, A.M. and Salem, N.M., 2012. Biosorption of cadmium (II) onto loquat leaves (Eriobotrya japonica) and their ash from aqueous solution, equilibrium, kinetics, and thermodynamic studies. *International Journal of Industrial Chemistry, 3*, 22.

Al-Haidary, A.M.A., Zanganah, F.H., Al-Azawi, S.R., Khalili, F.I. and Al-Dujaili, A.H., 2011a. A study on using date palm fibers and leaf base of palm as adsorbents for Pb (II) ions from its aqueous solution. *Water, Air, and Soil Pollution, 214*, 73-82.

Al-Haidary, A.M.A., Zanganah, F.H.H., Al-Azawi, S.R.F., Khalili, F.I. and Al-Dujaili, A.H., 2011b. A study on using date palmfibers and leaf base of palm as adsorbents for Pb(II) ions from its aqueous solution. *Water, Air, & Soil Pollution, 214*, 73-82.

Al-Masri, M., Amin, Y., Al-Akel, B. and Al-Naama, T., 2010. Biosorption of cadmium, lead, and uranium by powder of poplar leaves and branches. *Applied Biochemistry and Biotechnology, 160*, 976-987.

Al-Subu, M.M., 2002. The interaction effects of cypress (Cupressus sempervirens), cinchona (Eucalyptus longifolia) and pine (Pinus halepensis) leaves on their efficiencies for lead removal from aqueous solutions. *Advances in Environmental Research, 6*, 569-576.

Al Rmalli, S.W., Dahmani, A.A., Abuein, M.M. and Gleza, A.A., 2008. Biosorption of mercury from aqueous solutions by powdered leaves of castor tree (Ricinus communis L.). *Journal of Hazardous Materials, 152*, 955-959.

Ali, H. and Muhammad, S.K., 2008. Biosorption of crystal violet from water on leaf biomass of Calotropis procera. *Journal of Environmental Science and Technology, 1*, 143-150.

Ali, I. and Gupta, V.K., 2007. Advances in water treatment by adsorption technology. *Nature protocols, 1*, 2661.

Ali, I.H. and Alrafai, H., 2016. Kinetic, isotherm and thermodynamic studies on biosorption of chromium (VI) by using activated carbon from leaves of Ficus nitida. *Chemistry Central Journal, 10*, 36.

Alizadeh, N., Shariati, S. and Besharati, N., 2017. Adsorption of Crystal Violet and Methylene Blue on Azolla and Fig Leaves Modified with Magnetite Iron Oxide Nanoparticles. *International Journal of Environmental Research*, 1-10.

Amarasinghe, B.M.W.P.K. and Williams, R.A., 2007. Tea waste as a low cost adsorbent for the removal of Cu and Pb from wastewater. *Chemical Engineering Journal, 132*, 299-309.

Amirnia, S., Ray, M.B. and Margaritis, A., 2016. Copper ion removal by Acer saccharum leaves in a regenerable continuous-flow column. *Chemical Engineering Journal, 287*, 755-764.

Ammari, T.G., 2014. Utilization of a natural ecosystem bio-waste; leaves of Arundo donax reed, as a raw material of low-cost eco-biosorbent for cadmium removal from aqueous phase. *Ecological Engineering, 71*, 466-473.

Ansari, S.A., Khan, F. and Ahmad, A., 2016a. Cauliflower leave, an agricultural waste biomass adsorbent, and its application for the removal of MB dye from aqueous solution: Equilibrium, kinetics, and thermodynamic studies. *International Journal of Analytical Chemistry, 2016*, 10.

Ansari, S.A., Khan, F. and Ahmad, A., 2016b. Cauliflower Leave, an Agricultural Waste Biomass Adsorbent, and Its Application for the Removal of MB Dye from Aqueous Solution: Equilibrium, Kinetics, and Thermodynamic Studies. *International journal of analytical chemistry, 2016*.

Anwar, J., Shafique, U., Waheed uz, Z., un Nisa, Z., Munawar, M.A., Jamil, N., Salman, M., Dar, A., Rehman, R., Saif, J., Gul, H. and Iqbal, T., 2011. Removal of chromium on Polyalthia longifolia leaves biomass. *International Journal of Phytoremediation, 13*, 410-420.

Ang, X., Sethu, V., Andresen, J. and Sivakumar, M., 2013. Copper (II) ion removal from aqueous solutions using biosorption technology: thermodynamic and SEM–EDX studies. *Clean Technologies and Environmental Policy, 15*, 401-407.

Aoyama, M., 2003a. Comment on "Biosorption of chromium(VI) from aqueous solution by cone biomass of Pinus sylvestris". *Bioresource Technology, 89*, 317-318.

Aoyama, M., 2003b. Removal of Cr (VI) from aqueous solution by London plane leaves. *Journal of Chemical Technology and Biotechnology, 78*, 601-604.

Aoyama, M., 2003c. Removal of Cr(VI) from aqueous solution by London plane leaves. *Journal of Chemical Technology & Biotechnology, 78*, 601-604.

Aoyama, M., Sugiyama, T., Doi, S., Cho, N.-S. and Kim, H.-E., 1999a. Removal of hexavalent chromium from dilute aqueous solution by coniferous leaves. *Holzforschung, 53*, 365-368.

Aoyama, M., Sugiyama, T., Doi, S., Cho, N.S. and Kim, H.E., 1999b. Removal of hexavalent chromium from dilute aqueous solution by coniferous leaves, 365). Holzforschung.

Aoyama, M. and Tsuda, M., 2001. Removal of Cr(VI) from aqueous solutions by larch bark. *Wood Science and Technology, 35*, 425-434.

Aoyama, M., Tsuda, M., Seki, K., Doi, S., Kurimoto, Y. and Tamura, Y., 2000a. Adsorption of Cr (VI) from dichromate solutions onto black locust leaves. *Holzforschung, 54*, 340-342.

Aoyama, M., Tsuda, M., Seki, K., Doi, S., Kurimoto, Y. and Tamura, Y., 2000b. Adsorption of Cr(VI) from Dichromate Solutions onto Black Locust Leaves *Holzforschung*, 340).

Arshad, M., Zafar, M.N., Younis, S. and Nadeem, R., 2008. The use of Neem biomass for the biosorption of zinc from aqueous solutions. *Journal of Hazardous Materials, 157*, 534-540.

Asgarzadeh, S., Rostamian, R., Faez, E., Maleki, A. and Daraei, H., 2016. Biosorption of Pb(II), Cu(II), and Ni(II) ions onto novel lowcost P. eldarica leaves-based biosorbent: isotherm, kinetics, and operational parameters investigation. *Desalination and Water Treatment, 57*, 14544-14551.

Aslam, M., Rais, S., Alam, M. and Pugazhendi, A., 2013. Adsorption of Hg(II) from Aqueous Solution Using Adulsa (Justicia adhatoda) Leaves Powder: Kinetic and Equilibrium Studies. *Journal of Chemistry, 2013*, 11.

Awwad, A.M. and Salem, N.M., 2014. Kinetics and thermodynamics of Cd(II) biosorption onto loquat (Eriobotrya japonica) leaves. *Journal of Saudi Chemical Society, 18*, 486-493.

Aydin, M., Cavas, L. and Merdivan, M., 2012. An alternative evaluation method for accumulated dead leaves of Posidonia oceanica (L.) Delile on the beaches: removal of uranium from aqueous solutions. *Journal of Radioanalytical and Nuclear Chemistry, 293*, 489-496.

Babarinde, N., 2016. Kinetic, equilibrium and thermodynamic studies of the biosorption of Pb (II), Cd (II) and Cr (III) by neem leaf. *Journal of Innovative Research in Engineering and Sciences, 2*.

Babu, B.V. and Gupta, S., 2008. Adsorption of Cr(VI) using activated neem leaves: kinetic studies. *Adsorption, 14*, 85-92.

Baruah, S., Devi, A., Bhattacharyya, K. and Sarma, A., 2017. Developing a biosorbent from Aegle Marmelos leaves for removal of methylene blue from water. *International Journal of Environmental Science and Technology, 14*, 341-352.

Batool, F., Iqbal, S. and Akbar, J., 2017. Impact of metal ionic characteristics on adsorption potential of Ficus carica leaves using QSPR modeling. *Journal of Environmental Science and Health, Part B*, 1-6.

Bello, O.S., Adegoke, K.A. and Akinyunni, O.O., 2017. Preparation and characterization of a novel adsorbent from Moringa oleifera leaf. *Applied Water Science, 7*, 1295-1305.

Benadjemia, M., Millière, L., Reinert, L., Benderdouche, N. and Duclaux, L., 2011. Preparation, characterization and Methylene Blue adsorption of phosphoric acid activated carbons from globe artichoke leaves. *Fuel Processing Technology, 92*, 1203-1212.

Benaïssa, H., 2006. Screening of new sorbent materials for cadmium removal from aqueous solutions. *Journal of Hazardous Materials, 132*, 189-195.

Benaïssa, H. and Elouchdi, M.A., 2007. Removal of copper ions from aqueous solutions by dried sunflower leaves. *Chemical Engineering and Processing: Process Intensification, 46*, 614-622.

Bharali, R.K. and Bhattacharyya, K.G., 2015. Biosorption of fluoride on Neem (Azadirachta indica) leaf powder. *Journal of Environmental Chemical Engineering, 3*, 662-669.

Bhattacharyya, K.G. and Sarma, A., 2003. Adsorption characteristics of the dye, Brilliant Green, on Neem leaf powder. *Dyes and pigments, 57*, 211-222.

Bhattacharyya, K.G., Sarma, A. and Sarma, J., 2010. Adsorption of Cu(II) ions onto a cellulosic biosorbent, Azadirachta Indica leaf powder: Application in water treatment. *Adsorption Science & Technology, 28*, 869-883.

Bhattacharyya, K.G., Sarma, J. and Sarma, A., 2009. Azadirachta indica leaf powder as a biosorbent for Ni(II) in aqueous medium. *Journal of Hazardous Materials, 165*, 271-278.

Bhattacharyya, K.G. and Sharma, A., 2004. Adsorption of Pb(II) from aqueous solution by Azadirachta indica (Neem) leaf powder. *Journal of Hazardous Materials, 113*, 97-109.

Biggar, J.W. and Cheung, M.W., 1973. Adsorption of Picloram (4-Amino-3,5,6-Trichloropicolinic Acid) on Panoche, Ephrata, and Palouse Soils: A Thermodynamic Approach to the Adsorption Mechanism1. *Soil Science Society of America Journal, 37*, 863-868.

Blanchard, G., Maunaye, M. and Martin, G., 1984. Removal of heavy metals from waters by means of natural zeolites. *Water Research, 18*, 1501-1507.

Boparai, H.K., Joseph, M. and O'Carroll, D.M., 2011. Kinetics and thermodynamics of cadmium ion removal by adsorption onto nano zerovalent iron particles. *Journal of Hazardous Materials, 186*, 458-465.

Boruah, P., Sarma, A. and Bhattacharyya, K.G., 2015. Removal of Ni (II) ions from aqueous solution by using low cost biosorbent prepared from jackfruit (Artocarpus heterophyllus) leaf powder.

Bose, R.S., Bora, P.P., Deka, R.C. and Sarma, K.P., 2016. Removal of Cd(II) ion from aqueous solution by powdered leaf biomass of Boehmeria listeri: equilibrium and kinetic studies. *Desalination and Water Treatment, 57*, 20877-20888.

Boudrahem, F., Aissani-Benissad, F. and Soualah, A., 2011. Adsorption of Lead(II) from Aqueous Solution by Using Leaves of Date Trees As an Adsorbent. *Journal of Chemical & Engineering Data, 56*, 1804-1812.

Boveiri Monji, A., Javad Ahmadi, S. and Zolfonoun, E., 2008. Selective Biosorption of Zirconium and Hafnium from Acidic Aqueous Solutions by Rice Bran, Wheat Bran and Platanus Orientalis Tree Leaves. *Separation Science and Technology, 43*, 597-608.

Brahman, K.D., Kazi, T.G., Afridi, H.I., Baig, J.A., Abro, M.I., Arain, S.S., Ali, J. and Khan, S., 2016. Simultaneously removal of inorganic arsenic species from stored rainwater in arsenic endemic area by leaves of Tecomella undulata: A multivariate study. *Environmental Science and Pollution Research, 23*, 15149-15163.

Carvalho, d.R.P., Freitas, J.R., de Sousa, A.M.G., Moreira, R.L., Pinheiro, M.V.B. and Krambrock, K., 2003. Biosorption of copper ions by dried leaves: chemical bonds and site symmetry. *Hydrometallurgy, 71*, 277-283.

Çekim, M., Yildiz, S. and Dere, T., 2015. Biosorption of copper from synthetic waters by using tobacco leaf: Equilibrium, inetic and thermodynamic tests. *Journal of Environmental Engineering and Landscape Management, 23*, 172-182.

Cengiz, S. and Cavas, L., 2010. A promising evaluation method for dead leaves of Posidonia oceanica (L.) in the adsorption of methyl violet. *Marine Biotechnology, 12*, 728-736.

Copello, G.J., Garibotti, R.E., Varela, F., Tuttolomondo, M.V. and Diaz, L.E., 2011. Exhausted yerba mate leaves (Ilex Paraguariensis) as biosorbent for the removal of metals from aqueous solutions. *Journal of the Brazilian Chemical Society, 22*, 790-795.

Cukierman, A.L., 2007. Metal Ion Biosorption Potential of Lignocellulosic Biomasses and Marine Algae for Wastewater Treatment. *Adsorption Science & Technology, 25*, 227-244.

Chakraborty, S., Chowdhury, S. and Saha, P.D., 2012. Insight into biosorption equilibrium, kinetics and thermodynamics of crystal violet onto Ananas comosus (pineapple) leaf powder. *Applied Water Science, 2*, 135-141.

Chakravarty, S., Mohanty, A., Sudha, T.N., Upadhyay, A.K., Konar, J., Sircar, J.K., Madhukar, A. and Gupta, K.K., 2010. Removal of Pb(II) ions from aqueous solution by adsorption using bael leaves (Aegle marmelos). *Journal of Hazardous Materials, 173*, 502-509.

Chang, Y., Lai, J.-Y. and Lee, D.-J., 2016. Thermodynamic parameters for adsorption equilibrium of heavy metals and dyes from wastewaters: Research updated. *Bioresource Technology, 222*, 513-516.

Chao, H.-P. and Chen, S.-H., 2012. Adsorption characteristics of both cationic and oxyanionic metal ions on hexadecyltrimethylammonium bromide-modified NaY zeolite. *Chemical Engineering Journal, 193-194*, 283-289.

Chen, B., Yuan, M. and Liu, H., 2011a. Removal of polycyclic aromatic hydrocarbons from aqueous solution using plant residue materials as a biosorbent. *Journal of Hazardous Materials, 188*, 436-442.

Chen, H., Dai, G., Zhao, J., Zhong, A., Wu, J. and Yan, H., 2010a. Removal of copper(II) ions by a biosorbent—Cinnamomum camphora leaves powder. *Journal of Hazardous Materials, 177*, 228-236.

Chen, H., Zhao, J., Dai, G., Wu, J. and Yan, H., 2010b. Adsorption characteristics of Pb(II) from aqueous solution onto a natural biosorbent, fallen Cinnamomum camphora leaves. *Desalination, 262*, 174-182.

Chen, L., Ramadan, A., Lü, L., Shao, W., Luo, F. and Chen, J., 2011b. Biosorption of methylene blue from aqueous solution using lawny grass modified with citric acid. *Journal of Chemical & Engineering Data, 56*, 3392-3399.

Chen, L., Ramadan, A., Lü, L., Shao, W., Luo, F. and Chen, J., 2011c. Biosorption of methylene blue from aqueous solution using lawny grass modified with citric acid. *Journal of Chemical & Engineering Data, 56*, 3392-3399.

Chen, Y., Tang, G., Yu, Q.J., Zhang, T., Chen, Y. and Gu, T., 2009. Biosorption properties of hexavalent chromium on to biomass of tobacco-leaf residues. *Environmental Technology, 30*, 1003-1010.

Cheraghi, E., Ameri, E. and Moheb, A., 2015. Adsorption of cadmium ions from aqueous solutions using sesame as a low-cost biosorbent: kinetics and equilibrium studies. *International Journal of Environmental Science and Technology, 12*, 2579-2592.

Chojnacka, K., Chojnacki, A. and Górecka, H., 2005. Biosorption of Cr3+, Cd2+ and Cu2+ ions by blue–green algae Spirulina sp.: kinetics, equilibrium and the mechanism of the process. *Chemosphere, 59*, 75-84.

Choudhary, M., 2015. Aqueous removal of arsenic (III) using acid treated Devdaru (Polyalthia longifolia) leaf powder. *Journal of Applied and Fundamental Sciences, 1*, 98.

Chowdhury, S., Chakraborty, S. and Saha, P., 2011. Biosorption of Basic Green 4 from aqueous solution by Ananas comosus (pineapple) leaf powder. *Colloids and Surfaces B: Biointerfaces, 84*, 520-527.

Dabbagh, R., Ashtiani Moghaddam, Z. and Ghafourian, H., 2016. Removal of cobalt(II) ion from water by adsorption using intact and modified Ficus carica leaves as low-cost natural sorbent. *Desalination and Water Treatment, 57*, 19890-19902.

Deniz, F. and Karaman, S., 2011. Removal of Basic Red 46 dye from aqueous solution by pine tree leaves. *Chemical Engineering Journal, 170*, 67-74.

Deniz, F. and Saygideger, S.D., 2010. Equilibrium, kinetic and thermodynamic studies of Acid Orange 52 dye biosorption by Paulownia tomentosa Steud. leaf powder as a low-cost natural biosorbent. *Bioresource Technology, 101*, 5137-5143.

Deniz, F. and Saygideger, S.D., 2011. Removal of a hazardous azo dye (Basic Red 46) from aqueous solution by princess tree leaf. *Desalination, 268*, 6-11.

Devani, M.A., Munshi, B. and Oubagaranadin, J.U.K., 2015. Characterization and use of chemically activated Butea monosperma leaf dust for mercury (II) removal from solutions. *Journal of Environmental Chemical Engineering, 3*, 2212-2218.

Doğan, M., Türkyilmaz, A., Alkan, M. and Demirbaş, Ö., 2009. Adsorption of copper (II) ions onto sepiolite and electrokinetic properties. *Desalination, 238*, 257-270.

Dural, M.U., Cavas, L., Papageorgiou, S.K. and Katsaros, F.K., 2011. Methylene blue adsorption on activated carbon prepared from Posidonia oceanica (L.) dead leaves: Kinetics and equilibrium studies. *Chemical Engineering Journal, 168*, 77-85.

Edokpayi, J.N., Odiyo, J.O., Msagati, T.A. and Popoola, E.O., 2015. A Novel Approach for the removal of lead (II) ion from wastewater using mucilaginous leaves of diceriocaryum eriocarpum plant. *Sustainability, 7*, 14026-14041.

Elangovan, R., Philip, L. and Chandraraj, K., 2008. Biosorption of chromium species by aquatic weeds: Kinetics and mechanism studies. *Journal of Hazardous Materials, 152*, 100-112.

Fadzil, F., Ibrahim, S. and Hanafiah, M.A.K.M., 2016. Adsorption of lead (II) onto organic acid modified rubber leaf powder: Batch and column studies. *Process Safety and Environmental Protection, 100*, 1-8.

Farhan, A.M., Al-Dujaili, A.H. and Awwad, A.M., 2013a. Equilibrium and kinetic studies of cadmium (II) and lead (II) ions biosorption onto Ficus carcia leaves. *International Journal of Industrial Chemistry, 4*, 24.

Farhan, A.M., Al-Dujaili, A.H. and Awwad, A.M., 2013b. Equilibrium and kinetic studies of cadmium(II) and lead(II) ions biosorption onto Ficus carcia leaves. *International Journal of Industrial Chemistry, 4*, 24.

Febriana, N., Lesmana, S.O., Soetaredjo, F.E., Sunarso, J. and Ismadji, S., 2010. Neem leaf utilization for copper ions removal from aqueous solution. *Journal of the Taiwan Institute of Chemical Engineers, 41*, 111-114.

Gaikwad, R.W. and Kinldy, S.A.M., 2009. Studies on auramine dye adsorption on psidium guava leaves. *Korean Journal of Chemical Engineering, 26*, 102-107.

Gebrehawaria, G., Hussen, A. and Rao, V.M., 2015. Removal of hexavalent chromium from aqueous solutions using barks of Acacia albida and leaves of Euclea schimperi. *International Journal of Environmental Science and Technology, 12*, 1569-1580.

Ghosh, A., Das, P. and Sinha, K., 2015. Modeling of biosorption of Cu(II) by alkali-modified spent tea leaves using response surface methodology (RSM) and artificial neural network (ANN). *Applied Water Science, 5*, 191-199.

Gouamid, M., Ouahrani, M. and Bensaci, M., 2013. Adsorption equilibrium, kinetics and thermodynamics of methylene blue from aqueous solutions using date palm leaves. *Energy Procedia, 36*, 898-907.

Gowda, R., Nataraj, A. and Rao, N.M., 2012. Coconut leaves as a low cost adsorbent for the removal of nickel from electroplating effluents. *Int J Sci Eng Res, 2*, 1-5.

Goyal, P., Sharma, P., Srivastava, S. and Srivastava, M.M., 2008. Saraca indica leaf powder for decontamination of Pb: removal, recovery, adsorbent characterization and equilibrium modeling. *International Journal of Environmental Science & Technology, 5*, 27-34.

Guechi, E.-K. and Hamdaoui, O., 2013. Cattail leaves as a novel biosorbent for the removal of malachite green from liquid phase: data analysis by non-linear technique. *DESALINATION AND WATER TREATMENT, 51*, 3371-3380.

Guerrero-Coronilla, I., Morales-Barrera, L. and Cristiani-Urbina, E., 2015. Kinetic, isotherm and thermodynamic studies of amaranth dye biosorption from aqueous solution onto water hyacinth leaves. *Journal of Environmental Management, 152*, 99-108.

Gundogdu, A., Duran, C., Senturk, H.B., Soylak, M., Imamoglu, M. and Onal, Y., 2013. Physicochemical characteristics of a novel activated carbon produced from tea industry waste. *Journal of Analytical and Applied Pyrolysis, 104*, 249-259.

Gupta, N., Kushwaha, A.K. and Chattopadhyaya, M., 2012a. Adsorption studies of cationic dyes onto Ashoka (Saraca asoca) leaf powder. *Journal of the Taiwan Institute of Chemical Engineers, 43*, 604-613.

Gupta, N., Kushwaha, A.K. and Chattopadhyaya, M., 2016a. Application of potato (Solanum tuberosum) plant wastes for the removal of methylene blue and malachite green dye from aqueous solution. *Arabian Journal of Chemistry, 9*, S707-S716.

Gupta, N., Kushwaha, A.K. and Chattopadhyaya, M.C., 2012b. Adsorption studies of cationic dyes onto Ashoka (Saraca asoca) leaf powder. *Journal of the Taiwan Institute of Chemical Engineers, 43*, 604-613.

Gupta, N., Kushwaha, A.K. and Chattopadhyaya, M.C., 2016b. Application of potato (Solanum tuberosum) plant wastes for the removal of methylene blue and malachite green dye from aqueous solution. *Arabian Journal of Chemistry, 9*, S707-S716.

Gutha, Y., Munagapati, V.S., Naushad, M. and Abburi, K., 2015. Removal of Ni(II) from aqueous solution by Lycopersicum esculentum (Tomato) leaf powder as a low-cost biosorbent. *Desalination and Water Treatment, 54*, 200-208.

Hamdaoui, O., Saoudi, F., Chiha, M. and Naffrechoux, E., 2008. Sorption of malachite green by a novel sorbent, dead leaves of plane tree: Equilibrium and kinetic modeling. *Chemical Engineering Journal, 143*, 73-84.

Hamissa, A.M.B., Brouers, F., Mahjoub, B. and Seffen, M., 2007. Adsorption of textile dyes using Agave americana (L.) fibres: Equilibrium and kinetics modelling. *Adsorption Science & Technology, 25*, 311-325.

Hamissa, A.M.B., Lodi, A., Seffen, M., Finocchio, E., Botter, R. and Converti, A., 2010. Sorption of Cd(II) and Pb(II) from aqueous solutions onto Agave americana fibers. *Chemical Engineering Journal, 159*, 67-74.

Han, R., Zou, W., Yu, W., Cheng, S., Wang, Y. and Shi, J., 2007. Biosorption of methylene blue from aqueous solution by fallen phoenix tree's leaves. *Journal of Hazardous Materials, 141*, 156-162.

Han, X., Wang, W. and Ma, X., 2011. Adsorption characteristics of methylene blue onto low cost biomass material lotus leaf. *Chemical Engineering Journal, 171*, 1-8.

Han, X., Yuan, J. and Ma, X., 2014. Adsorption of malachite green from aqueous solutions onto lotus leaf: Equilibrium, kinetic, and thermodynamic studies. *Desalination and Water Treatment, 52*, 5563-5574.

Hanafiah, M., Zakaria, H. and Ngah, W.W., 2009a. Preparation, characterization, and adsorption behavior of Cu (II) ions onto alkali-treated weed (Imperata cylindrica) leaf powder. *Water, Air, and Soil Pollution, 201*, 43-53.

Hanafiah, M.A.K.M. and Ngah, W.S.W., 2009. Preparation, characterization and adsorption mechanism of Cu(II) onto protonated rubber leaf powder. *CLEAN – Soil, Air, Water, 37*, 696-703.

Hanafiah, M.A.K.M., Zakaria, H. and Wan Ngah, W.S., 2009b. Preparation, characterization, and adsorption behavior of Cu(II) Ions onto alkali-treated weed (Imperata cylindrica) leaf powder. *Water, Air, and Soil Pollution, 201*, 43-53.

Hanif, M.A., Nadeem, R., Bhatti, H.N., Ahmad, N.R. and Ansari, T.M., 2007. Ni(II) biosorption by Cassia fistula (Golden Shower) biomass. *Journal of Hazardous Materials, 139*, 345-355.

Hossain, M., Ngo, H., Guo, W., Nghiem, L., Hai, F., Vigneswaran, S. and Nguyen, T., 2014a. Competitive adsorption of metals on cabbage waste from multi-metal solutions. *Bioresource technology, 160*, 79-88.

Hossain, M.A., Kumita, M., Michigami, Y. and Mori, S., 2005. Optimization of parameters for Cr (VI) adsorption on used black tea leaves. *Adsorption, 11*, 561-568.

Hossain, M.A., Ngo, H.H., Guo, W., Zhang, J. and Liang, S., 2014b. A laboratory study using maple leaves as a biosorbent for lead removal from aqueous solutions. *Water Quality Research Journal of Canada, 49*, 195-209.

Hossain, M.A., Ngo, H.H., Guo, W.S., Nghiem, L.D., Hai, F.I., Vigneswaran, S. and Nguyen, T.V., 2014c. Competitive adsorption of metals on cabbage waste from multi-metal solutions. *Bioresource Technology, 160*, 79-88.

Hossain, M.A., Ngo, H.H., Guo, W.S., Nguyen, T.V. and Vigneswaran, S., 2014d. Performance of cabbage and cauliflower wastes for heavy metals removal. *Desalination and Water Treatment, 52*, 844-860.

Hymavathi, D. and Prabhakar, G., 2017. Studies on the Removal of Cobalt (II) from Aqueous solutions by Adsorption with Ficus benghalensis Leaf powder through Response Surface Methodology. *Chemical Engineering Communications, 204*, 1401-1411.

Immich, A.P.S., de Souza, A.A.U. and de Arruda Guelli Ulson de Souza, S.M., 2009. Adsorption of remazol blue RR from textile effluents using Azadirachta indica leaf powder as an alternative adsorbent. *Adsorption Science & Technology, 27*, 461-478.

Iqbal, M., Saeed, A. and Zafar, S.I., 2009. FTIR spectrophotometry, kinetics and adsorption isotherms modeling, ion exchange, and EDX analysis for understanding the mechanism of Cd2+ and Pb2+ removal by mango peel waste. *Journal of Hazardous Materials, 164*, 161-171.

Jain, S. and Gogate, P., 2017a. NaOH-treated dead leaves of Ficus racemosa as an efficient biosorbent for Acid Blue 25 removal. *International Journal of Environmental Science and Technology, 14*, 531-542.

Jain, S.N. and Gogate, P.R., 2017b. Acid Blue 113 removal from aqueous solution using novel biosorbent based on NaOH treated and surfactant modified fallen leaves of Prunus Dulcis. *Journal of Environmental Chemical Engineering, 5*, 3384-3394.

Jain, S.N. and Gogate, P.R., 2017c. Adsorptive removal of acid violet 17 dye from wastewater using biosorbent obtained from NaOH and H2SO4 activation of fallen leaves of Ficus racemosa. *Journal of Molecular Liquids, 243*, 132-143.

Jain, S.N. and Gogate, P.R., 2017d. Adsorptive removal of acid violet 17 dye from wastewater using biosorbent obtained from NaOH and H 2 SO 4 activation of fallen leaves of Ficus racemosa. *Journal of Molecular Liquids, 243*, 132-143.

Jain, S.N. and Gogate, P.R., 2018. Efficient removal of Acid Green 25 dye from wastewater using activated Prunus Dulcis as biosorbent: Batch and column studies. *Journal of environmental management, 210*, 226-238.

Jalil, A., Triwahyono, S., Yaakob, M., Azmi, Z., Sapawe, N., Kamarudin, N., Setiabudi, H., Jaafar, N., Sidik, S. and Adam, S., 2012a. Utilization of bivalve shell-treated Zea mays L.(maize) husk leaf as a low-cost biosorbent for enhanced adsorption of malachite green. *Bioresource Technology, 120*, 218-224.

Jalil, A.A., Triwahyono, S., Yaakob, M.R., Azmi, Z.Z.A., Sapawe, N., Kamarudin, N.H.N., Setiabudi, H.D., Jaafar, N.F., Sidik, S.M., Adam, S.H. and Hameed, B.H., 2012b. Utilization of bivalve shell-treated Zea mays L. (maize) husk leaf as a low-cost biosorbent for enhanced adsorption of malachite green. *Bioresource Technology, 120*, 218-224.

Javad, Z., Ali, S., Maryam, B., Dermanaki, F.S. and Peyman, Z., 2017. Chemometrics optimization for simultaneous adsorptive removal of ternary mixture of Cu(II), Cd(II), and Pb(II) by Fraxinus tree leaves. *Journal of Chemometrics, 31*, e2935.

Jenish, S. and Methodis, P.A., 2011. Fluoride removal from drinking water using used tea leaves as adsorbent. *Asian Journal of Chemistry, 23*, 2889.

Jeyaseelan, C. and Gupta, A., 2016a. Green Tea Leaves as a Natural Adsorbent for the Removal of Cr (VI) From Aqueous Solutions. *Air, Soil and Water Research, 9*, ASWR. S35227.

Jeyaseelan, C. and Gupta, A., 2016b. Green Tea Leaves as a Natural Adsorbent for the Removal of Cr(VI) from Aqueous Solutions. *Air, Soil and Water Research, 9*, ASWR.S35227.

Jorgetto, A.d.O., da Silva, A.C.P., Wondracek, M.H.P., Silva, R.I.V., Velini, E.D., Saeki, M.J., Pedrosa, V.A. and Castro, G.R., 2015. Multilayer adsorption of Cu(II) and Cd(II) over Brazilian Orchid Tree (Pata-de-vaca) and its adsorptive properties. *Applied Surface Science, 345*, 81-89.

Kahina, L. and Nasser, S.M., 2017. Adsorption of Auramine-O using activated Globe artichoke leaves: Kinetic and isotherm studies. *Asian Journal of Chemistry, 29*.

Kamar Firas, H., Nechifor Aurelia, C., Nechifor, G., Al-Musawi Tariq, J. and Mohammed Asem, H., 2017. Aqueous phase biosorption of Pb(II), Cu(II), and Cd(II) onto cabbage leaves powder *International Journal of Chemical Reactor Engineering*.

Kamaru, A.A., Sani, N.S. and Malek, N.A.N.N., 2016. Raw and surfactant-modified pineapple leaf as adsorbent for removal of methylene blue and methyl orange from aqueous solution. *Desalination and Water Treatment, 57*, 18836-18850.

Kamsonlian, S., Suresh, S., Majumder, C.B. and Chand, S., 2012a. Biosorption of Arsenic from Contaminated Water onto Solid Psidium guajava Leaf Surface: Equilibrium, Kinetics, Thermodynamics, and Desorption Study. *Bioremediation Journal, 16*, 97-112.

Kamsonlian, S., Suresh, S., Majumder, C.B. and Chand, S., 2012b. Biosorption of arsenic from contaminated water onto solid Psidium guajava leaf surface: Equilibrium, kinLetics, thermodynamics, and desorption study. *Bioremediation Journal, 16*, 97-112.

Kamsonlian, S., Suresh, S., Ramanaiah, V., Majumder, C.B., Chand, S. and Kumar, A., 2012c. Biosorptive behaviour of mango leaf powder and rice husk for arsenic(III) from aqueous solutions. *International Journal of Environmental Science and Technology, 9*, 565-578.

Kaouah, F., Berrama, T., Brahmi, L., Boumaza, S. and Bendjama, Z., 2014. Removal of cadmium from aqueous solution by Posidonia oceanica (L.) leaf sheaths fibres using discontinuous stirring tank reactor. *Desalination and Water Treatment, 52*, 2272-2281.

Kazmi, M., Ramzan, N., Feroze, N., Almas, Q., Zafar, M. and Saeed, Z., 2015. Removal of zinc and copper from contaminated water using Ficus religiosa leaves: kinetic, equilibrium and mechanistic studies. *Pak. J. Agri. Sci, 52*, 619-625.

Kılıç, M. and Solak, M., 2009. A comprehensive study on removal and recovery of copper (II) from aqueous solutions by NaOH-pretreated Marrubium globosum ssp. globosum leaves powder: Potential for utilizing the copper (II) condensed desorption solutions in agricultural applications. *Bioresource technology, 100*, 2130-2137.

Kılıç, M., Yazıcı, H. and Solak, M., 2009. A comprehensive study on removal and recovery of copper(II) from aqueous solutions by NaOH-pretreated Marrubium globosum ssp. globosum leaves powder: Potential for utilizing the copper(II) condensed desorption solutions in agricultural applications. *Bioresource Technology, 100*, 2130-2137.

King, P., Rakesh, N., Beenalahari, S., Prasanna Kumar, Y. and Prasad, V.S.R.K., 2007. Removal of lead from aqueous solution using Syzygium cumini L.: Equilibrium and kinetic studies. *Journal of Hazardous Materials, 142*, 340-347.

King, P., Rakesh, N., Lahari, S.B., Kumar, Y.P. and Prasad, V.S.R.K., 2008. Biosorption of zinc onto Syzygium cumini L.: Equilibrium and kinetic studies. *Chemical Engineering Journal, 144*, 181-187.

King, P., Srinivas, P., Kumar, Y.P. and Prasad, V.S.R.K., 2006. Sorption of copper(II) ion from aqueous solution by Tectona grandis l.f. (teak leaves powder). *Journal of Hazardous Materials, 136*, 560-566.

Kong, L., Gong, L. and Wang, J., 2015. Removal of methylene blue from wastewater using fallen leaves as an adsorbent. *DESALINATION AND WATER TREATMENT, 53*, 2489-2500.

Kumar, P.S., Kirthika, K. and Kumar, K.S., 2009. Bael Tree Leaves as a Natural Adsorbent for the Removal of Zinc(II) Ions from Industrial Effluents. *Adsorption Science & Technology, 27*, 503-512.

Kumar, Y.P., King, P. and Prasad, V.S.R.K., 2006. Zinc biosorption on Tectona grandis L.f. leaves biomass: Equilibrium and kinetic studies. *Chemical Engineering Journal, 124*, 63-70.

Kuppusamy, S., Thavamani, P., Megharaj, M., Venkateswarlu, K., Lee, Y.B. and Naidu, R., 2016. Potential of Melaleuca diosmifolia leaf as a low-cost adsorbent for hexavalent chromium removal from contaminated water bodies. *Process Safety and Environmental Protection, 100*, 173-182.

Kushwaha, A.K., Gupta, N. and Chattopadhyaya, M., 2014a. Removal of cationic methylene blue and malachite green dyes from aqueous solution by waste materials of Daucus carota. *Journal of Saudi Chemical Society, 18*, 200-207.

Kushwaha, A.K., Gupta, N. and Chattopadhyaya, M.C., 2014b. Removal of cationic methylene blue and malachite green dyes from aqueous solution by waste materials of Daucus carota. *Journal of Saudi Chemical Society, 18*, 200-207.

Kütahyali, C., Sert, Ş., Çetinkaya, B., Inan, S. and Eral, M., 2010. Factors Affecting Lanthanum and Cerium Biosorption on Pinus brutia Leaf Powder. *Separation Science and Technology, 45*, 1456-1462.

Kütahyalı, C., Sert, Ş., Çetinkaya, B., Yalçıntaş, E. and Bahadır Acar, M., 2012. Biosorption of Ce(III) onto modified Pinus brutia leaf powder using central composite design. *Wood Science and Technology, 46*, 721-736.

Khalir, W.M., Azira, W.K., Hanafiah, M., Kamal, M.A., So'ad, M., Zaiton, S., Ngah, W., Saime, W., Majid, A. and Azran, Z., 2012. Batch, column and thermodynamic of Pb (II) adsorption on xanthated rubber (Hevea brasiliensis) leaf powder. *Journal of Applied Sciences, 12*, 1142-1147.

Khan, A.A. and Singh, R.P., 1987. Adsorption thermodynamics of carbofuran on Sn (IV) arsenosilicate in H+, Na+ and Ca2+ forms. *Colloids and Surfaces, 24*, 33-42.

Khan Rao, R.A. and Khatoon, A., 2017. Aluminate treated Casuarina equisetifolia leaves as potential adsorbent for sequestering Cu(II), Pb(II) and Ni(II) from aqueous solution. *Journal of Cleaner Production, 165*, 1280-1295.

Khodabandehloo, A., Rahbar-Kelishami, A. and Shayesteh, H., 2017. Methylene blue removal using Salix babylonica (Weeping willow) leaves powder as a low-cost biosorbent in batch mode: Kinetic, equilibrium, and thermodynamic studies. *Journal of Molecular Liquids, 244*, 540-548.

Khokhar, A., Siddique, Z. and Misbah, 2015. Removal of heavy metal ions by chemically treated Melia azedarach L. leaves. *Journal of Environmental Chemical Engineering, 3*, 944-952.

Khorshidi, N. and Niazi, A., 2016. Optimization of pyrocatechol violet biosorption by Robinia pseudoacacia leaf powder using response surface methodology: kinetic, isotherm and thermodynamic studies. *Journal of Water Reuse and Desalination, 6*, 333-344.

Lafi, R., Hamdi, N. and Hafiane, A., 2015. Study of the performance of Esparto grass fibers as adsorbent of dyes from aqueous solutions. *Desalination and Water Treatment, 56*, 722-735.

Langmuir, I., 1918. The adsorption of gases on plane surfaces of glass, mica and platinum. *Journal of the American Chemical Society, 40*, 1361-1403.

Li, C., Fen-xia, Y., Shuai, Y., Shu-li, C. and Pei-qin, M., 2014. Removal of chromium from aqueous solutions using modified lettuce leaves. *Water Science and Technology, 69*, 2497-2503.

Li, Z., Tang, X., Chen, Y., Wei, L. and Wang, Y., 2009. Activation of Firmiana Simplex leaf and the enhanced Pb(II) adsorption performance: Equilibrium and kinetic studies. *Journal of Hazardous Materials, 169*, 386-394.

Liang, S., Ye, N., Hu, Y., Shi, Y., Zhang, W., Yu, W., Wu, X. and Yang, J., 2016. Lead adsorption from aqueous solutions by a granular adsorbent prepared from phoenix tree leaves. *RSC Advances, 6*, 25393-25400.

Lim, L., Priyantha, N. and Zaidi, N.M., 2016a. A superb modified new adsorbent, Artocarpus odoratissimus leaves, for removal of cationic methyl violet 2B dye. *Environmental Earth Sciences, 75*, 1179.

Lim, L.B.L., Priyantha, N. and Mohamad Zaidi, N.A.H., 2016b. A superb modified new adsorbent, Artocarpus odoratissimus leaves, for removal of cationic methyl violet 2B dye. *Environmental Earth Sciences, 75*, 1179.

Liu, H., Dong, Y., Liu, Y. and Wang, H., 2010a. Screening of novel low-cost adsorbents from agricultural residues to remove ammonia nitrogen from aqueous solution. *Journal of Hazardous Materials, 178*, 1132-1136.

Liu, H., Dong, Y., Wang, H. and Liu, Y., 2010b. Adsorption behavior of ammonium by a bioadsorbent–Boston ivy leaf powder. *Journal of Environmental Sciences, 22*, 1513-1518.

Liu, H., Dong, Y., Wang, H. and Liu, Y., 2010c. Adsorption behavior of ammonium by a bioadsorbent – Boston ivy leaf powder. *Journal of Environmental Sciences, 22*, 1513-1518.

Liu, H., Dong, Y., Wang, H. and Liu, Y., 2010d. Ammonium adsorption from aqueous solutions by strawberry leaf powder: Equilibrium, kinetics and effects of coexisting ions. *Desalination, 263*, 70-75.

Mahmoud, A.E.D., Fawzy, m. and Radwan, A., 2016. Optimization of Cadmium (CD2+) removal from aqueous solutions by novel biosorbent. *International Journal of Phytoremediation, 18*, 619-625.

Makeswari, M. and Santhi, T., 2014. Use of Ricinus communis leaves as a low-cost adsorbent for removal of Cu(II) ions from aqueous solution. *Research on Chemical Intermediates, 40*, 1157-1177.

Maleki, A., Hamesadeghi, U., Daraei, H., Hayati, B., Najafi, F., McKay, G. and Rezaee, R., 2017. Amine functionalized multi-walled carbon nanotubes: Single and binary systems for high capacity dye removal. *Chemical Engineering Journal, 313*, 826-835.

Malkoc, E. and Nuhoglu, Y., 2005. Investigations of nickel(II) removal from aqueous solutions using tea factory waste. *Journal of Hazardous Materials, 127*, 120-128.

Mambo, M., Admire, C. and Tichaona, N., 2016. Removal of Copper from Aqueous Solution Using Chemically Treated Potato (Solanum tuberosum) Leaf Powder. *CLEAN – Soil, Air, Water, 44*, 488-495.

Manahan, S., 2000. *Chapter 3. Fundamentals of Aquatic Chemistry. Environmental chemistry*: CRC press.

Markou, G., Mitrogiannis, D., Muylaert, K., Çelekli, A. and Bozkurt, H., 2016a. Biosorption and retention of orthophosphate onto Ca (OH) 2-pretreated biomass of Phragmites sp. *Journal of Environmental Sciences, 45*, 49-59.

Markou, G., Mitrogiannis, D., Muylaert, K., Çelekli, A. and Bozkurt, H., 2016b. Biosorption and retention of orthophosphate onto Ca(OH)2-pretreated biomass of Phragmites sp. *Journal of Environmental Sciences, 45*, 49-59.

Meseguer, V.F., Ortuño, J.F., Aguilar, M.I., Pinzón-Bedoya, M.L., Lloréns, M., Sáez, J. and Pérez-Marín, A.B., 2016. Biosorption of cadmium (II) from aqueous solutions by natural and modified non-living leaves of Posidonia oceanica. *Environmental Science and Pollution Research, 23*, 24032-24046.

Milonjić, S.K., 2009. Comments on "removal of uranium (VI) from aqueous solution by adsorption of hematite", by X. Shuibo, Z. Chun, Z. Xinghuo, Y. Jing, Z. Xiaojian, W. Jingsong. *Journal of Environmental Radioactivity, 100*, 921-922.

Mishra, V., Balomajumder, C. and Agarwal, V.K., 2010. Zn(II) Ion Biosorption onto Surface of Eucalyptus Leaf Biomass: Isotherm, Kinetic, and Mechanistic Modeling. *CLEAN – Soil, Air, Water, 38*, 1062-1073.

Mohammed, A.A., Abed, F.I. and Al-Musawi, T.J., 2016. Biosorption of Pb(II) from aqueous solution by spent black tea leaves and separation by flotation. *Desalination and Water Treatment, 57*, 2028-2039.

Mondal, D.K., Nandi, B.K. and Purkait, M.K., 2013. Removal of mercury (II) from aqueous solution using bamboo leaf powder: Equilibrium, thermodynamic and kinetic studies. *Journal of Environmental Chemical Engineering, 1*, 891-898.

Mozumder, M.S.I., Khan, M.M.R. and Islam, M.A., 2008. Kinetics and mechanism of Cr(VI) adsorption onto tea-leaves waste. *Asia-Pacific Journal of Chemical Engineering, 3*, 452-458.

Mucha, M. and Mucha, M., 2017. Ibuprofen and acetylsalicylic acid biosorption on the leaves of the knotweed Fallopia x bohemica. *New Journal of Chemistry, 41*, 7953-7959.

Muhammad, I., Silke, S. and Randall, C., 2009. Mechanistic elucidation and evaluation of biosorption of metal ions by grapefruit peel using FTIR spectroscopy, kinetics and isotherms modeling, cations displacement and EDX analysis. *Journal of Chemical Technology & Biotechnology, 84*, 1516-1526.

Murugan, T., Ganapathi, A. and Valliappan, R., 2010. Removal of dyes from aqueous solution by adsorption on biomass of mango (Mangifera indica) leaves. *Journal of Chemistry, 7*, 669-676.

Muthulaksmi, A., Baskaran, R. and Karthick, N.A., 2016. Removal of high concentrations of chromium from aqueous solutions using leaves of Tamarindus indica: Kinetics and equilibrium studies. *Journal of Environmental Biology, 37*, 1443.

Nadeem, M., Tan, I.B., Haq, M.R.U., Shahid, S.A., Shah, S.S. and McKay, G., 2006. Sorption of Lead Ions from Aqueous Solution by Chickpea Leaves, Stems and Fruit Peelings. *Adsorption Science & Technology, 24*, 269-282.

Nag, S., Mondal, A., Bar, N. and Das, S.K., 2017. Biosorption of chromium (VI) from aqueous solutions and ANN modelling. *Environmental Science and Pollution Research, 24*, 18817-18835.

Nag, S., Mondal, A., Mishra, U., Bar, N. and Das, S.K., 2016. Removal of chromium(VI) from aqueous solutions using rubber leaf powder: Batch and column studies. *Desalination and Water Treatment, 57*, 16927-16942.

Nagpal, U.M.K., Bankar, A.V., Pawar, N.J., Kapadnis, B.P. and Zinjarde, S.S., 2011. Equilibrium and Kinetic Studies on Biosorption of Heavy Metals by Leaf Powder of Paper Mulberry (Broussonetia papyrifera). *Water, Air, & Soil Pollution, 215*, 177-188.

Nakkeeran, E., Saranya, N., Giri Nandagopal, M.S., Santhiagu, A. and Selvaraju, N., 2016. Hexavalent chromium removal from aqueous solutions by a novel powder prepared from Colocasia esculenta leaves. *International Journal of Phytoremediation, 18*, 812-821.

Namdeti, R. and Pulipati, K., 2014. Lead removal from aqueous solution using Ficus Hispida leaves powder. *Desalination and Water Treatment, 52*, 339-349.

Ncibi, M.C., Mahjoub, B. and Seffen, M., 2006. Studies on the biosorption of textile dyes from aqueous solutions using Posidonia oceanica (L.) leaf sheath fibres. *Adsorption Science & Technology, 24*, 461-474.

Neupane, S., Ramesh, S., Gandhimathi, R. and Nidheesh, P., 2015. Pineapple leaf (Ananas comosus) powder as a biosorbent for the removal of crystal violet from aqueous solution. *DESALINATION AND WATER TREATMENT, 54*, 2041-2054.

Ngah, W.S.W. and Hanafiah, M.A.K.M., 2008. Biosorption of copper ions from dilute aqueous solutions on base treatedrubber (Hevea brasiliensis) leaves powder: Kinetics, isotherm, and biosorption mechanisms. *Journal of Environmental Sciences, 20*, 1168-1176.

Ngah, W.S.W. and Hanafiah, M.A.K.M., 2009. Surface modification of rubber (Hevea brasiliensis) leaves for the adsorption of copper ions: kinetic, thermodynamic and binding mechanisms. *Journal of Chemical Technology & Biotechnology, 84*, 192-201.

Pandey, R., Prasad, R.L., Ansari, N.G. and Murthy, R.C., 2015a. Utilization of NaOH modified Desmostachya bipinnata (Kush grass) leaves and Bambusa arundinacea (bamboo) leaves for Cd (II) removal from aqueous solution. *Journal of Environmental Chemical Engineering, 3*, 593-602.

Pandey, R., Prasad, R.L., Ansari, N.G. and Murthy, R.C., 2015b. Utilization of NaOH modified Desmostachya bipinnata (Kush grass) leaves and Bambusa arundinacea (bamboo) leaves for Cd(II) removal from aqueous solution. *Journal of Environmental Chemical Engineering, 3*, 593-602.

Panneerselvam, P., Morad, N. and Tan, K.A., 2011. Magnetic nanoparticle (Fe3O4) impregnated onto tea waste for the removal of nickel (II) from aqueous solution. *Journal of Hazardous Materials, 186*, 160-168.

Park, D., Yun, Y.-S., Lee, D.S. and Park, J.M., 2011. Optimum condition for the removal of Cr(VI) or total Cr using dried leaves of Pinus densiflora. *Desalination, 271*, 309-314.

Park, D., Yun, Y.-S. and Park, J.M., 2005. Studies on hexavalent chromium biosorption by chemically-treated biomass of Ecklonia sp. *Chemosphere, 60*, 1356-1364.

Pennesi, C., Totti, C. and Beolchini, F., 2013. Removal of vanadium (III) and molybdenum (V) from wastewater using Posidonia oceanica (Tracheophyta) biomass. *PloS One, 8*, e76870.

Peng, C., Yan, X.-b., Wang, R.-t., Lang, J.-w., Ou, Y.-j. and Xue, Q.-j., 2013. Promising activated carbons derived from waste tea-leaves and their application in high performance supercapacitors electrodes. *Electrochimica Acta, 87*, 401-408.

Peydayesh, M. and Rahbar-Kelishami, A., 2015. Adsorption of methylene blue onto Platanus orientalis leaf powder: Kinetic, equilibrium and thermodynamic studies. *Journal of Industrial and Engineering Chemistry, 21*, 1014-1019.

Ponnusami, V., Gunasekar, V. and Srivastava, S., 2009a. Kinetics of methylene blue removal from aqueous solution using gulmohar (Delonix regia) plant leaf powder: multivariate regression analysis. *Journal of Hazardous Materials, 169*, 119-127.

Ponnusami, V., Gunasekar, V. and Srivastava, S.N., 2009b. Kinetics of methylene blue removal from aqueous solution using gulmohar (Delonix regia) plant leaf powder: Multivariate regression analysis. *Journal of Hazardous Materials, 169*, 119-127.

Ponou, J., Kim, J., Wang, L.P., Dodbiba, G. and Fujita, T., 2011. Sorption of Cr(VI) anions in aqueous solution using carbonized or dried pineapple leaves. *Chemical Engineering Journal, 172*, 906-913.

Prasad, A.L. and Thirumalisamy, S., 2013. Evaluation of the use of acacia nilotica leaf as an ecofriendly adsorbent for Cr(VI) and its suitability in real waste water: Study of residual errors. *Journal of Chemistry, 2013*, 7.

Prasanna Kumar, Y., King, P. and Prasad, V.S.R.K., 2006. Equilibrium and kinetic studies for the biosorption system of copper(II) ion from aqueous solution using Tectona grandis L.f. leaves powder. *Journal of Hazardous Materials, 137*, 1211-1217.

Purai, A. and Rattan, V., 2012. Biosorption of Leather Dye (Acid Blue 193) from Aqueous Solution using Ash Prepared from Cow Dung, Mango Stone, Parthenium Leaves and Activated Carbon. *Indian Chemical Engineer, 54*, 190-209.

Qaiser, S., Saleemi, A.R. and Mahmood Ahmad, M., 2007. Heavy metal uptake by agro based waste materials. *Electronic Journal of Biotechnology, 10*, 409-416.

Qaiser, S., Saleemi, A.R. and Umar, M., 2009. Biosorption of lead from aqueous solution by Ficus religiosa leaves: Batch and column study. *Journal of Hazardous Materials, 166*, 998-1005.

Qi, B.C. and Aldrich, C., 2008. Biosorption of heavy metals from aqueous solutions with tobacco dust. *Bioresource Technology, 99*, 5595-5601.

Qi, W., Zhao, Y., Zheng, X., Ji, M. and Zhang, Z., 2016. Adsorption behavior and mechanism of Cr(VI) using Sakura waste from aqueous solution. *Applied Surface Science, 360*, 470-476.

Rahmat, N.A., Ali, A.A., Hussain, N., Muhamad, M.S., Kristanti, R.A. and Hadibarata, T., 2016. Removal of Remazol Brilliant Blue R from Aqueous Solution by Adsorption Using Pineapple Leaf Powder and Lime Peel Powder. *Water, Air, and Soil Pollution, 227*, 105.

Raju, D., Kiran, G.R. and Rao, D.V., 2013. Comparison studies on biosorption of lead (II) from an aqueous solution using anacardium occidentale and carica papaya leaves powder. *J. Emerging Trends In Engineering and Development, 3*, 273-283.

Ramakul, P., Yanachawakul, Y., Leepipatpiboon, N. and Sunsandee, N., 2012. Biosorption of palladium (II) and platinum (IV) from aqueous solution using tannin from Indian almond (Terminalia catappa L.) leaf biomass: Kinetic and equilibrium studies. *Chemical engineering journal, 193*, 102-111.

Ramrakhiani, L., Halder, A., Majumder, A., Mandal, A.K., Majumdar, S. and Ghosh, S., 2017. Industrial waste derived biosorbent for toxic metal remediation: Mechanism studies and spent biosorbent management. *Chemical Engineering Journal, 308*, 1048-1064.

Rangabhashiyam, S., Nakkeeran, E., Anu, N. and Selvaraju, N., 2015. Biosorption potential of a novel powder, prepared from Ficus auriculata leaves, for sequestration of hexavalent chromium from aqueous solutions. *Research on Chemical Intermediates, 41*, 8405-8424.

Rao, K., 2010. Equilibrium and kinetic studies for Cd (II) adsorption from aqueous solution on Terminalia catappa Linn leaf powder biosorbent.

Rao, K., Anand, S. and Venkateswarlu, P., 2011a. Modeling the kinetics of Cd (II) adsorption on Syzygium cumini L leaf powder in a fixed bed mini column. *Journal of Industrial and Engineering Chemistry, 17*, 174-181.

Rao, K., Anand, S. and Venkateswarlu, P., 2010a. Psidium guvajava L leaf powder—a potential low-cost biosorbent for the removal of cadmium(II) Ions from wastewater. *Adsorption Science & Technology, 28*, 163-178.

Rao, K.S., Anand, S. and Venkateswarlu, P., 2010b. Adsorption of cadmium (II) ions from aqueous solution by Tectona grandis LF (teak leaves powder). *BioResources, 5*, 438-454.

Rao, K.S., Anand, S. and Venkateswarlu, P., 2011b. Adsorption of cadmium from aqueous solution by Ficus religiosa leaf powder and characterization of loaded biosorbent. *CLEAN – Soil, Air, Water, 39*, 384-391.

Rao, K.S., Anand, S. and Venkateswarlu, P., 2010c. Cadmium removal from aqueous solutions using biosorbent Syzygium cumini leaf powder: Kinetic and equilibrium studies. *Korean Journal of Chemical Engineering, 27*, 1547-1554.

Rao, R.A.K. and Khan, U., 2017. Adsorption studies of Cu(II) on Boston fern (Nephrolepis exaltata Schott cv. Bostoniensis) leaves. *Applied Water Science, 7*, 2051-2061.

Raza, M.H., Sadiq, A., Farooq, U., Athar, M., Hussain, T., Mujahid, A. and Salman, M., 2015. Phragmites karka as a Biosorbent for the Removal of Mercury Metal Ions from Aqueous Solution: Effect of Modification. *Journal of Chemistry, 2015*, 12.

Reddy, D.H.K., Harinath, Y., Seshaiah, K. and Reddy, A.V.R., 2010. Biosorption of Pb(II) from aqueous solutions using chemically modified Moringa oleifera tree leaves. *Chemical Engineering Journal, 162*, 626-634.

Reddy, D.H.K., Seshaiah, K., Reddy, A.V.R. and Lee, S.M., 2012. Optimization of Cd(II), Cu(II) and Ni(II) biosorption by chemically modified Moringa oleifera leaves powder. *Carbohydrate Polymers, 88*, 1077-1086.

Rehman, R., Anwar, J. and Mahmud, T., 2014. Adsorptive Elimination of Chromium (III) and Nickel (II) from Water by Spent Eugenia jambolana Leaves: Isothermal and Thermodynamical Studies. *Asian Journal of Chemistry, 26*, 644.

Rehman, R., Mahmud, T., Anwar, J. and Salman, M., 2012. Isothermal modeling of batch biosorption of Brilliant Green dye from water by chemically modified Eugenia jambolana leaves. *J Chem Soc Pak, 34*, 136-143.

Rehman, R., Mahmud, T., Ejaz, R., Rauf, A. and Mitu, L., 2017. Sorptive removal of Direct Blue-15 dye from water using Camellia sinensis and Carica papaya leaves. *BULGARIAN CHEMICAL COMMUNICATIONS, 49*, 20-25.

Rehman, R., Shafique, U., Anwar, J. and Ghafoor, S., 2013. Kinetic and isothermal biosorption studies of Co (II), Cu (II) and Ni (II) using Polyalthia longifolia leaf powder. *Asian Journal of Chemistry, 25*, 8285.

Ren, X., Xiao, W., Zhang, R., Shang, Y. and Han, R., 2015. Adsorption of crystal violet from aqueous solution by chemically modified phoenix tree leaves in batch mode. *DESALINATION AND WATER TREATMENT, 53*, 1324-1334.

Romero-González, J., Peralta-Videa, J.R., Rodríguez, E., Ramirez, S.L. and Gardea-Torresdey, J.L., 2005. Determination of thermodynamic parameters of Cr(VI) adsorption from aqueous solution onto Agave lechuguilla biomass. *The Journal of Chemical Thermodynamics, 37*, 343-347.

Rostami, B. and Niazi, A., 2013. Biosorption of a textile dye (Eosin) by eucalyptus tree leaves biomass: estimation of equilibrium, thermodynamic and kinetic parameters. *Advanced Science Focus, 1*, 50-56.

Ruiyi, F., Qingping, Y., Yucong, X., Feng, X., Qinglin, Z. and Zhengrong, L., 2016. Enhanced adsorption and recovery of Pb(II) from aqueous solution by alkali-treated persimmon fallen leaves. *Journal of Applied Polymer Science, 133*.

Saha, G.C., Hoque, M.I.U., Miah, M.A.M., Holze, R., Chowdhury, D.A., Khandaker, S. and Chowdhury, S., 2017. Biosorptive removal of lead from aqueous solutions onto Taro (Colocasiaesculenta(L.) Schott) as a low cost bioadsorbent: Characterization, equilibria, kinetics and biosorption-mechanism studies. *Journal of Environmental Chemical Engineering, 5*, 2151-2162.

Saha, P.D., Chakraborty, S. and Chowdhury, S., 2012a. Batch and continuous (fixed-bed column) biosorption of crystal violet by Artocarpus heterophyllus (jackfruit) leaf powder. *Colloids and Surfaces B: Biointerfaces, 92*, 262-270.

Saha, P.D., Chakraborty, S. and Chowdhury, S., 2012b. Batch and continuous (fixed-bed column) biosorption of crystal violet by Artocarpus heterophyllus (jackfruit) leaf powder. *Colloids and surfaces B: Biointerfaces, 92*, 262-270.

Saha, R. and Saha, B., 2014. Removal of hexavalent chromium from contaminated water by adsorption using mango leaves (Mangifera indica). *Desalination and Water Treatment, 52*, 1928-1936.

Salehi, P., Asghari, B. and Mohammadi, F., 2008. Removal of heavy metals from aqueous solutions by Cercis siliquastrum L. *Journal of the Iranian Chemical Society, 5*, S80-S86.

Sangi, M.R., Shahmoradi, A., Zolgharnein, J., Azimi, G.H. and Ghorbandoost, M., 2008. Removal and recovery of heavy metals from aqueous solution using Ulmus carpinifolia and Fraxinus excelsior tree leaves. *Journal of Hazardous Materials, 155*, 513-522.

Sarada, B., Prasad, M.K., Kumar, K.K. and Murthy, C., 2013a. POTENTIAL USE OF LEAF BIOMASS, ARAUCARIA HETEROPHYLLA FOR REMOVAL OF Pb+2. *International Journal of Phytoremediation, 15*, 756-773.

Sarada, B., Prasad, M.K., Kumar, K.K. and Murthy, C., 2013b. Potential use of leaf biomass, Araucaria heterophylla for removal OF Pb+ 2. *International journal of phytoremediation, 15*, 756-773.

Sathish, T., Vinithkumar, N.V., Dharani, G. and Kirubagaran, R., 2015. Efficacy of mangrove leaf powder for bioremediation of chromium (VI) from aqueous solutions: kinetic and thermodynamic evaluation. *Applied Water Science, 5*, 153-160.

Sawalha, M.F., Peralta-Videa, J.R., Romero-González, J., Duarte-Gardea, M. and Gardea-Torresdey, J.L., 2007. Thermodynamic and isotherm studies of the biosorption of Cu(II), Pb(II), and Zn(II) by leaves of saltbush (Atriplex canescens). *The Journal of Chemical Thermodynamics, 39*, 488-492.

Sen, T.K., Azman, A.F.B., Maitra, S. and Dutta, B.K., 2011. Removal of mercury (II) from aqueous solutions using the leaves of the rambai tree (Baccaurea motleyana). *Water Environment Research, 83*, 834-842.

Sert, Ş., Kütahyali, C., İnan, S., Talip, Z., Çetinkaya, B. and Eral, M., 2008. Biosorption of lanthanum and cerium from aqueous solutions by Platanus orientalis leaf powder. *Hydrometallurgy, 90*, 13-18.

Setiabudi, H., Jusoh, R., Suhaimi, S. and Masrur, S., 2016a. Adsorption of methylene blue onto oil palm (Elaeis guineensis) leaves: process optimization, isotherm, kinetics and thermodynamic studies. *Journal of the Taiwan Institute of Chemical Engineers, 63*, 363-370.

Setiabudi, H.D., Jusoh, R., Suhaimi, S.F.R.M. and Masrur, S.F., 2016b. Adsorption of methylene blue onto oil palm (Elaeis guineensis) leaves: Process optimization, isotherm, kinetics and thermodynamic studies. *Journal of the Taiwan Institute of Chemical Engineers, 63*, 363-370.

Shafique, U., Ijaz, A., Salman, M., Zaman, W.u., Jamil, N., Rehman, R. and Javaid, A., 2012. Removal of arsenic from water using pine leaves. *Journal of the Taiwan Institute of Chemical Engineers, 43*, 256-263.

Shah, J., Jan, M.R., Haq, A.u. and Zeeshan, M., 2015a. Equilibrium, kinetic and thermodynamic studies for sorption of Ni (II) from aqueous solution using formaldehyde treated waste tea leaves. *Journal of Saudi Chemical Society, 19*, 301-310.

Shah, J., Jan, M.R., ul Haq, A. and Zeeshan, M., 2015b. Equilibrium, kinetic and thermodynamic studies for sorption of Ni (II) from aqueous solution using formaldehyde treated waste tea leaves. *Journal of Saudi Chemical Society, 19*, 301-310.

Shanthi, T. and Selvarajan, V.M., 2013. Removal of Cr(VI) and Cu(II) Ions from Aqueous Solution by Carbon Prepared from Henna Leaves. *Journal of Chemistry, 2013*, 6.

Sharma, A. and Bhattacharyya, K.G., 2005. Adsorption of Chromium (VI) on Azadirachta Indica (Neem) Leaf Powder. *Adsorption, 10*, 327-338.

Sharma, A. and Bhattacharyya, K.G., 2008. Interactions of Pb (II), Cd (II) and Cr (VI) with Neem (Azadirachta indica) leaf powder: kinetics and thermodynamics. *International Journal of Environment and Pollution, 34*, 374-399.

Sharma, D.C. and Forster, C.F., 1994. The treatment of chromium wastewaters using the sorptive potential of leaf mould. *Bioresource Technology, 49*, 31-40.

Sheen, O.P., Ong, S.T. and Hung, Y.T., 2013. Utilization of Mango Leaf as A Low-Cost Adsorbent for The Removal of Cu (II) Ions from Aqueous Solution. *Asian Journal of Chemistry, 25*, 6141.

Shi, J., Fang, Z., Zhao, Z., Sun, T. and Liang, Z., 2016a. Comparative study on Pb(II), Cu(II), and Co(II) ions adsorption from aqueous solutions by arborvitae leaves. *Desalination and Water Treatment, 57*, 4732-4739.

Shi, J., Zhao, Z., Liang, Z. and Sun, T., 2016b. Adsorption characteristics of Pb(II) from aqueous solutions onto a natural biosorbent, fallen arborvitae leaves. *Water Science and Technology, 73*, 2422-2429.

Singha, B. and Das, S.K., 2012. Removal of Pb(II) ions from aqueous solution and industrial effluent using natural biosorbents. *Environmental Science and Pollution Research, 19*, 2212-2226.

Sinha, V., Pakshirajan, K. and Chaturvedi, R., 2015a. Evaluation of Cr (VI) Exposed and Unexposed Plant Parts of Tradescantia pallida (Rose) DR Hunt. for Cr Removal from Wastewater by Biosorption. *International journal of phytoremediation, 17*, 1204-1211.

Sinha, V., Pakshirajan, K. and Chaturvedi, R., 2015b. Evaluation of Cr(VI) Exposed and Unexposed Plant Parts of Tradescantia pallida (Rose) D. R. Hunt. for Cr Removal from Wastewater by Biosorption. *International Journal of Phytoremediation, 17*, 1204-1211.

Srinivasa Rao, K., Anand, S. and Venkateswarlu, P., 2010. *Adsorption of cadmium (II) ions from aqueous solution by Tectona grandis LF (teak leaves powder)*. BioResources.

Srivastava, V.C., Mall, I.D. and Mishra, I.M., 2006. Equilibrium modelling of single and binary adsorption of cadmium and nickel onto bagasse fly ash. *Chemical Engineering Journal, 117*, 79-91.

Tamez Uddin, M., Rukanuzzaman, M., Maksudur Rahman Khan, M. and Akhtarul Islam, M., 2009. Adsorption of methylene blue from aqueous solution by jackfruit (Artocarpus heteropyllus) leaf powder: A fixed-bed column study. *Journal of Environmental Management, 90*, 3443-3450.

Tran, H.N. and Chao, H.-P., 2018. Adsorption and desorption of potentially toxic metals on modified biosorbents through new green grafting process. *Environmental Science and Pollution Research*.

Tran, H.N., Lee, C.-K., Nguyen, T.V. and Chao, H.-P., 2017a. Saccharide-derived microporous spherical biochar prepared from hydrothermal carbonization and different pyrolysis temperatures: synthesis, characterization, and application in water treatment. *Environmental Technology*, 1-14.

Tran, H.N., You, S.-J., Hosseini-Bandegharaei, A. and Chao, H.-P., 2017b. Mistakes and inconsistencies regarding adsorption of contaminants from aqueous solutions: A critical review. *Water Research, 120*, 88-116.

Tran, H.N., You, S.-J., Nguyen, T.V. and Chao, H.-P., 2017c. Insight into the adsorption mechanism of cationic dye onto biosorbents derived from agricultural wastes. *Chemical Engineering Communications, 204*, 1020-1036.

Uddin, M.T., Islam, M.A., Mahmud, S. and Rukanuzzaman, M., 2009. Adsorptive removal of methylene blue by tea waste. *Journal of Hazardous Materials, 164*, 53-60.

V., G.V. and Misra, A.K., 2018. Copper contaminated wastewater – An evaluation of bioremedial options. *Indoor and Built Environment, 27*, 84-95.

Van Suc, N. and Son, L.N., 2016. Mistletoe leaves as a biosorbent for removal of Pb(II) and Cd(II) from aqueous solution. *Desalination and Water Treatment, 57*, 3606-3618.

Venkateswarlu, P., Durga, G.V., Babu, N.C. and Rao, M.V., 2008. Biosorption of Zn (II) from an aqueous solution by Erythrina variegata orientalis leaf powder. *International Journal of Physical Sciences, 3*, 197-204.

Vijaya Lakshmi, G., Chitti Babu, N., Ravi Kumar, P.V., Subba Rao, D. and Venkateswarlu, P., 2008. POTENTIAL OF ERYTHRINA VARIEGATA ORIENTALIS LEAF POWDER FOR THE REMOVAL OF COBALT(II). *Chemical Engineering Communications, 196*, 463-480.

Vilvanathan, S. and Shanthakumar, S., 2016. Removal of Ni(II) and Co(II) ions from aqueous solution using teak (Tectona grandis) leaves powder: adsorption kinetics, equilibrium and thermodynamics study. *Desalination and Water Treatment, 57*, 3995-4007.

Volesky, B., 2007. Biosorption and me. *Water Research, 41*, 4017-4029.

Wahab, M.A., Boubakri, H., Jellali, S. and Jedidi, N., 2012. Characterization of ammonium retention processes onto Cactus leaves fibers using FTIR, EDX and SEM analysis. *Journal of Hazardous Materials, 241-242*, 101-109.

Wan Ngah, W.S. and Hanafiah, M.A.K.M., 2008. Adsorption of copper on rubber (Hevea brasiliensis) leaf powder: Kinetic, equilibrium and thermodynamic studies. *Biochemical Engineering Journal, 39*, 521-530.

Wan, S., Ma, Z., Xue, Y., Ma, M., Xu, S., Qian, L. and Zhang, Q., 2014. Sorption of Lead(II), Cadmium(II), and Copper(II) Ions from Aqueous Solutions Using Tea Waste. *Industrial & Engineering Chemistry Research, 53*, 3629-3635.

Wang, C., Wang, H. and Liu, Y., 2016. Purification of Pb (II) ions from aqueous solution by camphor leaf modified with succinic anhydride. *Colloids and Surfaces A: Physicochemical and Engineering Aspects, 509*, 80-85.

Wenfang, Q., Yue, W., Min, J., Yingxin, Z. and Zhenya, Z., 2015. Highly efficient adsorption of Cr (VI) by Sakura leaves from aqueous solution. *Chemistry Letters, 44*, 697-699.

Weng, C.-H., Lin, T.Y., Chu, S.-H. and Yuan, C., 2006. Laboratory-scale evaluation of Cr (VI) removal from clay by electrokinetics incorporated with Fe (O) barrier. *Practice Periodical of Hazardous, Toxic, and Radioactive Waste Management, 10*, 171-178.

Weng, C.-H., Lin, Y.-T., Hong, D.-Y., Sharma, Y.C., Chen, S.-C. and Tripathi, K., 2014a. Effective removal of copper ions from aqueous solution using base treated black tea waste. *Ecological Engineering, 67*, 127-133.

Weng, C.-H., Lin, Y.-T., Hong, D.-Y., Sharma, Y.C., Chen, S.-C. and Tripathi, K., 2014b. Effective removal of copper ions from aqueous solution using base treated black tea waste. *Ecological engineering, 67*, 127-133.

Weng, C.-H., Lin, Y.-T. and Tzeng, T.-W., 2009. Removal of methylene blue from aqueous solution by adsorption onto pineapple leaf powder. *Journal of Hazardous Materials, 170*, 417-424.

Weng, C.-H. and Wu, Y.-C., 2012. Potential low-cost biosorbent for copper removal: Pineapple leaf powder. *Journal of Environmental Engineering, 138*, 286-292.

Xia, L., Tan, K., Wang, X., Zheng, W., Liu, W. and Deng, C., 2013. Uranium Removal from Aqueous Solution by Banyan Leaves: Equilibrium, Thermodynamic, Kinetic, and Mechanism Studies. *Journal of Environmental Engineering, 139*, 887-895.

Xiao, X., Xue, J., Ding, D., He, B., He, D., Tan, L. and Liao, L., 2016. Adsorption of low concentration of uranium(VI) from aqueous solution by diethylenetriamine functionalized Cycas revoluta leaves. *Journal of Radioanalytical and Nuclear Chemistry, 308*, 1027-1037.

Yagub, M.T., Sen, T.K. and Ang, H., 2012. Equilibrium, kinetics, and thermodynamics of methylene blue adsorption by pine tree leaves. *Water, Air, and Soil Pollution, 223*, 5267-5282.

Yang, J.-X. and Hong, G.-B., 2018a. Adsorption behavior of modified Glossogyne tenuifolia leaves as a potential biosorbent for the removal of dyes. *Journal of Molecular Liquids, 252*, 289-295.

Yang, J.-X. and Hong, G.-B., 2018b. Adsorption behavior of modified Glossogyne tenuifolia leaves as a potential biosorbent for the removal of dyes. *Journal of Molecular Liquids*.

Yu, J.-x., Feng, L.-y., Cai, X.-l., Wang, L.-y. and Chi, R.-a., 2015. Adsorption of Cu2+, Cd2+ and Zn2+ in a modified leaf fixed-bed column: competition and kinetics. *Environmental Earth Sciences, 73*, 1789-1798.

Yuvaraja, G., Krishnaiah, N., Subbaiah, M.V. and Krishnaiah, A., 2014. Biosorption of Pb(II) from aqueous solution by Solanum melongena leaf powder as a low-cost biosorbent prepared from agricultural waste. *Colloids and Surfaces B: Biointerfaces, 114*, 75-81.

Yuvaraja, G., Subbaiah, M.V. and Krishnaiah, A., 2012. Caesalpinia bonducella leaf powder as biosorbent for Cu(II) removal from aqueous environment: Kinetics and isotherms. *Industrial & Engineering Chemistry Research, 51*, 11218-11225.

Zahedi, R., Dabbagh, R., Ghafourian, H. and Behbahanini, A., 2015. Nickel removal by Nymphaea alba leaves and effect of leaves treatment on the sorption capacity: A kinetic and thermodynamic study. *Water Resources, 42*, 690-698.

Zhang, Y., Li, X. and Li, Y., 2015. Influence of solution chemistry on heavy metals removal by bioadsorbent tea waste modified by poly (vinyl alcohol). *Desalination and Water Treatment, 53*, 2134-2143.

Zhou, Q., Xie, C., Gong, W., Xu, N. and Zhou, W., 2011. Comments on the method of using maximum absorption wavelength to calculate Congo Red solution concentration published in J. Hazard. Mater. *Journal of Hazardous Materials, 198*, 381-382.

Zhu, L., Wang, Y., He, T., You, L. and Shen, X., 2016. Assessment of potential capability of water bamboo leaves on the adsorption removal efficiency of cationic dye from aqueous solutions. *Journal of Polymers and the Environment, 24*, 148-158.

Zolgharnein, J., Adhami, Z., Shahmoradi, A. and Mousavi, S.N., 2010. Optimization of removal of methylene blue by Platanus tree leaves using response surface methodology. *Analytical Sciences, 26*, 111-116.

Zolgharnein, J., Asanjarani, N. and Shariatmanesh, T., 2013a. Taguchi L16 orthogonal array optimization for Cd (II) removal using Carpinus betulus tree leaves: Adsorption characterization. *International Biodeterioration & Biodegradation, 85*, 66-77.

Zolgharnein, J. and Bagtash, M., 2015. Hybrid central composite design optimization for removal of Methylene blue by Acer tree leaves: characterization of adsorption. *DESALINATION AND WATER TREATMENT, 54*, 2601-2610.

Zolgharnein, J., Bagtash, M., Feshki, S., Zolgharnein, P. and Hammond, D., 2017a. Crossed mixture process design optimization and adsorption characterization of multi-metal (Cu (II), Zn (II) and Ni (II)) removal by modified Buxus sempervirens tree leaves. *Journal of the Taiwan Institute of Chemical Engineers, 78*, 104-117.

Zolgharnein, J., Bagtash, M., Feshki, S., Zolgharnein, P. and Hammond, D., 2017b. Crossed mixture process design optimization and adsorption characterization of multi-metal (Cu(II), Zn(II) and Ni(II)) removal by modified Buxus sempervirens tree leaves. *Journal of the Taiwan Institute of Chemical Engineers, 78*, 104-117.

Zolgharnein, J., Gholami, F., Asanjarani, N., Zolgharnein, P. and Azimi, G., 2014. Removal of Methyl Violet Dye from Aqueous Solution by sf Platanus Carpinifolia Tree Leaves as Highly Efficient Sorbent: Multivariate Optimization, Isotherm Modeling, and Kinetic Studies. *Separation Science and Technology, 49*, 752-762.

Zolgharnein, J. and Shahmoradi, A., 2010. Characterization of Sorption Isotherms, Kinetic Models, and Multivariate Approach for Optimization of Hg(II) Adsorption onto Fraxinus Tree Leaves. *Journal of Chemical & Engineering Data, 55*, 5040-5049.

Zolgharnein, J., Shahmoradi, A., Zolgharnein, P. and Amani, S., 2016. Multivariate Optimization and Adsorption Characterization of As(III) by Using Fraxinus Tree Leaves. *Chemical Engineering Communications, 203*, 210-223.

Zolgharnein, J., Shariatmanesh, T. and Asanjarani, N., 2013b. Cercis siliquastrum tree leaves as an efficient adsorbent for removal of Ag(I): Response surface optimization and characterization of biosorption. *CLEAN – Soil, Air, Water, 41*, 1183-1195.

Zolgharnein, J., Shariatmanesh, T., Asanjarani, N. and Zolanvari, A., 2015. Doehlert design as optimization approach for the removal of Pb(II) from aqueous solution by Catalpa Speciosa tree leaves: adsorption characterization. *Desalination and Water Treatment, 53*, 430-445.